Cover image: Microscopic image of a neointimal lesion after ligation of the left common carotid artery characterised by vascular smooth muscle cell senescence (blue).

Cover design: Anita Muys

Printed by: D. Provo nv – Brulens 23B – 2275 Gierle

The research described in this thesis was performed at the laboratory of Physiopharmacology at the University of Antwerp. Mandy Grootaert is a PhD fellow of the Agency for Innovation by Science and Technology in Flanders (IWT). This work was supported financially by the Fund for Scientific Research Flanders (FWO) and the University of Antwerp.

Faculteit Farmaceutische, Biomedische en Diergeneeskundige Wetenschappen

Departement Farmaceutische wetenschappen

Inhibition of apoptosis, autophagy and necrosis in atherosclerosis: potential strategies for plaque stabilisation?

Inhibitie van apoptose, autofagie en necrose in atherosclerose: potentiële strategieën voor plaquestabilisatie?

Proefschrift voorgelegd tot het behalen van de graad van doctor in de Farmaceutische Wetenschappen aan de Universiteit Antwerpen te verdedigen door

Mandy GROOTAERT

Promotoren: Prof. dr. Wim Martinet

Prof. dr. Dorien M Schrijvers

Antwerpen, 2016

Members of the jury

Internal doctoral committee

Prof. dr. Ingrid De Meester (Chair)

Laboratory of Medical Biochemistry - University of Antwerp

Prof. dr. Wim Martinet (Promotor)

Laboratory of Physiopharmacology - University of Antwerp

Prof. dr. Dorien M Schrijvers (Promotor)

Laboratory of Physiopharmacology - University of Antwerp

Prof. dr. Pieter Van der Veken (Member)

Laboratory of Medicinal Chemistry (UAMC) - University of Antwerp

External members of the jury

Prof. dr. Patrizia Agostinis

Cell Death Research and Therapy Lab, Department Cellular & Molecular Medicine, KULeuven, Belgium

Prof. dr. Martin R Bennett

Division of Cardiovascular Medicine, Department of Medicine, University of Cambridge, UK

“ Everything happens for a reason”

Aristotle

TABLE OF CONTENTS

ACKNOWLEDGEMENTS - DANKWOORD

Een doctoraat, dat zou in de synoniemenlijst opgenomen moeten worden als ‘een onderzoekstudieweg met vallen en opstaan”. Ik ben een paar keer gevallen, maar gelukkig niet te hard, en snel weer opgestaan dankzij de positieve wendingen tijdens mijn doctoraat en de veelbetekenende steun van mijn promotoren, collega’s, vrienden en familie. Zij verdienen hier een woordje van dank…

Eén van de eerste die ik wens te bedanken is mijn promotor prof. Dorien Schrijvers. Dorien, Ik heb zoveel aan jou te danken dat ik niet goed weet waar te beginnen. Eén ding weet ik zeker: mijn doctoraat en zelfs mijn verdere toekomst had er helemaal anders uitgezien als ik jou niet als promotor had gehad. Vanaf dag 1 stond je klaar voor mij om me alles in het labo te leren en gaande weg liet je me meer en meer los (of probeerde ik mezelf al een beetje los te wrikken ☺) zodat ik voldoende zelfstandigheid als onderzoeker kon opbouwen. Maar als er iets fout liep, kon ik meteen bij jou terecht! Ik weet nog hoe enthousiast we konden worden van een mooi western blot resultaat! Goh, wat heb ik onze brainstorm - thinking outside the box - momentjes al gemist maar wat heb ik daar veel van geleerd! Bedankt om mij altijd zo goed te steunen in mijn wetenschappelijke ideeën (ik denk bijv. aan de ligatiestudie) en mij het gevoel te geven dat ik goed bezig was. Het laatste jaar hebben we mekaar nu wel minder gezien, maar op de cruciale momenten kon ik nog steeds op jou rekenen! Als laatste wil ik jou heel erg bedanken om mij te steunen en te sturen in mijn nieuw postdoc avontuur. Dankzij jouw inzet en connecties kan ik nu beginnen aan een nieuwe uitdaging!

Ook mijn promotor prof. Wim Martinet wil ik uitvoerig bedanken. Wim, op u kon ik altijd rekenen! Voor experimentele problemen maar ook manuscripten werden binnen de 24u verbeterd. Ik moet de tel zijn kwijtgeraakt van hoeveel manuscriptversies u heeft verbeterd voor mij. In feite, heeft ú me leren wetenschappelijk schrijven! “Een artikel moet een mooi, duidelijk verhaal brengen en volgt zelden de chronologische volgorde van de uitgevoerde experimenten.” Als we de opbouw van mijn thesis bekijken, denk ik dat ik uw raad goed heb opgevolgd! Ik apprecieer enorm uw oprechtheid en nuchtere kijk, ook al waren we het af en toe wel eens oneens over iets.☺ Daarenboven zou ik u graag willen bedanken voor de kansen die ik heb gekregen (bijv. het bijwonen van het autofagie congres in Texas) en uw vertrouwen in mij zodat ik steeds al mijn, soms wildste,

experimentele ideeën mocht uitwerken. Als laatste zou ik u graag nog willen bedanken om op 6 weken tijd mijn thesis na te lezen. Zonder u had ik op zo'n korte tijd nooit mijn doctoraat kunnen afleggen!

Guido, u bent misschien niet officieel mijn promotor, maar zo voelt het alleszins niet aan want ook bij u kon ik steeds terecht voor vragen over statistiek, het uitwisselen van gedachten over wetenschap én onderwijs, en zelfs een peptalk ☺. Ik weet dat u mijn zin voor verantwoordelijkheid enorm apprecieert, en dat doet me veel plezier. Bedankt om alles in het werk te stellen zodat ik mijn doctoraat in een versneld tempo kon afwerken om mijn dromen verder na te jagen. Als laatste wens ik u nog veel wetenschappelijk voorspoed want ik weet dat dit labo u nauw aan het hart ligt en u er heel veel voor doet!

I would like to thank the members of the jury, prof. Patrizia Agostinis and prof. Martin Bennett for the critical evaluation of this thesis. I thank the members of the doctoral committee, prof. Ingrid De Meester and prof. Pieter Van der Veken for the interesting discussions and questions at my pre-defence which enforced me to critically reflect my PhD work and to further improve my thesis.

Vervolgens wens ik graag mijn 2 bureaugenootjes Lynn en Miche te bedanken! Samen hebben we heel veel leuke momenten beleefd (op congres in Cambridge, samen soezen bakken voor het kerstfeest,..) maar ook tijdens de mindere momenten vonden we steun bij elkaar. Lynn, tijdens de afgelopen 5 jaar is er een hechte vriendschap tussen ons ontstaan. De eerste banden werden gesmeed op congres in Wiesbaden waar we het recordaantal voetbleinen hadden opgelopen.:) Jij kent me ondertussen door en door, zowel mijn sterktes als mijn zwaktes, mijn dromen en mijn bekommernissen. Ik vond het heel erg fijn dat jij ook jouw perikelen aan mij kon toevertrouwen. Daarnaast waardeer ik enorm jouw mening die altijd eerlijk en oprecht is met de juiste dosis nuchterheid én gevoeligheid. Lieve Lynn, je bent een doorzetter en een steengoede onderzoeker met een hart die klopt voor wetenschappelijke uitdagingen. Ik wens je veel succes toe in je verdere carrière en een bijzonder mooie toekomst samen met Brett en de kleine spruit die opkomst is! Miche, het afgelopen jaar is onze band alleen maar sterker geworden. Alle twee zaten we immers in hetzelfde schuitje: een doctoraatsthesis schrijven dat gepaard gaat met de nodige deadlines, de laatste papers trachten zo snel mogelijk buiten te sturen en hopen op milde commentaren van de reviewers én geen Dorien binnen handbereik. We hebben alle twee de nodige stressmomentjes gehad de afgelopen

maanden maar konden daarbij op elkaars steun rekenen! Ik weet nog hoe blij je voor me was toen ik eind april bericht kreeg dat ik een postdoc mocht beginnen in Cambridge. Jij stond te springen in den bureau terwijl ik nog in de paniekfase zat. Lieve Miche, ik vind jou een straffe vrouw die heel nuchter en zelfstandig in het leven staat maar ook in het labo een juiste, kritische onderzoekersmentaliteit hanteert. Ik wens je heel veel succes toe met je doctoraatsverdediging en alle andere avonturen die je nog te wachten staat!

Isabelle en Dorien, we delen nog maar een jaar een bureau maar dat is lang genoeg voor mij om te weten dat jullie 2 toffe madammen zijn, met veel zin én vuur om het PhD avontuur aan te gaan. Ook al waren jullie dit jaar getuigen van een aantal stressmomentjes bij de anciens, hopelijk hebben we jullie ook kunnen overtuigen van de mooie dingen van het onderzoek! Ik wens jullie alleszins heel veel succes!

Ook de farmacostudenten van de andere bureau (zogezegd den 'tofste' bureau maar dat spreek ik graag tegen ☺) zou ik graag willen bedanken voor de leuke sfeer en hen veel succes wensen met het verder afwerken van hun doctoraat. Ammar, het einde van je doctoraat is in zicht en de eindspurt is inmiddels ingezet. Je hebt heel mooie resultaten behaald hier op T2 dus dat zullen we ongetwijfeld vertaald zien in een mooie thesis! Succes! Bieke, ik denk dat jij een duidelijke visie hebt naar waar jouw onderzoek naartoe moet gaan. Blijf je intuïtie volgen en dit zal leiden tot mooie publicaties. Arthur, jij en ik, wij verschillen nogal veel van mekaar, maar ik respecteer jou en jouw onderzoekersmentaliteit! Je gaat nog grootste dingen verwezenlijken, daar ben ik zeker van! Hadis, ik heb je leren kennen als een behulpzaam en zachtaardig persoon én uiterst gemotiveerd. "Waar een wil is, is een weg", zeg ik altijd, en dit zal je ver kunnen brengen! Dries, je zal ondertussen wel de perfecte balans gevonden hebben tussen je PhD en je gezin, met beide wens ik je heel veel geluk!

Rita, wat jij voor mij allemaal gedaan hebt, is onbeschrijfelijk maar ik zal het toch maar proberen.☺ Een dikke merci voor al die (duizenden?) coupes die jij voor mij hebt gesneden en gekleurd. Ikzelf ben de tel kwijtgeraakt maar jij wellicht niet, want volgens jouw logboek was ik 2 jaar geleden zelfs 'de winnaar'. Zonder jou had ik alleszins maar een heel dunne thesis én niet zo'n mooie cover gehad! Wat ik ook zo fijn vind aan jou, is dat jij altijd bereid was om een nieuwe kleuring of antilichaam uit te testen. Weliswaar uit te voeren op jouw manier (!) ☺, maar je ging wel met veel plezier de uitdaging aan. Lieve

Rita, bedankt voor al jouw werk én voor de leuke babbels tussen het snijden/kleuren door!

Min, bedankt voor jouw hulp bij de genotyperingen, cholesterolbepalingen en qPCR. Ik apprecieer enorm jouw manier van werken: precies, accuraat en alles ordelijk gedocumenteerd. Dankjewel voor de hele fijne samenwerking!

Anne-Elise, ook jij bedankt voor de vele genotyperingen die je voor mij hebt uitgevoerd; dat heeft me veel werk én tijd bespaard. Dankjewel voor de lieve woorden en gesprekken. Het was heel fijn samenwerken met jou!

Cor en Paul, met jullie gewiekste vragen op de werkvergaderingen, probleemoplossende geest en altijd paraat om te helpen en kennis te delen, zijn jullie een uiterst kostbare waarde op T2. Bedankt voor alle hulp én raad!

Maya, met jouw aan boord, waait er een nieuwe, frisse wind bij T2. Ik wens je heel veel succes! Katrien, bedankt voor de wetenschappelijke babbels en ik wens je nog veel geluk in je verdere loopbaan én met je gezin!

Inn, bedankt om steeds de bestellingen in goede banen te leiden voor ons. Je maakte er nooit een probleem van als ik wéér iets last-minute aan de bestellinglijst wou toevoegen. Ook bedankt voor de kaartjes met mijn verjaardag en met kerst, dat was altijd een leuke verrassing! Ik hoop ten zeerste dat je nu iemand anders vindt die ‘stopjes’ voor jou wilt verzamelen! ☺

Ook de collega’s van de fysio wil ik graag bedanken voor de leuke momenten die we samen hebben beleefd. Leni, samen zijn wij gestart op T2 en werden de eerste banden gesmeed met het voorlezen van onze nieuwjaarsbrief. Maar ondertussen ben jij al een paar stapjes verder in je leven: je hebt een nieuwe job die je vlotjes lijkt te combineren met het moederschap over Ellie en Pauline. Ik wens je op alle gebied heel veel geluk! Zarha, voor jou komt de eindfase ook stilletjes aan in zicht. Je hebt prachtige resultaten behaald hier op T2 en ik zie je harde werk dan ook bekroond worden door een mooie publicatie én indrukwekkende thesis. Daarenboven wens ik je heel veel succes met je postdoc avontuur in het grote Amerika! Lindsey, jouw PhD avontuur staat nog maar in de startblokken, maar je bent vlot, leergierig en gemotiveerd dus dat kan niet anders dan goedkomen! Succes! Katrien, ik heb heel graag met jouw het celcultuur labo gedeeld. Alles netjes en ordelijk houden, daar kwamen we goed in overeen! Sinds kort heb je T2

verlaten en ik hoop dan ook ten zeerste dat je hetgene vindt waar naar je opzoek bent! Annie, als 'de mama van T2' stond je altijd klaar om iedereen te helpen. Bedankt en geniet van je pensioen! Maria, bij jou in het lab is alles begonnen! Samen aan de Langendorf opstelling prutsen heeft een band gesmeed tussen ons. Goh, wat hebben we toen veel gelachen (én hard gewerkt natuurlijk ☺)! Tijdens mijn masterproef heb ik de smaak van het onderzoek echt te pakken gekregen! Lieve Maria, ik wens je een deugddoend pensioen! Marc, als onze MacGyver van dienst, stond je altijd klaar om te helpen om de door ons afgeschreven technische apparatuur opnieuw leven in te blazen. Bedankt voor je hulp! Gilles, uw kritische en meer 'klinisch gerichte' vragen op de werkvergaderingen waardeer ik enorm. Ook tijdens de IWT oefensessies bleken uw vragen niet van de poes maar die verplichtte me wel om alles in een breder kader te plaatsen. Bedankt! Vincent, ik heb helaas niet de kans gehad om nauw met u samen te werken, jammer, want ik hoor alleen maar lovende woorden over u. Ik wens u alleszins veel succes toe met uw carrière én gezin! Chris, bedankt voor al je hulp met de bestellingen en de post. Ik vind het fantastisch hoe je elke dag je best doet om er piekfijn uit te zien (zelfs na een fietstocht door weer en wind!) en altijd álles assorti! Lieve Chris, toen ik je vertelde dat ik naar Cambridge verhuis voor 3 jaar, was je ontroerd en dat ontroerde mij. Bedankt voor je lieve woorden! Ik wens je een deugddoend en welverdiend pensioen! Sonja, bedankt om ons verdiep altijd zo proper te houden! Ik zie het altijd meteen wanneer jij op vakantie bent! ☺ Op vlak van netheid konden we het dan ook zeer goed met elkaar vinden en hebben we veel plezante babbels gehad! Lieve Sonja, je hebt een hart van goud en ik wens jou en jouw familie heel veel geluk toe!

Vervolgens wens ik graag de gastro collega's te bedanken. Onze bureaus vlak naast elkaar waren een ideale uitvalsbasis om snel even bij te babbelen, frustraties te delen en bij te benen met de laatste roddels. Het laatste in acht nemend, begin ik dan best bij Sara! ☺ Wat ben jij een topwijf! Is er iets wat jij niet kan?! Je hebt ontzettend hard gewerkt op het labo, mooie resultaten geboekt en tegen dat je dit leest, ook hoogstwaarschijnlijk een bangelijke verdediging afgelegd. Ik wens je heel veel succes toe in je verdere loopbaan maar ook daarbuiten! Wilco, bij jou kon ik steeds terecht met wetenschappelijke beslommeringen, medische vragen en voor het ventileren van frustraties. Ik hoop dat ik voor jou evenveel een luisterend oor heb kunnen bieden dan jij voor mij. Ik wens je veel succes in je verdere carrière, waar die zich ook zou mogen afspelen. Ik zou zeggen: just follow your gut feeling.☺ Hanne, jij was mijn eerste masterstudent die ik mocht

begeleiden. En wat was ik fier toen ik hoorde dat jij een doctoraat ging beginnen, hier bij ons op T2. 't Was wel bij de gastro en niet bij de farmaco maar bon, daar kon ik wel mee leven.☺ Je bent iemand die hard en snel werkt, kritisch denkt en goede ideeën aanbrengt, een ideale combinatie aan kwaliteiten lijkt me om je doctoraat tot een mooi einde te brengen! Veel succes! Hannah, je bent gedreven, vlot in omgang en je weet wat je wilt. Jouw doctoraat kende een vlotte start en zal ongetwijfeld ook fantastisch eindigen! Succes! Joris, ik heb je leren kennen als een zeer warm, zachtaardig persoon die altijd klaar staat om anderen te helpen. Wij hebben helaas nooit de mogelijkheid gehad om samen te werken, maar ik weet dat het gastro team jouw kennis en expertise enorm waardeert. Bénédicte, waar zal ik beginnen? Waar jij de energie vandaan haalt om een heel labo in goede banen te leiden en dan nog een heel huishouden met 4 kinderen (i.e. 4 jongens), daar heb ik het raden naar. Ik bewonder jouw doorzettingsvermogen, jouw inzet voor het lab én onderwijs en jouw veerkracht na een tegenslag. Ik wens jou nog heel veel geluk toe in werk en privé!

Er zijn ook nog heel wat ex-collega's die ik graag zou willen bedanken voor de fijne tijd hier op T2. Carole en Cé, als ex-bureaugenoten hebben we vele leuke en komische momenten gedeeld. Ik wens jullie nog veel geluk in alles! Annemie, wat een fantastisch avontuur ben jij begonnen in de down under. Ik wens je een heel succesvolle carrière toe, een mooie toekomst samen met Michaël en we houden zeker nog contact via mail! Ook al andere ex-T2'ers: Inge, Ilse, Rachid, Marthe, Wim, Nathalie, Johanna, Anne-Sophie, Maria, prof. Bult en prof. Herman zou ik graag willen bedanken en nog veel geluk toewensen. De leuke momenten die we samen beleefd hebben op kerstfeestjes, lentefeestjes, labo uitstapjes en 'dronken dinsdagen' zal ik niet snel vergeten!

Ook buiten het labo zijn er aantal mensen die een bedankje verdienen. En dat is in de eerste plaats Nicole uit Maastricht. Met jouw magische handen werd de ligatiestudie een schot in de roos en heb jij een uiterst significante bijdrage geleverd aan dit werk. Een autorit van 2x1,5uur, komen werken op zondag,.. dat was voor jou allemaal geen probleem! Bovendien draag jij het welzijn van de dieren hoog in het vaandel! Een hele, hele dikke merci voor al jouw hulp!

Ook alle andere co-auteurs zou ik graag willen bedanken voor de fijne samenwerking!

Daarnaast ook een bedankje gericht aan het labo Oncologie, Medische Biochemie en Proteïnechemie waar ik regelmatig binnenviel opzoek naar een antilichaam of om één van hun toestellen te bezetten.☺

Uiteraard zou ik ook alle medewerkers van het animalarium, met in het bijzonder Brendy, Annelies en manager Christel, willen bedanken om zo goed voor onze muisjes te zorgen.

Ook mijn 2 masterstudenten Hanne en Marthe zou ik graag willen bedanken voor hun inzet en harde werk. Ik wens jullie beide heel veel succes in jullie verdere loopbaan!

Mijn doctoraat had ik nooit op zo'n positieve manier kunnen afleggen zonder de onvoorwaardelijke steun van familie en vrienden. Eva en Jorien, bedankt voor jullie steun, jullie interesse in mijn onderzoek en jullie enthousiasme toen ik over Cambridge vertelde. Ik hoop dat onze vriendschap er eentje voor het leven is, en dat de komende toenemende afstand tussen ons alleen maar op geografische vlak zal gelden. In het bijzonder zou ik ook heel graag mijn ouders bedanken. Mama en papa, wat heb ik jullie allemaal aangedaan in de afgelopen 10 jaar? Eerst 5 jaar met een livingtafel vol met boeken en kaften (en met kringen van de tassen koffie (sorry ☺)) en een kort lontje tijdens de examenperiodes, gevolgd door nog eens 5 jaar met opnieuw een overvolle livingtafel (dit keer vol met wetenschappelijke artikels), IWT-stress en geklaag over muizen die niet doen wat ze moeten doen, lege CO_2 flessen en onredelijke reviewers. En nu kom ik af met het idee om een postdoc te beginnen in Cambridge! Lieve mama en papa, bedankt om mij altijd in alles te steunen, mij op te voeden met de juiste waarden en normen en mij een warme en liefdevolle thuis te geven. Kortom, jullie hebben mij een perfect starterspakket meegegeven en nu ben ik klaar voor de volgende stap! Dankjewel! Ik zie jullie graag!

SCIENTIFIC CURRICULUM VITAE

Mandy Odile Julie Grootaert

Date of birth	July 11, 1988
Nationality	Belgian
E-mail	mandygrootaert@pandora.be

Education

2009-2011	Master's degree in Pharmaceutical Sciences, Drug development, University of Antwerp *Magna cum laude*
2006-2009	Bachelor's degree in Pharmaceutical Sciences, University of Antwerp *Magna cum laude*
2000-2006	Sciences-Mathematics, Saint-Ludgardis School

Additional courses

2015	Language course French, University of Antwerp (Linguapolis)
2012	Giving presentations in English, University of Antwerp (Linguapolis)
2011	Laboratory Animal Science for project leaders (FELASA certificate C), University of Antwerp

Scientific career

09/2011-09/2016 ***PhD in Pharmaceutical Sciences***

Laboratory of Physiopharmacology, University of Antwerp

PhD thesis: Inhibition of apoptosis, autophagy and necrosis in atherosclerosis: potential strategies for plaque stabilisation?

Supervisors: Prof. dr. Wim Martinet and Prof. dr. Dorien Schrijvers

Scientific output

Publications

Peer-reviewed research papers

- Defective autophagy in vascular smooth muscle cells accelerates senescence and promotes neointima formation and atherosclerosis**. Grootaert MOJ**, Da Costa Martins P, Bitsch N, Pintelon I, De Meyer GRY, Martinet W, Schrijvers DM. *Autophagy*, 2015 Nov 2;11(11):2014-2032.

- Inhibitor screening and enzymatic activity determination for autophagy target Atg4B using a gel electrophoresis based assay. Cleenewerck M, **Grootaert MOJ**, Gladysz R, Adriaenssens Y, Roelandt R, Joossens J, Lambeir AM, De Meyer GRY, Declercq W, Augustyns K, Martinet W, Van der Veken P. *European Journal of Medicinal Chemistry*, 2016 Jul 31; 123: 631-638.

- NecroX-7 reduces necrotic core formation in atherosclerotic plaques of ApoE knockout mice. **Grootaert MOJ**, Schrijvers DM, Van Spaendonk H, Breynaert A, Hermans N, Van Hoof VO, Nozomi T, Vandenabeele P, Kim SH, De Meyer GRY, Martinet W. *Atherosclerosis***,** 2016 DOI: 10.1016/j.atherosclerosis.2016.06.045

- Caspase-3 deletion promotes necrosis in atherosclerotic plaques of ApoE knockout mice. **Grootaert MOJ**, Schrijvers DM, Hermans M, De Meyer GRY, Martinet W. *Oxidative Medicine and Cellular Longevity*, 2016 *(in revision)*

- Prolonged disturbance of the dendritic cell pool using the Zbtb46-DTR mouse model does not stabilize advanced atherosclerotic lesions. Rombouts M, Cools N, **Grootaert MOJ**, de Bakker F, Van Brussel I, Wouters A, De Meyer GRY, De Winter BY, Schrijvers DM. *Atherosclerosis*, 2016 *(submitted)*

Review articles

- Autophagy in vascular disease. De Meyer GRY, **Grootaert MOJ**, Michiels CF, Kurdi A, Schrijvers DM, Martinet W. *Circulation Research*, 2015 Jan 30;116(3):468-79.

- Defective autophagy in atherosclerosis: to die or to senesce? **Grootaert MOJ**, Schrijvers DM, De Meyer GRY, Martinet W. *(in preparation)*

Book chapter

- **Grootaert MOJ**, Kurdi A, De Munck DG, Martinet W, De Meyer GRY. Autophagy in Atherosclerosis. In: Hayat MA, ed., Autophagy: cancer, other pathologies, inflammation, immunity, infection, and aging, Volume 10. Oxford: Elsevier, 2016: 249-264.

Abstracts for oral presentations

- The role of autophagy in the regulation of vascular smooth muscle cell survival and phenotype. **Grootaert MOJ**, Pintelon I, Biessen E, Bochaton-Piallat ML, Bult H, De Meyer GRY, Martinet W, Schrijvers DM. Belgian Society of Pharmacology and Physiology, Brussels, Belgium, October 18, 2013.

- Defective autophagy in vascular smooth muscle cells promotes neointima formation via induction of senescence. **Grootaert MOJ**, Bitsch N, Da Costa Martins P, Biessen E, De Meyer GRY, Martinet W, Schrijvers DM. PhysPhar 2014, 2nd Benelux congress on physiology and pharmacology, Maastricht, The Netherlands, April 4-5, 2014.

- Defective autophagy in vascular smooth muscle cells promotes neointima formation via induction of senescence. **Grootaert MOJ**, Bitsch N, Da Costa Martins P, Biessen E, De Meyer GRY, Martinet W, Schrijvers DM. Coeur Symposium: Current Cardiac and Vascular Aging Research at Erasmus MC, Rotterdam, The Netherlands, June 20, 2014.

- Crosstalk between autophagy and vascular smooth muscle cell senescence: impact on neointima formation and atherogenesis. **Grootaert MOJ**, Da Costa Martins P, Bitsch N, Pintelon I, De Meyer GRY, Martinet W, Schrijvers DM. 83rd European Atherosclerosis Society (EAS) Congress, Glasgow, UK, March 22-25, 2015.

- NecroX-7 reduces necrosis in atherosclerotic plaques of ApoE knockout mice. **Grootaert MOJ**, Kim SH, Van Spaendonk H, De Meyer GRY, Schrijvers DM, Martinet W. Belgian Society of Physiology and Pharmacology, Brussels, Belgium, November 6, 2015.

Abstracts for poster presentations

- Balancing life and death: the role of autophagy in atherosclerosis. Schrijvers DM, **Grootaert M**, Bult H, De Meyer GRY, Martinet W. International Vascular Biology Meeting (IVBM), Wiesbaden, Germany, June 2-5, 2012.

- Balancing life and death: the role of autophagy in atherosclerosis. Schrijvers DM, **Grootaert M**, Bult H, De Meyer GRY, Martinet W. Abcam Meeting, Munich, Germany, September 20, 2012.

- Defective autophagy in vascular smooth muscle cells induces cellular senescence and promotes neointima formation. **Grootaert MOJ**, Bitsch N, Da Costa Martins P, Biessen E, Pintelon I, De Meyer GRY, Martinet W, Schrijvers DM. Keystone Symposia, Autophagy: Fundamentals to Disease, Texas, USA, May 23-28, 2014.

- NecroX-7 attenuates atherosclerosis and plaque necrosis in ApoE knockout mice. **Grootaert MOJ**, Kim SH, Van Spaendonk H, De Meyer GRY, Schrijvers DM, Martinet W. British Atherosclerosis Society (BAS), Autumn meeting, Cambridge, UK, September 9-11, 2015.

- Depletion of conventional dendritic cells in atherosclerosis using the zbtb46-DTR mouse model. Rombouts M, De Bakker F, Van Brussel I, **Grootaert MOJ**, Wouters A, Staelens S, De Meyer G, De Winter BY, Cools N, Schrijvers DM. 22nd Annual Scandinavian Atherosclerosis Conference, Humlebaek, Denmark, April 13-16, 2016.

Grants and Awards

- Best Oral Presentation Award for the abstract “Defective autophagy in vascular smooth muscle cells promotes neointima formation via induction of senescence” at PhysPhar 2014, 2nd Benelux congress on physiology and pharmacology, Maastricht, The Netherlands, April 4-5, 2014.

- IWT (Agency for Innovation by Science and Technology in Flanders) doctoral grant for strategic basic research

LIST OF ABBREVIATIONS

7-KC	7-ketocholesterol
8-oxodG	8-oxo-2'-deoxyguanosine
AC	Apoptotic cells
ACOX1	Acyl-coA oxidase 1
ATG5	Autophagy-related 5
ATG7	Autophagy-related 7
ATG12	Autophagy-related 12
ATP	Adenosine 5'-triphosphate
ApoE	Apolipoprotein E
ARE	Antioxidant response element
BMDM	Bone marrow-derived macrophages
BrdU	5-bromo-2'-deoxyuridine
Casp3	Caspase-3
CD36	Cluster of differentiation 36
CHX	Cycloheximide
COL1A1/2	Collagen type I alpha 1/2
COL3A1	Colagen type III alpha 1
CPTa1	Carnitine palmitoyl transferase
CVD	Cardiovascular disease
DAMPs	Damage-associated molecular patterns
DCFDA	Dichlorofluorescin diacetate
DGAT	Diacylglycerol O-acyltransferase
EBSS	Earle's balanced salt solution
EC	Endothelial cells
ECM	Extracellular matrix
EDD	End-diastolic diameter
eNOS	Endothelial nitric oxide synthase
ER	Endoplasmic reticulum
ESD	End-systolic diameter
FASN	Fatty acid synthase
FS	Fractional shortening

GAPDH	Glyceraldehyde 3-phosphate dehydrogenase
GSTα	Glutathione S-transferase alpha
H&E	haematoxylin-eosin
HMGB1	high mobility group box 1
HPRT	Hypoxanthine-guanine phosphoribosyltransferase
IFNɣ	Interferon gamma
IL	Interleukin
i.p.	Intraperitoneal
iNOS	Inducible nitric oxide synthase
KEAP1	Kelch-like ECH-associated protein 1
LC3	Microtubule-associated protein 1 light chain 3
LCCA	Left common carotid artery
LCCM	L-cell conditioned medium
LDL(R)	Low-density lipoprotein (receptor)
LPS	Lipopolysaccharide
Mac-3	Macrophage 3
Moma-2	Monocyt/macrophage 2
M-CSF	Monocyte colony stimulating factor
MDA	Malondialdehyde
MMP	Matrix metalloproteinases
Mφ	Macrophages
M(O)MP	Mitochondrial (outer) membrane permeabilisation
mPTP	Mitochondrial permeability transition pore
mtROS	Mitochondrial reactive oxygen species
mTOR	Mammalian target of rapamycin
NAPDH	Nicotinamide adenine dinucleotide phosphate
Nec-1	Necrostatin-1
NF-κB	Nuclear factor kappa light-chain-enhancer of activated B cells
NLRP3	NLR family pyrin domain containing 3
NO	Nitric oxide
NQO1	NAD(P)H:quinone oxidoreductase 1
NRF2	Nuclear factor erythroid 2-related factor
NX-7	NecroX-7
OCT	Optimal Cutting Temperature

ORO	Oil Red O
oxLDL	Oxidised low-density lipoprotein
PARP1	Poly(ADP)ribose polymerase 1
PDGF	Platelet-derived growth factor
PI	Propidium iodide
PM	Puromycin
PNPLA2	Patatin like phospholipase domain containing 2
PPIA	Peptidylprolyl isomerase A
PS	Phosphatidylserine
RAGE	Receptor for advanced glycation end products
RB	Retinoblastoma protein
RIPK	Receptor interacting protein kinase
ROS	Reactive oxygen species
SA-β-gal	Senescence-associated β-galactosidase
SASP	Senescence-associated secretory phenotype
SDF1	Stromal cell-derived factor 1
SIPS	Stress-induced premature senescence
SIRT1	Sirtuin 1 deacetylase
SQSTM1	Sequestosome 1
STEMI	ST-segment elevated myocardial infarction
tBHP	*tert*-butyl hydroperoxide
TEM	Transmission electron microscopy
TGFβ	Transforming growth factor beta
TLR	Toll-like receptor
TNFα	Tumour necrosis factor alpha
TUNEL	Terminal deoxynucleotidyl transferase dUTP nick end labelling
UPR	Unfolded protein response
Veh	Vehicle
VSMC	Vascular smooth muscle cell
WD	Western-type diet
XBP1	X-box binding protein 1
zVAD-fmk	Carbobenzoxy-valyl-alanyl-aspartyl-[O-methyl]-fluoromethylketone

LIST OF CELL DEATH MODULATING DRUGS

USED IN THIS STUDY

Name	Mode of Action	Chemical Structure
Cycloheximide (CHX)	Protein synthesis inhibitor Apoptosis inducer	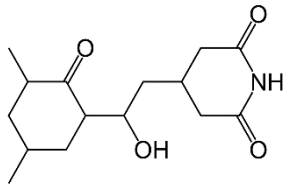
Lipopolysaccharide (LPS)	TLR4 agonist NF-κB activator Macrophage polarisation into pro-inflammatory (M1) phenotype Apoptosis inducer (via caspase-8) Induces necroptosis when combined with zVAD-fmk (vide infra)	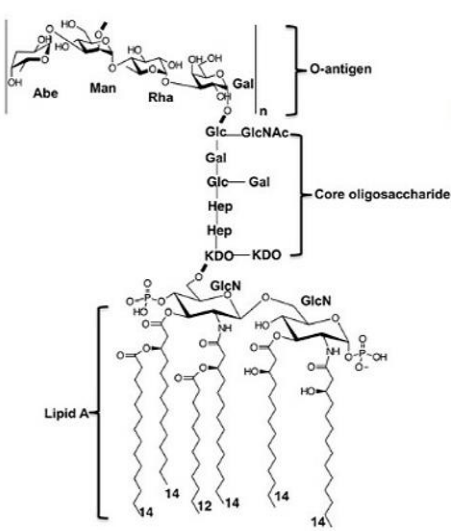
Necrostatin-1 (Nec-1)	RIPK1 inhibitor Necroptosis inhibitor	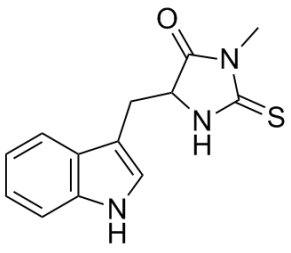

NecroX-7 (NX-7)	NADPH oxidase inhibitor ROS/RNS scavenger Necrosis inhibitor	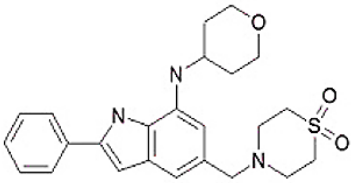
Puromycin (PM)	Protein synthesis inhibitor Apoptosis inducer	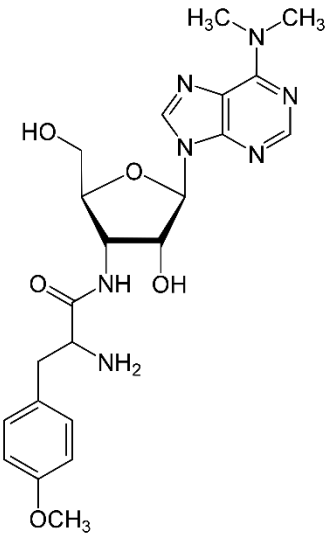
Carbobenzoxy-valyl-alanyl-aspartyl-[O-methyl]-fluoromethylketone (zVAD-fmk)	Pan-caspase inhibitor	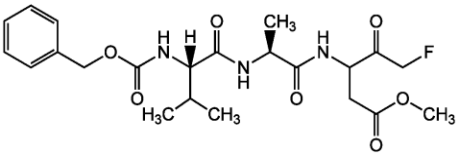

CHAPTER 1

Introduction

1.1 Atherosclerosis

Atherosclerosis is a chronic, progressive, inflammatory disease characterised by the formation of atherosclerotic plaques in the vessel wall of medium-sized and large arteries.[1, 2] These lesions start to develop quite early in life, approximately around the age of twenty, but then evolve slowly and silently over multiple decades, until suddenly, life-threatening clinical symptoms manifest.[3] Most common manifestations are coronary artery disease and ischemic stroke as a result of luminal narrowing (i.e. stenosis) or arterial occlusion by thrombi that obstruct the blood flow to the heart or brain.[4, 5] Atherosclerotic plaques preferentially develop at branching points or curved regions along the artery where blood flow is low and/or disrupted and the barrier function of the endothelial cell (EC) layer covering the vessel wall, is compromised.[6]

Epidemiological studies have identified a large number of risk factors for atherosclerosis including hyperlipidaemia, hypertension, diabetes, obesity and smoking.[7] Some risk factors are genetically determined while others are environmental and thus modifiable by means of life style changes and drug therapy. Nevertheless, despite the remarkable advances in surgical and pharmacological interventions, atherosclerosis remains a leading cause of death and morbidity in the western world (approximately 370 000 deaths/year in the USA).[8] With the rapid ageing population and the improved survival after a myocardial infarction, the prevalence of coronary heart disease is expected to increase in the upcoming years.[9, 10]

1.1.1 The pathogenesis of atherosclerosis

Lesion initiation

The primary event in the initiation of atherosclerosis, is the accumulation of low density lipoproteins (LDL) in the subendothelial matrix as a result of endothelial dysfunction **(Fig. 1.1a)**.[11, 12] Due to the increased permeability of the EC layer, LDL particles passively diffuse into the subendothelial space where they are retained by binding to matrix proteoglycans.[13] Once in the intima, native LDL is biochemically modified into minimally oxidised LDL (oxLDL)[14] and stimulates the expression of adhesion molecules such as vascular adhesion molecule 1 (VCAM-1) and intracellular adhesion molecule 1 (ICAM-1) on the EC surface.[1, 15] In this way, monocytes are recruited from the blood into the intima

where they differentiate into macrophages upon exposure to monocyte colony stimulating factor (M-CSF).[1, 15]

Fatty streak

The intimal macrophages convert into so-called foam cells by the uptake of oxLDL via their scavenger receptors (e.g. SR-A and CD36).[16] The accumulation of foam cells in the intima leads to the formation of a fatty streak (**Fig. 1.1b)**.[1] However, macrophages may express different polarisation phenotypes and exert different effects in the plaque.[17, 18] Most plaque macrophages exhibit a pro-inflammatory M1-like phenotype, possibly through LDL scavenging, and produce reactive oxygen species (ROS) and pro-inflammatory cytokines that amplify local inflammation. Other macrophages may have an M2-like phenotype and secrete factors to limit inflammation. Besides macrophages, other immune cells of both the innate (dendritic cells, neutrophils, mast cells) and adaptive (T cells, B cells) immune system are recruited to the plaque and contribute to the inflammatory responses associated with this disease.[19, 20] After antigen-specific activation, T helper 1 (Th1) cells secrete the pro-inflammatory cytokine IFNγ which can augment plaque inflammation while regulatory T cells exert anti-inflammatory actions.[20]

Fibrous stable plaque

Macrophage and T-cell-derived growth factors and cytokines promote the migration and proliferation of vascular smooth muscle cells (VSMCs) from the media into the intima.[21] During this migration step, VSMCs switch from a contractile to a synthetic phenotype[22] and start synthesising extracellular matrix (ECM) such as collagen, proteoglycans and elastin. The intimal VSMCs together with the ECM form a fibrous cap that covers the plaque **(Fig. 1.1c)**. The thickness of the fibrous cap is critical for the stability of the plaque.[3] Nevertheless, alternative origins of plaque VSMCs have been suggested, including circulating bone marrow-derived progenitor cells[23-25] or multipotent stem cells in the media[26] or adventitia,[27] though, no compelling evidence has been obtained so far for a significant contribution of these alternative sources to the vast majority of plaque VSMCs. Furthermore, plaque growth results in hypoxia which triggers the formation of intra-plaque microvessels.[28] These neovessels promote further plaque growth and inflammation via the influx of leukocytes and cholesterol, and may cause intra-plaque haemorrhages.[29, 30]

Unstable, rupture-prone plaques

As the plaque progresses, inflammatory cells tend to accumulate, particularly in the shoulder regions of the plaque, and produce pro-inflammatory cytokines that promote VSMC death.[2] Moreover, macrophages secrete proteolytic enzymes such as matrix metalloproteinases (MMPs) that degrade the extracellular matrix.[31] Also mast cells have the potential to degrade ECM components.[32] Loss of VSMCs and collagen leads to thinning of the fibrous cap and contributes to plaque destabilisation.[3] Apoptotic and necrotic cell death of lipid-laden VSMCs and macrophages promote the accumulation of cellular debris and lipids in the centre of the plaque, forming a lipid-rich necrotic core.[33] Hence, unstable atherosclerotic plaques are characterised by an increased inflammatory cell count, a thin fibrous cap and a large lipid-rich necrotic core.[3, 12] Rupture of the plaque preferentially occurs at sites where the fibrous cap is very weak and most infiltrated by macrophage foam cells **(Fig. 1.1d)**.[3, 5] The weakest spot in the plaque is thus often located at the shoulder regions or at the margins of the cap.[5] The underlying necrotic core is rich in tissue factor, a key initiator of the coagulation cascade released by dead macrophages. Once the fibrous cap ruptures, the pro-thrombogenic content of the necrotic core is exposed to coagulation factors and platelets in the blood, triggering thrombus formation.[34, 35]

1.1.2 Anti-atherosclerotic therapies

Current treatment strategies for atherosclerosis are predominantly based on reducing the multiple risk factors.

Lipid lowering, by diet and/or statin therapy, are essential in the primary and secondary prevention of cardiovascular disease (CVD).[36] Statins inhibit the cholesterol synthesis in the liver by inhibition of the HMG-CoA reductase enzyme and therefore reduces total cholesterol and LDL in plasma.[37] Moreover, statins exert pleiotropic effects such as improving endothelial dysfunction and plaque stability, and reducing vascular inflammation, that are considered beneficial in the struggle against atherosclerosis.[38]

Lowering of blood pressure via antihypertensive drugs such as β-blokkers, calcium channel blockers, thiazide diuretics and angiotensin converting enzyme-inhibitors, reduces the risk of cardiovascular mortality and morbidity significantly.[39]

Inhibition of platelet aggregation by low doses (80-100mg) of acetylsalicylic acid (ASA) has been proven highly successful in the (primary and) secondary prevention of CVD.[40] For patients who have undergone coronary artery stenting, double anti-platelet therapy with ASA and clopidogrel for 6-12 months is recommended.[41]

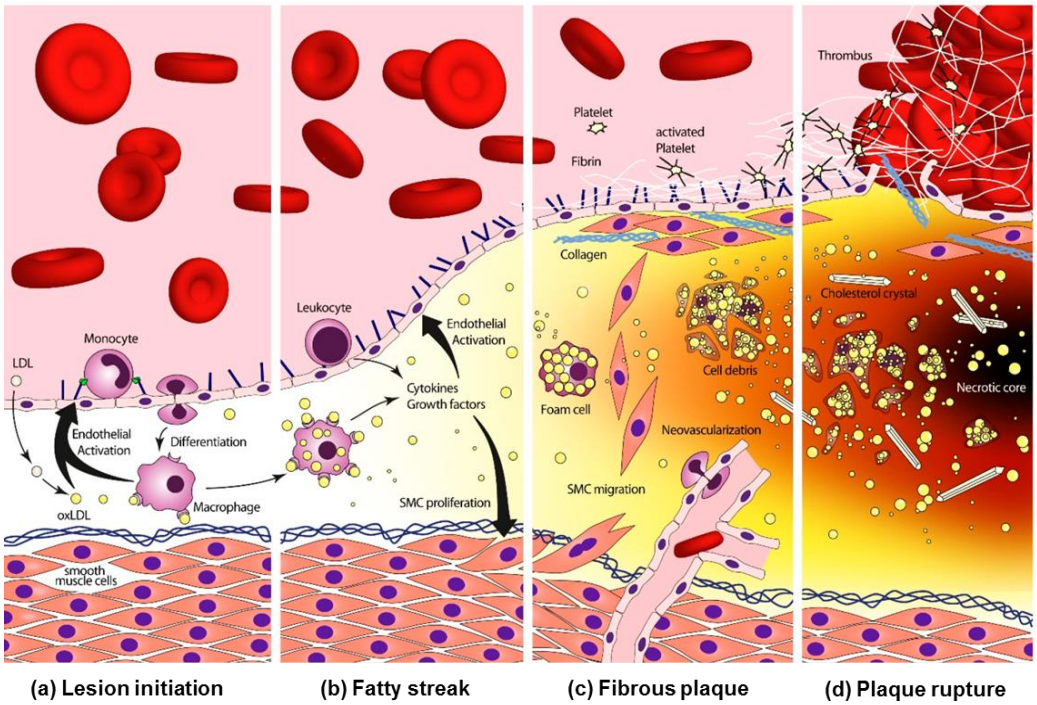

Figure 1.1: The development of the atherosclerotic plaque. (a) Plaque formation is initiated by the accumulation of LDL in the subendothelial space. LDL is modified into oxLDL which stimulates the expression of adhesion molecules on the endothelium to recruit monocytes and other leukocytes (e.g. T cells) to the intima. **(b)** After differentiation, macrophages take up oxLDL and turn into foam cells, forming a fatty streak. **(c)** Growth factors and cytokines derived from macrophages and T cells promote the migration of vascular smooth muscles cells (VSMCs) from the media into the plaque. The intimal VSMCs produce collagen and form a protective fibrous cap. In response to hypoxia, neovessels are formed and penetrate into the plaque. **(d)** The plaque becomes vulnerable due to thinning of the fibrous cap and the formation of a large lipid-rich necrotic core. When the plaque ruptures, pro-coagulant material of the necrotic core is exposed to the blood and triggers thrombus formation. Modified from [42]

1.1.3 Mouse models to study atherosclerosis

The use of murine models has been shown to be extremely valuable to study the biological processes underlying this disease and to test new approaches to target the mechanisms leading to plaque destabilisation. In the present study, we used the apolipoprotein E-deficient (*ApoE*$^{-/-}$) mouse, which is perhaps the most widely-used mouse model to study atherosclerosis.[43] ApoE associates with VLDL in the plasma and binds to the LDLR on the liver to promote lipoprotein uptake.[44] Deficiency in *ApoE* results in high levels of VLDL (and LDL) and promotes spontaneous plaque development, which can be accelerated by feeding the mice a high cholesterol western-type diet.[43] Another frequently used model is the LDL receptor knockout (*Ldlr*$^{-/-}$) mouse. These mice show only an increase in LDL and require a western-type diet to induce significant plaque development.[43]

1.2 Cell death

Cell death is a crucial event in maintaining organismal homeostasis by controlling tissue cell turnover. Cell death enables the organism to kill and eliminate unwanted cells during normal as well as pathological development. However, abnormal regulation of this process facilitates disease progression.[45]

A cell is considered dead when a so-called 'point-of-no-return' has been trespassed.[46] These 'points-of-no-return' include loss of plasma membrane integrity, mitochondrial membrane permeabilisation, cell fragmentation or engulfment by adjacent cells. According to morphological criteria, cell death can be classified into 3 major catabolic processes, namely, apoptosis, autophagy and necrosis, often referred to as type I, type II and type III cell death, respectively. Even though recent guidelines discourage the use of these Roman numerals to indicate the different types of cell death,[46] we followed this system of classification to order the different types of cell death discussed in this thesis.

Besides changes in cell morphology, the different types of cell death are characterised by distinct biochemical changes such as activation of proteases, mitochondrial membrane depolarisation and phagocytic recognition **(Table 1.1)**. It is highly recommended to combine both morphological and molecular criteria to determine the type of cell death. Of note, dying cells can show mixed features or overlapping

mechanisms or decease via other cell death pathways (e.g. anoikis[47], entosis[48] and mitotic catastrophe[49]).

Table 1.1 Morphological and biochemical features of apoptosis, autophagy and necrosis

	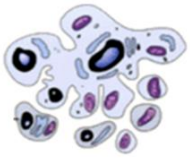 **Apoptosis**	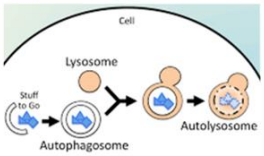 **Autophagy**	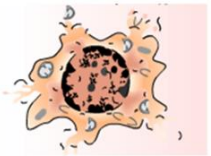 **Necrosis**
Morphological features	Cell shrinkage Membrane blebbing	Cell shrinkage Autophagic vacuoles	Cell swelling Loss of membrane integrity
	Chromatin condensation Internucleosomal DNA fragmentation	Chromatin condensation possible but not DNA fragmentation	Random DNA fragmentation
Biochemical features	Caspases	ATG proteins	Necroptosis: RIPK1/RIPK3
	Cytochrome c release Mitochondrial depolarisation PS exposure	LC3 processing Mitophagy	LDH, HMGB1 release Mitochondrial depolarisation
	Properly phagocytised	Properly phagocytised	Poorly phagocytised
	Energy required	Energy not required	Energy not required

1.2.1 Apoptosis

Apoptosis is the best-studied form of programmed cell death. The term apoptosis was firstly introduced by Kerr, Wyllie and Currie in 1972, and comes from the Greek words 'apo' + 'ptosis', meaning 'falling off'.[50] Apoptosis can be morphologically distinguished by cellular shrinkage, chromatin condensation, membrane blebbing and internucleosomal DNA fragmentation.[50] The remaining apoptotic bodies may be phagocytised (also known as efferocytosis) by adjacent cells without further inflammation. The demolition of the cell during apoptosis is governed by **c**ysteine **asp**artate specific prote**ases**, termed **caspases**. These proteases are expressed as zymogens (i.e. inactive precursors) but are activated by cleavage at specific aspartic residues in response to death stimuli.[51] Caspases are generally subdivided in initiator and effector caspases. Initiator caspases (caspase-2, -8, -9 and -10) act upstream of the apoptotic pathway and bind to adaptor

molecules that promote caspase oligomerisation and activation. In contrast, the effector caspases (caspase-3, -6 and -7) are located downstream of the pathway and are activated by cleavage via the initiator caspases to provoke the dismantling of the cell.[52] For example, cleaving of cellular substrates involved in cytoskeleton reorganisation (e.g. α-fodrin and gelsolin) alters the cellular shape while cleaving of lamins and the inhibitor of caspase-activated DNase (ICAD) causes nuclear degradation.[53] In detail, cleaving of ICAD relieves the inhibition on the endonuclease CAD, resulting in internucleosomal DNA fragmentation.[54] Moreover, during apoptosis, phosphatidylserine (PS) is translocated from the inner leaflet to the outer side of the plasma membrane to facilitate the recognition and removal of apoptotic cells by phagocytes,[55] thereby minimising inflammation. Of note, also non-apoptotic caspases have been identified, termed inflammatory caspases (caspase -1, -4, -5 -11), which play a role in the maturation of pro-inflammatory cytokines and in the promotion of innate immune responses.[56]

There are 2 major signalling pathways for the regulation of apoptosis: the extrinsic and the intrinsic pathway **(Fig. 1.2)**. The first pathway involves membrane-bound death receptors such as TNFR1, Fas, DR4 and DR5.[57] Binding of the receptors to their ligands (TNFα, FasL and TRAIL respectively) results in the recruitment of adaptor proteins (e.g. FADD) and pro-caspase-8. The subsequent oligomerisation activates caspase-8, which in turn can activate the effector caspases. The intrinsic pathway involves the release of cytochrome c from the mitochondria, mediated by the pro-apoptotic proteins (e.g. Bax and Bak) of the Bcl-2 family.[58] Bax and Bak permeabilise the outer mitochondrial membrane (MOMP), which can be prevented by the anti-apoptotic proteins Bcl-2 and Bcl-XL. Once released, cytochrome c forms a complex with Apaf-1 and pro-caspase-9 (called the 'apoptosome'), which activates caspase-9 and subsequently activates the downstream caspases.[59] Moreover, crosstalk between the two pathways has been described. Caspase-8 can cleave the Bcl-2 family member Bid into the pro-apoptotic molecule, tBid, that triggers cytochrome c release.[60] Furthermore, the mitochondrial apoptotic pathway may also be engaged by the tumour suppressor p53. p53 can activate the transcription of multiple pro-apoptotic genes encoding for members of the Bcl-2 family such as Bax, Noxa and PUMA.[61]

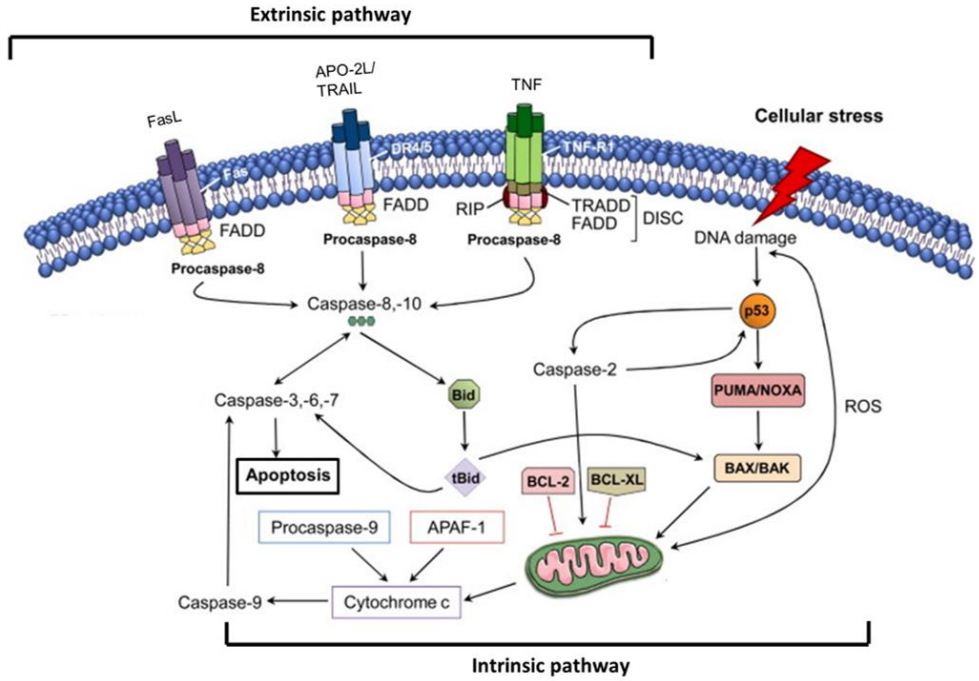

Figure 1.2: Schematic overview of the extrinsic and intrinsic pathway of apoptosis. The extrinsic pathway is activated by binding of ligands (FasL, TRAIL, TNF) to their death receptors (Fas, DR4/5, TNFR). These receptors recruit FADD and activate caspase-8 and -10 which in turn activates the effector caspases (caspase-3,-6,-7). In the intrinsic pathway, death signals reach the mitochondria where pro-apoptotic proteins of the Bcl-2 family (Bax, Bak) permeabilise the mitochondrial outer membrane to release cytochrome c. Next, cytochrome c forms a complex with Apaf-1 and pro-caspase-9, which leads to caspase-9 activation and subsequent activation of the effector caspases. Cytochrome c release is prevented by the anti-apoptotic proteins Bcl-2 and Bcl-XL. The mitochondrial pathway may also be triggered by p53 and caspase-2 upon DNA damage. Crosstalk between the intrinsic and extrinsic pathway involves caspase-8-mediated cleavage of Bid into tBid, which may promote cytochrome c release. Modified from [62]

1.2.2 Autophagy

Autophagy is a cellular catabolic process involved in the delivery of long-lived proteins and organelles to lysosomes for degradation.[63-65] The term autophagy comes from the Greek words 'auto' + 'phagy' meaning 'to eat oneself' referring to the self-digesting properties of autophagy. At least three forms of autophagy have been described: (1) macroautophagy, in which cytoplasmic material is sequestered in double-membrane vacuoles, termed autophagosomes, and delivered to the lysosome, (2) microautophagy, in which cytoplasm is directly engulfed by the lysosome, and (3) chaperon-mediated autophagy, in which cytoplasmic proteins are incorporated into the lysosome by selective binding to a specific receptor.[63-65] In this thesis, we will only focus on macroautophagy

(herein further referred to as autophagy), which is the most studied form of autophagy. Autophagy occurs at low levels in the cell to perform homeostatic functions by recycling the engulfed cargo into new building blocks (e.g. amino acids, carbohydrates, fatty acids and nucleotides). When cells are exposed to intracellular (e.g. accumulation of damaged organelles) or extracellular (e.g. nutrient deprivation, hypoxia) stressful stimuli, autophagy is upregulated and serves as a cell survival mechanism.[66] However, unrestrained excessive stimulation of autophagy results in autophagic cell death due to the degradation of major cytosolic components such as the mitochondria and the endoplasmic reticulum, leading to final cellular collapse.[67] The term 'autophagic cell death' has been heavily under debate in the past few years[68, 69] because it can be interpreted in two ways: (1) 'cell death associated with autophagy' during which autophagy is activated in dying cells as a futile attempt to prevent final cell demise or (2) 'cell death fully executed by autophagy'. According to the latest recommendations of the Nomenclature Committee on Cell Death (NCCD), the term 'autophagic cell death' can be used when describing cell death that can be suppressed by inhibition of the autophagic pathway (e.g. by chemicals or genetic interventions).[46]

The autophagic machinery is regulated by specific proteins called **ATG** (**A**u**T**opha**G**y regulated genes) proteins. Each of these proteins play a specific role in the distinct stages of the process **(Fig. 1.3)**.[70] The induction of autophagosome formation is firstly regulated by the ATG1/ULK complex, and is controlled by mammalian target of rapamycin (mTOR)-dependent and mTOR-independent pathways (vide infra). The second stage includes the formation of the isolation membrane or phagophore (= vesicle nucleation) which is mediated by proteins of the PI3K (phosphatidylinositol 3 kinase) complex (including Beclin-1 and Vps34/PI3K class III). The third step, the vesicle elongation, is controlled by two ubiquitin-like conjugation systems (ATG12 and ATG8 systems). ATG12 is activated by ATG7 and forms a complex with ATG5 and ATG16. ATG8, better known as pro-LC3, is cleaved by ATG4 into LC3-I and activated by ATG7. Then, LC3-I is conjugated to phosphoethanolamine (PE) to form LC3-II. The mature autophagosome then fuses with a lysosome to form an autolysosome where the incorporated cargo is degraded by lysosomal hydrolases.[70] During this process, also the membrane bound LC3-II is degraded together with the cargo receptor p62 that targets polyubiquitinated proteins to the autophagosome.

The autophagic process can be controlled by multiple upstream signalling pathways such as mTOR (i.e. negative regulator) and AMPK (i.e. positive regulator). In case of nutrient excess, mTOR is activated, resulting in ULK1 inhibition and suppression of autophagy whereas in conditions of nutrient deprivation, mTOR is inactivated to allow autophagy-mediated degradation of biomolecules.[71] The energy sensor AMP-activated protein kinase (AMPK) induces autophagy indirectly by inhibition of mTOR or directly through phosphorylation and activation of ULK1.[72]

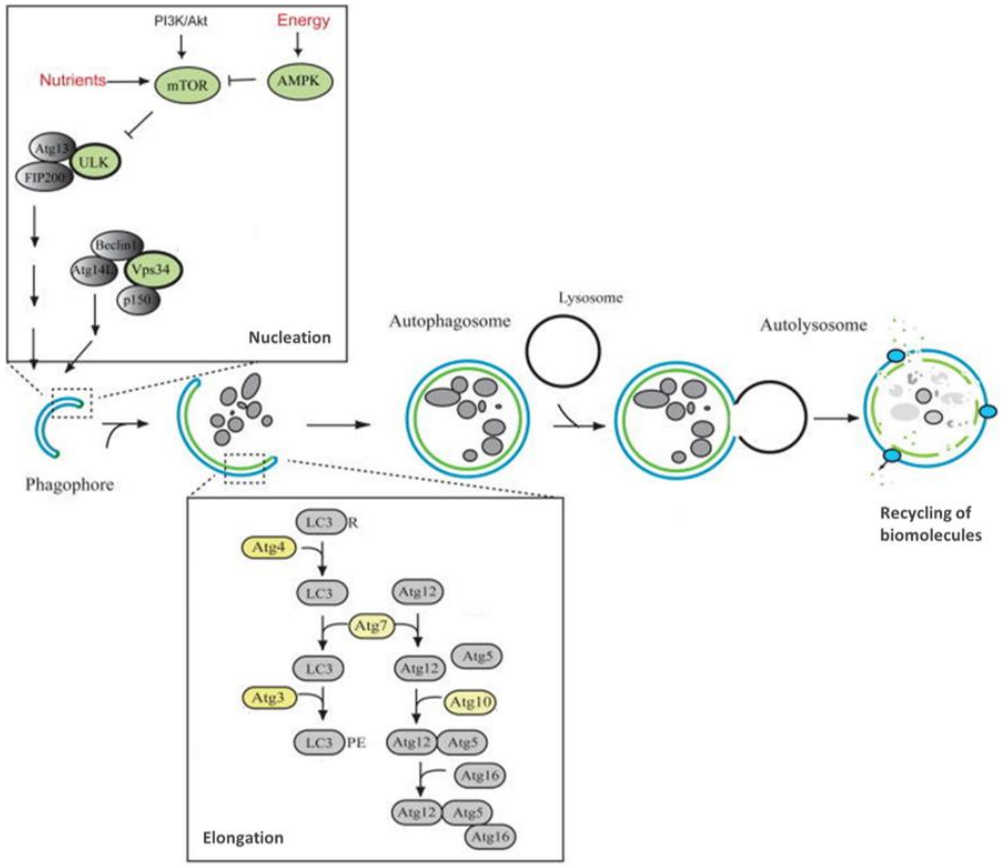

Figure 1.3: Schematic overview of the regulation of autophagy. The induction of autophagosome formation is regulated by the ULK1 complex which is under control of mTOR and AMPK pathways. During the vesicle nucleation stage, the formation of the phagophore is controlled by the PI3K complex. Two ubiquitin-like conjugation systems (ATG12 and ATG8) regulate the vesicle elongation. When the autophagosome is completed, it fuses with a lysosome to form an autolysosome. The incorporated material including the inner membrane is degraded by lysosomal hydrolases. Modified from [73]

1.2.3 Necrosis

Necrosis, meaning 'death' in Greek, is probably the oldest known type of cellular demise. Necrosis can be morphologically distinguished from the other forms of cell death by a gain in cell volume (oncosis) and swelling of organelles, followed by rupture of the plasma membrane and the release of the intracellular content.[74] Besides rapid loss of membrane integrity, bioenergetic failure (i.e. ATP depletion) is considered as a key event of necrosis.[75] The passive release of damage-associated molecular patterns (DAMPs), pro-inflammatory molecules and/or proteases from necrotic cells into the surrounding environment evokes an inflammatory response. Moreover, it has been described that necrotic cells are less efficiently cleared by phagocytes as compared to apoptotic cells.[76]

Though necrosis was originally considered as an accidental, non-programmed form of cell death (due to physio-chemical stress), accumulating evidence indicates that necrosis can be regulated via different signalling transduction pathways including death receptor activation, opening of the mitochondrial permeability transition pore (mPTP) and poly(ADP)ribose polymerase 1 (PARP1) overactivation **(Fig. 1.4)**.[77, 78] These signalling routes share common mediators (e.g. Ca^{2+} and ROS) that are involved in the different stages of the necrotic process (initiation/propagation/execution).[79] Necrotic cell death is finally executed in different ways such as the formation of pores in the plasma membrane, random DNA fragmentation and depletion of ATP.

Death receptor-mediated necrosis

Necrosis triggered by activation of the TNFR1 is the most well-known form of regulated necrosis, also termed 'necroptosis', and requires activation of the receptor-interacting proteins RIPK1 and RIPK3.[80] The ubiquitination state of RIPK1 determines whether it functions as a pro-survival scaffold molecule or as a kinase that promotes cell death.[81, 82] Polyubiquitination of RIPK1 by the cellular inhibitors of apoptosis proteins (cIAPs) promotes activation of the NF-κB survival pathway[83] whereas deubiquitination of RIPK1 (by CYLD deubiquitinase) promotes the formation of apoptotic or necrotic signalling complexes.[84] When apoptosis is blocked by caspase 8 inactivation, RIPK3 is recruited to the FADD, caspase-8 and RIPK1 containing complex, called the 'necrosome'. RIPK1 and RIPK3 interact via their RHIM-domain, become activated through (auto)phosphorylation and trigger necroptotic signalling.[85, 86] Due to the existence of RIPK3-dependent but

RIPK1-independent necrosis,[80] necroptosis should rather be defined as RIPK3-dependent regulated necrosis.[78]

RIPK3 executes necrosis via multiple ways. Firstly, RIPK3 interacts with several bioenergetic enzymes in the mitochondria such as glycogen phosphorylase (PYGL), glutamate-ammonia ligase (GLUL) and glutamate dehydrogenase 1 (GLUD1).[87] Enhanced glycogenolysis and glutaminolysis causes overproduction of ROS, which in turn triggers mitochondrial membrane permeabilisation and subsequent necrosis. However, necroptosis may also occur independently of ROS. In some cells, RIPK1 disrupts the interaction between adenine nucleotide translocase (ANT) and cyclophilin D (CYPD), two components of the mPTP (vide infra), compromising the ADP-ATP exchange between the cytosol and the mitochondria.[88, 89] More recent evidence has identified mixed lineage kinase domain-like (MLKL) as a direct effector mechanism of necroptosis. MLKL is recruited to the necrosome via interaction with RIPK3 and is activated through RIPK3-mediated phosphorylation.[90] MLKL then translocates to the plasma membrane where it binds to phosphatidylinositol phosphate and causes membrane leakage and concomitant necrosis.[91] Moreover, relocalisation of MLKL to the plasma membrane promotes influx of Ca^{2+} ions via transient receptor potential cation channels.[92]

mPTP-mediated necrosis

In response to ROS or Ca^{2+}, the mPTP localised in the mitochondrial inner membrane, is opened and may provoke necrotic cell death. Persistent mPTP opening leads to mitochondrial depolarisation, inhibition of the respiratory chain and subsequent ATP depletion.[93] Until now, only CYPD has been identified as the key regulatory component of the mPTP. Recent evidence shows that the pro-necrotic activity of CYPD may be regulated by the tumour suppressor protein p53.[94]

PARP1-mediated necrosis

In response to DNA damage, PARP1 is recruited to the DNA at the site of damage and catalyses the poly(ADP)ribosylation of nuclear proteins (e.g. histones) by converting NAD into nicotinamide and ADP-ribose.[95] In case of severe DNA damage, PARP1 becomes overactivated and promotes necrosis via different ways. Firstly, PARP1-overactivion leads to the depletion of cytosolic NAD^+ and subsequently prevents glycolysis-dependent

ATP production.[96] Secondly, PARP1 overactivation results in the release of AIF from the mitochondria and its translocation to the nucleus where it operates as an endonuclease to evoke large-scale DNA fragmentation.[97, 98] This form of PARP-1-mediated necrosis is also known as 'parthanatos'. Some studies have reported activation of RIPK1/JNK pathways downstream of PARP1. JNK affects mitochondrial membrane permeability and finally causes necrosis.[77, 99]

NAPDH-mediated necrosis

The membrane-bound nicotinamide adenine dinucleotide phosphate (NADPH) oxidase enzymes (also known as NOX enzymes) generate superoxide anions, leading to the formation of other ROS, such as H_2O_2.[100] Moreover, NOX1 has been implicated in TNFα-induced necroptosis.[101] NOX1 is recruited to the TNFR complex and activated in a RIPK1-dependent manner. NOX1 activation results in the generation of ROS, contributing to sustained JNK activation and necrosis.[101]

Ca^{2+}-mediated necrosis

During necrosis, Ca^{2+}-dependent proteases are activated in case of intracellular Ca^{2+}-overload.[102] For example, Ca^{2+}-dependent calpains cleave different substrates including cytoskeleton proteins, membrane proteins, ion transporters, etc.[103] Calpain-mediated cleaving of the Na^+/Ca^{2+} exchanger in the plasma membrane results in a sustained secondary Ca^{2+}-overload followed by necrosis.[104] Moreover, calpains can cause lysosomal membrane permeability, which leads to the release of lysosomal cathepsins B and L.[105] Degradation of intracellular molecules by cathepsins and calpains eventually leads to necrotic cell death.

Toll-like receptor-mediated necrosis

Toll-like receptors (TLRs) belong to the group of pattern recognition receptors (PRRs) and recognize both pathogen- (PAMPs) and damage-associated molecular patterns (DAMPs). Triggering of TLR4 by lipopolysaccharide (LPS) induces RIPK1/RIPK3-dependent necroptosis when caspase-8 is suppressed.[87, 106, 107] However, recognition of DAMPs, released by necrotic cells (e.g. HMGB1), does not induce necrosis but triggers an inflammatory response.[108]

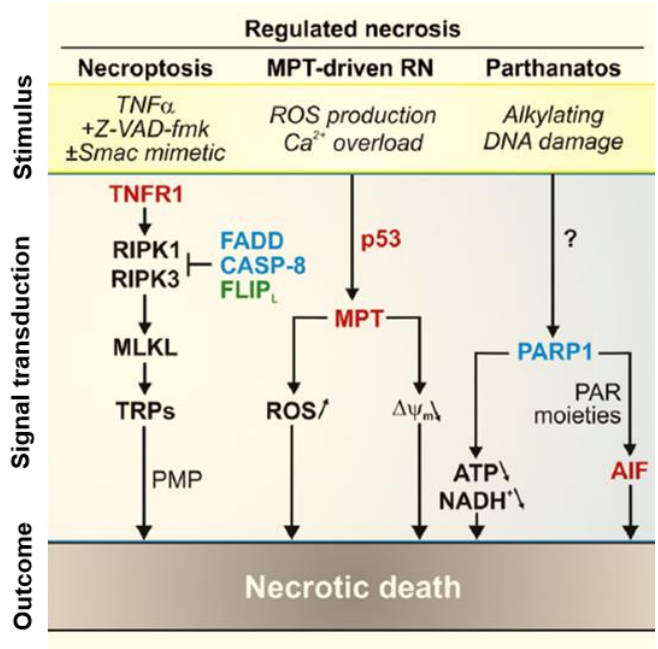

Figure 1.4: Schematic overview of the 3 main signalling transductions pathways of regulated necrosis. (Left panel) TNFα-induced necroptosis involves formation of the necrosome containing FADD, caspase-8, RIPK1 and RIPK3. The caspase-8-FLIP$_L$ heterodimer controls necrosis by cleaving RIPK1 and RIPK3. The downstream activation of MLKL triggers necrosis by increasing plasma membrane permeability (PMP) and promoting cation influx via transient receptor potential cation channels (TRPs). (Middle panel) Increased levels of ROS and/or intracellular Ca^{2+} trigger opening of the mitochondrial permeability transition (MPT) pore leading to mitochondrial depolarisation and subsequent necrosis. Activation of CYPD during MPT pore opening may involve p53. (Right panel) Severe DNA damage causes PARP1 overactivation, also called parthanatos, and leads to ATP depletion and large scale DNA fragmentation as a result of AIF release. Modified from [78]

Pyroptosis

Pyroptosis involves activation of caspase-1 upon exposure to PAMPs and DAMPs.[79] Caspase-1 forms, together with the adaptor molecule ASC, a supramolecular complex, called the 'pyroptosome' where it converts pro-IL1β and pro-IL18 into their active form.[109] Pyroptosis is therefore considered a highly pro-inflammatory form of regulated necrosis.[79] Pyroptosis is characterised by loss of membrane integrity, release of intracellular content and large-scale DNA fragmentation.[110] The loss of membrane integrity is thought to result from caspase 1-dependent formation of pores in the plasma membrane causing rapid osmotic cell lysis.[111]

Ferroptosis

Ferroptosis is a recently recognised form of regulated necrotic cell death characterised by the accumulation of lipid peroxidation products and lethal amounts of ROS derived from iron metabolism.[79, 112] Ferroptosis can be morphologically distinguished by smaller mitochondria, reduced mitochondrial cristae and rupture of the outer mitochondrial membrane.[113] Glutathion (GSH) peroxidase 4 (GPX4) is a crucial inhibitor of ferroptosis by the suppression of lipoxygenase enzymes (LOX), and its activation relies on GSH levels. Thus, GSH depletion leads to loss-of-function of GPX4, resulting in lipid peroxidation.[114]

1.3 Cell death in atherosclerosis

The very first observation of cell death in atherosclerosis was made by the vascular pathologist Virchow in 1858. He stated that atherosclerotic plaques are formed by a dynamic interplay between cell replication and cell death.[115] At that time, plaque cell death was generally, though often incorrectly, described as non-programmed necrosis. Most evidence for apoptosis in atherosclerosis was gathered in the early 1990's while the first indications for autophagy in atherosclerotic plaques were not reported until the beginning of this century. All three major forms of cell death (apoptosis, autophagy, necrosis) have now been identified in the different plaque cell types and are involved in the development of the disease **(Fig. 1.5)**. The consequences of cell death in atherosclerosis, however, depends on the specific cell type that is involved, the developmental stage of the plaque, and of course, the type of cell death itself.

1.3.1 Apoptosis in atherosclerosis

Several studies have shown evidence for apoptotic cell death in both human and animal atherosclerotic plaques.[116-123] The level of apoptosis is low in early plaques but increases as lesions become more and more advanced.[124] Overall, the apoptotic index of advanced plaques averages at 1-2%.[116, 120] Apoptotic cells mostly accumulate in the fibrous cap, at sites of rupture, close to lipid deposits and necrotic cores, and in the presence of inflammatory cells.[117, 119, 121, 125]

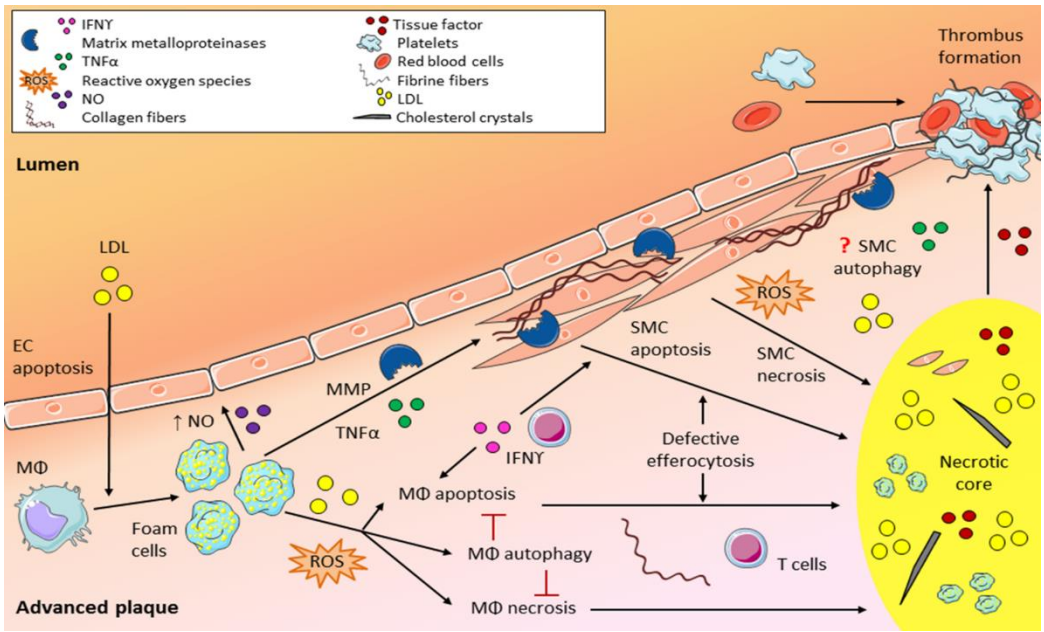

Figure 1.5: Cell death in atherosclerosis. Macrophage (MΦ) foam cells produce high levels of NO and pro-inflammatory cytokines (e.g. TNFα) which induce apoptosis of endothelial cells (EC) and smooth muscle cells (SMC). MΦ-derived matrix metalloproteinases (MMP) degrade the collagen fibres in the fibrous cap. Infiltrated Th1 cells produce IFNγ and induce MΦ and SMC apoptosis. The level of ROS and oxLDL in the plaque may determine whether a cell dies by apoptosis or necrosis. Necrotic MΦ and SMC accumulate in the necrotic core (NC) and release their lipid-rich content. Tissue factor present in the NC triggers thrombus formation after plaque rupture. Defective efferocytosis of apoptotic MΦ and SMC contributes to the enlargement of the NC. Autophagy, triggered by low levels of ROS and oxLDL, plays a protective role in macrophages by inhibiting apoptosis and necrosis. The role of autophagy in SMC is still unknown.

1.3.1.1 Quantification of apoptosis

The most standard technique for quantification of apoptosis in atherosclerotic tissue is terminal deoxynucleotidyl transferase dUTP nick end labelling (TUNEL) that marks the execution phase of apoptosis by the detection of DNA fragments. However, as with each technique, TUNEL does not come without pitfalls. For example, non-apoptotic cells that show signs of active RNA splicing may stain false positive for TUNEL.[126] Indeed, RNA transcription is in fact abolished during apoptosis due to caspase-3 mediated cleaving of the splicing factor U1 snRNP.[127] Moreover, the TUNEL assay may give rise to artefacts in case of improper tissue sectioning or in regions of the plaque where necrotic debris accumulates.[128-130] Therefore, TUNEL should always be combined with other apoptotic markers, for example cleaved caspase-3. Furthermore, one should take into account that

these markers only measure the frequency of apoptosis but provide neither information on the rate of apoptosis nor on the efficacy of apoptotic body clearance.[130]

1.3.1.2 Potential apoptosis inducers

In endothelial cells

Endothelial cell damage is a critical event in the initiation of atherosclerosis. Lesion-prone aortic regions are characterised by an increased turnover of EC, most likely due to increased apoptosis,[131] resulting from low blood flow and/or low shear stress.[132] Well-known risk factors for atherosclerosis such as high glucose and increased advanced glycation end products (AGE) levels,[133, 134] increased oxLDL,[135, 136] oxidative stress and angiotensin II levels[137, 138] stimulate EC apoptosis. Moreover, pro-inflammatory mediators (e.g. TNFα) may initiate pro-apoptotic pathways in EC.[139, 140] Exposure of EC to high levels of nitric oxide (NO), produced by iNOS-expressing macrophages, increases apoptosis by promoting cytochrome c release, activating p53 and altering the expression of Bcl-2 family proteins.[141] In an highly oxidative environment, NO can react with superoxide to form peroxynitrite, which can cause DNA damage and subsequent apoptosis.[142] In normal and physiological conditions, however, low levels of NO produced by endothelial NOS in response to shear stress, prevent EC apoptosis by activation of cGMP-dependent protein kinases[143] or by direct inactivation of caspases through *S*-nitrosylation.[144] Besides shear stress, cell-to-cell and cell-to-matrix contacts are necessary for EC survival.[145]

In vascular smooth muscle cells

Diverse factors have been identified to induce VSMC apoptosis including pro-inflammatory cytokines, oxLDL, high levels of NO and mechanical injury.[146] Pro-inflammatory cytokines secreted by plaque macrophages (e.g. TNFα) and T cells (e.g. IFNγ), sensitize VSMCs to Fas-mediated apoptosis by promoting Fas trafficking to the cell surface.[147, 148] Fas-mediated apoptosis is also involved in oxLDL-induced apoptosis in VSMCs.[149] Nevertheless, VSMC apoptosis can be counterbalanced by so-called survival factors, usually growth factors such as PDGF, IGF-1 and FGF.[150] With regard to apoptosis regulating genes, plaque VSMCs are very sensitive to p53-mediated apoptosis.[151] High levels of p53 induce apoptosis in human plaque VSMCs in low serum conditions but not in normal medial VSMCs. In fact, p53 activation sensitizes human

VSMCs to Fas-mediated apoptosis by transiently increasing surface Fas expression by transport from the Golgi apparatus.[152] Moreover, sensitivity to p53-mediated apoptosis increases when VSMCs are driven to proliferate.[151] Paradoxically, high levels of apoptosis together with low levels of proliferation have been observed in VSMCs in human plaques.[150] This may be explained by the predominance of the hypophosphorylated form of the tumour suppressor retinoblastoma protein (RB) in plaque VSMCs that promotes cellular senescence, a state of irreversible growth arrest.[153]

In macrophages

Multiple atherosclerosis-related stimuli such as high levels of oxLDL, TNFα and ROS have shown to induce macrophage apoptosis.[154, 155] The ability of oxLDL to induce apoptosis is thought to be mediated by 7-ketocholesterol (7-KC),[156] one of its primary oxysterols, and involves activation of the mitochondrial pathway.[157] Paradoxically, low levels of LDL may promote macrophage survival and proliferation[158, 159] suggesting that the response of macrophages to oxLDL depends on the dose, the exposure time and the degree of oxidation of oxLDL.[154] Another key inducer of macrophage apoptosis in advanced atherosclerosis is the accumulation of free (i.e. unesterified) cholesterol (FC) in the endoplasmic reticulum (ER) of the cell.[160, 161,155] This event triggers the unfolded protein response (UPR) and, in case of prolonged ER-stress, apoptosis via its downstream effector CHOP. FC-induced macrophage apoptosis involves activation of the pro-apoptotic STAT1, induction of the death receptor Fas and stimulation of the mitochondria-cytochrome c pathway.[162] Moreover, in case of low ER-stress, so-called 'second hits' are required to induce macrophage apoptosis such as the activation of the scavenger receptor CD36 and the toll-like receptor 2.[163]

1.3.1.3 Mouse models to target apoptosis in atherosclerosis

The current knowledge on the role of apoptosis in plaque development and stability has been significantly improved owing to the use of numerous mouse models designed to modulate apoptotic cell death. Moreover, these models enable us to explore the potential of apoptosis-targeting therapeutic strategies. The different mouse models used to either induce or inhibit apoptosis in atherosclerosis are listed in **Table 1.2**.

Table 1.2: Overview of the different mouse models to target apoptosis in atherosclerosis

Mouse model	Experimental design	Effect on apoptosis	Effect on atherosclerosis	Reference
Induction of apoptosis				
+TRAIL in *ApoE-/-*	+ streptozotocin-induced diabetes	↑ Mφ apoptosis but not VSMC apoptosis	↓ atherosclerosis	164
AdFASL/ApoE-/-	/	↑	↑ plaque vulnerability	165
cIAP2-/-ApoE-/-	4wk and 12wk diet	↑	↓ atherosclerosis	166
AIM-/-Ldlr-/-	5 wk and12wk diet	↑ Mφ	↓ atherosclerosis	167
Bcl-X-/-ApoE-/- (LysM Cre)	10wk diet 27wk diet	↑ Mφ apoptosis	= atherosclerosis (+ ↑ cholesterol) ↑ atherosclerosis, ↑ necrosis	168
Bcl-2-/-ApoE-/- (LysM Cre)	10wk diet	↑ Mφ apoptosis	↑ atherosclerosis, ↑ necrosis	169
CD11b-hDTR/ApoE-/- - ACUTE: - CHRONIC :	10wk diet + DT (early) 10wk diet followed by one DT dose (advanced) 10wk diet followed by 10wk diet + DT (advanced)	= ↑ Mφ apoptosis = apoptosis	↓ atherogenesis (↓ necrosis) ↓ Mφ but = inflammation = Mφ (due to Mφ reinfiltration) = plaque size	170
CD11c-hDTR/ApoE-/- - ACUTE: - CHRONIC:	8wk diet followed by one DT dose 5wk diet followed by 7wk diet + DT	↑ Mφ apoptosis ↑ Mφ apoptosis	↑ new Mφ and ↑ inflammation = Mφ (due to Mφ reinfiltration) ↑ plaque size	171
SM22α-hDTR/ApoE-/-	10wk diet + DT (early) 12wk diet followed by 10 wk diet + DT (advanced)	↑ VSMC apoptosis ↑ VSMC apoptosis	↑ atherogenesis ↑ plaque size and ↑ vulnerability ↑ calcification	172, 173

Inhibition of apoptosis				
TNFR1 -/- (p55) C57Bl/6	14wk	N.D.	↑ atherosclerosis (↑ fatty streak)	174
TNFα-/-ApoE-/-	10wk and 20wk	N.D.	↓ atherosclerosis	175
Gld.ApoE-/- (FASL mutation)	12wk	↑ # apoptotic cells ?!	↑ atherosclerosis	176
FAS-/-ApoE-/-	/	↑ # apoptotic cells ?!	↑ atherosclerosis	177
TRAIL-/-ApoE-/-	12wk	N.D.	↑ calcification	178
Bax-/-Ldlr-/- (BMT)	10wk	↓ Mφ apoptosis	↑ atherosclerosis (↑ necrosis)	179
CD68-hBcl-2 ApoE-/-	5wk 15wk	↓ Mφ apoptosis	↑ atherosclerosis ↓ plaque size	171
p53-/-ApoE-/- (full KO)	6,10,15wk	= apoptosis ↑ proliferation	↑ atherosclerosis	180
p53-/-ApoE-/- (BMT)	15wk and 20wk	= apoptosis ↑ proliferation	↑ atherosclerosis ↑ necrosis	181
*p53-/-ApoE-/-*3-Leiden* (BMT)	12wk	↓ apoptosis = proliferation	↑ plaque size ↑ necrosis	182
p53-/-ApoE-/- *(LysM Cre)*	7wk and 11wk	↓ apoptosis = proliferation	= plaque size ↑ necrosis	183
p53-/-ApoE-/- (full KO)	14wk	↓ Mφ and VSMC apoptosis ↑ proliferation	↑ atherosclerosis	184
p19(ARF)-/- ApoE-/-	4wk and 9wk	↓ Mφ and VSMC apoptosis = proliferation	↑ atherosclerosis	185
CHOP-/-Ldlr-/-	12wk	↓ Mφ ER stress-induced apoptosis	↓ atherogenesis ↓ apoptosis and ↓ necrosis	186

Mφ = macrophages; VSMC = vascular smooth muscle cell; wk = weeks; DT = diphtheria toxin; N.D. = not determined

1.3.1.4 Consequences of apoptosis on plaque stability

The different mouse models have demonstrated that the consequences of apoptosis in atherosclerosis strongly depend on the stage of the plaque as well as on the cell type that is involved.

With regard to macrophages, apoptosis may dampen inflammation in early lesions by reducing the release of cytotoxic cytokines and collagen-degrading proteases. However, in advanced lesions, increased macrophage apoptosis has been shown to increase plaque vulnerability for several reasons. Firstly, apoptosis of lesional macrophages coupled with defective efferocytosis leads to the accumulation of apoptotic bodies, followed by secondary necrosis and enlargement of the necrotic core.[162] In this way, macrophage apoptosis may contribute to plaque inflammation. Secondly, loss of professional phagocytes may further compromise apoptotic cell removal.[187] Thirdly, apoptotic macrophages may shed membrane micro-particles containing pro-coagulant material such as tissue factor, which may facilitate thrombosis after plaque rupture.[188]

In contrast to macrophages, VSMC death is detrimental in all developmental stages of the plaque. VSMC apoptosis accelerates atherogenesis and leads to fibrous cap weakening, compromising plaque stability.[173,189] These observations counterbalance the former hypothesis that VSMC apoptosis may limit atherogenesis and may retard plaque progression.[173] In advanced plaques, VSMC apoptosis contributes to increased plaque vulnerability (i.e. thinning of the fibrous cap, loss of collagen, enlarged necrotic core), plaque calcification, stenosis and medial degeneration.[172, 173] Moreover, VSMC apoptosis may promote plaque thrombogenicity by exposing PS on their surface that can act as a substrate for thrombin generation and activation of the coagulant cascade.[190] Furthermore, VSMC apoptosis may contribute to plaque inflammation. Analogous with macrophages, human VSMCs have been shown to be potent phagocytes of apoptotic VSMCs, though, their phagocytic capacity is significantly reduced by hyperlipidaemia.[191] Inefficient clearance of apoptotic VSMCs results in secondary necrosis and subsequent IL1-driven inflammation.[191]

1.3.2 Autophagy in atherosclerosis

In the past decade, multiple research groups have gathered evidence for the occurrence of autophagy in human atherosclerosis.[192-195] The autophagic cells are characterised by engulfment of amorphous material in membranous cytosolic vacuoles, which are distinguishable from lipid droplets and lysosomes. They are mainly localised in the fibrous cap and around the necrotic core but at relatively low frequencies, approximately 1.5%, comparable with the incidence of apoptosis. The role of autophagy in atherosclerosis is dependent on the stage of plaque development.[196] In early lesions, autophagy serves as a cell survival mechanism against oxidative and metabolic stress, and inflammation. In advanced lesions, however, autophagy is unable to cope with the excess amount of (oxidative) stress, and therefore becomes insufficient and promotes apoptosis.[197] Besides this maladaptive response, evidence is accumulating that the process of autophagy becomes defective during the progression of atherosclerosis.[198] Multiple reports support the current hypothesis that the lysosomal-mediated degradation of engulfed cytoplasmic material (e.g. p62-enriched proteins) is hampered in advanced atherosclerosis rather than the initiation of autophagy itself.[197, 199-201]

1.3.2.1 Quantification of autophagy

Although several techniques have been developed over the past few years,[202, 203] the unambiguous detection of autophagy in atherosclerotic plaques remains difficult and it is therefore highly recommended to use a combination of different techniques. Besides electron microscopy, detection of the autophagic marker LC3-II by means of western blot analysis or immunohistochemistry is mostly applied to identify autophagy in atherosclerotic tissue. However, the expression of LC3-II does not give any information on the autophagic flux. For example, a decrease in LC3-II likely reflects a decline in autophagy, but an increase in autophagic turnover of LC3-II should not be excluded. Another important and widely used autophagic marker is p62. Given its role in targeting polyubiquitinated proteins to the autophagosome and the subsequent degradation of the incorporated proteins and p62 itself, an increase in p62 expression indicates a defect in the autophagic machinery.[203]

1.3.2.2 Potential autophagy inducers

In endothelial cells

Autophagy is activated in endothelial cells in response to multiple atherosclerosis-related stimuli including oxLDL,[204] ROS,[205] hypoxia[206] and AGE[207] to allow cell survival. The signalling pathways leading to autophagy stimulation in EC may be mTOR-dependent or mTOR-independent. For example, ROS stimulates the AMPK pathway, which promotes autophagy via inhibition of mTOR.[208] Autophagy induced by oxLDL promotes EC survival through oxLDL degradation,[204] whereas high levels of oxLDL, trigger upregulation of lectin-like oxLDL receptor and attenuate autophagy, promoting EC apoptosis.[209] ROS and oxLDL may also trigger autophagy via induction of ER-stress. Splicing of the mRNA of X-box binding protein 1 (XBP1) triggers an autophagic response in EC through transcriptional activation of Beclin 1.[210] Furthermore, laminar shear stress promotes EC autophagy through redox regulation and upregulation of sirtuin-1 (SIRT1).[211]

In vascular smooth muscle cells

Atherosclerosis-related stimuli such as ROS and oxidised lipids stimulate autophagy in VSMCs, which offers cytoprotection, at least *in vitro*. As in EC, the effect of oxLDL on cell death is concentration-dependent. Exposure of VSMCs to modest concentrations of oxLDL (10-40µg/ml) enhances autophagy, whereas high concentrations (≥60µg/ml) stimulate apoptosis.[212] 7-KC induces VSMC autophagy through upregulation of NADPH oxidase 4 and increased H_2O_2 production.[213] The lipid peroxidation product 4-hydroxnonenal (4-HNE) activates autophagy in VSMCs via induction of ER stress to promote the removal of 4-HNE modified proteins.[214] VSMC autophagy may also be regulated by different cytokines (e.g. osteopontin) and growth factors (PDGF).[215] Many of these autophagy inducers have been shown to influence VSMC phenotype and proliferation. For example, the growth factor PDGF decreases the expression of contractile proteins but upregulates synthetic VSMC markers and enhances their migration and proliferation potential.[216] Also osteopontin and AGE promote VSMC proliferation *in vitro*.[215] Although these findings suggest that autophagy is important in the development of a hyperproliferative VSMC phenotype, numerous cardiovascular drugs with autophagy-inducing potential such as simvastatin, verapamil and everolimus (in drug-eluting stents) have shown to inhibit VSMC proliferation.[217-219]

In macrophages

Analogous with VSMCs, macrophage autophagy can be activated by multiple atherosclerosis-related stimuli such as ROS and oxidised lipids. oxLDL and 7-KC may stimulate autophagy directly or indirectly via induction of ER-stress. For example, 7-KC in combination with the ER-stressor thapsigargin, induces autophagy in primary macrophages.[220] ER-stress triggers the activation of the UPR and induces autophagy in a JNK-dependent manner.[221] Simvastatin has been shown to stimulate oxLDL-induced autophagy in macrophages but attenuates lipid accumulation.[222]

1.3.2.3 The role of autophagy in atherosclerosis

To further define the role of macrophage autophagy in atherosclerosis, cell type-specific autophagy deficient knockout mice were created and crossbred with *Ldlr* knockout mice. Macrophage-specific deletion of *Atg5* accelerates atherosclerotic plaque development in *Ldlr*$^{-/-}$ mice.[220] Plaques of *Atg5*$^{-/-}$*Ldlr*$^{-/-}$ mice are characterised by elevated expression of oxidative stress and apoptotic markers, and increased plaque necrosis. *In vitro*, *Atg5* deficient macrophages show increased susceptibility for apoptosis upon treatment with 7-KC in combination with thapsigargin due to elevated NADPH oxidase activity and subsequent ROS generation. Moreover, *Atg5* deficient macrophages show reduced efferocytosis, suggesting that apoptotic autophagy deficient macrophages are poorly recognised and cleared by phagocytes.[220] In addition, plaques of *Atg5*$^{-/-}$*Ldlr*$^{-/-}$ mice show increased accumulation of cholesterol crystals that could promote hyperactivation of the NLRP3 inflammasome. Indeed, *Atg5* deficient macrophages secrete high levels of IL1β, a well-known characteristic of NLRP3 inflammasome activation, upon treatment with lipopolysaccharide (LPS) and cholesterol crystals.[198] Furthermore, lipid-loaded *Atg5* deficient macrophages show impaired cholesterol efflux, indicating that autophagy is involved in macrophage reverse cholesterol transport.[223] More recent evidence shows that defective macrophage autophagy stimulates inflammation by promoting macrophage polarisation into a pro-inflammatory M1 phenotype.[224] Taken together, macrophage autophagy is involved in key atherosclerotic processes including cholesterol transport and inflammation, indicating that its role in macrophages goes far beyond cellular protection against apoptotic and oxidative insults.

The current knowledge on EC autophagy, as described above, is mainly based on *in vitro* experiments. However, growing evidence suggests that autophagy may play a crucial role in preserving EC function. For instance, autophagy stimulates the maturation and secretion of the von Willebrand factor (vWF)[225] while impaired autophagy has been shown to contribute to arterial aging.[226] These findings indicate that defective autophagy in EC may have a prominent role in age-related arterial dysfunction.

Similar to EC, the knowledge on VSMC autophagy is mainly based on cell culture experiments. Additional *in vivo* experiments would be essential to elucidate the role of autophagy in VSMC survival and phenotype in arterial disease (investigated and described in chapter 4).

1.3.3 Necrosis in atherosclerosis

Cellular debris of necrotic cells, as well as the accumulation of lipids released by necrotic foam cells, contribute to necrotic core formation.[227] Examination of advanced human plaques showed that 80% of necrotic cores appeared to be larger than 1 mm^2 and comprised >10% of the lesion area.[228] In 66% of the examined plaques with plaque rupture, the necrotic core occupied >25% of the lesion area, suggesting that necrotic cell death is associated with plaque vulnerability.[229] Both plaque VSMCs and macrophages show morphological features typical of necrosis,[119] yet most reports suggest that the necrotic core contains predominantly macrophage debris.[227, 230]

1.3.3.1 Quantification of necrosis

The fact that reliable methods to detect and quantify (plaque) necrosis are currently lacking, is probably one of the main reasons why necrotic cell death has been so poorly investigated in atherosclerosis. The most standard method used to quantify plaque necrosis is measuring the size of the necrotic core on a H&E staining as described by Seimon et al.[231] This method, however, is not 100% correct since the necrotic core also contains lipid material (e.g. membranes of red blood cells (RBC), cholesterol esters, cholesterol crystals).

1.3.3.2 Potential necrosis inducers

(ox)LDL

As previously mentioned, the type of cell death in response to oxLDL depends on the dose and the degree of oxidation of oxLDL. Overall, highly oxidised LDL or high levels of mildly oxidised LDL induce necrosis rather than apoptosis.[232] Furthermore, the accumulation of free cholesterol in lipid-loaded macrophages leads to the formation of cholesterol crystals inside the cell.[233] These sharp-needled crystals can cause necrosis directly by puncturing the plasma membrane.[232]

(Mitochondrial) ROS

High levels of ROS cause irreversible oxidative damage to key cellular components (DNA, lipids, proteins). Severe DNA damage can cause PARP overactivation[96] whereas the generated lipid peroxidation products can disrupt organelles and the plasma membrane, leading to necrosis.[234] Mitochondria and NADPH oxidase enzymes are the major sources of ROS in cardiovascular disease.[235, 236] Moreover, according to various reports, excessive mitochondrial ROS (mtROS) promotes the progression of atherosclerosis in both patients and mouse models.[237-241] Excess mtROS causes mitochondrial depolarisation, ATP depletion and eventually necrosis.

ATP depletion

Depletion of the cytosolic ATP pool switches cell fate from apoptosis to necrosis.[242] Loss of function of ATP-dependent ion channels in the plasma membrane, causes cell swelling due to the uncontrolled influx of cations, and finally rupture of the plasma membrane.[75] ATP depletion can be the result of PARP overactivation (vide supra), accumulation of mtROS or mitochondrial Ca^{2+}-overload.[75]

Intracellular Ca^{2+}-overload

Increased intracellular calcium levels induce necrosis via activation of calcium-dependent proteases (e.g.calpains) and/or increased mtROS generation (in case of mitochondrial Ca^{2+}-overload).[75, 243] Loss of function of ATP-dependent Ca^{2+}-channels promotes Ca^{2+}-influx from the extracellular environment or from the ER, causing intracellular Ca^{2+}-overload.

Defective efferocytosis

Phagocytosis of apoptotic cells plays a central role in the resolution of inflammation.[244] The engulfment of apoptotic cells suppresses the secretion of pro-inflammatory cytokines (e.g. TNFα) and upregulates anti-inflammatory mediators (e.g. TGFβ).[245] Several reports have shown that the clearance of apoptotic cells (AC) by phagocytes is impaired in advanced atherosclerotic plaques.[246, 247] Multiple mechanisms of defective efferocytosis have been suggested including competition between AC, oxRBC and oxLDL for the uptake via the same receptors (e.g. SR-A, CD36, CD68),[248, 249] binding of auto-antibodies against oxLDL to phagocytic ligands on the AC,[250] exposure to free radicals,[251] incorporation of indigestible material[251] or red blood cells,[142, 252] and downregulation of the bridging molecule MFG-E8[253] or the mertk efferocytosis receptor[254]. As a consequence, the AC accumulate, undergo secondary necrosis and contribute to the enlargement of the necrotic core.

1.3.3.3 Consequences of necrosis on plaque stability

Increased inflammation

The necrotic debris is a major source of pro-inflammatory cytokines (e.g. IL6) and damage-associated molecular patterns (DAMP) (e.g. high mobility group box 1 [HMGB1])[255] and may hamper plaque stability by promoting inflammation. HMGB1 is passively released from necrotic or damaged cells, but not during apoptosis and secondary necrosis.[256] Once released, HMGB1 stimulates macrophages to produce pro-inflammatory cytokines such as TNFα, IL6 and IL1β through binding with the receptor for advanced glycation end products (RAGE) or members of the toll-like receptor family (e.g. TLR4).[257, 258] Necrotic VSMCs have been shown to secrete IL1α whereas during secondary necrosis, both IL1α and IL1β are released.[191] Both cytokines act on the surrounding viable VSMCs, stimulating them to produce pro-inflammatory cytokines such as IL6 and monocyte chemotactic protein 1 (MCP1), amplifying inflammation.[191]

Increased plaque vulnerability

The formation and enlargement of the necrotic core plays a key role in plaque vulnerability. The larger the necrotic core, the higher the risk of plaque rupture.[228, 229] Besides the size of the core, its consistency is important for plaque stability. Soft cores, consisting of cholesterol esters, are considered more vulnerable than crystalline

cholesterol containing cores because they are less able to bear the imposed mechanical stresses.[259] Furthermore, necrotic cores are rich in matrix metalloproteinases (MMPs), released by necrotic cells, that degrade the extracellular matrix and contribute to plaque destabilisation.[255]

Increased plaque thrombogenicity

The necrotic core also contains pro-thrombotic factors such as tissue factor, presumably derived from macrophages undergoing secondary necrosis.[260] Tissue factor facilitates thrombus formation after plaque rupture.[5]

1.3.3.4 The role of necroptosis in atherosclerosis

The discovery of RIPK3 as a key regulator of necroptosis led to the generation of *Ripk3*$^{-/-}$*Ldlr*$^{-/-}$ knockout mice to investigate the role of RIPK3 in atherosclerosis. Deletion of *Ripk3* in *Ldlr*$^{-/-}$ mice reduces atherosclerotic plaque size after 16 weeks on western-type diet but has no effect on early atherosclerosis.[261] Moreover, necrotic core size is significantly reduced in plaques of *Ripk3*$^{-/-}$*Ldlr*$^{-/-}$mice as compared to *Ripk3*$^{+/+}$*Ldlr*$^{-/-}$ mice while plaque apoptosis is not altered, indicating that RIPK3 does not play a role in macrophage apoptosis but only promotes plaque (primary) necrosis. Furthermore, plaques of *Ripk3*$^{-/-}$ *Ldlr*$^{-/-}$ mice show reduced accumulation of macrophages and decreased mRNA expression levels of TNFα and VCAM-1,[261] underscoring the link between necrosis and inflammation.

1.3.3.5 Potential therapeutic strategies to target necrosis

The recent understanding that necrosis can occur in a highly regulated manner, has led to the development of novel small molecules that target regulated necrosis. Most of these compounds have been shown to be highly effective in reducing ischemia-reperfusion injury in different animal models, though, in most cases, they have never been tested as a potential anti-atherosclerotic therapy. Compounds that potentially may inhibit necrosis in atherosclerosis are listed in **Table 1.3**.

Table 1.3: Overview of compounds with potential anti-necrotic effects in atherosclerosis

Compound	Target	Application	Possible unwanted effects	References
Inhibition of necroptosis				
Necrostatin-1 (Nec-1)	RIPK1 inhibitor	Protection against inflammatory diseases in mouse models of sepsis, NAFLD and against neurodegenerative diseases (stroke) ↓ **plaque** size, ↑ **plaque** stability in WD-fed *ApoE*$^{-/-}$ mice	Toxic and less specific	262-264
Nec-1s		↓ TNF-induced lethality in SIRS mice	↓ toxic, ↑ stability, ↑ specificity	
GSK 840 GSK 843 GSK 872	RIPK3 inhibitor	↓ LPS or TNF+zVAD induced necroptosis in (mouse) Mφ	GSK 843, 872: high conc triggers TNF induced RIPK1-dep. apoptosis GSK840: only targets human RIPK3	265
Necrosulfonamide (NSA)	MLKL inhibitor	↓ TNF+zVAD induced necroptosis in Jurkat cells	NSA only targets human MLKL	90
Inhibition of mPTP-mediated necrosis				
Cyclosporin A	CYPD inhibitor	↓ IR injury after myocardial infarction ↑ **atherosclerosis** in WD-fed mice: ↓ inflammation but ↑ cholesterol levels	Strong immunosuppressive Hyperlipidemia ↑ risk of atherosclerosis	266-268
Inhibition of PARP-mediated necrosis				
3-aminobenzamide	PARP1 inhibitor	↑ anti-tumour effects of chemotherapeutic agents in clinical trials ↓ myocardial infarct size (animal + clinical studies) ↓ **plaque** size, ↑ **plaque** stability in WD-fed *ApoE*$^{-/-}$ mice	No severe drug-related side effects were observed	269

Table 1.3 Overview of compounds with potential anti-necrotic effects in atherosclerosis (continued)

Inhibition of ferroptosis				
Ferrostatin-1 Ferrostatin derivatives	Inhibits lipid peroxidation	↓ IR injury in mouse kidney	↓ plasma and metabolic stability ↑ ADME properties, ↑ potency	270, 271
LOXBlock-1 Novel LOX inhibitors	Inhibits lipid peroxidation	↓ brain infarct size in mouse models of stroke	↓ selectivity ↑ potency and selectively	272, 273
Inhibition of NADPH oxidase				
NecroX compounds	Inhibits NOX ↓ mtROS	↓ oxidative stress-induced necrosis in cardiomyocytes ↓ myocardial/hepatic/renal IR injury in animals	No adverse effects reported after acute administration in patients	274-277
Stimulation of efferocytosis				
Glucocorticoids	↑ Mφ phagocytic capacity	↑ efferocytosis capacity is associated with reorganisation of cytoskeleton elements	Strong immunosuppressive Many adverse effects: dyslipidemia, hyperglycemia, hypertension	278, 279
Lovastatin	↑ Mφ phagocytic capacity	↑ efferocytosis in alveolar Mφ in a HMG-coA reductase-dependent manner		280
Metformin	↑ Mφ phagocytic capacity	↑ efferocytosis of apoptotic neutrophils by Mφ is AMPK-dependent ↓ **atherosclerosis** in *ApoE*$^{-/-}$ mice		281, 282

Mφ = macrophages; NOX = NADPH oxidase

1.4 References

(1) Lusis AJ. Atherosclerosis. *Nature* 2000;407(6801):233-41.
(2) Hansson GK. Inflammation, atherosclerosis, and coronary artery disease. *N Engl J Med* 2005;352(16):1685-95.
(3) Falk E, Nakano M, Bentzon JF, Finn AV, Virmani R. Update on acute coronary syndromes: the pathologists' view. *Eur Heart J* 2013;34(10):719-28.
(4) Libby P. Mechanisms of acute coronary syndromes and their implications for therapy. *N Engl J Med* 2013;368(21):2004-13.
(5) Bentzon JF, Otsuka F, Virmani R, Falk E. Mechanisms of plaque formation and rupture. *Circ Res* 2014;114(12):1852-66.
(6) Gimbrone MA, Jr. Vascular endothelium, hemodynamic forces, and atherogenesis. *Am J Pathol* 1999;155(1):1-5.
(7) Wong ND. Epidemiological studies of CHD and the evolution of preventive cardiology. *Nat Rev Cardiol* 2014;11(5):276-89.
(8) Mozaffarian D et al. Heart Disease and Stroke Statistics-2016 Update: A Report From the American Heart Association. *Circulation* 2016;133(4):e38-e360.
(9) Laslett LJ, Alagona P, Jr., Clark BA, III, Drozda JP, Jr., Saldivar F, Wilson SR, Poe C, Hart M. The worldwide environment of cardiovascular disease: prevalence, diagnosis, therapy, and policy issues: a report from the American College of Cardiology. *J Am Coll Cardiol* 2012;60(25 Suppl):S1-49.
(10) Townsend N, Nichols M, Scarborough P, Rayner M. Cardiovascular disease in Europe--epidemiological update 2015. *Eur Heart J* 2015;36(40):2696-705.
(11) Sitia S et al. From endothelial dysfunction to atherosclerosis. *Autoimmun Rev* 2010;9(12):830-4.
(12) Tabas I, Garcia-Cardena G, Owens GK. Recent insights into the cellular biology of atherosclerosis. *J Cell Biol* 2015;209(1):13-22.
(13) Tabas I, Williams KJ, Boren J. Subendothelial lipoprotein retention as the initiating process in atherosclerosis: update and therapeutic implications. *Circulation* 2007;116(16):1832-44.
(14) Steinberg D. The LDL modification hypothesis of atherogenesis: an update. *J Lipid Res* 2009;50 Suppl:S376-S381.
(15) Libby P, Ridker PM, Maseri A. Inflammation and atherosclerosis. *Circulation* 2002;105(9):1135-43.
(16) Kunjathoor VV et al. Scavenger receptors class A-I/II and CD36 are the principal receptors responsible for the uptake of modified low density lipoprotein leading to lipid loading in macrophages. *J Biol Chem* 2002;277(51):49982-8.
(17) Stoger JL, Gijbels MJ, van d, V, Manca M, van der Loos CM, Biessen EA, Daemen MJ, Lutgens E, de Winther MP. Distribution of macrophage polarization markers in human atherosclerosis. *Atherosclerosis* 2012;225(2):461-8.
(18) Leitinger N and Schulman IG. Phenotypic polarization of macrophages in atherosclerosis. *Arterioscler Thromb Vasc Biol* 2013;33(6):1120-6.
(19) Hansson GK and Hermansson A. The immune system in atherosclerosis. *Nat Immunol* 2011;12(3):204-12.
(20) Witztum JL and Lichtman AH. The influence of innate and adaptive immune responses on atherosclerosis. *Annu Rev Pathol* 2014;9:73-102.
(21) Johnson JL. Emerging regulators of vascular smooth muscle cell function in the development and progression of atherosclerosis. *Cardiovasc Res* 2014;103(4):452-60.
(22) Alexander MR and Owens GK. Epigenetic control of smooth muscle cell differentiation and phenotypic switching in vascular development and disease. *Annu Rev Physiol* 2012;74:13-40.
(23) Sata M et al. Hematopoietic stem cells differentiate into vascular cells that participate in the pathogenesis of atherosclerosis. *Nat Med* 2002;8(4):403-9.
(24) Caplice NM, Bunch TJ, Stalboerger PG, Wang S, Simper D, Miller DV, Russell SJ, Litzow MR, Edwards WD. Smooth muscle cells in human coronary atherosclerosis can originate from cells administered at marrow transplantation. *Proc Natl Acad Sci U S A* 2003;100(8):4754-9.
(25) Yu H, Stoneman V, Clarke M, Figg N, Xin HB, Kotlikoff M, Littlewood T, Bennett M. Bone marrow-derived smooth muscle-like cells are infrequent in advanced primary atherosclerotic plaques but promote atherosclerosis. *Arterioscler Thromb Vasc Biol* 2011;31(6):1291-9.
(26) Tang Z, Wang A, Yuan F, Yan Z, Liu B, Chu JS, Helms JA, Li S. Differentiation of multipotent vascular stem cells contributes to vascular diseases. *Nat Commun* 2012;3:875.
(27) Hu Y, Zhang Z, Torsney E, Afzal AR, Davison F, Metzler B, Xu Q. Abundant progenitor cells in the adventitia contribute to atherosclerosis of vein grafts in ApoE-deficient mice. *J Clin Invest* 2004;113(9):1258-65.
(28) Sluimer JC and Daemen MJ. Novel concepts in atherogenesis: angiogenesis and hypoxia in atherosclerosis. *J Pathol* 2009;218(1):7-29.

(29) Kolodgie FD et al. Intraplaque hemorrhage and progression of coronary atheroma. *N Engl J Med* 2003;349(24):2316-25.
(30) Moreno PR, Purushothaman KR, Zias E, Sanz J, Fuster V. Neovascularization in human atherosclerosis. *Curr Mol Med* 2006;6(5):457-77.
(31) Libby P. Collagenases and cracks in the plaque. *J Clin Invest* 2013;123(8):3201-3.
(32) Kovanen PT. Mast cells in atherogenesis: actions and reactions. *Curr Atheroscler Rep* 2009;11(3):214-9.
(33) Moore KJ and Tabas I. Macrophages in the pathogenesis of atherosclerosis. *Cell* 2011;145(3):341-55.
(34) Virmani R, Kolodgie FD, Burke AP, Farb A, Schwartz SM. Lessons from sudden coronary death: a comprehensive morphological classification scheme for atherosclerotic lesions. *Arterioscler Thromb Vasc Biol* 2000;20(5):1262-75.
(35) Insull W, Jr. The pathology of atherosclerosis: plaque development and plaque responses to medical treatment. *Am J Med* 2009;122(1 Suppl):S3-S14.
(36) Catapano AL et al. ESC/EAS Guidelines for the management of dyslipidaemias: the Task Force for the management of dyslipidaemias of the European Society of Cardiology (ESC) and the European Atherosclerosis Society (EAS). *Atherosclerosis* 2011;217 Suppl 1:S1-44.
(37) Nicholls SJ, Pisaniello AD, Kataoka Y, Puri R. Lipid pharmacotherapy for treatment of atherosclerosis. *Expert Opin Pharmacother* 2014;15(8):1119-25.
(38) Davignon J. Beneficial cardiovascular pleiotropic effects of statins. *Circulation* 2004;109(23 Suppl 1):III39-III43.
(39) Perk J et al. European Guidelines on cardiovascular disease prevention in clinical practice (version 2012). The Fifth Joint Task Force of the European Society of Cardiology and Other Societies on Cardiovascular Disease Prevention in Clinical Practice (constituted by representatives of nine societies and by invited experts). *Eur Heart J* 2012;33(13):1635-701.
(40) Hennekens CH. Aspirin in the treatment and prevention of cardiovascular disease: current perspectives and future directions. *Curr Atheroscler Rep* 2007;9(5):409-16.
(41) Levine GN et al. 2016 ACC/AHA Guideline Focused Update on Duration of Dual Antiplatelet Therapy in Patients With Coronary Artery Disease: A Report of the American College of Cardiology/American Heart Association Task Force on Clinical Practice Guidelines. *Circulation* 2016.
(42) Steinl DC and Kaufmann BA. Ultrasound imaging for risk assessment in atherosclerosis. *Int J Mol Sci* 2015;16(5):9749-69.
(43) Getz GS and Reardon CA. Animal models of atherosclerosis. *Arterioscler Thromb Vasc Biol* 2012;32(5):1104-15.
(44) Getz GS and Reardon CA. Apoprotein E as a lipid transport and signaling protein in the blood, liver, and artery wall. *J Lipid Res* 2009;50 Suppl:S156-S161.
(45) Fuchs Y and Steller H. Programmed cell death in animal development and disease. *Cell* 2011;147(4):742-58.
(46) Kroemer G et al. Classification of cell death: recommendations of the Nomenclature Committee on Cell Death 2009. *Cell Death Differ* 2009;16(1):3-11.
(47) Grossmann J. Molecular mechanisms of "detachment-induced apoptosis" - Anoikis. *Apoptosis* 2002;7(3):247-60.
(48) Overholtzer M, Mailleux AA, Mouneimne G, Normand G, Schnitt SJ, King RW, Cibas ES, Brugge JS. A nonapoptotic cell death process, entosis, that occurs by cell-in-cell invasion. *Cell* 2007;131(5):966-79.
(49) Castedo M, Perfettini JL, Roumier T, Andreau K, Medema R, Kroemer G. Cell death by mitotic catastrophe: a molecular definition. *Oncogene* 2004;23(16):2825-37.
(50) Kerr JF, Wyllie AH, Currie AR. Apoptosis: a basic biological phenomenon with wide-ranging implications in tissue kinetics. *Br J Cancer* 1972;26(4):239-57.
(51) Hengartner MO. The biochemistry of apoptosis. *Nature* 2000;407(6805):770-6.
(52) Cohen GM. Caspases: the executioners of apoptosis. *Biochem J* 1997;326 (Pt 1):1-16.
(53) Porter AG and Janicke RU. Emerging roles of caspase-3 in apoptosis. *Cell Death Differ* 1999;6(2):99-104.
(54) Sakahira H, Enari M, Nagata S. Cleavage of CAD inhibitor in CAD activation and DNA degradation during apoptosis. *Nature* 1998;391(6662):96-9.
(55) Fadok VA, Bratton DL, Frasch SC, Warner ML, Henson PM. The role of phosphatidylserine in recognition of apoptotic cells by phagocytes. *Cell Death Differ* 1998;5(7):551-62.
(56) Martinon F and Tschopp J. Inflammatory caspases and inflammasomes: master switches of inflammation. *Cell Death Differ* 2007;14(1):10-22.
(57) Schmitz I, Kirchhoff S, Krammer PH. Regulation of death receptor-mediated apoptosis pathways. *Int J Biochem Cell Biol* 2000;32(11-12):1123-36.
(58) Cai J, Yang J, Jones DP. Mitochondrial control of apoptosis: the role of cytochrome c. *Biochim Biophys Acta* 1998;1366(1-2):139-49.

(59) Hill MM, Adrain C, Duriez PJ, Creagh EM, Martin SJ. Analysis of the composition, assembly kinetics and activity of native Apaf-1 apoptosomes. *EMBO J* 2004;23(10):2134-45.
(60) Eposti MD. The roles of Bid. *Apoptosis* 2002;7(5):433-40.
(61) Benchimol S. p53-dependent pathways of apoptosis. *Cell Death Differ* 2001;8(11):1049-51.
(62) Ghavami S et al. Autophagy and apoptosis dysfunction in neurodegenerative disorders. *Prog Neurobiol* 2014;112:24-49.
(63) Klionsky DJ and Emr SD. Autophagy as a regulated pathway of cellular degradation. *Science* 2000;290(5497):1717-21.
(64) Levine B and Klionsky DJ. Development by self-digestion: molecular mechanisms and biological functions of autophagy. *Dev Cell* 2004;6(4):463-77.
(65) Yorimitsu T and Klionsky DJ. Autophagy: molecular machinery for self-eating. *Cell Death Differ* 2005;12 Suppl 2:1542-52.
(66) Mizushima N and Komatsu M. Autophagy: renovation of cells and tissues. *Cell* 2011;147(4):728-41.
(67) Levine B and Yuan J. Autophagy in cell death: an innocent convict? *J Clin Invest* 2005;115(10):2679-88.
(68) Shen S, Kepp O, Kroemer G. The end of autophagic cell death? *Autophagy* 2012;8(1):1-3.
(69) Clarke PG and Puyal J. Autophagic cell death exists. *Autophagy* 2012;8(6):867-9.
(70) Feng Y, He D, Yao Z, Klionsky DJ. The machinery of macroautophagy. *Cell Res* 2014;24(1):24-41.
(71) Jung CH, Ro SH, Cao J, Otto NM, Kim DH. mTOR regulation of autophagy. *FEBS Lett* 2010;584(7):1287-95.
(72) Mao K and Klionsky DJ. AMPK activates autophagy by phosphorylating ULK1. *Circ Res* 2011;108(7):787-8.
(73) Cheong H, Lu C, Lindsten T, Thompson CB. Therapeutic targets in cancer cell metabolism and autophagy. *Nat Biotechnol* 2012;30(7):671-8.
(74) Majno G and Joris I. Apoptosis, oncosis, and necrosis. An overview of cell death. *Am J Pathol* 1995;146:3-15.
(75) Zong WX and Thompson CB. Necrotic death as a cell fate. *Genes Dev* 2006;20(1):1-15.
(76) Krysko DV, Vanden Berghe T, D'Herde K, Vandenabeele P. Apoptosis and necrosis: detection, discrimination and phagocytosis. *Methods* 2008;44(3):205-21.
(77) Festjens N, Vanden Berghe T, Vandenabeele P. Necrosis, a well-orchestrated form of cell demise: signalling cascades, important mediators and concomitant immune response. *Biochim Biophys Acta* 2006;1757(9-10):1371-87.
(78) Galluzzi L, Kepp O, Krautwald S, Kroemer G, Linkermann A. Molecular mechanisms of regulated necrosis. *Semin Cell Dev Biol* 2014;35:24-32.
(79) Vanden Berghe T, Linkermann A, Jouan-Lanhouet S, Walczak H, Vandenabeele P. Regulated necrosis: the expanding network of non-apoptotic cell death pathways. *Nat Rev Mol Cell Biol* 2014;15(2):135-47.
(80) Vanlangenakker N, Bertrand MJ, Bogaert P, Vandenabeele P, Vanden Berghe T. TNF-induced necroptosis in L929 cells is tightly regulated by multiple TNFR1 complex I and II members. *Cell Death Dis* 2011;2:e230.
(81) Festjens N, Vanden Berghe T, Cornelis S, Vandenabeele P. RIP1, a kinase on the crossroads of a cell's decision to live or die. *Cell Death Differ* 2007;14(3):400-10.
(82) Declercq W, Vanden Berghe T, Vandenabeele P. RIP kinases at the crossroads of cell death and survival. *Cell* 2009;138(2):229-32.
(83) Mahoney DJ et al. Both cIAP1 and cIAP2 regulate TNFalpha-mediated NF-kappaB activation. *Proc Natl Acad Sci U S A* 2008;105(33):11778-83.
(84) Hitomi J, Christofferson DE, Ng A, Yao J, Degterev A, Xavier RJ, Yuan J. Identification of a molecular signaling network that regulates a cellular necrotic cell death pathway by a genome wide siRNA screen. *Cell* 2008;135(7):1311-23.
(85) Cho YS, Challa S, Moquin D, Genga R, Ray TD, Guildford M, Chan FK. Phosphorylation-driven assembly of the RIP1-RIP3 complex regulates programmed necrosis and virus-induced inflammation. *Cell* 2009;137(6):1112-23.
(86) He S, Wang L, Miao L, Wang T, Du F, Zhao L, Wang X. Receptor interacting protein kinase-3 determines cellular necrotic response to TNF-alpha. *Cell* 2009;137(6):1100-11.
(87) Zhang DW, Shao J, Lin J, Zhang N, Lu BJ, Lin SC, Dong MQ, Han J. RIP3, an energy metabolism regulator that switches TNF-induced cell death from apoptosis to necrosis. *Science* 2009;325(5938):332-6.
(88) Temkin V, Huang Q, Liu H, Osada H, Pope RM. Inhibition of ADP/ATP exchange in receptor-interacting protein-mediated necrosis. *Mol Cell Biol* 2006;26(6):2215-25.
(89) Moquin D and Chan FK. The molecular regulation of programmed necrotic cell injury. *Trends Biochem Sci* 2010;35(8):434-41.
(90) Sun L et al. Mixed lineage kinase domain-like protein mediates necrosis signaling downstream of RIP3 kinase. *Cell* 2012;148(1-2):213-27.

(91) Dondelinger Y et al. MLKL compromises plasma membrane integrity by binding to phosphatidylinositol phosphates. *Cell Rep* 2014;7(4):971-81.
(92) Cai Z, Jitkaew S, Zhao J, Chiang HC, Choksi S, Liu J, Ward Y, Wu LG, Liu ZG. Plasma membrane translocation of trimerized MLKL protein is required for TNF-induced necroptosis. *Nat Cell Biol* 2014;16(1):55-65.
(93) Kinnally KW, Peixoto PM, Ryu SY, Dejean LM. Is mPTP the gatekeeper for necrosis, apoptosis, or both? *Biochim Biophys Acta* 2011;1813(4):616-22.
(94) Vaseva AV, Marchenko ND, Ji K, Tsirka SE, Holzmann S, Moll UM. p53 opens the mitochondrial permeability transition pore to trigger necrosis. *Cell* 2012;149(7):1536-48.
(95) D'Amours D, Desnoyers S, D'Silva I, Poirier GG. Poly(ADP-ribosyl)ation reactions in the regulation of nuclear functions. *Biochem J* 1999;342 (Pt 2):249-68.
(96) Ha HC and Snyder SH. Poly(ADP-ribose) polymerase is a mediator of necrotic cell death by ATP depletion. *Proc Natl Acad Sci U S A* 1999;96(24):13978-82.
(97) David KK, Andrabi SA, Dawson TM, Dawson VL. Parthanatos, a messenger of death. *Front Biosci (Landmark Ed)* 2009;14:1116-28.
(98) Fatokun AA, Dawson VL, Dawson TM. Parthanatos: mitochondrial-linked mechanisms and therapeutic opportunities. *Br J Pharmacol* 2014;171(8):2000-16.
(99) Xu Y, Huang S, Liu ZG, Han J. Poly(ADP-ribose) polymerase-1 signaling to mitochondria in necrotic cell death requires RIP1/TRAF2-mediated JNK1 activation. *J Biol Chem* 2006;281(13):8788-95.
(100) Lambeth JD. NOX enzymes and the biology of reactive oxygen. *Nat Rev Immunol* 2004;4(3):181-9.
(101) Kim YS, Morgan MJ, Choksi S, Liu ZG. TNF-induced activation of the Nox1 NADPH oxidase and its role in the induction of necrotic cell death. *Mol Cell* 2007;26(5):675-87.
(102) Liu X, Van VT, Schnellmann RG. The role of calpain in oncotic cell death. *Annu Rev Pharmacol Toxicol* 2004;44:349-70.
(103) Rami A. Ischemic neuronal death in the rat hippocampus: the calpain-calpastatin-caspase hypothesis. *Neurobiol Dis* 2003;13(2):75-88.
(104) Bano D, Young KW, Guerin CJ, Lefeuvre R, Rothwell NJ, Naldini L, Rizzuto R, Carafoli E, Nicotera P. Cleavage of the plasma membrane Na+/Ca2+ exchanger in excitotoxicity. *Cell* 2005;120(2):275-85.
(105) Yamashima T. Ca2+-dependent proteases in ischemic neuronal death: a conserved 'calpain-cathepsin cascade' from nematodes to primates. *Cell Calcium* 2004;36(3-4):285-93.
(106) Ma Y, Temkin V, Liu H, Pope RM. NF-kappaB protects macrophages from lipopolysaccharide-induced cell death: the role of caspase 8 and receptor-interacting protein. *J Biol Chem* 2005;280(51):41827-34.
(107) He S, Liang Y, Shao F, Wang X. Toll-like receptors activate programmed necrosis in macrophages through a receptor-interacting kinase-3-mediated pathway. *Proc Natl Acad Sci U S A* 2011;108(50):20054-9.
(108) Vanlangenakker N, Vanden Berghe T, Vandenabeele P. Many stimuli pull the necrotic trigger, an overview. *Cell Death Differ* 2012;19(1):75-86.
(109) Fernandes-Alnemri T, Wu J, Yu JW, Datta P, Miller B, Jankowski W, Rosenberg S, Zhang J, Alnemri ES. The pyroptosome: a supramolecular assembly of ASC dimers mediating inflammatory cell death via caspase-1 activation. *Cell Death Differ* 2007;14(9):1590-604.
(110) Bergsbaken T, Fink SL, Cookson BT. Pyroptosis: host cell death and inflammation. *Nat Rev Microbiol* 2009;7(2):99-109.
(111) Fink SL and Cookson BT. Caspase-1-dependent pore formation during pyroptosis leads to osmotic lysis of infected host macrophages. *Cell Microbiol* 2006;8(11):1812-25.
(112) Conrad M, Angeli JP, Vandenabeele P, Stockwell BR. Regulated necrosis: disease relevance and therapeutic opportunities. *Nat Rev Drug Discov* 2016;15(5):348-66.
(113) Xie Y, Hou W, Song X, Yu Y, Huang J, Sun X, Kang R, Tang D. Ferroptosis: process and function. *Cell Death Differ* 2016;23(3):369-79.
(114) Yang WS et al. Regulation of ferroptotic cancer cell death by GPX4. *Cell* 2014;156(1-2):317-31.
(115) Virchow R. Die Cellularpathologie: Sechszehnte verlesung, 14 April 1858, Goerge Olms, Hildesheim, Germany. 317-329. 1966.
(116) Isner JM, Kearney M, Bortman S, Passeri J. Apoptosis in human atherosclerosis and restenosis. *Circulation* 1995;91(11):2703-11.
(117) Geng YJ and Libby P. Evidence for apoptosis in advanced human atheroma. Colocalization with interleukin-1 beta-converting enzyme. *Am J Pathol* 1995;147(2):251-66.
(118) Han DK, Haudenschild CC, Hong MK, Tinkle BT, Leon MB, Liau G. Evidence for apoptosis in human atherogenesis and in a rat vascular injury model. *Am J Pathol* 1995;147(2):267-77.
(119) Crisby M, Kallin B, Thyberg J, Zhivotovsky B, Orrenius S, Kostulas V, Nilsson J. Cell death in human atherosclerotic plaques involves both oncosis and apoptosis. *Atherosclerosis* 1997;130(1-2):17-27.

(120) Kockx MM, De Meyer GR, Muhring J, Bult H, Bultinck J, Herman AG. Distribution of cell replication and apoptosis in atherosclerotic plaques of cholesterol-fed rabbits. *Atherosclerosis* 1996;120(1-2):115-24.
(121) Bjorkerud S and Bjorkerud B. Apoptosis is abundant in human atherosclerotic lesions, especially in inflammatory cells (macrophages and T cells), and may contribute to the accumulation of gruel and plaque instability. *Am J Pathol* 1996;149(2):367-80.
(122) Bauriedel G, Schluckebier S, Hutter R, Welsch U, Kandolf R, Luderitz B, Prescott MF. Apoptosis in restenosis versus stable-angina atherosclerosis: implications for the pathogenesis of restenosis. *Arterioscler Thromb Vasc Biol* 1998;18(7):1132-9.
(123) Kockx MM, De Meyer GR, Muhring J, Jacob W, Bult H, Herman AG. Apoptosis and related proteins in different stages of human atherosclerotic plaques. *Circulation* 1998;97(23):2307-15.
(124) Geng YJ and Libby P. Progression of atheroma: a struggle between death and procreation. *Arterioscler Thromb Vasc Biol* 2002;22(9):1370-80.
(125) Kolodgie FD, Narula J, Burke AP, Haider N, Farb A, Hui-Liang Y, Smialek J, Virmani R. Localization of apoptotic macrophages at the site of plaque rupture in sudden coronary death. *Am J Pathol* 2000;157(4):1259-68.
(126) Kockx MM, Muhring J, Knaapen MW, De Meyer GR. RNA synthesis and splicing interferes with DNA in situ end labeling techniques used to detect apoptosis. *Am J Pathol* 1998;152(4):885-8.
(127) Casciola-Rosen LA, Miller DK, Anhalt GJ, Rosen A. Specific cleavage of the 70-kDa protein component of the U1 small nuclear ribonucleoprotein is a characteristic biochemical feature of apoptotic cell death. *J Biol Chem* 1994;269(49):30757-60.
(128) Galluzzi L et al. Guidelines for the use and interpretation of assays for monitoring cell death in higher eukaryotes. *Cell Death Differ* 2009;16(8):1093-107.
(129) Vanden Berghe T, Grootjans S, Goossens V, Dondelinger Y, Krysko DV, Takahashi N, Vandenabeele P. Determination of apoptotic and necrotic cell death in vitro and in vivo. *Methods* 2013;61(2):117-29.
(130) Figg N and Bennett MR. Quantification of Apoptosis in Mouse Atherosclerotic plaques. *Methods Mol Biol* 2015;1339:191-9.
(131) Dimmeler S, Hermann C, Zeiher AM. Apoptosis of endothelial cells. Contribution to the pathophysiology of atherosclerosis? *Eur Cytokine Netw* 1998;9(4):697-8.
(132) Tricot O, Mallat Z, Heymes C, Belmin J, Leseche G, Tedgui A. Relation between endothelial cell apoptosis and blood flow direction in human atherosclerotic plaques. *Circulation* 2000;101(21):2450-3.
(133) Du XL, Sui GZ, Stockklauser-Farber K, Weiss J, Zink S, Schwippert B, Wu QX, Tschope D, Rosen P. Introduction of apoptosis by high proinsulin and glucose in cultured human umbilical vein endothelial cells is mediated by reactive oxygen species. *Diabetologia* 1998;41(3):249-56.
(134) Min C, Kang E, Yu SH, Shinn SH, Kim YS. Advanced glycation end products induce apoptosis and procoagulant activity in cultured human umbilical vein endothelial cells. *Diabetes Res Clin Pract* 1999;46(3):197-202.
(135) Dimmeler S, Haendeler J, Galle J, Zeiher AM. Oxidized low-density lipoprotein induces apoptosis of human endothelial cells by activation of CPP32-like proteases. A mechanistic clue to the 'response to injury' hypothesis. *Circulation* 1997;95(7):1760-3.
(136) Galle J, Schneider R, Heinloth A, Wanner C, Galle PR, Conzelmann E, Dimmeler S, Heermeier K. Lp(a) and LDL induce apoptosis in human endothelial cells and in rabbit aorta: role of oxidative stress. *Kidney Int* 1999;55(4):1450-61.
(137) Dimmeler S, Rippmann V, Weiland U, Haendeler J, Zeiher AM. Angiotensin II induces apoptosis of human endothelial cells. Protective effect of nitric oxide. *Circ Res* 1997;81(6):970-6.
(138) Galle J and Heermeier K. Angiotensin II and oxidized LDL: an unholy alliance creating oxidative stress. *Nephrol Dial Transplant* 1999;14(11):2585-9.
(139) Robaye B, Mosselmans R, Fiers W, Dumont JE, Galand P. Tumor necrosis factor induces apoptosis (programmed cell death) in normal endothelial cells in vitro. *Am J Pathol* 1991;138(2):447-53.
(140) Karsan A, Yee E, Harlan JM. Endothelial cell death induced by tumor necrosis factor-alpha is inhibited by the Bcl-2 family member, A1. *J Biol Chem* 1996;271(44):27201-4.
(141) Chung HT, Pae HO, Choi BM, Billiar TR, Kim YM. Nitric oxide as a bioregulator of apoptosis. *Biochem Biophys Res Commun* 2001;282(5):1075-9.
(142) Kockx MM and Herman AG. Apoptosis in atherosclerosis: beneficial or detrimental? *Cardiovasc Res* 2000;45(3):736-46.
(143) Polte T, Oberle S, Schroder H. Nitric oxide protects endothelial cells from tumor necrosis factor-alpha-mediated cytotoxicity: possible involvement of cyclic GMP. *FEBS Lett* 1997;409(1):46-8.
(144) Dimmeler S, Haendeler J, Nehls M, Zeiher AM. Suppression of apoptosis by nitric oxide via inhibition of interleukin-1beta-converting enzyme (ICE)-like and cysteine protease protein (CPP)-32-like proteases. *J Exp Med* 1997;185(4):601-7.

(145) Stoneman VE and Bennett MR. Role of apoptosis in atherosclerosis and its therapeutic implications. *Clin Sci (Lond)* 2004;107(4):343-54.
(146) Mallat Z and Tedgui A. Apoptosis in the vasculature: mechanisms and functional importance. *Br J Pharmacol* 2000;130(5):947-62.
(147) Rosner D, Stoneman V, Littlewood T, McCarthy N, Figg N, Wang Y, Tellides G, Bennett M. Interferon-gamma induces Fas trafficking and sensitization to apoptosis in vascular smooth muscle cells via a. *Am J Pathol* 2006;168(6):2054-63.
(148) Boyle JJ, Weissberg PL, Bennett MR. Tumor necrosis factor-alpha promotes macrophage-induced vascular smooth muscle cell apoptosis by direct and autocrine mechanisms. *Arterioscler Thromb Vasc Biol* 2003;23(9):1553-8.
(149) Lee T and Chau L. Fas/Fas ligand-mediated death pathway is involved in oxLDL-induced apoptosis in vascular smooth muscle cells. *Am J Physiol Cell Physiol* 2001;280(3):C709-C718.
(150) Bennett MR, Evan GI, Schwartz SM. Apoptosis of human vascular smooth muscle cells derived from normal vessels and coronary atherosclerotic plaques. *J Clin Invest* 1995;95(5):2266-74.
(151) Bennett MR, Littlewood TD, Schwartz SM, Weissberg PL. Increased sensitivity of human vascular smooth muscle cells from atherosclerotic plaques to p53-mediated apoptosis. *Circ Res* 1997;81(4):591-9.
(152) Bennett M, Macdonald K, Chan SW, Luzio JP, Simari R, Weissberg P. Cell surface trafficking of Fas: a rapid mechanism of p53-mediated apoptosis. *Science* 1998;282(5387):290-3.
(153) Bennett MR, Macdonald K, Chan SW, Boyle JJ, Weissberg PL. Cooperative interactions between RB and p53 regulate cell proliferation, cell senescence, and apoptosis in human vascular smooth muscle cells from atherosclerotic plaques. *Circ Res* 1998;82(6):704-12.
(154) Martinet W and Kockx MM. Apoptosis in atherosclerosis: focus on oxidized lipids and inflammation. *Curr Opin Lipidol* 2001;12(5):535-41.
(155) Tabas I. Apoptosis and plaque destabilization in atherosclerosis: the role of macrophage apoptosis induced by cholesterol. *Cell Death Differ* 2004;11 Suppl 1:S12-S16.
(156) Colles SM, Irwin KC, Chisolm GM. Roles of multiple oxidized LDL lipids in cellular injury: dominance of 7 beta-hydroperoxycholesterol. *J Lipid Res* 1996;37(9):2018-28.
(157) Panini SR and Sinensky MS. Mechanisms of oxysterol-induced apoptosis. *Curr Opin Lipidol* 2001;12(5):529-33.
(158) Hamilton JA, Myers D, Jessup W, Cochrane F, Byrne R, Whitty G, Moss S. Oxidized LDL can induce macrophage survival, DNA synthesis, and enhanced proliferative response to CSF-1 and GM-CSF. *Arterioscler Thromb Vasc Biol* 1999;19(1):98-105.
(159) Hundal RS, Gomez-Munoz A, Kong JY, Salh BS, Marotta A, Duronio V, Steinbrecher UP. Oxidized low density lipoprotein inhibits macrophage apoptosis by blocking ceramide generation, thereby maintaining protein kinase B activation and Bcl-XL levels. *J Biol Chem* 2003;278(27):24399-408.
(160) Fazio S, Major AS, Swift LL, Gleaves LA, Accad M, Linton MF, Farese RV, Jr. Increased atherosclerosis in LDL receptor-null mice lacking ACAT1 in macrophages. *J Clin Invest* 2001;107(2):163-71.
(161) Feng B, Zhang D, Kuriakose G, Devlin CM, Kockx M, Tabas I. Niemann-Pick C heterozygosity confers resistance to lesional necrosis and macrophage apoptosis in murine atherosclerosis. *Proc Natl Acad Sci U S A* 2003;100(18):10423-8.
(162) Tabas I, Seimon T, Timmins J, Li G, Lim W. Macrophage apoptosis in advanced atherosclerosis. *Ann N Y Acad Sci* 2009;1173 Suppl 1:E40-E45.
(163) Seimon TA et al. Atherogenic lipids and lipoproteins trigger CD36-TLR2-dependent apoptosis in macrophages undergoing endoplasmic reticulum stress. *Cell Metab* 2010;12(5):467-82.
(164) Secchiero P, Candido R, Corallini F, Zacchigna S, Toffoli B, Rimondi E, Fabris B, Giacca M, Zauli G. Systemic tumor necrosis factor-related apoptosis-inducing ligand delivery shows antiatherosclerotic activity in apolipoprotein E-null diabetic mice. *Circulation* 2006;114(14):1522-30.
(165) Zadelaar AS et al. Increased vulnerability of pre-existing atherosclerosis in ApoE-deficient mice following adenovirus-mediated Fas ligand gene transfer. *Atherosclerosis* 2005;183(2):244-50.
(166) Sleiman L, Beanlands R, Hasu M, Thabet M, Norgaard A, Chen YX, Holcik M, Whitman S. Loss of cellular inhibitor of apoptosis protein 2 reduces atherosclerosis in atherogenic apoE-/- C57BL/6 mice on high-fat diet. *J Am Heart Assoc* 2013;2(5):e000259.
(167) Arai S et al. A role for the apoptosis inhibitory factor AIM/Spalpha/Api6 in atherosclerosis development. *Cell Metab* 2005;1(3):201-13.
(168) Shearn AI et al. Bcl-x inactivation in macrophages accelerates progression of advanced atherosclerotic lesions in Apoe(-/-) mice. *Arterioscler Thromb Vasc Biol* 2012;32(5):1142-9.
(169) Thorp E, Li Y, Bao L, Yao PM, Kuriakose G, Rong J, Fisher EA, Tabas I. Brief report: increased apoptosis in advanced atherosclerotic lesions of Apoe-/- mice lacking macrophage Bcl-2. *Arterioscler Thromb Vasc Biol* 2009;29(2):169-72.

(170) Stoneman V, Braganza D, Figg N, Mercer J, Lang R, Goddard M, Bennett M. Monocyte/macrophage suppression in CD11b diphtheria toxin receptor transgenic mice differentially affects atherogenesis and established plaques. *Circ Res* 2007;100(6):884-93.
(171) Gautier EL, Huby T, Witztum JL, Ouzilleau B, Miller ER, Saint-Charles F, Aucouturier P, Chapman MJ, Lesnik P. Macrophage apoptosis exerts divergent effects on atherogenesis as a function of lesion stage. *Circulation* 2009;119(13):1795-804.
(172) Clarke MC, Littlewood TD, Figg N, Maguire JJ, Davenport AP, Goddard M, Bennett MR. Chronic apoptosis of vascular smooth muscle cells accelerates atherosclerosis and promotes calcification and medial degeneration. *Circ Res* 2008;102(12):1529-38.
(173) Clarke MC, Figg N, Maguire JJ, Davenport AP, Goddard M, Littlewood TD, Bennett MR. Apoptosis of vascular smooth muscle cells induces features of plaque vulnerability in atherosclerosis. *Nat Med* 2006;12(9):1075-80.
(174) Schreyer SA, Peschon JJ, LeBoeuf RC. Accelerated atherosclerosis in mice lacking tumor necrosis factor receptor p55. *J Biol Chem* 1996;271(42):26174-8.
(175) Branen L, Hovgaard L, Nitulescu M, Bengtsson E, Nilsson J, Jovinge S. Inhibition of tumor necrosis factor-alpha reduces atherosclerosis in apolipoprotein E knockout mice. *Arterioscler Thromb Vasc Biol* 2004;24(11):2137-42.
(176) Aprahamian T, Rifkin I, Bonegio R, Hugel B, Freyssinet JM, Sato K, Castellot JJ, Jr., Walsh K. Impaired clearance of apoptotic cells promotes synergy between atherogenesis and autoimmune disease. *J Exp Med* 2004;199(8):1121-31.
(177) Feng X et al. ApoE-/-Fas-/- C57BL/6 mice: a novel murine model simultaneously exhibits lupus nephritis, atherosclerosis, and osteopenia. *J Lipid Res* 2007;48(4):794-805.
(178) Di Bartolo BA, Cartland SP, Harith HH, Bobryshev YV, Schoppet M, Kavurma MM. TRAIL-deficiency accelerates vascular calcification in atherosclerosis via modulation of RANKL. *PLoS One* 2013;8(9):e74211.
(179) Liu J, Thewke DP, Su YR, Linton MF, Fazio S, Sinensky MS. Reduced macrophage apoptosis is associated with accelerated atherosclerosis in low-density lipoprotein receptor-null mice. *Arterioscler Thromb Vasc Biol* 2005;25(1):174-9.
(180) Guevara NV, Kim HS, Antonova EI, Chan L. The absence of p53 accelerates atherosclerosis by increasing cell proliferation in vivo. *Nat Med* 1999;5(3):335-9.
(181) Merched AJ, Williams E, Chan L. Macrophage-specific p53 expression plays a crucial role in atherosclerosis development and plaque remodeling. *Arterioscler Thromb Vasc Biol* 2003;23(9):1608-14.
(182) van Vlijmen BJ et al. Macrophage p53 deficiency leads to enhanced atherosclerosis in APOE*3-Leiden transgenic mice. *Circ Res* 2001;88(8):780-6.
(183) Boesten LS et al. Macrophage p53 controls macrophage death in atherosclerotic lesions of apolipoprotein E deficient mice. *Atherosclerosis* 2009;207(2):399-404.
(184) Mercer J, Figg N, Stoneman V, Braganza D, Bennett MR. Endogenous p53 protects vascular smooth muscle cells from apoptosis and reduces atherosclerosis in ApoE knockout mice. *Circ Res* 2005;96(6):667-74.
(185) Gonzalez-Navarro H, Abu Nabah YN, Vinue A, Andres-Manzano MJ, Collado M, Serrano M, Andres V. p19(ARF) deficiency reduces macrophage and vascular smooth muscle cell apoptosis and aggravates atherosclerosis. *J Am Coll Cardiol* 2010;55(20):2258-68.
(186) Thorp E, Li G, Seimon TA, Kuriakose G, Ron D, Tabas I. Reduced apoptosis and plaque necrosis in advanced atherosclerotic lesions of Apoe-/- and Ldlr-/- mice lacking CHOP. *Cell Metab* 2009;9(5):474-81.
(187) Van Vre EA, Ait-Oufella H, Tedgui A, Mallat Z. Apoptotic cell death and efferocytosis in atherosclerosis. *Arterioscler Thromb Vasc Biol* 2012;32(4):887-93.
(188) Mallat Z, Hugel B, Ohan J, Leseche G, Freyssinet JM, Tedgui A. Shed membrane microparticles with procoagulant potential in human atherosclerotic plaques: a role for apoptosis in plaque thrombogenicity. *Circulation* 1999;99(3):348-53.
(189) Clarke M and Bennett M. The emerging role of vascular smooth muscle cell apoptosis in atherosclerosis and plaque stability. *Am J Nephrol* 2006;26(6):531-5.
(190) Flynn PD, Byrne CD, Baglin TP, Weissber PL, Bennett MR. Thrombin generation by apoptotic vascular smooth muscle cells. *Blood* 1997;89(12):4378-84.
(191) Clarke MC, Talib S, Figg NL, Bennett MR. Vascular smooth muscle cell apoptosis induces interleukin-1-directed inflammation: effects of hyperlipidemia-mediated inhibition of phagocytosis. *Circ Res* 2010;106(2):363-72.
(192) Martinet W and De Meyer GRY. Autophagy in atherosclerosis: a cell survival and death phenomenon with therapeutic potential. *Circ Res* 2009;104(3):304-17.
(193) Perrotta I. The use of electron microscopy for the detection of autophagy in human atherosclerosis. *Micron* 2013;50:7-13.

(194) Swaminathan B, Goikuria H, Vega R, Rodriguez-Antiguedad A, Lopez MA, Freijo MM, Vandenbroeck K, Alloza I. Autophagic marker MAP1LC3B expression levels are associated with carotid atherosclerosis symptomatology. *PLoS One* 2014;9(12):e115176.
(195) Liu H, Cao Y, Tong T, Shi J, Zhang Y, Yang Y, Liu C. Autophagy in atherosclerosis: a phenomenon found in human carotid atherosclerotic plaques. *Chin Med J (Engl)* 2015;128(1):69-74.
(196) Grootaert MOJ, Kurdi A, De Munck DG, Martinet W, De Meyer GRY. Autophagy in Atherosclerosis. In: Hayat MA, ed. *Autophagy*.Oxford: Elsevier; 2016. p. 251-68.
(197) Kiffin R, Bandyopadhyay U, Cuervo AM. Oxidative stress and autophagy. *Antioxid Redox Signal* 2006;8(1-2):152-62.
(198) Razani B et al. Autophagy links inflammasomes to atherosclerotic progression. *Cell Metab* 2012;15(4):534-44.
(199) Kurz T, Terman A, Brunk UT. Autophagy, ageing and apoptosis: the role of oxidative stress and lysosomal iron. *Arch Biochem Biophys* 2007;462(2):220-30.
(200) Duewell P et al. NLRP3 inflammasomes are required for atherogenesis and activated by cholesterol crystals. *Nature* 2010;464(7293):1357-61.
(201) De Meyer GRY, Grootaert MOJ, Michiels CF, Kurdi A, Schrijvers DM, Martinet W. Autophagy in vascular disease. *Circ Res* 2015;116(3):468-79.
(202) Martinet W, Timmermans JP, De Meyer GRY. Methods to assess autophagy in situ - Transmission electron microscopy versus immunohistochemistry. In: Galluzzi L, Kroemer G, eds. *Methods in Enzymology: cell-wide metabolic alterations associated with malignancy*.Waltham, Massachusetts: Academic Press; 2014. p. 89-114.
(203) Klionsky DJ. Guidelines for the use and interpretation of assays for monitoring autophagy (3rd edition). *Autophagy* 2016;12(1):1-222.
(204) Zhang YL, Cao YJ, Zhang X, Liu HH, Tong T, Xiao GD, Yang YP, Liu CF. The autophagy-lysosome pathway: a novel mechanism involved in the processing of oxidized LDL in human vascular endothelial cells. *Biochem Biophys Res Commun* 2010;394(2):377-82.
(205) Mattart L et al. The peroxynitrite donor 3-morpholinosydnonimine activates Nrf2 and the UPR leading to a cytoprotective response in endothelial cells. *Cell Sign* 2012;24(1):199-213.
(206) Chen G et al. Hypoxia-induced autophagy in endothelial cells: a double-edged sword in the progression of infantile haemangioma? *Cardiovasc Res* 2013;98(3):437-48.
(207) Xie Y, You SJ, Zhang YL, Han Q, Cao YJ, Xu XS, Yang YP, Li J, Liu CF. Protective role of autophagy in AGE-induced early injury of human vascular endothelial cells. *Mol Med Rep* 2011;4(3):459-64.
(208) Shafique E et al. Oxidative stress improves coronary endothelial function through activation of the pro-survival kinase AMPK. *Aging (Albany NY)* 2013;5(7):515-30.
(209) Mollace V et al. Oxidized LDL attenuates protective autophagy and induces apoptotic cell death of endothelial cells: Role of oxidative stress and LOX-1 receptor expression. *Int J Cardiol* 2015;184:152-8.
(210) Margariti A et al. XBP1 mRNA splicing triggers an autophagic response in endothelial cells through BECLIN-1 transcriptional activation. *J Biol Chem* 2013;288(2):859-72.
(211) Liu J et al. Shear stress regulates endothelial cell autophagy via redox regulation and Sirt1 expression. *Cell Death Dis* 2015;6:e1827.
(212) Ding Z, Wang X, Schnackenberg L, Khaidakov M, Liu S, Singla S, Dai Y, Mehta JL. Regulation of autophagy and apoptosis in response to ox-LDL in vascular smooth muscle cells, and the modulatory effects of the microRNA hsa-let-7 g. *Int J Cardiol* 2013;168(2):1378-85.
(213) He C, Zhu H, Zhang W, Okon I, Wang Q, Li H, Le YZ, Xie Z. 7-Ketocholesterol induces autophagy in vascular smooth muscle cells through Nox4 and Atg4B. *Am J Pathol* 2013;183(2):626-37.
(214) Hill BG, Haberzettl P, Ahmed Y, Srivastava S, Bhatnagar A. Unsaturated lipid peroxidation-derived aldehydes activate autophagy in vascular smooth-muscle cells. *Biochem J* 2008;410(3):525-34.
(215) Salabei JK and Hill BG. Implications of autophagy for vascular smooth muscle cell function and plasticity. *Free Radic Biol Med* 2013;65:693-703.
(216) Salabei JK, Cummins TD, Singh M, Jones SP, Bhatnagar A, Hill BG. PDGF-mediated autophagy regulates vascular smooth muscle cell phenotype and resistance to oxidative stress. *Biochem J* 2013;451(3):375-88.
(217) Martin KA, Rzucidlo EM, Merenick BL, Fingar DC, Brown DJ, Wagner RJ, Powell RJ. The mTOR/p70 S6K1 pathway regulates vascular smooth muscle cell differentiation. *Am J Physiol Cell Physiol* 2004;286(3):C507-C517.
(218) Salabei JK, Balakumaran A, Frey JC, Boor PJ, Treinen-Moslen M, Conklin DJ. Verapamil stereoisomers induce antiproliferative effects in vascular smooth muscle cells via autophagy. *Toxicol Appl Pharmacol* 2012;262(3):265-72.
(219) Wei YM, Li X, Xu M, Abais JM, Chen Y, Riebling CR, Boini KM, Li PL, Zhang Y. Enhancement of autophagy by simvastatin through inhibition of Rac1-mTOR signaling pathway in coronary arterial myocytes. *Cell Physiol Biochem* 2013;31(6):925-37.

(220) Liao X, Sluimer JC, Wang Y, Subramanian M, Brown K, Pattison JS, Robbins J, Martinez J, Tabas I. Macrophage autophagy plays a protective role in advanced atherosclerosis. *Cell Metab* 2012;15(4):545-53.
(221) Raciti M, Lotti LV, Valia S, Pulcinelli FM, Di Renzo L. JNK2 is activated during ER stress and promotes cell survival. *Cell Death Dis* 2012;3:e429.
(222) Huang B, Jin M, Yan H, Cheng Y, Huang D, Ying S, Zhang L. Simvastatin enhances oxidizedlow density lipoproteininduced macrophage autophagy and attenuates lipid aggregation. *Mol Med Rep* 2015;11(2):1093-8.
(223) Ouimet M, Franklin V, Mak E, Liao X, Tabas I, Marcel YL. Autophagy regulates cholesterol efflux from macrophage foam cells via lysosomal acid lipase. *Cell Metab* 2011;13(6):655-67.
(224) Liu K, Zhao E, Ilyas G, Lalazar G, Lin Y, Haseeb M, Tanaka KE, Czaja MJ. Impaired macrophage autophagy increases the immune response in obese mice by promoting proinflammatory macrophage polarization. *Autophagy* 2015;11(2):271-84.
(225) Torisu T et al. Autophagy regulates endothelial cell processing, maturation and secretion of von Willebrand factor. *Nat Med* 2013;19(10):1281-7.
(226) LaRocca TJ, Henson GD, Thorburn A, Sindler AL, Pierce GL, Seals DR. Translational evidence that impaired autophagy contributes to arterial ageing. *J Physiol* 2012;590(14):3305-16.
(227) Tabas I. Consequences and therapeutic implications of macrophage apoptosis in atherosclerosis: the importance of lesion stage and phagocytic efficiency. *Arterioscler Thromb Vasc Biol* 2005;25(11):2255-64.
(228) Virmani R, Burke AP, Willerson J, Farb A, Narula J, Kolodgie FD. The pathology of vulnerable plaque. In: Virmani R, Narula J, Leon M, Willerson J, eds. *The vulnerable atherosclerotic plaque: strategies for diagnosis and management*. Malden: Blackwell Futura; 2007. p. 21-36.
(229) Fok PW. Growth of necrotic cores in atherosclerotic plaque. *Math Med Biol* 2012;29(4):301-27.
(230) Ball RY, Stowers EC, Burton JH, Cary NR, Skepper JN, Mitchinson MJ. Evidence that the death of macrophage foam cells contributes to the lipid core of atheroma. *Atherosclerosis* 1995;114(1):45-54.
(231) Seimon TA, Wang Y, Han S, Senokuchi T, Schrijvers DM, Kuriakose G, Tall AR, Tabas IA. Macrophage deficiency of p38alpha MAPK promotes apoptosis and plaque necrosis in advanced atherosclerotic lesions in mice. *J Clin Invest* 2009;119(4):886-98.
(232) Martinet W, Schrijvers DM, De Meyer GRY. Necrotic cell death in atherosclerosis. *Basic Res Cardiol* 2011;106(5):749-60.
(233) Tangirala RK, Jerome WG, Jones NL, Small DM, Johnson WJ, Glick JM, Mahlberg FH, Rothblat GH. Formation of cholesterol monohydrate crystals in macrophage-derived foam cells. *J Lipid Res* 1994;35(1):93-104.
(234) van LK, Duvoisin RM, Engelhardt H, Wiedmann M. A function for lipoxygenase in programmed organelle degradation. *Nature* 1998;395(6700):392-5.
(235) Griendling KK, Sorescu D, Ushio-Fukai M. NAD(P)H oxidase: role in cardiovascular biology and disease. *Circ Res* 2000;86(5):494-501.
(236) Madamanchi NR and Runge MS. Mitochondrial dysfunction in atherosclerosis. *Circ Res* 2007;100(4):460-73.
(237) Ballinger SW et al. Mitochondrial integrity and function in atherogenesis. *Circulation* 2002;106(5):544-9.
(238) Harrison CM, Pompilius M, Pinkerton KE, Ballinger SW. Mitochondrial oxidative stress significantly influences atherogenic risk and cytokine-induced oxidant production. *Environ Health Perspect* 2011;119(5):676-81.
(239) Ari E, Kaya Y, Demir H, Cebi A, Alp HH, Bakan E, Odabasi D, Keskin S. Oxidative DNA damage correlates with carotid artery atherosclerosis in hemodialysis patients. *Hemodial Int* 2011;15(4):453-9.
(240) Wang Y, Wang GZ, Rabinovitch PS, Tabas I. Macrophage mitochondrial oxidative stress promotes atherosclerosis and nuclear factor-kappaB-mediated inflammation in macrophages. *Circ Res* 2014;114(3):421-33.
(241) Tabas I and Wang Y. Emerging Roles of Mitochondria ROS in Atherosclerotic Lesions: Causation or Association? *J Atheroscler Thromb* 2014.
(242) Nicotera P, Leist M, Ferrando-May E. Intracellular ATP, a switch in the decision between apoptosis and necrosis. *Toxicol Lett* 1998;102-103:139-42.
(243) Phair RD. Cellular calcium and atherosclerosis: a brief review. *Cell Calcium* 1988;9(5-6):275-84.
(244) Voll RE, Herrmann M, Roth EA, Stach C, Kalden JR, Girkontaite I. Immunosuppressive effects of apoptotic cells. *Nature* 1997;390(6658):350-1.
(245) Huynh ML, Fadok VA, Henson PM. Phosphatidylserine-dependent ingestion of apoptotic cells promotes TGF-beta1 secretion and the resolution of inflammation. *J Clin Invest* 2002;109(1):41-50.
(246) Schrijvers DM, De Meyer GRY, Herman AG, Martinet W. Phagocytosis in atherosclerosis: Molecular mechanisms and implications for plaque progression and stability. *Cardiovasc Res* 2007;73(3):470-80.

(247) Thorp E and Tabas I. Mechanisms and consequences of efferocytosis in advanced atherosclerosis. *J Leukoc Biol* 2009;86(5):1089-95.
(248) Sambrano GR, Parthasarathy S, Steinberg D. Recognition of oxidatively damaged erythrocytes by a macrophage receptor with specificity for oxidized low density lipoprotein. *Proc Natl Acad Sci U S A* 1994;91(8):3265-9.
(249) Sambrano GR and Steinberg D. Recognition of oxidatively damaged and apoptotic cells by an oxidized low density lipoprotein receptor on mouse peritoneal macrophages: role of membrane phosphatidylserine. *Proc Natl Acad Sci U S A* 1995;92(5):1396-400.
(250) Chang MK, Bergmark C, Laurila A, Horkko S, Han KH, Friedman P, Dennis EA, Witztum JL. Monoclonal antibodies against oxidized low-density lipoprotein bind to apoptotic cells and inhibit their phagocytosis by elicited macrophages: evidence that oxidation-specific epitopes mediate macrophage recognition. *Proc Natl Acad Sci U S A* 1999;96(11):6353-8.
(251) Schrijvers DM, De Meyer GRY, Kockx MM, Herman AG, Martinet W. Phagocytosis of apoptotic cells by macrophages is impaired in atherosclerosis. *Arterioscler Thromb Vasc Biol* 2005;25(6):1256-61.
(252) Loegering DJ, Raley MJ, Reho TA, Eaton JW. Macrophage dysfunction following the phagocytosis of IgG-coated erythrocytes: production of lipid peroxidation products. *J Leukoc Biol* 1996;59(3):357-62.
(253) Ait-Oufella H et al. Lactadherin deficiency leads to apoptotic cell accumulation and accelerated atherosclerosis in mice. *Circulation* 2007;115(16):2168-77.
(254) Thorp E, Cui D, Schrijvers DM, Kuriakose G, Tabas I. Mertk receptor mutation reduces efferocytosis efficiency and promotes apoptotic cell accumulation and plaque necrosis in atherosclerotic lesions of apoe-/- mice. *Arterioscler Thromb Vasc Biol* 2008;28(8):1421-8.
(255) Seimon T and Tabas I. Mechanisms and consequences of macrophage apoptosis in atherosclerosis. *J Lipid Res* 2009;50 Suppl:S382-S387.
(256) Scaffidi P, Misteli T, Bianchi ME. Release of chromatin protein HMGB1 by necrotic cells triggers inflammation. *Nature* 2002;418(6894):191-5.
(257) Andersson U et al. High mobility group 1 protein (HMG-1) stimulates proinflammatory cytokine synthesis in human monocytes. *J Exp Med* 2000;192(4):565-70.
(258) Erlandsson HH and Andersson U. Mini-review: The nuclear protein HMGB1 as a proinflammatory mediator. *Eur J Immunol* 2004;34(6):1503-12.
(259) Lundberg B. Chemical composition and physical state of lipid deposits in atherosclerosis. *Atherosclerosis* 1985;56(1):93-110.
(260) Hutter R et al. Caspase-3 and tissue factor expression in lipid-rich plaque macrophages: evidence for apoptosis as link between inflammation and atherothrombosis. *Circulation* 2004;109(16):2001-8.
(261) Lin J et al. A role of RIP3-mediated macrophage necrosis in atherosclerosis development. *Cell Rep* 2013;3(1):200-10.
(262) Degterev A, Maki JL, Yuan J. Activity and specificity of necrostatin-1, small-molecule inhibitor of RIP1 kinase. *Cell Death Differ* 2013;20(2):366.
(263) Takahashi N et al. Necrostatin-1 analogues: critical issues on the specificity, activity and in vivo use in experimental disease models. *Cell Death Dis* 2012;3:e437.
(264) Karunakaran D et al. Targeting macrophage necroptosis for therapeutic and diagnostic interventions in atherosclerosis. *Sci. Adv.* 2016;2:e1600224.
(265) Mandal P et al. RIP3 induces apoptosis independent of pronecrotic kinase activity. *Mol Cell* 2014;56(4):481-95.
(266) Piot C et al. Effect of cyclosporine on reperfusion injury in acute myocardial infarction. *N Engl J Med* 2008;359(5):473-81.
(267) Emeson EE and Shen ML. Accelerated atherosclerosis in hyperlipidemic C57BL/6 mice treated with cyclosporin A. *Am J Pathol* 1993;142(6):1906-15.
(268) Kockx M, Jessup W, Kritharides L. Cyclosporin A and atherosclerosis--cellular pathways in atherogenesis. *Pharmacol Ther* 2010;128(1):106-18.
(269) Pacher P and Szabo C. Role of poly(ADP-ribose) polymerase 1 (PARP-1) in cardiovascular diseases: the therapeutic potential of PARP inhibitors. *Cardiovasc Drug Rev* 2007;25(3):235-60.
(270) Linkermann A et al. Synchronized renal tubular cell death involves ferroptosis. *Proc Natl Acad Sci U S A* 2014;111(47):16836-41.
(271) Hofmans S, Vanden Berghe T, Devisscher L, Hassannia B, Lyssens S, Joossens J, van d, V, Vandenabeele P, Augustyns K. Novel Ferroptosis Inhibitors with Improved Potency and ADME Properties. *J Med Chem* 2016;59(5):2041-53.
(272) Yigitkanli K et al. Inhibition of 12/15-lipoxygenase as therapeutic strategy to treat stroke. *Ann Neurol* 2013;73(1):129-35.
(273) van LK, Holman TR, Maloney DJ. The potential of 12/15-lipoxygenase inhibitors in stroke therapy. *Future Med Chem* 2014;6(17):1853-5.
(274) Kim HJ et al. NecroX as a novel class of mitochondrial reactive oxygen species and ONOO scavenger. *Arch Pharm Res* 2010;33(11):1813-23.

(275) Choi JM, Park KM, Kim SH, Hwang DW, Chon SH, Lee JH, Lee SY, Lee YJ. Effect of necrosis modulator necrox-7 on hepatic ischemia-reperfusion injury in beagle dogs. *Transplant Proc* 2010;42(9):3414-21.
(276) Park J et al. NecroX-7 prevents oxidative stress-induced cardiomyopathy by inhibition of NADPH oxidase activity in rats. *Toxicol Appl Pharmacol* 2012;263(1):1-6.
(277) Jin SA et al. Beneficial Effects of Necrosis Modulator, Indole Derivative NecroX-7, on Renal Ischemia-Reperfusion Injury in Rats. *Transplant Proc* 2016;48(1):199-204.
(278) Giles KM, Ross K, Rossi AG, Hotchin NA, Haslett C, Dransfield I. Glucocorticoid augmentation of macrophage capacity for phagocytosis of apoptotic cells is associated with reduced p130Cas expression, loss of paxillin/pyk2 phosphorylation, and high levels of active Rac. *J Immunol* 2001;167(2):976-86.
(279) Strohmayer EA and Krakoff LR. Glucocorticoids and cardiovascular risk factors. *Endocrinol Metab Clin North Am* 2011;40(2):409-17, ix.
(280) Morimoto K et al. Lovastatin enhances clearance of apoptotic cells (efferocytosis) with implications for chronic obstructive pulmonary disease. *J Immunol* 2006;176(12):7657-65.
(281) Bae HB, Zmijewski JW, Deshane JS, Tadie JM, Chaplin DD, Takashima S, Abraham E. AMP-activated protein kinase enhances the phagocytic ability of macrophages and neutrophils. *FASEB J* 2011;25(12):4358-68.
(282) Forouzandeh F, Salazar G, Patrushev N, Xiong S, Hilenski L, Fei B, Alexander RW. Metformin beyond diabetes: pleiotropic benefits of metformin in attenuation of atherosclerosis. *J Am Heart Assoc* 2014;3(6):e001202.

CHAPTER 2

Aims of the study

2.1 Aims of the study

We are challenged to develop new therapeutic opportunities to fight atherosclerotic disease as not all patients benefit from the current pharmacotherapy and the risk of a recurrent event after an acute coronary syndrome remains unacceptably high (approx. 10-20% within the first 12 months).[1] Recent clinical observations confirmed that plaque rupture is the most common cause of coronary thrombosis in dying patients but also in those who survive.[2] In fact, the composition and the vulnerability of the plaque, rather than its size or the consequent degree of stenosis, are currently considered to be the most important determinants for acute coronary syndromes.[3-5] These findings underscore the need for rupture-preventive approaches that specifically target the mechanisms leading to plaque destabilisation.

One of the main mechanisms converting a stable lesion into a vulnerable, rupture-prone plaque is lesional cell death.[6, 7] Numerous studies have demonstrated that increased apoptotic and necrotic cell death of macrophages and vascular smooth muscle cells (VSMCs), particularly in advanced lesions, promotes thinning of the fibrous cap,[8, 9] enlargement of the necrotic core[10, 11] and induction of inflammatory responses[12]. Although it seems intuitively reasonable that increased cell death may actually reduce atherosclerosis by limiting the cellular build-up in plaques, this approach will only be adequate if the clearance of these dead cells by phagocytes occurs in a fast, efficient and inflammation-resolving manner. However, compelling evidence indicates that the phagocytic clearance of apoptotic cells is defective in advanced atherosclerotic plaques.[13, 14] Also necrotic cells have been shown to be less efficiently cleared.[15] The increased incidence of apoptotic and necrotic cell death in advanced atherosclerotic plaques coupled with defective dead cell clearance, leads to increased plaque vulnerability. In contrast to apoptosis and necrosis, the consequences of autophagy on atherosclerotic plaque stability are still not fully explored, yet, worthwhile to investigate given its role as a 'balancer' between life and death. Accumulating evidence suggest that autophagy becomes dysfunctional during the progression of atherosclerosis.[16] Moreover, loss-of-function studies in macrophages showed that defective autophagy promotes plaque apoptosis,[17] plaque necrosis[17] and inflammasome hyperactivation[16], whereas the consequences of defective autophagy in VSMCs in atherosclerosis are still unknown.

Therefore, the three main research questions addressed in this thesis were **(Fig. 2.1)**:

1) Does apoptosis impairment improve plaque stability?

2) What are the consequences of defective autophagy in VSMCs in atherosclerosis?

3) Is inhibition of necrosis a good strategy for plaque stabilisation?

In **chapter 3**, *ApoE*$^{-/-}$ mice lacking the effector caspase-3 were used as a model for defective apoptosis in atherosclerosis. Although different mouse models have already been designed over the last 10 years to inhibit apoptosis,[18-28] caspase-3 has never been explored as a suitable target to modulate apoptotic cell death in atherosclerosis. By genetic disruption of caspase-3, we aimed to block the execution of apoptosis and to prevent subsequent necrotic core enlargement. To investigate the impact on plaque stability, cellular composition and the degree of cell death was analysed in plaques of *Casp3*$^{-/-}$*ApoE*$^{-/-}$ mice versus *Casp3*$^{+/+}$*ApoE*$^{-/-}$ mice after 16 weeks of western-type diet (WD).

In **chapter 4**, we aimed to investigate the role of autophagy in VSMC phenotype, death and survival using VSMC-specific *Atg7* deficient mice. Firstly, a ligation-injury model was applied to study the role of VSMC autophagy in neointima formation. Secondly, VSMC-specific *Atg7* deficient mice were crossbred with *ApoE*$^{-/-}$ mice to study the consequences of defective VSMC autophagy in early (10 weeks WD) and advanced (14 weeks WD) atherosclerosis. In this way, we were able to explore whether autophagy in VSMCs plays a similar role as in macrophages in atherosclerosis.

In **chapter 5**, we applied a pharmacological approach to inhibit necrosis formation in 16 weeks WD-fed *ApoE*$^{-/-}$ mice. Up till now, not many strategies have been performed to specifically target plaque necrosis, despite the well-known consequences of necrosis on atherosclerotic plaque stability. In this study, we investigated the plaque stabilising potential of NecroX-7, a newly developed necrosis inhibitor that targets mitochondrial reactive oxygen species.[29, 30] Besides plaque composition, different markers of cell death, oxidative stress and inflammation were analysed in plaques of NecroX-7-treated mice versus controls.

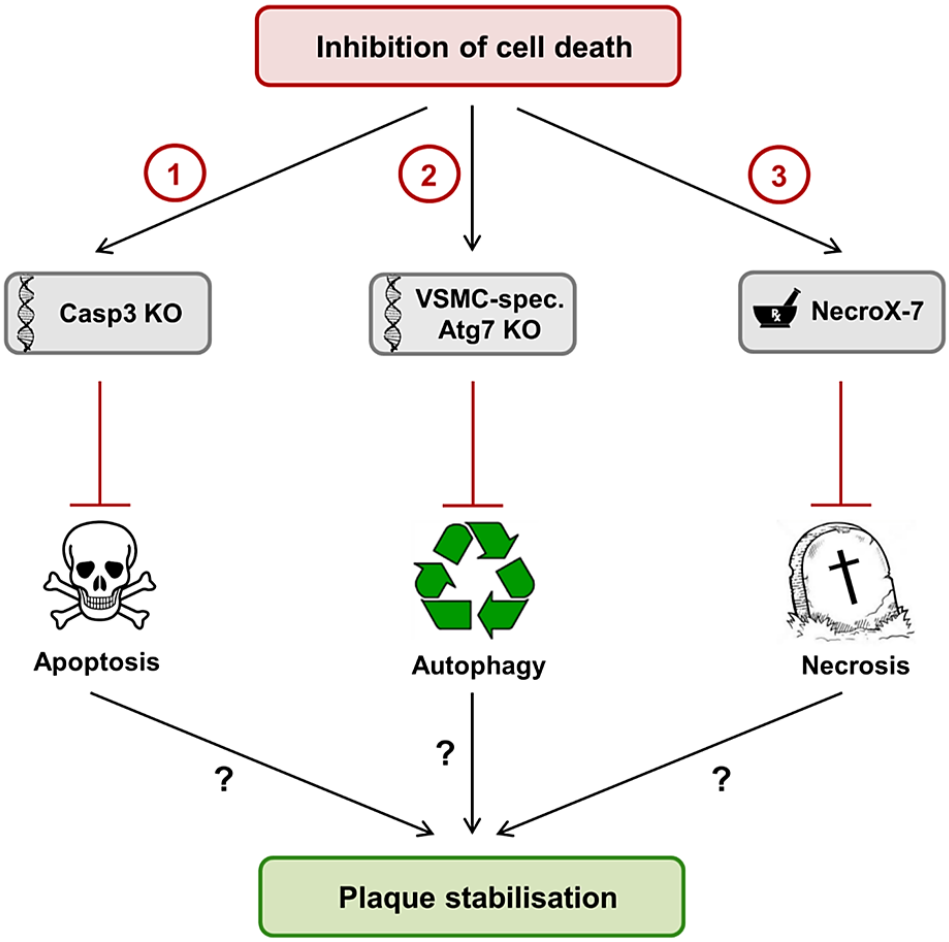

Figure 2.1: Schematic overview of the three different approaches, implemented in this thesis, to inhibit cell death in atherosclerosis as potential plaque stabilising strategies.
(1) *ApoE*$^{-/-}$ mice with a genetic disruption of the effector caspase-3 were used as a model for defective apoptosis in atherosclerosis. **(2)** To investigate the role of autophagy in vascular smooth muscle cells (VSMCs) in atherosclerosis, VSMC-specific *Atg7* deficient mice were crossbred with *ApoE*$^{-/-}$ mice. **(3)** In the third study, a pharmacological approach was applied to inhibit necrosis. The plaque stabilising potential of the necrosis inhibitor NecroX-7 was tested in *ApoE*$^{-/-}$ mice.

2.2 References

(1) Libby P, Bornfeldt KE, Tall AR. Atherosclerosis: Successes, Surprises, and Future Challenges. *Circ Res* 2016;118(4):531-4.
(2) Falk E, Nakano M, Bentzon JF, Finn AV, Virmani R. Update on acute coronary syndromes: the pathologists' view. *Eur Heart J* 2013;34(10):719-28.
(3) Falk E, Shah PK, Fuster V. Coronary plaque disruption. *Circulation* 1995;92(3):657-71.
(4) Mann JM and Davies MJ. Vulnerable plaque. Relation of characteristics to degree of stenosis in human coronary arteries. *Circulation* 1996;94(5):928-31.
(5) Pasterkamp G, Falk E, Woutman H, Borst C. Techniques characterizing the coronary atherosclerotic plaque: influence on clinical decision making? *J Am Coll Cardiol* 2000;36(1):13-21.
(6) Silvestre-Roig C, de Winther MP, Weber C, Daemen MJ, Lutgens E, Soehnlein O. Atherosclerotic plaque destabilization: mechanisms, models, and therapeutic strategies. *Circ Res* 2014;114(1):214-26.
(7) Martinet W, Schrijvers DM, De Meyer GRY. Pharmacological modulation of cell death in atherosclerosis: A promising approach toward plaque stabilization? *Br J Pharmacol* 2011.
(8) Clarke MC, Figg N, Maguire JJ, Davenport AP, Goddard M, Littlewood TD, Bennett MR. Apoptosis of vascular smooth muscle cells induces features of plaque vulnerability in atherosclerosis. *Nat Med* 2006;12(9):1075-80.
(9) Clarke MC, Littlewood TD, Figg N, Maguire JJ, Davenport AP, Goddard M, Bennett MR. Chronic apoptosis of vascular smooth muscle cells accelerates atherosclerosis and promotes calcification and medial degeneration. *Circ Res* 2008;102(12):1529-38.
(10) Thorp E, Li Y, Bao L, Yao PM, Kuriakose G, Rong J, Fisher EA, Tabas I. Brief report: increased apoptosis in advanced atherosclerotic lesions of Apoe-/- mice lacking macrophage Bcl-2. *Arterioscler Thromb Vasc Biol* 2009;29(2):169-72.
(11) Shearn AI et al. Bcl-x inactivation in macrophages accelerates progression of advanced atherosclerotic lesions in Apoe(-/-) mice. *Arterioscler Thromb Vasc Biol* 2012;32(5):1142-9.
(12) Gautier EL, Huby T, Witztum JL, Ouzilleau B, Miller ER, Saint-Charles F, Aucouturier P, Chapman MJ, Lesnik P. Macrophage apoptosis exerts divergent effects on atherogenesis as a function of lesion stage. *Circulation* 2009;119(13):1795-804.
(13) Schrijvers DM, De Meyer GRY, Kockx MM, Herman AG, Martinet W. Phagocytosis of apoptotic cells by macrophages is impaired in atherosclerosis. *Arterioscler Thromb Vasc Biol* 2005;25(6):1256-61.
(14) Thorp E and Tabas I. Mechanisms and consequences of efferocytosis in advanced atherosclerosis. *J Leukoc Biol* 2009;86(5):1089-95.
(15) Krysko DV, Brouckaert G, Kalai M, Vandenabeele P, D'Herde K. Mechanisms of internalization of apoptotic and necrotic L929 cells by a macrophage cell line studied by electron microscopy. *J Morphol* 2003;258(3):336-45.
(16) Razani B et al. Autophagy links inflammasomes to atherosclerotic progression. *Cell Metab* 2012;15(4):534-44.
(17) Liao X, Sluimer JC, Wang Y, Subramanian M, Brown K, Pattison JS, Robbins J, Martinez J, Tabas I. Macrophage autophagy plays a protective role in advanced atherosclerosis. *Cell Metab* 2012;15(4):545-53.
(18) Schreyer SA, Peschon JJ, LeBoeuf RC. Accelerated atherosclerosis in mice lacking tumor necrosis factor receptor p55. *J Biol Chem* 1996;271(42):26174-8.
(19) Aprahamian T, Rifkin I, Bonegio R, Hugel B, Freyssinet JM, Sato K, Castellot JJ, Jr., Walsh K. Impaired clearance of apoptotic cells promotes synergy between atherogenesis and autoimmune disease. *J Exp Med* 2004;199(8):1121-31.
(20) Branen L, Hovgaard L, Nitulescu M, Bengtsson E, Nilsson J, Jovinge S. Inhibition of tumor necrosis factor-alpha reduces atherosclerosis in apolipoprotein E knockout mice. *Arterioscler Thromb Vasc Biol* 2004;24(11):2137-42.
(21) Feng X et al. ApoE-/-Fas-/- C57BL/6 mice: a novel murine model simultaneously exhibits lupus nephritis, atherosclerosis, and osteopenia. *J Lipid Res* 2007;48(4):794-805.
(22) Liu J, Thewke DP, Su YR, Linton MF, Fazio S, Sinensky MS. Reduced macrophage apoptosis is associated with accelerated atherosclerosis in low-density lipoprotein receptor-null mice. *Arterioscler Thromb Vasc Biol* 2005;25(1):174-9.
(23) Guevara NV, Kim HS, Antonova EI, Chan L. The absence of p53 accelerates atherosclerosis by increasing cell proliferation in vivo. *Nat Med* 1999;5(3):335-9.
(24) van Vlijmen BJ et al. Macrophage p53 deficiency leads to enhanced atherosclerosis in APOE*3-Leiden transgenic mice. *Circ Res* 2001;88(8):780-6.
(25) Merched AJ, Williams E, Chan L. Macrophage-specific p53 expression plays a crucial role in atherosclerosis development and plaque remodeling. *Arterioscler Thromb Vasc Biol* 2003;23(9):1608-14.

(26) Mercer J, Figg N, Stoneman V, Braganza D, Bennett MR. Endogenous p53 protects vascular smooth muscle cells from apoptosis and reduces atherosclerosis in ApoE knockout mice. *Circ Res* 2005;96(6):667-74.
(27) Boesten LS et al. Macrophage p53 controls macrophage death in atherosclerotic lesions of apolipoprotein E deficient mice. *Atherosclerosis* 2009;207(2):399-404.
(28) Gonzalez-Navarro H, Abu Nabah YN, Vinue A, Andres-Manzano MJ, Collado M, Serrano M, Andres V. p19(ARF) deficiency reduces macrophage and vascular smooth muscle cell apoptosis and aggravates atherosclerosis. *J Am Coll Cardiol* 2010;55(20):2258-68.
(29) Kim HJ et al. NecroX as a novel class of mitochondrial reactive oxygen species and ONOO scavenger. *Arch Pharm Res* 2010;33(11):1813-23.
(30) Park J et al. NecroX-7 prevents oxidative stress-induced cardiomyopathy by inhibition of NADPH oxidase activity in rats. *Toxicol Appl Pharmacol* 2012;263(1):1-6.

CHAPTER 3

Caspase-3 deletion promotes necrosis in atherosclerotic plaques of ApoE knockout mice

Adapted from:
Grootaert MOJ, Schrijvers DM, Hermans M, De Meyer GRY, Martinet W. Caspase-3 deletion promotes necrosis in atherosclerotic plaques of *ApoE* knockout mice. *Oxidative Medicine and Cellular Longevity*, 2016 *(in revision)*

3.1 Introduction

Increasing evidence shows that vulnerable, rupture-prone plaques display higher levels of apoptosis than stable lesions.[1, 2] Apoptotic cell death of macrophages and vascular smooth muscle cells (VSMCs) have a detrimental impact on the stability of advanced atherosclerotic lesions. Specifically, apoptosis of VSMCs promotes plaque vulnerability by disintegration of the protective fibrous cap,[3] while macrophage apoptosis promotes necrotic core enlargement.[4, 5] Because the phagocytic clearance of apoptotic cells is impaired in advanced plaques, apoptotic bodies accumulate and undergo secondary necrosis.[6, 7]

The development of different strategies to target apoptosis in atherosclerosis using various experimental mouse models has been an important objective for many years. However, up till now, caspases have never been explored as a suitable target to modulate apoptotic cell death in atherosclerosis. Because previous studies have identified cleaved caspase-3 in both human[8] and mouse[9] atherosclerotic plaques, where it colocalizes with dead macrophages and lipid-rich plaque components,[10] we aimed to investigate the impact of caspase-3 deletion on atherogenesis by crossbreeding caspase 3 knockout (*Casp3*$^{-/-}$) mice with ApoE knockout (*ApoE*$^{-/-}$) mice.

3.2 Materials and methods

3.2.1 Mice

Caspase-3 deficient (*Casp3*$^{-/-}$) mice (C57BL/6, Jackson Laboratory, stock number 006233) were crossbred with atherosclerosis-prone Apolipoprotein E deficient (*ApoE*$^{-/-}$) mice (C57BL/6, Jackson Laboratory, stock number 002052). Male *Casp3*$^{+/+}$*ApoE*$^{-/-}$ (n=19) and *Casp3*$^{-/-}$*ApoE*$^{-/-}$ (n=18) mice were fed a western-type diet (WD) (4021.90, AB Diets) for 16 weeks to induce plaque formation. Mice were housed in a temperature-controlled room with a 12h light/dark cycle and food and water ad libitum. After 16 weeks on WD, mice were anesthetised with sevoflurane (8% for induction and 4,5% for maintenance, SevoFlo®, Penlon vaporizer) to perform transthoracic echocardiograms using a Toshiba diagnostic ultrasound system (SSA-700A) equipped with a 15 MHz transducer. End-diastolic diameter (EDD) and end-systolic diameter (ESD) were measured and fractional shortening (FS) was calculated as follows: ([EDD-

ESD]/EDD)*100. Next, mice were fasted overnight and blood was collected by cardiac puncture under terminal anaesthesia. Total cholesterol, LDL cholesterol and triglyceride levels were measured on a Dimension Vista® System (Siemens Healthcare Diagnostics) with reagents from the same manufacturer. Tissues were fixed in formalin 4% for 24h before paraffin imbedding. In some experiments, tissues were imbedded in OCT and stored at -80°C. All experiments were approved by the Ethical Committee of the University of Antwerp.

3.2.2 Cell culture

Bone marrow-derived macrophages (BMDM) were harvested by flushing bone marrow from the hind limbs of *Casp3*$^{+/+}$*ApoE*$^{-/-}$ and *Casp3*$^{-/-}$*ApoE*$^{-/-}$ mice. Cells were cultured for 7 days in RPMI medium (Gibco Life Technologies) supplemented with 15% L-cell conditioned medium (LCCM) containing monocyte colony stimulating factor (M-CSF). VSMCs were isolated from the aorta as previously described.[11, 12] Briefly, aortas were incubated in 1mg/ml collagenase type II CLS (Worthington), 1mg/ml soybean trypsin inhibitor (Worthington) and 0.74units/ml elastase (Worthington) for 15min at 37°C to remove the adventitia. Thereafter, the aortas were placed in fresh enzyme solution for 1h. Isolated cells were collected, washed and resuspended in DMEM/F-12 medium (Gibco Life Technologies) supplemented with 20% FBS (Sigma Aldrich). To induce apoptosis, BMDM and VSMCs were treated with cycloheximide (Sigma-Aldrich) for 8h or puromycin (Sigma-Aldrich) for 16h, respectively. zVAD-fmk (Enzo Life Sciences) was used as a pan-caspase inhibitor. Apoptosis was monitored by a TUNEL staining (S7101, Millipore) and a caspase 3/7 activity fluorometric assay (K105-100, BioVision). Necrosis was monitored by propidium iodide (PI, Molecular Probes) labelling using fluorescence microscopy (EVOS® FL Cell Imaging System, ThermoFisher Scientific). Necrostatin-1 (Nec-1, Enzo Life Sciences), a RIPK1 inhibitor, was used to inhibit necroptosis while the combination of 100ng/ml LPS (Sigma-Aldrich) and 20µmol/l zVAD-fmk was used as a positive control for necroptosis induction.

3.2.3 Western blotting

Cells were lysed in Laemmli sample buffer (Bio-rad) containing β-mercaptoethanol (Sigma-Aldrich) and boiled for 4min. Samples were loaded on Bolt 4-12% Bis-Tris gels (Life Technologies) and after electrophoresis transferred to Immobilon-FL membranes (Millipore). Membranes were probed with rabbit anti-cleaved caspase-3 (9661, Cell

Signaling Technologies) or mouse anti-β-actin (A5441, clone AC-15, Sigma-Aldrich) primary antibodies. Subsequently, membranes were incubated with infrared (IR)-conjugated secondary antibodies (IgG926-32211 (anti-rabbit); IgG926-68070 (anti-mouse); LI-COR Biosciences) to allow IR fluorescence detection using an Odyssey SA infrared imaging system (LI-COR Biosciences).

3.2.4 Histological analysis

Atherosclerotic plaques located in the aortic root were analysed in 4 different sections sliced at equally spaced intervals (every 50µm). Apoptosis was evaluated using a TUNEL (S7101, Millipore) and an Annexin-PE (559763, BD Pharmingen) staining on paraffin-embedded or frozen sections, respectively. All other stainings were performed on paraffin-embedded sections. Necrosis was measured on a haematoxylin-eosin (H&E) staining according to a standard method.[13] The percentage necrosis was calculated as the size of the necrotic core divided by the total plaque size. A 3000µm^2 minimum threshold was implemented in order to avoid counting of regions that likely do not represent substantial areas of necrosis. Total collagen was detected by a Sirius red staining (Sigma-Aldrich). Plaques were further analysed by immunohistochemistry with rabbit anti-Mac-3 (553322, BD Pharmingen) and mouse anti-α-SMC-actin (A2547, Sigma-Aldrich) primary antibodies. Thereafter, tissue sections were incubated with species-appropriate HRP-conjugated secondary antibodies followed by 60min of reactive ABC. 3,3'-diaminobenzidine or 3-amino-9-ethyl-carbazole were used as a chromogen. All images were acquired with Universal Grab 6.1 software using an Olympus BX40 microscope or the EVOS® fluorescent microscope (Annexin-PE staining), and quantified with Image J software.

3.2.5 Statistical analysis

All data were analysed with SPSS 23.0 software (SPSS Inc.) and presented as mean ± SEM. Statistical tests are mentioned in the figure legends. Differences were considered significant at $P<0.05$.

3.3 Results

3.3.1 Apoptosis is inhibited in caspase-3 deficient macrophages and vascular smooth muscle cells

Bone marrow-derived macrophages (BMDM) and aortic vascular smooth muscle cells (VSMCs) were isolated from *Casp3*$^{-/-}$*ApoE*$^{-/-}$ mice and treated with apoptosis-inducers cycloheximide (CHX) (1µg/ml; 10µg/ml; 30µg/ml) and puromycin (PM) (1µg/ml; 10µg/ml; 30µg/ml), respectively, to validate their inability to undergo apoptosis. Western blot analysis confirmed the absence of cleaved caspase-3 in *Casp3*$^{-/-}$*ApoE*$^{-/-}$ BMDM and *Casp3*$^{-/-}$*ApoE*$^{-/-}$ VSMCs in both untreated and treated conditions **(Fig. 3.1A)**. Moreover, TUNEL staining showed a clear reduction in DNA fragmentation in CHX-treated *Casp3*$^{-/-}$*ApoE*$^{-/-}$ BMDM and PM-treated *Casp3*$^{-/-}$*ApoE*$^{-/-}$ VSMCs as compared to *Casp3*$^{+/+}$*ApoE*$^{-/-}$ BMDM and *Casp3*$^{+/+}$*ApoE*$^{-/-}$ VSMCs **(Fig. 3.1B)**. To rule out the possibility that caspase-7, which shares similar substrate specificity with caspase-3, is compensatory activated in *Casp3*$^{-/-}$*ApoE*$^{-/-}$ BMDM and *Casp3*$^{-/-}$*ApoE*$^{-/-}$ VSMCs, a fluorometric DEVD substrate-based caspase activity assay was performed. In contrast to *Casp3*$^{+/+}$*ApoE*$^{-/-}$ BMDM and *Casp3*$^{+/+}$*ApoE*$^{-/-}$ VSMCs, treatment of *Casp3*$^{-/-}$*ApoE*$^{-/-}$ BMDM and *Casp3*$^{-/-}$*ApoE*$^{-/-}$ VSMCs with apoptosis-inducers did not increase activity of caspase-3/7 **(Fig. 3.1C)**. Co-treatment with the apoptosis-inhibitor zVAD-fmk completely abolished caspase-3/7 activity in CHX-treated *Casp3*$^{+/+}$*ApoE*$^{-/-}$ BMDM and PM-treated *Casp3*$^{+/+}$*ApoE*$^{-/-}$ VSMCs. However, zVAD-fmk did not further decrease caspase activity in CHX-treated *Casp3*$^{-/-}$*ApoE*$^{-/-}$ BMDM and PM-treated *Casp3*$^{-/-}$*ApoE*$^{-/-}$ VSMCs, indicating that there is no residual caspase 7 activity in caspase-3 deficient BMDM and VSMCs.

3.3.2 Caspase-3 deficiency triggers a switch from apoptosis to necrosis

Casp3$^{-/-}$*ApoE*$^{-/-}$ BMDM treated with the apoptosis-inducer CHX were not protected against cell death but underwent necrosis **(Fig. 3.2A left panel)**. According to a morphological analysis, CHX-treated *Casp3*$^{-/-}$*ApoE*$^{-/-}$ BMDM were characterised by cell oncosis (i.e. increased cell volume) and a translucent cytoplasm, indicative of necrosis. In contrast, *Casp3*$^{+/+}$*ApoE*$^{-/-}$ BMDM showed membrane blebbing and cellular shrinkage upon CHX treatment, which are typical characteristics of apoptotic cell death.

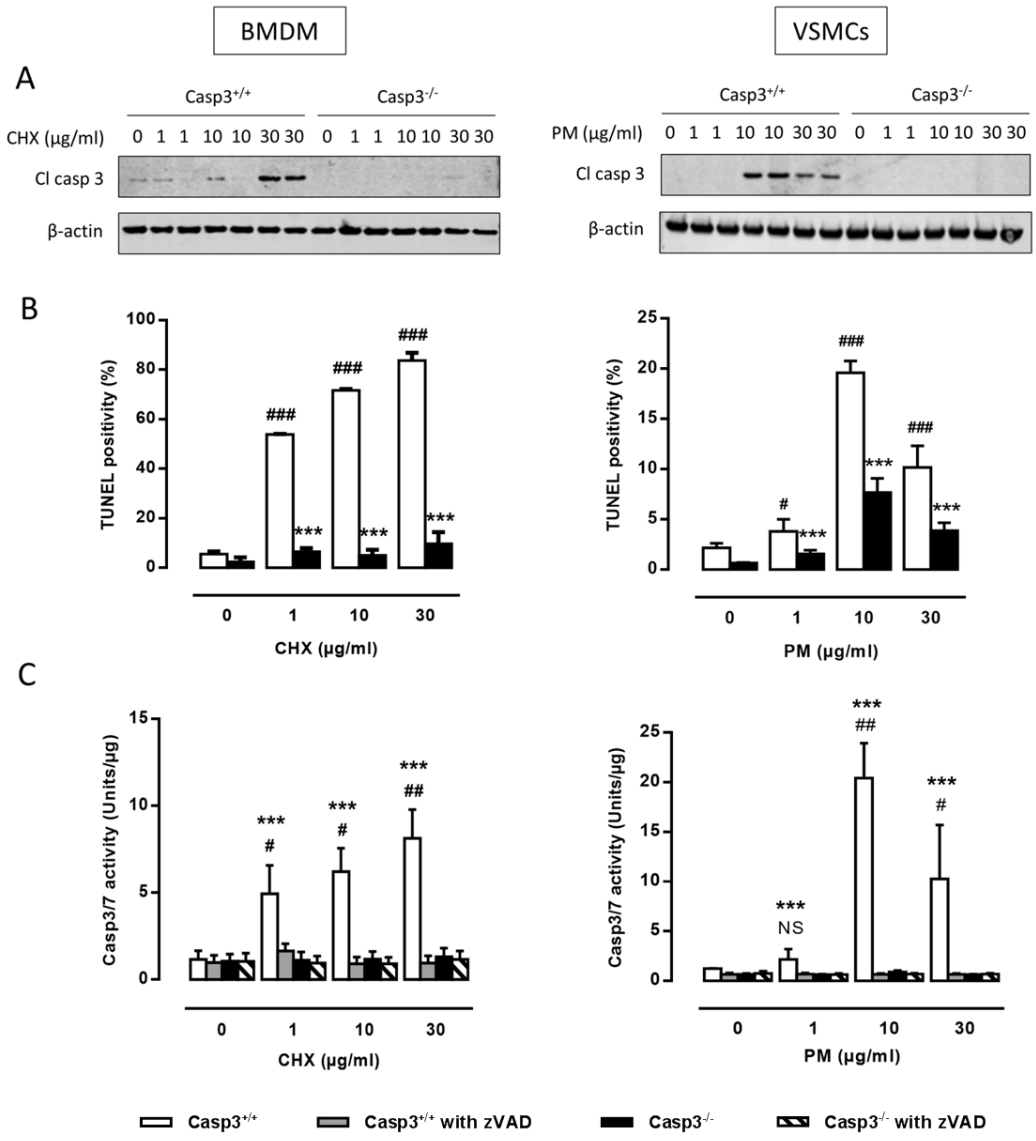

Figure 3.1 Apoptosis is inhibited in caspase-3 deficient macrophages and vascular smooth muscle cells. BMDM and VSMCs were isolated from *Casp3*$^{+/+}$*ApoE*$^{-/-}$ (*Casp3*$^{+/+}$) and *Casp3*$^{-/-}$ *ApoE*$^{-/-}$ (*Casp3*$^{-/-}$) mice and treated with cycloheximide (CHX) (0-30μg/ml) and puromycin (PM) (0-30μg/ml), respectively. Apoptosis was monitored by **(A)** western blot analysis for cleaved caspase-3 (β-actin was used as loading control), **(B)** TUNEL staining (n=2 independent experiments with 2 counting regions of 200 cells/region in duplicate; $^{###}P$<0.001, $^{#}P$<0.05 vs. 0μg/ml; $^{***}P$<0.001 vs. *Casp3*$^{+/+}$; Factorial ANOVA with genotype and treatment as category factors; Dunnett Post Hoc) and **(C)** caspase-3/7 fluorometric activity assay (Data were collected as relative fluorescent units and normalised to cell protein content) (n=3 independent experiments; $^{##}P$<0.01, $^{#}P$<0.05, NS, not significant vs. 0μg/ml; $^{***}P$<0.001 vs. *Casp3*$^{-/-}$; Factorial ANOVA with genotype and treatment as category factors; Dunnett Post Hoc).

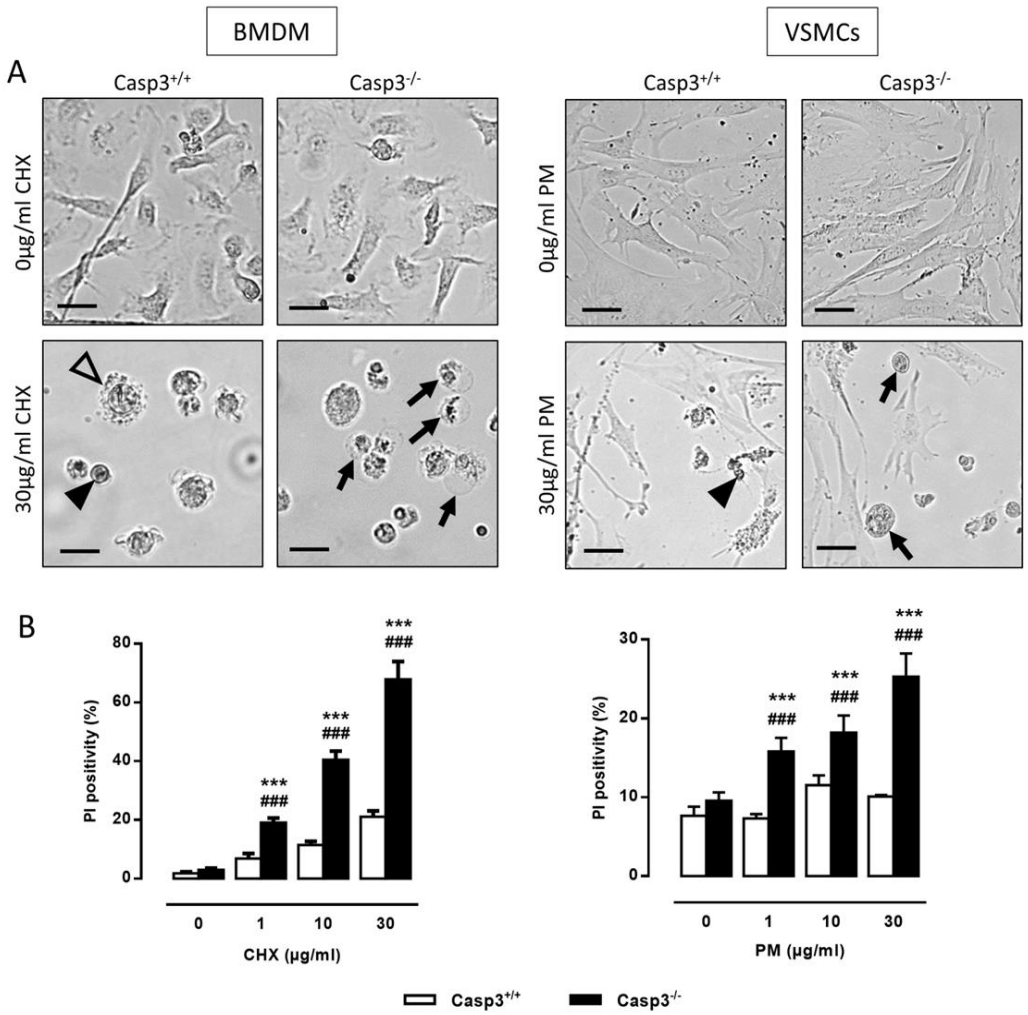

Figure 3.2: Caspase-3 deficiency triggers a switch from apoptosis to primary necrosis. BMDM and VSMCs were isolated from *Casp3*$^{+/+}$*ApoE*$^{-/-}$ (*Casp3*$^{+/+}$) and *Casp3*$^{-/-}$*ApoE*$^{-/-}$ (*Casp3*$^{-/-}$) mice and treated with cycloheximide (CHX) (0-30µg/ml) and puromycin (PM) (0-30µg/ml), respectively. Necrosis was monitored by **(A)** morphological analysis (necrotic cells were characterised by cellular oncosis (black arrows) while apoptotic cells showed cellular shrinkage (black arrowheads) and membrane blebbing (open arrowhead)) Scale bars: 25µm (BMDM) and 50µm (VSMCs) **(B)** PI labelling (n=3 independent experiments with 2 counting regions of 150 cells/region in duplicate; $^{###}P$<0.001 vs. 0µg/ml; $^{***}P$<0.001 vs. *Casp3*$^{+/+}$; Factorial ANOVA with genotype and treatment as category factors; Dunnett Post Hoc).

Furthermore, CHX-treated *Casp3*$^{-/-}$*ApoE*$^{-/-}$ BMDM were characterised by a loss of membrane integrity as shown by increased PI labelling **(Fig. 3.2B left panel)**. Consistent with BMDM, *Casp3*$^{-/-}$*ApoE*$^{-/-}$ VSMCs showed increased susceptibility to necrosis when treated with the apoptosis-inducer PM as illustrated by increased cell oncosis **(Fig. 3.2A right panel)** and PI labelling **(Fig. 3.2B right panel)**.

To investigate whether *Casp3*$^{-/-}$*ApoE*$^{-/-}$ BMDM undergo necroptosis (i.e. programmed primary necrosis), PI positivity of CHX-treated BMDM was examined in the presence or absence of Necrostatin-1 (Nec-1), a well-known necroptosis inhibitor **(Fig. 3.3)**. Co-treatment with Nec-1 did not affect the degree of necrosis in CHX-treated *Casp3*$^{-/-}$*ApoE*$^{-/-}$ BMDM and *Casp3*$^{+/+}$*ApoE*$^{-/-}$ BMDM, indicating that caspase-3 deficiency does not trigger a switch to necroptosis. Of note, treatment of *Casp3*$^{-/-}$*ApoE*$^{-/-}$ and *Casp3*$^{+/+}$*ApoE*$^{-/-}$ BMDM with the necroptosis inducer LPS/zVAD-fmk showed that *Casp3*$^{-/-}$*ApoE*$^{-/-}$ BMDM were as efficient as *Casp3*$^{+/+}$*ApoE*$^{-/-}$ BMDM to undergo necroptosis.

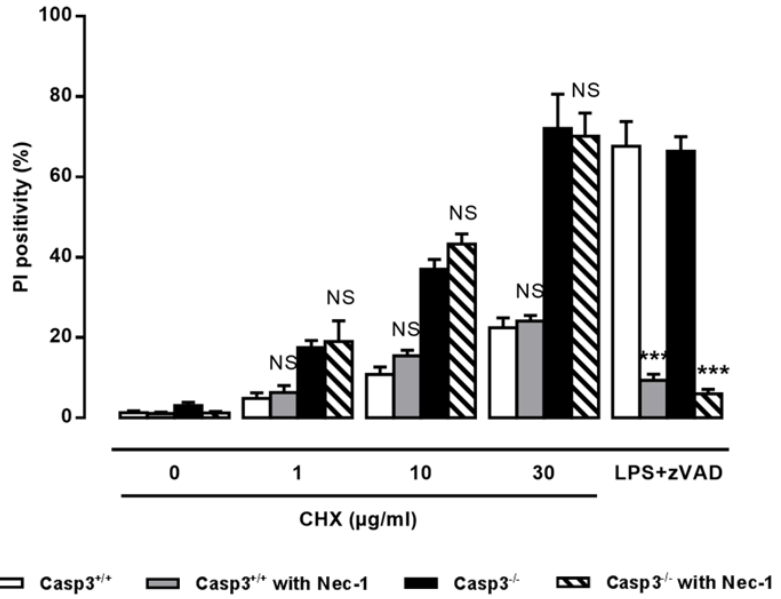

Figure 3.3: Caspase-3 deficiency does not trigger a switch to necroptosis. BMDM were isolated from *Casp3*$^{+/+}$*ApoE*$^{-/-}$ (*Casp3*$^{+/+}$) and *Casp3*$^{-/-}$*ApoE*$^{-/-}$ (*Casp3*$^{-/-}$) mice and treated with cycloheximide (CHX) (0-30µg/ml) in the presence or absence of the necroptosis inhibitor Necrostatin-1 (Nec-1) (30µmol/l). BMDM treated with 100ng/ml LPS and 20µmol/l zVAD-fmk were used as positive control for necroptosis induction. Necrosis was monitored by PI labelling (n=2 independent experiments with 2 counting regions of 150 cells/region in duplicate; NS, not significant; $^{***}P$<0.001 vs. *Casp3*$^{+/+}$ and *Casp3*$^{-/-}$ without Nec-1; Factorial ANOVA with genotype and treatment as category factors; Dunnett Post Hoc).

3.3.3 Caspase-3 deficiency increases total plaque size and plaque necrosis in *ApoE*$^{-/-}$ mice

To investigate the role of caspase-3 in atherosclerosis, *Casp3*$^{+/+}$*ApoE*$^{-/-}$ and *Casp3*$^{-/-}$ *ApoE*$^{-/-}$ mice were fed a western-type diet for 16 weeks. Body weight, heart weight, total cholesterol, LDL-cholesterol and triglycerides were not different between *Casp3*$^{+/+}$*ApoE*$^{-/-}$ mice and *Casp3*$^{-/-}$*ApoE*$^{-/-}$ mice **(Table 3.1)**. Echocardiography did not reveal any signs of left ventricle dilatation or impaired cardiac function as a result of caspase-3 deficiency **(Table 3.1)**.

Table 3.1: Characteristics of *Casp3*$^{+/+}$*ApoE*$^{-/-}$ mice and *Casp3*$^{-/-}$*ApoE*$^{-/-}$ mice after 16 weeks on western-type diet

	Casp3$^{+/+}$*ApoE*$^{-/-}$	*Casp3*$^{-/-}$*ApoE*$^{-/-}$
General		
Body weight (g)[a]	34±1	33±1
Heart weight (mg)[a]	150±3	161±16
Lipids		
Total cholesterol (mg/dl)[a]	473±32	423±38
LDL cholesterol (mg/dl)[a]	309±21	258±29
Triglycerides (mg/dl)[a]	114±7	105±18
Cardiac function		
EDD LV (mm)[a]	4.2±0.1	4.0±0.2
ESD LV (mm)[a]	2.7±0.1	2.6±0.1
FS (%)[a]	36±2	35±1

([a], Student t test, P>0.05)

To validate apoptosis deficiency *in vivo*, aortic root atherosclerotic plaques of *Casp3*$^{+/+}$*ApoE*$^{-/-}$ and *Casp3*$^{-/-}$*ApoE*$^{-/-}$ mice were stained with TUNEL to detect DNA fragmentation. Remarkably, plaques of *Casp3*$^{-/-}$*ApoE*$^{-/-}$ mice showed increased TUNEL positivity as compared to *Casp3*$^{+/+}$*ApoE*$^{-/-}$ mice **(Fig. 3.4A)**. Further statistical analysis showed that the cellular localisation of the TUNEL staining (nuclear vs. cytoplasmic) depended on the presence of necrosis (Chi-square, P = 0.024). If there was no necrotic core present in the plaque, the TUNEL staining was exclusively nuclear, indicative of apoptosis. However, when a necrotic core was present, 9 out of 24 plaques showed extensive cytosolic TUNEL staining, presumably due to the detection of large DNA fragments released into the cytoplasm during necrosis. In this way, increased TUNEL positivity in plaques of *Casp3*$^{-/-}$*ApoE*$^{-/-}$ mice likely reflected necrosis rather than apoptosis.

Therefore, we searched for an alternative apoptosis marker. Staining with Annexin-PE was considered a suitable and reliable marker for the detection of apoptosis *in vivo*. Annexin-PE labelling revealed a significant decrease in apoptotic cell number in plaques of *Casp3*$^{-/-}$*ApoE*$^{-/-}$ mice as compared to *Casp3*$^{+/+}$*ApoE*$^{-/-}$ mice **(Fig. 3.4B)**, indicating that apoptosis is reduced in atherosclerotic plaques of *Casp3*$^{-/-}$*ApoE*$^{-/-}$ mice.

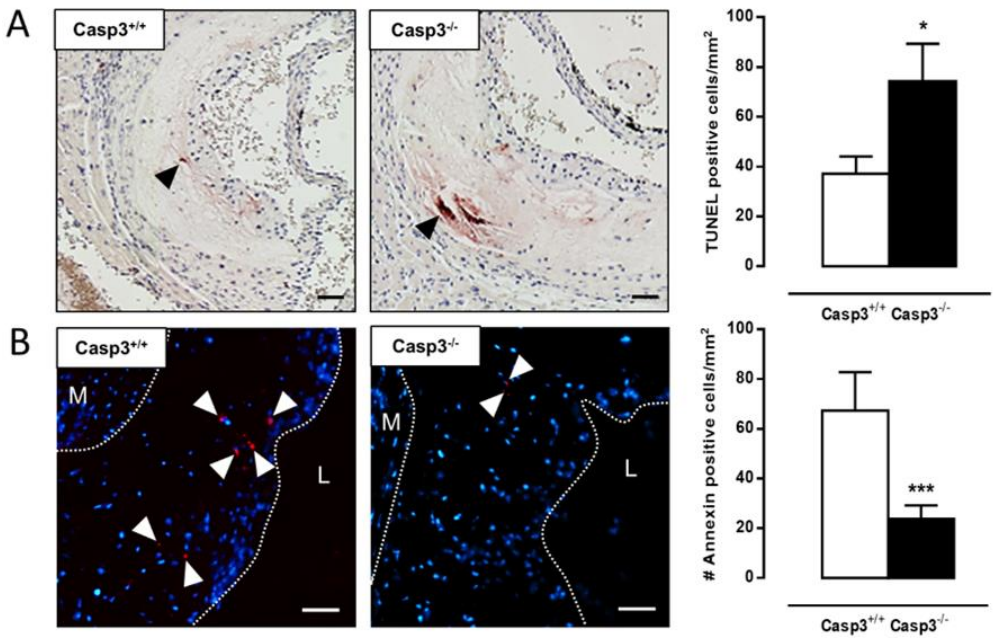

Figure 3.4: Caspase-3 deficiency reduces apoptosis in *ApoE*$^{-/-}$ mice. *Casp3*$^{+/+}$*ApoE*$^{-/-}$ mice (*Casp3*$^{+/+}$) and *Casp3*$^{-/-}$*ApoE*$^{-/-}$ mice (*Casp3*$^{-/-}$) were fed a western-type diet for 16 weeks. **(A)** TUNEL staining on aortic root atherosclerotic plaques to detect DNA fragmentation (depicted by black arrowheads) ($^{*}P$<0.05 vs. *Casp3*$^{+/+}$; n=8; Repeated Measure) **(B)** Annexin-PE labelling to detect phosphatisylserine exposure on apoptotic cell membranes (Red Annexin positive cells are depicted by white arrowheads) and counterstaining with DAPI (blue nuclei) ($^{***}P$<0.001 vs. *Casp3*$^{+/+}$; n=11; Univariate). M, media; L, lumen. Scale bar: 50µm.

Further analysis showed that the atherosclerotic plaques of *Casp3*$^{-/-}$*ApoE*$^{-/-}$ mice (144±8 x10^3 µm^2) were significantly larger as compared to *Casp3*$^{+/+}$*ApoE*$^{-/-}$ mice (108±6 x10^3 µm^2). Moreover, plaques of *Casp3*$^{-/-}$*ApoE*$^{-/-}$ mice showed increased plaque necrosis **(Fig. 3.5A)** as suspected by the false positive TUNEL staining. The necrotic cores in plaques of *Casp3*$^{-/-}$*ApoE*$^{-/-}$ mice were not only larger but also more abundantly present. Furthermore, plaque macrophage content was significantly reduced in *Casp3*$^{-/-}$*ApoE*$^{-/-}$ mice **(Fig. 3.5B)** while smooth muscle cell and collagen content were not different between both groups **(Fig. 3.5C and 3.5D)**.

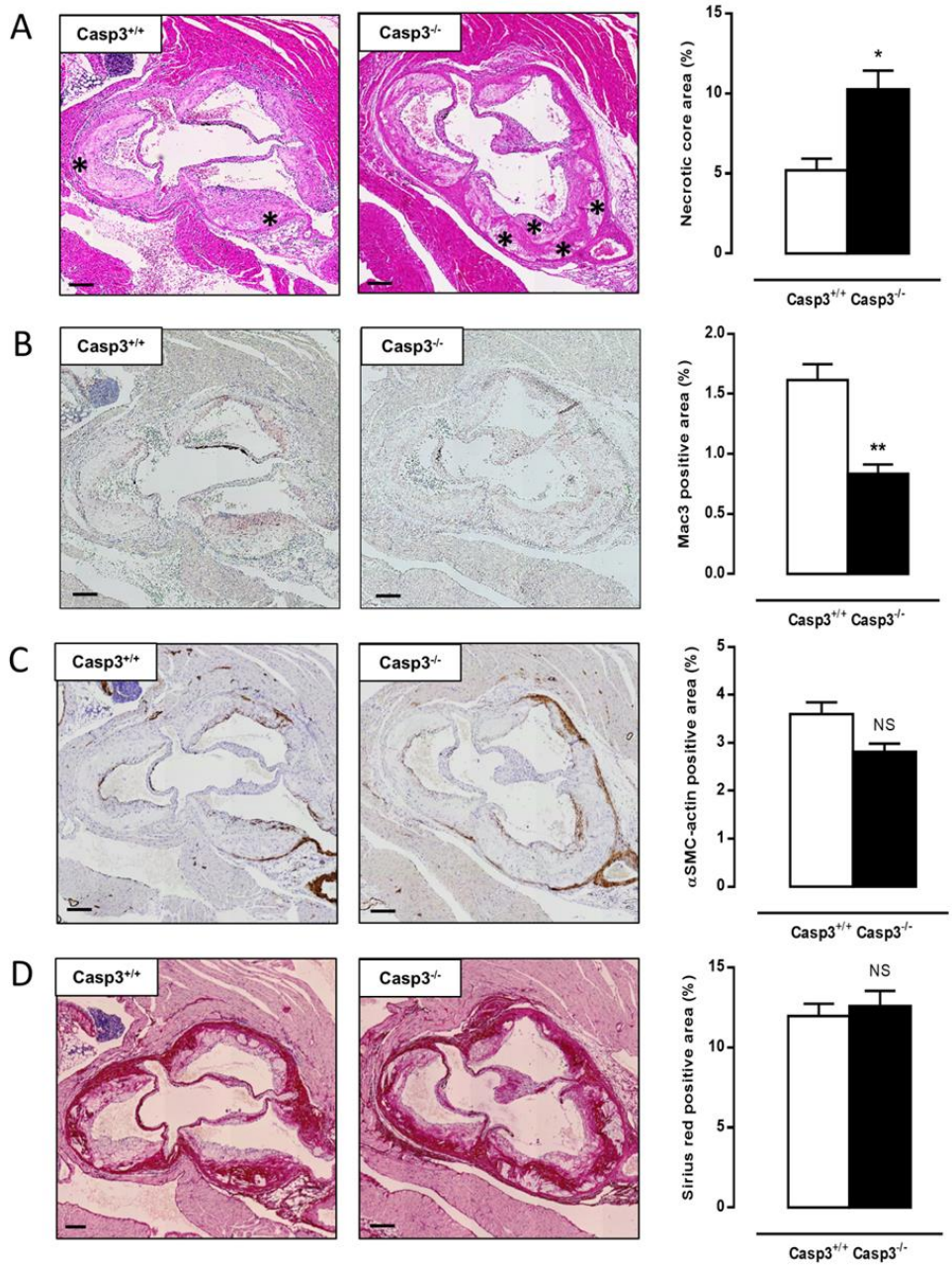

Figure 3.5 Caspase-3 deficiency increases plaque necrosis in *ApoE*$^{-/-}$ mice. *Casp3*$^{+/+}$*ApoE*$^{-/-}$ mice (*Casp3*$^{+/+}$) (n=8) and *Casp3*$^{-/-}$*ApoE*$^{-/-}$ mice (*Casp3*$^{-/-}$) (n=7) were fed a western-type diet for 16 weeks. **(A)** Aortic root atherosclerotic plaques were stained with H&E to quantify plaque necrosis (the necrotic cores are indicated by an asterisk). **(B,C)** Serial sections were immunostained for Mac-3 and α-SMC-actin to determine macrophage content and smooth muscle cell content, respectively. **(D)** Serial sections were stained with Sirius red to quantify total collagen content. ($^{*}P$<0.05, $^{**}P$<0.01, NS, not significant, vs. *Casp3*$^{+/+}$; Repeated Measures) Scale bar: 150μm.

3.4 Discussion

Given the detrimental consequences of macrophage and VSMC apoptosis in advanced atherosclerosis, further improving our knowledge on the regulation of apoptosis in atherosclerosis is imperative to explore the potential of anti-apoptotic plaque stabilising strategies. Because caspases are an unexplored yet attractive target to modulate apoptotic cell death in atherosclerosis, we chose to examine the impact of caspase-3 deletion on atherosclerosis by crossbreeding caspase-3 knockout (*Casp3*$^{-/-}$) mice with ApoE knockout (*ApoE*$^{-/-}$) mice.

Bone marrow-derived macrophages (BMDM) and vascular smooth muscle cells (VSMCs), two major constituents of atherosclerotic plaques, were isolated from *Casp3*$^{-/-}$*ApoE*$^{-/-}$ and *Casp3*$^{+/+}$*ApoE*$^{-/-}$ mice and subjected to the apoptosis inducers cycloheximide[14] or puromycin[15], respectively, to validate our experimental model. Caspase-3 deficient BMDM and VSMCs showed resistance to apoptosis as illustrated by reduced TUNEL positivity. Moreover, deletion of caspase-3 did not evoke a compensatory activation of caspase-7 in *Casp3*$^{-/-}$*ApoE*$^{-/-}$ macrophages and VSMCs, despite their shared substrate specificity. These experiments underline the critical role of caspase-3 in the execution of apoptotic cell death and confirm the successful inhibition of apoptosis in this model. Nevertheless, caspase-3 deficient BMDM and VSMCs were not resistant to cell death but instead showed increased susceptibility to primary necrosis. Indeed, *Casp3*$^{-/-}$*ApoE*$^{-/-}$ macrophages and VSMCs showed cell oncosis and increased PI labelling upon exposure to apoptotic stimuli. The observed switch between apoptotic and necrotic cell death in anti-apoptotic conditions has been reported previously by others.[16-18] Moreover, knockdown of caspase-8 in L929 cells triggers TNFα-induced necroptosis (i.e. programmed necrosis regulated by RIPK1 and RIPK3) due to the absence of caspase-8-mediated inactivation of RIPK1 and RIPK3.[19] In the present study, treatment of CHX-treated macrophages with the necroptosis inhibitor Necrostatin-1 did not influence the degree of necrosis, indicating that caspase-3, in contrast to caspase-8, does not play a role in the regulation of necroptosis. Taken together, caspase-3 deletion protects macrophages and vascular smooth muscle cells against apoptosis but triggers a switch to primary necrosis. These data indicate that caspase-3 plays a crucial role in the execution of apoptosis though deletion of caspase-3 does not prevail cell death.

To investigate the consequences of caspase-3 deletion on plaque development, *Casp3*$^{+/+}$*ApoE*$^{-/-}$ and *Casp3*$^{-/-}$*ApoE*$^{-/-}$ mice were fed a western-type diet for 16 weeks. Plasma total cholesterol, LDL cholesterol and triglyceride levels, and cardiac parameters (EDD, ESD, FS) were not different between *Casp3*$^{-/-}$*ApoE*$^{-/-}$ mice and *Casp3*$^{+/+}$*ApoE*$^{-/-}$ mice, indicating that deletion of caspase-3 affected neither lipid metabolism nor cardiac function. Analysis of the atherosclerotic lesions showed that *Casp3*$^{-/-}$*ApoE*$^{-/-}$ mice developed larger plaques as compared to *Casp3*$^{+/+}$*ApoE*$^{-/-}$ mice and were characterised by increased plaque necrosis. The increased abundancy of necrotic cores in plaques of *Casp3*$^{-/-}$*ApoE*$^{-/-}$ mice was associated with non-nuclear TUNEL staining. According to previous reports, TUNEL staining can give rise to false positivity because this technique does not allow to distinguish between DNA fragments generated during apoptosis (internucleosomal DNA fragmentation) and necrosis (large-scale DNA fragmentation).[20-24] When large DNA fragments are released into the cytoplasm following nuclear membrane degradation, a cytoplasmic TUNEL staining pattern appears.[21] Our data combined with these previous reports emphasise that TUNEL staining should always be interpreted critically and should be combined with other apoptosis markers. In the present study, labelling with Annexin-PE revealed a significant decrease in apoptotic cell number in plaques of *Casp3*$^{-/-}$*ApoE*$^{-/-}$ mice as compared to *Casp3*$^{+/+}$*ApoE*$^{-/-}$ mice, indicating that *Casp3*$^{-/-}$*ApoE*$^{-/-}$ mice were a suitable model to study apoptosis deficiency in atherosclerosis. With regard to the cellular composition, plaques of *Casp3*$^{-/-}$*ApoE*$^{-/-}$ mice showed a significant decrease in macrophage content and a trend towards reduced VSMC content as compared to *Casp3*$^{+/+}$*ApoE*$^{-/-}$ plaques. The decrease in macrophage (and VSMC) content most likely reflects the observed rise in plaque necrosis. Necrotic macrophages (and VSMCs) accumulate in the necrotic core while losing their cell-type specific antigens, hindering their detection.

These findings are in line with previous observations in mice lacking the pro-apoptotic protein Bax[25], the death receptors TNFR1[26] and Fas[27] or the tumour suppressor proteins p53[28-32] and p19(ARF)[33]. Macrophage specific deletion of Bax reduces macrophage apoptosis and stimulates the development of advanced atherosclerotic plaques in *Ldlr*$^{-/-}$ mice.[25] Knockout of TNFR1 accelerates atherosclerosis in western-type diet-fed mice due to increased foam cell formation, though the effect on apoptosis and necrosis was not determined.[26] Impairment of Fas-mediated apoptosis, by targeting the Fas receptor[27] or its ligand[34], also accelerates atherosclerosis in *ApoE*$^{-/-}$ mice. Genetic disruption of p53,

either generally or macrophage-specifically, promotes atherosclerosis in *ApoE*$^{-/-}$ mice[28, 31] and is often accompanied by increased plaque necrosis.[29, 30, 32] Moreover, deletion of the tumour suppressor p19(ARF) in *ApoE*$^{-/-}$ mice reduces apoptosis in plaque macrophages and VSMCs, and aggravates atherosclerosis, though the effect on plaque necrosis was not examined.[33]

In conclusion, caspase-3 deletion inhibits apoptosis in murine macrophages and vascular smooth muscle cells but causes a switch to primary necrosis. Moreover, caspase-3 deficiency promotes plaque growth and plaque necrosis in 16 week western-type diet-fed *ApoE*$^{-/-}$ mice. Considering the pro-inflammatory and pro-thrombotic properties of plaque necrosis,[35] inhibition of apoptosis may not be a favourable strategy to improve atherosclerotic plaque stability.

3.5 References

(1) Kolodgie FD, Narula J, Burke AP, Haider N, Farb A, Hui-Liang Y, Smialek J, Virmani R. Localization of apoptotic macrophages at the site of plaque rupture in sudden coronary death. *Am J Pathol* 2000;157(4):1259-68.

(2) Geng YJ and Libby P. Progression of atheroma: a struggle between death and procreation. *Arterioscler Thromb Vasc Biol* 2002;22(9):1370-80.

(3) Clarke MC, Figg N, Maguire JJ, Davenport AP, Goddard M, Littlewood TD, Bennett MR. Apoptosis of vascular smooth muscle cells induces features of plaque vulnerability in atherosclerosis. *Nat Med* 2006;12(9):1075-80.

(4) Stoneman V, Braganza D, Figg N, Mercer J, Lang R, Goddard M, Bennett M. Monocyte/macrophage suppression in CD11b diphtheria toxin receptor transgenic mice differentially affects atherogenesis and established plaques. *Circ Res* 2007;100(6):884-93.

(5) Gautier EL, Huby T, Witztum JL, Ouzilleau B, Miller ER, Saint-Charles F, Aucouturier P, Chapman MJ, Lesnik P. Macrophage apoptosis exerts divergent effects on atherogenesis as a function of lesion stage. *Circulation* 2009;119(13):1795-804.

(6) Schrijvers DM, De Meyer GRY, Herman AG, Martinet W. Phagocytosis in atherosclerosis: Molecular mechanisms and implications for plaque progression and stability. *Cardiovasc Res* 2007;73(3):470-80.

(7) Seimon T and Tabas I. Mechanisms and consequences of macrophage apoptosis in atherosclerosis. *J Lipid Res* 2009;50 Suppl:S382-S387.

(8) Mallat Z, Ohan J, Leseche G, Tedgui A. Colocalization of CPP-32 with apoptotic cells in human atherosclerotic plaques. *Circulation* 1997;96(2):424-8.

(9) Nhan TQ, Liles WC, Chait A, Fallon JT, Schwartz SM. The p17 cleaved form of caspase-3 is present within viable macrophages in vitro and in atherosclerotic plaque. *Arterioscler Thromb Vasc Biol* 2003;23(7):1276-82.

(10) Hutter R et al. Caspase-3 and tissue factor expression in lipid-rich plaque macrophages: evidence for apoptosis as link between inflammation and atherothrombosis. *Circulation* 2004;109(16):2001-8.

(11) Owens GK, Loeb A, Gordon D, Thompson MM. Expression of smooth muscle-specific alpha-isoactin in cultured vascular smooth muscle cells: relationship between growth and cytodifferentiation. *J Cell Biol* 1986;102(2):343-52.

(12) Geisterfer AA, Peach MJ, Owens GK. Angiotensin II induces hypertrophy, not hyperplasia, of cultured rat aortic smooth muscle cells. *Circ Res* 1988;62(4):749-56.

(13) Seimon TA, Wang Y, Han S, Senokuchi T, Schrijvers DM, Kuriakose G, Tall AR, Tabas IA. Macrophage deficiency of p38alpha MAPK promotes apoptosis and plaque necrosis in advanced atherosclerotic lesions in mice. *J Clin Invest* 2009;119(4):886-98.

(14) Croons V, Martinet W, Herman AG, Timmermans JP, De Meyer GRY. Selective clearance of macrophages in atherosclerotic plaques by the protein synthesis inhibitor cycloheximide. *J Pharmacol Exp Ther* 2007;320(3):986-93.

(15) Croons V, Martinet W, Herman AG, De Meyer GRY. Differential effect of the protein synthesis inhibitors puromycin and cycloheximide on vascular smooth muscle cell viability. *J Pharmacol Exp Ther* 2008;325(3):824-32.

(16) Scheller C, Knoferle J, Ullrich A, Prottengeier J, Racek T, Sopper S, Jassoy C, Rethwilm A, Koutsilieri E. Caspase inhibition in apoptotic T cells triggers necrotic cell death depending on the cell type and the proapoptotic stimulus. *J Cell Biochem* 2006;97(6):1350-61.

(17) Lemaire C, Andreau K, Souvannavong V, Adam A. Inhibition of caspase activity induces a switch from apoptosis to necrosis. *FEBS Lett* 1998;425(2):266-70.

(18) Meilhac O, Escargueil-Blanc I, Thiers JC, Salvayre R, Negre-Salvayre A. Bcl-2 alters the balance between apoptosis and necrosis, but does not prevent cell death induced by oxidized low density lipoproteins. *FASEB J* 1999;13(3):485-94.

(19) Vanlangenakker N, Bertrand MJ, Bogaert P, Vandenabeele P, Vanden Berghe T. TNF-induced necroptosis in L929 cells is tightly regulated by multiple TNFR1 complex I and II members. *Cell Death Dis* 2011;2:e230.

(20) Grasl-Kraupp B, Ruttkay-Nedecky B, Koudelka H, Bukowska K, Bursch W, Schulte-Hermann R. In situ detection of fragmented DNA (TUNEL assay) fails to discriminate among apoptosis, necrosis, and autolytic cell death: a cautionary note. *Hepatology* 1995;21(5):1465-8.

(21) Jaeschke H and Lemasters JJ. Apoptosis versus oncotic necrosis in hepatic ischemia/reperfusion injury. *Gastroenterology* 2003;125(4):1246-57.

(22) Galluzzi L et al. Guidelines for the use and interpretation of assays for monitoring cell death in higher eukaryotes. *Cell Death Differ* 2009;16(8):1093-107.

(23) Vanden Berghe T, Grootjans S, Goossens V, Dondelinger Y, Krysko DV, Takahashi N, Vandenabeele P. Determination of apoptotic and necrotic cell death in vitro and in vivo. *Methods* 2013;61(2):117-29.
(24) Figg N and Bennett MR. Quantification of Apoptosis in Mouse Atherosclerotic plaques. *Methods Mol Biol* 2015;1339:191-9.
(25) Liu J, Thewke DP, Su YR, Linton MF, Fazio S, Sinensky MS. Reduced macrophage apoptosis is associated with accelerated atherosclerosis in low-density lipoprotein receptor-null mice. *Arterioscler Thromb Vasc Biol* 2005;25(1):174-9.
(26) Schreyer SA, Peschon JJ, LeBoeuf RC. Accelerated atherosclerosis in mice lacking tumor necrosis factor receptor p55. *J Biol Chem* 1996;271(42):26174-8.
(27) Feng X et al. ApoE-/-Fas-/- C57BL/6 mice: a novel murine model simultaneously exhibits lupus nephritis, atherosclerosis, and osteopenia. *J Lipid Res* 2007;48(4):794-805.
(28) Guevara NV, Kim HS, Antonova EI, Chan L. The absence of p53 accelerates atherosclerosis by increasing cell proliferation in vivo. *Nat Med* 1999;5(3):335-9.
(29) van Vlijmen BJ et al. Macrophage p53 deficiency leads to enhanced atherosclerosis in APOE*3-Leiden transgenic mice. *Circ Res* 2001;88(8):780-6.
(30) Merched AJ, Williams E, Chan L. Macrophage-specific p53 expression plays a crucial role in atherosclerosis development and plaque remodeling. *Arterioscler Thromb Vasc Biol* 2003;23(9):1608-14.
(31) Mercer J, Figg N, Stoneman V, Braganza D, Bennett MR. Endogenous p53 protects vascular smooth muscle cells from apoptosis and reduces atherosclerosis in ApoE knockout mice. *Circ Res* 2005;96(6):667-74.
(32) Boesten LS et al. Macrophage p53 controls macrophage death in atherosclerotic lesions of apolipoprotein E deficient mice. *Atherosclerosis* 2009;207(2):399-404.
(33) Gonzalez-Navarro H, Abu Nabah YN, Vinue A, Andres-Manzano MJ, Collado M, Serrano M, Andres V. p19(ARF) deficiency reduces macrophage and vascular smooth muscle cell apoptosis and aggravates atherosclerosis. *J Am Coll Cardiol* 2010;55(20):2258-68.
(34) Aprahamian T, Rifkin I, Bonegio R, Hugel B, Freyssinet JM, Sato K, Castellot JJ, Jr., Walsh K. Impaired clearance of apoptotic cells promotes synergy between atherogenesis and autoimmune disease. *J Exp Med* 2004;199(8):1121-31.
(35) Martinet W, Schrijvers DM, De Meyer GRY. Necrotic cell death in atherosclerosis. *Basic Res Cardiol* 2011;106(5):749-60.

CHAPTER 4

Defective autophagy in vascular smooth muscle cells accelerates senescence and promotes neointima formation and atherosclerosis

Adapted from:
Grootaert MOJ, Da Costa Martins P, Bitsch N, Pintelon I, De Meyer GRY, Martinet W, Schrijvers DM. Defective autophagy in vascular smooth muscle cells accelerates senescence and promotes neointima formation and atherosclerosis**.** *Autophagy*, 2015 Nov 2;11(11):2014-2032.

4.1 Introduction

Vascular smooth muscle cells (VSMCs) are the major components of the blood vessel wall and play crucial roles in both physiological (e.g. regulation blood pressure and vascular tone) and pathological processes (e.g. restenosis and atheroma formation). Accumulating evidence suggests that autophagy is activated in VSMCs in response to various stimuli including lipids, reactive oxygen species, cytokines and growth factors and may promote VSMC survival.[1-7] Moreover, PDGF-induced autophagy promotes the development of a synthetic and proliferative VSMC phenotype,[6] suggesting that autophagy may regulate VSMC phenotype and function.[8] Because our knowledge on the regulation of autophagy in VSMCs is mainly based on cell culture experiments, we focused on the role of VSMC autophagy in arterial disease such as post-injury neointima formation and atherosclerosis. At this moment, the relation between autophagy and neointima formation is debatable because induction of autophagy by PDGF stimulates VSMC proliferation (vide supra) while the autophagy inducer rapamycin or derivatives thereof (e.g. everolimus) are essentially used to prevent restenosis.[9, 10] Even though autophagy occurs in VSMCs of atherosclerotic plaques,[11, 12] the role of VSMC autophagy in atherosclerosis has not been investigated. To study the role of autophagy in VSMCs *in vitro* and *in vivo*, a mouse model was constructed with defective autophagy in VSMCs only, by genetic deletion of the essential autophagy gene *Atg7*.

4.2 Materials and Methods

4.2.1 Mouse studies

Mice homozygous for a vector that disrupts *Atg7* in exon 14 by Cre-loxP technology (*Atg7$^{F/F}$* mice)[13] were crossbred for > 10 generations with *SM22α-Cre*$^{+}$ mice (C57BL/6, Jackson Laboratory, 004746), which express *Cre* recombinase under the control of the mouse *SM22α* promoter, to obtain VSMC-specific *Atg7* knockout mice (referred to as *Atg7$^{F/F}$SM22α-Cre*$^{+}$ mice or simply *Atg7$^{F/F}$* mice). To induce neointimal lesions, blood flow was disrupted in the left common carotid artery of *Atg7*$^{+/+}$ and *Atg7$^{F/F}$* mice for 5 days (n=4/group) or 5 weeks (n=14/group) by ligating the vessel near the bifurcation. During the surgical procedure, 0.1mg/g BW ketamine i.p. (Anesketin, 100mg/ml, Eurovet) and 0.01mg/g BW xylazine i.p. (Rompun, 20mg/ml, Bayer Health Care) were used as

anesthetics and 0.1mg/kg BW brupenorfine s.c. (Temgesic, 0.3mg/ml, Schering-Plough) as analgesic agent. For atherosclerosis studies, *Atg7*$^{+/+}$ and *Atg7*$^{F/F}$ mice were crossbred with *ApoE*$^{-/-}$ mice (C57BL/6, Jackson Laboratory, 002052) and fed a western-type diet (Harlan Teklad, TD88137) for 10 (n=16/group) or 14 weeks (n=16/group). At the end of the experiment, mice were fasted overnight and blood was collected by puncture of the retro-orbital plexus. Plasma lipoprotein profiles were determined by fast performance liquid chromatography gel filtration on a Superose 6 column. Cholesterol levels were assessed by a commercially available kit (Randox, CH200). Tissues were fixed in formalin 4% for 24h before paraffin imbedding. In some experiments, tissues were imbedded in OCT and stored at -80°C. Macrophage-specific *Atg7* knockouts were obtained by crossbreeding *Atg7*$^{F/F}$ mice for > 10 generations with *LysM-Cre*$^{+}$ mice (C57BL/6, Jackson Laboratory, 004781) which express *Cre* recombinase under the control of the mouse lysozyme M promoter. All experiments were approved by the Ethics Committee of the University of Antwerp.

4.2.2 Cell culture

VSMCs were isolated from mouse aorta as previously described.[14, 15] Briefly, aortas were preincubated in HBSS (Gibco Life Technologies) containing 1mg/ml collagenase (Worthington, type II CLS), 1mg/ml soybean trypsin inhibitor (Worthington) and 0.74units/ml elastase (Worthington) for 15min at 37°C, in 95% air/5% CO_2. Next, the adventitia was stripped off and the aorta was opened longitudinally to remove blood clots and endothelial cells. Subsequently, aortas were placed in fresh enzyme solution and incubated for 1h (37°C, in 95% air/5% CO_2). Isolated cells were centrifuged, washed and resuspended in DMEM/F-12 medium (Gibco Life Technologies) supplemented with 20% FBS (Sigma Aldrich). Cells were used from passage 4 till 10 and cultured in DMEM/F-12 medium supplemented with 10% FBS. Cells were isolated from 2 or 3 mice. In each individual experiment, cells from the same passage number were used. Bone marrow-derived macrophages (BMDM) were harvested by flushing bone marrow from the hind limbs of mice. Cells were cultured for 7 days in RPMI medium (Gibco Life Technologies) supplemented with 15% L-cell conditioned medium (LCCM). LCCM is produced by L929 cells cultured in RPMI medium. Once cells are confluent, medium is changed and cells are left alone for 7 days to secrete M-CSF (monocyte colony-stimulating factor). Then, the medium (=LCCM) is collected and stored at -80°C. To induce oxidative stress, cells were treated with 25µmol/l *tert*-butyl hydroperoxide (tBHP; Sigma-Aldrich) or 50µg/ml

oxidised LDL (oxLDL, Kalen Biomedical) for 24h. In some experiments, cells were treated with 10µmol/l puromycin (Sigma Aldrich) for 12h or exposed to UV-irradiation for 10min to induce apoptosis. Cell viability was evaluated by a neutral red assay.[16] ROS production was determined using the fluorogenic marker carboxy-H_2DCFDA (Molecular Probes, I36007). The DCFDA-positive cells were immediately visualised by fluorescence microscopy and then quantified using Image J software. To measure cellular size, VSMCs were labelled with 1µmol/l calcein AM (Molecular probes, C3099) and visualised with an inverted microscope attached to a microlens-enhanced dual spinning disk confocal system (UltraVIEW VoX, PerkinElmer). Images were analysed with Volocity software (PerkinElmer). Cellular protein quantity was determined using the BCA method. To induce starvation-induced autophagy, cells were incubated in Earle balanced salt solution (EBSS; Gibco Life Technologies) for 48h.

4.2.3 Transmission electron microscopy

Samples were prepared for transmission electron microscopy (TEM) as previously described.[17] Sections were examined with a Tecnai microscope (FEI, Eindhoven, The Netherlands) at 120kV.

4.2.4 Radio-active amino acid incorporation assay

VSMCs were incubated with radioactive labelled amino acids (EasyTag Express Protein Labeling Mix [^{35}S]-, NEG772002MC, PerkinElmer) for 2h. Next, cells were lysed in hypotonic lysis buffer, collected and trichloroacetic acid was added (final concentration 10%) to allow protein precipitation. After centrifugation at 14000rpm for 10min, the pellet was resuspended in 0.2mol/l NaOH and radioactivity was measured with a liquid scintillation counter to evaluate protein synthesis.

4.2.5 Analysis of proliferation, collagen amount and migration

Cellular proliferation was assessed using a BrdU incorporation test. Once 80% confluent, BMDM and VSMCs were treated with 10µmol/l BrdU (Sigma-Aldrich, B5002) for 2h or 6h respectively, followed by an anti-BrdU staining (rat anti-BrdU antibody; Abcam, ab6326). The BrdU-positive nuclei were quantified using Image J software. Collagen synthesis in VSMCs was stimulated by 10ng/ml TGFβ (Peprotech) for 48h in serum-free medium. Total collagen amount was assayed using Sirius red staining as previously described.[18] COL1A1/2 and COL3A1 expression was analysed by immunofluorescence with rabbit

anti-COL1A1/2 antibody (Abcam, ab21286) and anti-rabbit Alexa Fluor 555 secondary antibody (Molecular Probes, A21428), and goat anti-COL3A1 antibody (Biodesign, T33330G) and anti-goat Alexa Fluor 488 secondary antibody (Molecular Probes, A11078). The migratory capacity was evaluated, independently of cell size and chemotactic effects, using an Oris™ Cell Migration Assay (Platypus Technologies). Briefly, $2.5x10^4$ cells/well were added to a 96-well plate with Cell Seeding Inserts and incubated overnight to permit cell attachment. Subsequently, the stoppers were removed to allow cell migration into the empty zone. 24h later, cells were fixed and stained with 0.1% crystal violet (Sigma Aldrich) in 20% methanol for 3min to visualise and quantify the migrated cells using an inverted microscope. The migratory capacity of the cells was evaluated by measuring the percentage closure area: 100 x $((premigration)_{area} - (migration)_{area}) / (premigration)_{area}$

4.2.6 Western blotting

Cells were lysed in Laemmli sample buffer (Bio-Rad) containing β-mercaptoethanol (Sigma Aldrich) and boiled for 4 min. Protein samples were loaded on NuPAGE 4-12% Bis-Tris gels (Life Technologies) and after electrophoresis transferred to Immobilon-P membranes (Millipore). Membranes were probed with the following primary antibodies: goat anti-GSTα (ab53940), rabbit anti-Nrf2 (ab137550), mouse anti-p16 (ab54210) and rabbit anti-p21 (ab7960) from Abcam; rabbit anti-SDF1 (Bioss, bs-4938); rabbit anti-GAPDH (14C10), rabbit anti-TGFβ (3711) and rabbit anti-phospho RB (8516) from Cell Signaling Technology; mouse anti-LC3 (Nanotools, clone 5F10, 0231-100); rabbit anti-NQO1 (Novus Biologicals, NBP1-40663); rabbit anti-PARP1 (sc-7150), rabbit anti-p16 (sc-1207) and rabbit anti-total RB (sc-50) from Santa Cruz Biotechnology; mouse anti-β-actin (clone AC-15, A5441), rabbit anti-ATG7 (A2856), rabbit anti-ATG5 (A0856), rabbit anti-p62 (P0067) and rabbit anti-acetyl-p53 (SAB4503014) from Sigma-Aldrich. Thereafter, membranes were incubated with HRP-conjugated secondary antibodies (Dako, anti-rabbit P0399, anti-mouse P0260, anti-goat P0160) to allow chemiluminescent detection. In some experiments, cytoplasmic and nuclear fractions were isolated from cultured VSMCs and BMDM using the NE-PER® Nuclear and Cytoplasmic Extraction kit (Thermo Scientific, 78833) prior to western blot analysis. Tissue samples were homogenised (see section gelatin zymography) before western blot analysis.

4.2.7 Gelatin zymography

Ligated left common carotid arteries were collected, gently flushed to remove all blood clots and immediately snap frozen. Tissues were homogenised in RIPA buffer and protein content was determined using the BCA method. Samples were mixed with Laemmli sample buffer without β-mercaptoethanol before loading on a 10% Zymogram Gelatin gel (Life Technologies). After electrophoresis in Tris-Glycine SDS Running Buffer (Life Technologies), proteins were renaturated in Zymogram Renaturing Buffer (Life Technologies) and incubated with Zymogram Developing Buffer (Life Technologies) overnight. Gels were stained with Coomassie Brilliant Blue (Merck) for 3h and subsequently destained twice for 1h. Finally, gels were scanned to visualise the gelatinolytic activity of MMP9 and MMP2 in the left common carotid artery.

4.2.8 MicroArray

Total RNA was prepared using the Absolutely RNA Miniprep Kit (Agilent, 400800) and treated with RNase-free DNase I. RNA quality was verified on an Agilent 2100 Bioanalyzer System (Agilent Technologies) using the RNA 6000 Nano LabChip kit (Agilent Technologies). Samples were then analysed by the Microarray Facility of the Flanders Interuniversity Institute for Biotechnology using a Whole Mouse Genome Oligo Microarray Kit (Agilent Technologies) representing over 41,000 mouse genes and transcripts.

4.2.9 PCR analysis of XBP1 mRNA splicing

VSMCs were treated with 20µmol/l thapsigargin (R&D Systems) for 2h to induce ER-stress. Total RNA was isolated (vide supra) and cDNA was prepared using SuperScript® II reverse transcriptase (Invitrogen). Splicing of X-box-binding protein (XBP)1 mRNA was examined by PCR using XBP1-specific primers: 5'-GATCCTGACGAGGTTCCAGAGGTG-3' (FW) and 5'-GAGTCAGAGTCCATGGGAAGATGTTCTG-3' (RV) and the following thermocycling parameters: 94°C for 2min followed by 40 cycles of 94°C for 15s, 60°C for 30s and 72°C for 30s. The PCR products were then analysed on 4% E-gels (Invitrogen).

4.2.10 Real time RT-PCR

TaqMan gene expression assays (Applied Biosystems) for Nrf2, GSTα, NQO1 and p62 were performed in duplicate on an ABI Prism 7300 sequence detector system (Applied

Biosystems, Foster city, CA, USA) in 25µl reaction volumes containing Universal PCR Master Mix (Applied Biosystems). mRNA expression of IL1α, IL1β and NLRP3 was analysed using SYBR Green (GC Biotech) and the following gene-specific primers (Sigma-Aldrich): IL1α, 5'-AAGACAAGCCTGTGTTGCTGAAGG-3' (FW) and 5'-TCCCAGAAGAAAATGAGGTCGGTC-3' (RV); IL1β, 5'-TGAAATGCCACCTTTTGACAG-3' (FW) and 5'- CCACAGCCACAATGAGTGATAC-3' (RV); NLRP3, 5'-GCTCCAACCATTCTCTGACC-3' (FW) and 5'-AAGTAAGGCCGGAATTCACC-3' (RV). The parameters for PCR amplification were 95°C for 10min followed by 40 cycles of 95°C for 15sec and 60°C for 1min. In case of SYBR Green analysis, an additional step of 72°C for 30sec and a dissociation stage were added. Relative expression of mRNA was calculated using the comparative threshold cycle method. All data were normalised for quantity of cDNA input by performing measurements on the endogenous reference gene β-actin.

4.2.11 Nrf2 silencing and p16 and p62 overexpression

VSMCs were transfected with 100nmol/l Nrf2-specific siRNA (ON-TARGET*plus*® SMART Pool, Mouse Nrf2, Dharmacon, L-040766-00-0005) or siRNA control (ON-TARGET*plus*® Control Pool, nontargeting pool, Dharmacon, D-001810-10-05) via nucleofection using the Human AoSMC Nucleofector™ Kit (Amaxa, VPC-1001). Silencing efficiency was assessed by real time RT-PCR and western blotting.

To overexpress p16 or p62 in VSMCs, full-length cDNA encoding mouse p16 or p62 protein was amplified by PCR from VSMCs using Platinum Pfx DNA polymerase (Invitrogen, 11708-013). The following primers were used: 5'-CCAAGCTTAGCAGCATGGAGTCCGCTGCAGACAG-3' (p16 FW), 5'-CCTCTAGATTAGCTCTGCTCTTGGGATTGGCC-3' (p16 RV), 5'-CAGAATTCGTTATGGCGTCGTTCACGGTGAAGGC-3' (p62 FW) and 5'-CAGCGGCCGCTATCACAATGGTGGAGGGTGCTTCG-3' (p62 RV) from Sigma Aldrich. The resultant PCR products were HindIII/XbaI (p16) or EcoRI/NotI (p62) digested and cloned in the similarly opened plasmid pEGFP-N3 (Clontech, 6080-1), thereby replacing the eGFP coding sequence. After sequencing, VSMCs were transfected with 5µg plasmid DNA via nucleofection using the Human AoSMC Nucleofector™ kit (Amaxa, VPC-1001).

4.2.12 Analysis of cellular senescence

Senescence was determined using the Senescence Cells Histochemical Staining Kit (Sigma-Aldrich, CS0030). Briefly, $1x10^4$ cells were incubated with 1x Fixation Buffer for 7min at RT. Next, cells were washed and incubated with staining mixture (containing X-gal) at 37°C for 24h and then counterstained with Nuclear Fast Red. The percentage of senescence-associated β-gal-positive cells was quantified using Image J software. Cell cycle analysis was performed according to the Vindelov method.[19] Briefly, cells were permeabilised with trypsin, followed by ribonuclease treatment to ensure only DNA staining. Finally, nuclei are stained with propidium iodide (Molecular Probes) and analysed by flow cytometry (BD FACScan) to quantify DNA content. Results were analysed with FCS Express 4 Flow software (De Novo Software). To detect DNA damage, a comet assay was performed as previously described.[20] Briefly, $1x10^3$ cells/µl were mixed with 1% low melting point agarose and embedded on agarose-coated glass slides on ice. Next, cells were lysed in a hypertonic lysis buffer for 1h at 4°C followed by alkaline electrophoresis. During electrophoresis, DNA strand breaks migrated to the positive pole resulting in comet tail formation. After washing with neutralising buffer, slides were fixed in ice-cold ethanol, air-dried and then stained with 20µg/ml ethidium bromide (Sigma-Aldrich) for 10min. DNA damage was evaluated by fluorescence microscopy. Cells treated with 0.5mmol/l H_2O_2 for 10min were used as positive control.

4.2.13 Histological analysis

The percentage neointima formation after ligation [(neointima area/lumen area) x 100] as well as the plaque area and necrotic core in the brachiocephalic artery and aortic root were measured on H&E sections. Atherosclerotic plaques located in the aortic root were analysed in 5 different sections sliced at equally spaced intervals (every 50µm). A 3000 μm^2 minimum threshold was implemented to avoid counting of regions that likely do not represent substantial areas of necrosis.[21] Lesions were further analysed by immunohistochemistry with the following primary antibodies: rabbit anti-Mac-3 (BD Pharmingen, 553322), rabbit anti-cleaved casp-3 (Cell Signaling Technology, 9661), rabbit anti-phospho RB (Cell Signaling Technology, 8516), rabbit anti-p16 (Santa Cruz Biotechnology, sc-1207), goat anti-SM22α (Abcam, ab10135), mouse anti-α-SMC-actin (FITC labelled; Sigma-Aldrich, A2547) and rabbit anti-p62 (Sigma Aldrich, P0067). Thereafter, tissue sections were incubated with species-appropriate HRP-conjugated

secondary antibodies followed by 60 min of reactive ABC (Vector Laboratories, pk4001). 3,3'-diaminobenzidine or 3-amino-9-ethyl-carbazole were used as a chromogen. A Sirius red staining was used for detection of total collagen and COL1A1/2 under polarised light. COL3A1 was detected using goat anti-COL3A1 antibody (Biodesign, T33330G). Frozen tissue sections were stained with Oil Red O and visualised under polarised light to detect cholesterol crystals. The Senescence Cells Histochemical Staining Kit (Sigma Aldrich, CS0030) was applied on the left common carotid artery (LCCA) and aortic root. Frozen sections of the LCCA were counterstained with periodic acid-Schiff (PAS) to visualise the basal lamina. Sections of the aortic root were counterstained with Nuclear Fast Red. Consecutive sections were double stained with rabbit anti-phospho-RB antibody (Cell Signaling Technology, 8516) and anti-rabbit Alexa Fluor 555 secondary antibody (Molecular Probes, A21428), and mouse anti-α-SMC-actin-FITC (Sigma Aldrich, F3777) antibody and visualised by fluorescence microscopy. All other images were acquired with Universal Grab 6.1 software using an Olympus BX40 microscope and quantified with Image J software.

4.2.14 Statistical analysis

All data were analysed with SPSS 22.0 software (SPSS Inc.) and presented as mean ± SEM. Differences were considered significant at $P<0.05$.

4.3 Results

4.3.1 Autophagy is defective in *Atg7$^{F/F}$SM22α-Cre^{+}* (*Atg7$^{F/F}$*) VSMCs

The essential autophagy gene *Atg7* was deleted in VSMCs by cross-breeding mice homozygous for the *Atg7^{Flox}* allele (*Atg7$^{F/F}$*) with a transgenic mouse strain that expresses *Cre* recombinase under control of the mouse VSMC-specific *SM22α* promoter. To validate our experimental mouse model, VSMCs were isolated from the aorta of *Atg7$^{+/+}$SM22α-Cre^{+}* (further referred to as *Atg7$^{+/+}$*) and *Atg7$^{F/F}$SM22α-Cre^{+}* (further referred to as *Atg7$^{F/F}$*) mice. According to western blot analysis, the lack of ATG7 expression in *Atg7$^{F/F}$* VSMCs was associated with typical features of impaired autophagy such as severe p62 accumulation, decreased levels of the ATG12–ATG5 complex, an increased amount of unconjugated ATG5 and a marked decrease of LC3-II levels with respect to *Atg7$^{+/+}$* VSMCs **(Fig. 4.1A)**. Moreover, *Atg7$^{F/F}$* VSMCs did not show enhanced processing of LC3-I into LC3-II upon treatment with EBSS, a well-known stimulus of starvation-induced autophagy **(Fig. 4.1B)**. In addition, electron microscopic analysis did not reveal autophagosome formation in *Atg7$^{F/F}$* VSMCs in both untreated and EBSS-treated conditions. *Atg7$^{+/+}$* VSMCs however, showed increased formation of autophagosomes upon EBSS treatment **(Fig. 4.1C)**. The autophagic vacuoles can be distinguished by the incorporation of dense degraded material**.** These experiments confirm that *Atg7$^{F/F}$* VSMCs were unable to initiate autophagy.

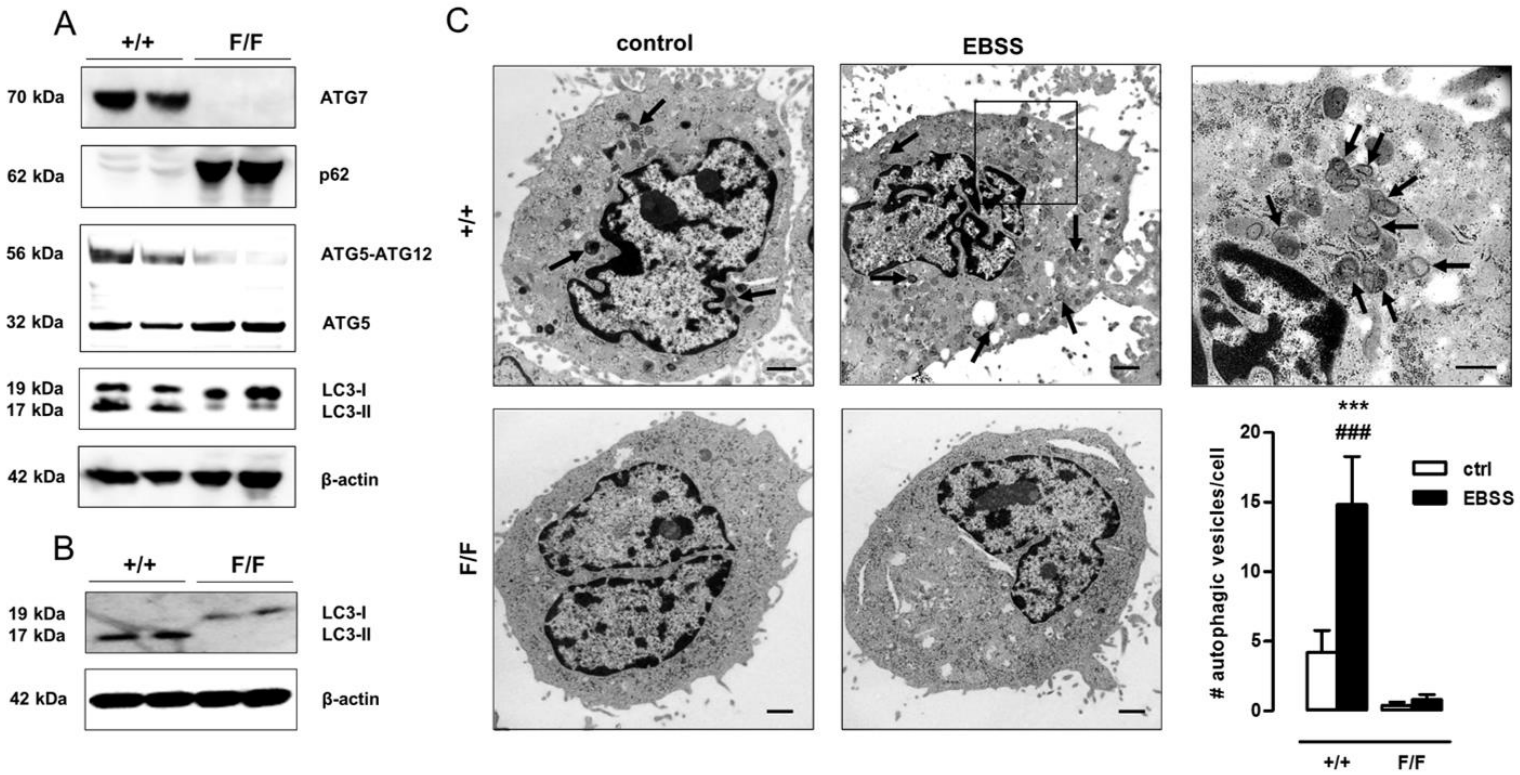

Figure 4.1 Autophagy is defective in *Atg7$^{F/F}$SM22α-Cre^{+}* VSMCs. (A) VSMCs were isolated from the aorta of *Atg7$^{+/+}$SM22α-Cre^{+}* (+/+) and *Atg7$^{F/F}$SM22α-Cre^{+}* (F/F) mice. Western blot analysis of ATG7, p62, ATG12-ATG5 and LC3-II in untreated *Atg7$^{+/+}$* and *Atg7$^{F/F}$* VSMCs. β-actin was used as loading control. **(B,C)** *Atg7$^{+/+}$* and *Atg7$^{F/F}$* VSMCs were treated with EBSS for 48h, followed by western blot analysis of LC3-II (B) or transmission electron microscopy (C). Autophagic vesicles, characterised by incorporated dense degraded material and indicated by arrows, were quantified per cell (***, $P<0.001$ vs. *Atg7$^{F/F}$*; ###, $P<0.001$ vs. control; Two-way ANOVA with genotype and treatment as category factors). Scale bar: 1µm. The right panel shows a high-power image of autophagosomes in EBSS-treated *Atg7$^{+/+}$* VSMCs. Scale bar: 500nm.

4.3.2 Defective autophagy in VSMCs triggers an antioxidative backup mechanism

ROS production, oxidative damage and cell death are major events in cardiovascular disease[22, 23] and may be regulated by autophagy.[24, 25] To test the role of autophagy in VSMC survival against oxidative stress, *Atg7*$^{+/+}$ *and Atg7*$^{F/F}$ VSMCs were treated with 25µmol/l tBHP or 50µg/ml oxLDL for 24h. *Atg7*$^{F/F}$ VSMCs were much more resistant to oxidative stress-induced cell death than *Atg7*$^{+/+}$ VSMCs **(Fig. 4.2A)**. Along these lines, treatment with 100µmol/l tBHP for 6h stimulated ROS production in *Atg7*$^{+/+}$ VSMCs but not in *Atg7*$^{F/F}$ VSMCs **(Fig. 4.2B)**. Interestingly, *Atg7*$^{F/F}$ VSMCs treated with 10µmol/l puromycin for 12h or exposed to UV-irradiation for 10min did not reveal improved protection against apoptosis **(Fig. 4.2C)**.

To explain the observed cytoprotection against oxidative stress, RNA of untreated *Atg7*$^{+/+}$ and *Atg7*$^{F/F}$ VSMCs was analysed. Microarray analysis revealed an upregulation of the genes encoding several antioxidative enzymes such as GSTα1/3/4 (glutathione S-transferase, alpha 1/3/4) and NQO1 (NAD[P]H dehydrogenase, quinone 1) in *Atg7*$^{F/F}$ VSMCs. The microarray data are available via the National Center for Biotechnology Information Gene Expression Omnibus at: http://www.ncbi.nlm.nih.gov/geo/query /acc.cgi?token=ytuzumoktdqzpif&acc=GSE54019. Upregulation of GSTα and NQO1 was confirmed by real-time RT-PCR and western blotting **(Fig. 4.2D and 4.2E)**. Because accumulation of p62 induces nuclear factor erythroid 2-like 2 (Nrf2)-dependent transcription of detoxifying enzymes such as GSTα,[26] this pathway was further studied by western blot analysis. Cytoplasmic and nuclear fractions of *Atg7*$^{F/F}$ VSMCs showed enhanced translocation of Nrf2 into the nucleus **(Fig. 4.2F)**. Silencing of Nrf2 completely suppressed GSTα and NQO1 expression and abolished the protection of *Atg7*$^{F/F}$ VSMCs against tBHP and oxLDL **(Fig. 4.2G and 4.2H)**. These experiments indicate that the Nrf2 signalling pathway is activated in *Atg7*$^{F/F}$ VSMCs as a backup mechanism to protect against oxidative stress. Overall, *Atg7* deletion in VSMCs did not result in a general pro-survival status but only protected VSMCs against oxidative stress-mediated cell death via upregulation of antioxidative enzymes.

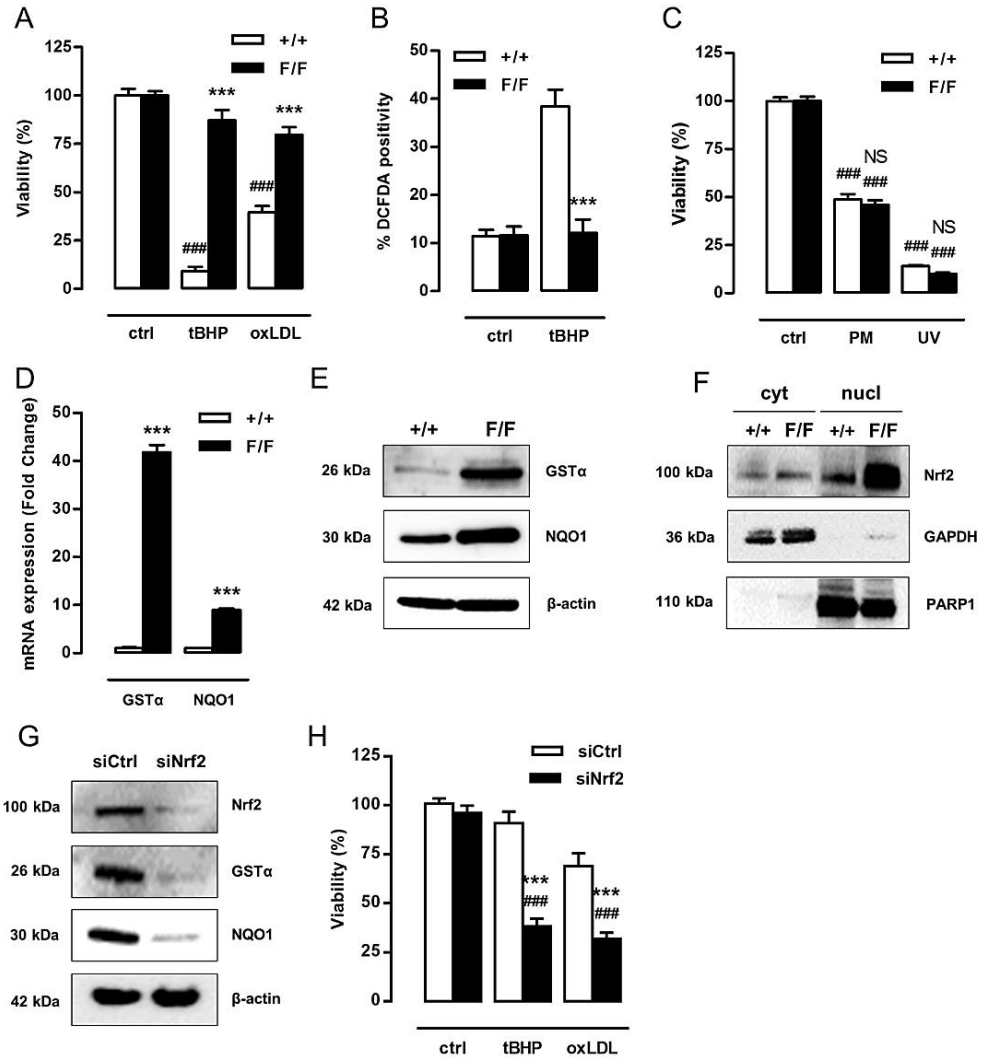

Figure 4.2 Defective autophagy in VSMCs results in increased protection against oxidative stress-induced cell death. (A) *Atg7$^{+/+}$SM22α-Cre^{+}* (+/+) and *Atg7$^{F/F}$SM22α-Cre^{+}* (F/F) VSMCs were treated with 25µmol/l tBHP or 50µg/ml oxLDL for 24h (***, *P*<0.001 vs. Atg7$^{+/+}$; ###, *P*<0.001 vs. control; n=3 experiments in triplicate; Two-way ANOVA with genotype and treatment as category factors, Dunnett Post Hoc). **(B)** To measure ROS production, *Atg7$^{+/+}$* and *Atg7$^{F/F}$* VSMCs were left untreated or treated with 100µmol/l tBHP for 6h, followed by a DCFDA staining (***, *P*<0.001 vs. *Atg7$^{+/+}$*; n=200 cells/condition in duplicate; Two-way ANOVA. **(C)** *Atg7$^{+/+}$* and *Atg7$^{F/F}$* VSMCs were exposed to 10µmol/l puromycin (PM) for 12h or UV-irradiation for 10min (NS, not significant vs. *Atg7$^{+/+}$*; ###, *P*<0.001 vs. control; n=2 experiments in triplicate; Two-way ANOVA). **(D,E)** Analysis of GSTα and NQO1 expression in *Atg7$^{+/+}$* and *Atg7$^{F/F}$* VSMCs by real time RT-PCR (D) (***, *P*<0.001; n=2 experiments in duplicate; Student t test) and western blotting (E). **(F)** Western blot analysis of Nrf2 in cytoplasmic and nuclear fractions of *Atg7$^{+/+}$* and *Atg7$^{F/F}$* VSMCs. **(G,H)** *Atg7$^{F/F}$* VSMCs were transfected with 100nmol/l siRNA against Nrf2 (siNrf2) or nontargeting siRNA (siCtrl). After 72h, silencing efficiency was confirmed by western blotting by assessment of Nrf2, GSTα and NQO1 expression (G) and VSMCs were treated with tBHP or oxLDL for 24h (H) (***, *P*<0.001 vs. siCtrl; ###, *P*<0.001 vs. control; n=3 experiments in duplicate; Two-way ANOVA with genotype and treatment as category factors and Dunnett Post Hoc).

4.3.3 Defective autophagy in VSMCs elicits cellular hypertrophy, improves migration capacity, and promotes synthesis of inflammasome components and collagen

Microscopic analysis of *Atg7*$^{F/F}$ VSMCs did not reveal a typical spindle-shaped phenotype as compared to *Atg7*$^{+/+}$ VSMCs. Instead, *Atg7*$^{F/F}$ VSMCs were characterised by a more rhomboid shape and an increase in cellular size **(Fig. 4.3A)**. *In vivo*, the medial thickness of *Atg7*$^{F/F}$ aorta was significantly increased as compared to *Atg7*$^{+/+}$ aorta **(Fig. 3.4B)**, though the number of VSMC layers was not altered. Also TEM images of *Atg7*$^{F/F}$ aorta showed an increase in size of the individual VSMCs **(Fig. 4.3C)**. These findings indicate that defective autophagy in VSMCs results in cellular hypertrophy *in vitro* and *in vivo*. Furthermore, *Atg7*$^{F/F}$ VSMCs showed a significant increase in protein content as compared to *Atg7*$^{+/+}$ VSMCs, indicating that the hypertrophic phenotype of *Atg7*$^{F/F}$ VSMCs is not just a result of cytosolic dilation but is associated with increased protein quantity **(Fig. 4.3D)**. To investigate whether the increased protein content was due to increased accumulation (owing to impaired autophagic clearance of proteins) and/or to increased protein synthesis, a radio-active amino acid incorporation assay was performed. *Atg7*$^{F/F}$ VSMCs showed increased radio-active protein labelling as compared to *Atg7*$^{+/+}$ VSMCs **(Fig. 4.3E)**. Importantly, the hypersynthetic state of *Atg7*$^{F/F}$ VSMCs did not trigger activation of the unfold protein response (UPR), as evidenced by the lack of XBP1 splicing **(Fig. 4.3F)**, indicating that autophagy deficiency in VSMCs does not provoke ER stress.

Further characterisation of *Atg7*$^{F/F}$ VSMCs revealed a substantial upregulation of the inflammasome components IL1β and NLRP3, but not of IL1α **(Fig. 4.4A)**. Moreover, according to western blot analysis, the expression of the pro-migratory growth factors TGFβ and SDF1 was significantly elevated in *Atg7*$^{F/F}$ VSMCs **(Fig. 4.4B)**. Indeed, an Oris migration assay revealed enhanced spontaneous migration of *Atg7*$^{F/F}$ VSMCs as compared to *Atg7*$^{+/+}$ VSMCs **(Fig. 4.4C).** To test the influence on collagen content, *Atg7*$^{+/+}$ and *Atg7*$^{F/F}$ VSMCs were treated with 10ng/ml TGFβ for 48h. *Atg7*$^{F/F}$ VSMCs showed a significant increase in collagen amount in both control and TGFβ-treated conditions as compared to *Atg7*$^{+/+}$ VSMCs **(Fig. 4.4D)**. Further analysis of COL1A1/2 and COL3A1 by immunofluorescence showed that *Atg7*$^{F/F}$ VSMCs express less COL1A1/2 but more COL3A1 as compared to *Atg7*$^{+/+}$ VSMCs **(Fig. 4.4E)**. TGFβ treatment augmented COL1A1/2 and COL3A1 expression in both genotypes.

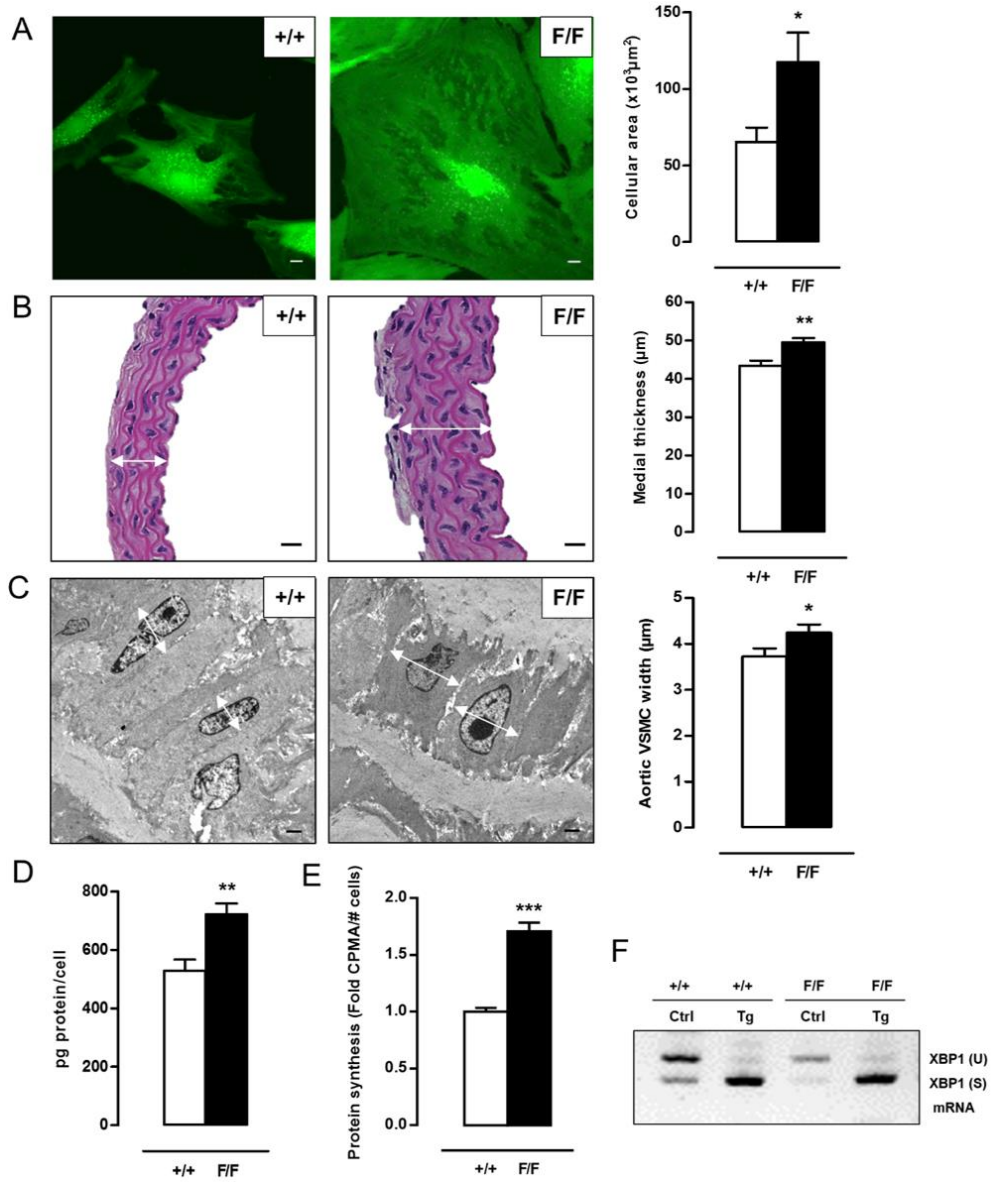

Figure 4.3 Defective autophagy in VSMCs elicits cellular hypertrophy and increases protein synthesis. (A) VSMCs isolated from *Atg7*$^{+/+}$*SM22α-Cre*$^{+}$ (+/+) and *Atg7*$^{F/F}$*SM22α-Cre*$^{+}$ aorta were labelled with calcein AM and visualised by confocal fluorescence microscopy. Scale bar: 10µm. Cell size was measured using z-stack images (*, *P*<0.05; n=2 experiments; Student t test). **(B)** Thoracic aorta of *Atg7*$^{+/+}$ and *Atg7*$^{F/F}$ mice were stained with H&E to measure the width of the media (white arrows) (**, *P*<0.01; n=6 regions/aorta; Univariate). Scale bar: 25µm. **(C)** TEM images of the aorta of *Atg7*$^{+/+}$ and *Atg7*$^{F/F}$ mice to quantify VSMC width (white arrows). Scale bar: 1µm. (*, *P*<0.05; n=38 cells/aorta; Student t test). **(D)** Determination of protein quantity in *Atg7*$^{+/+}$ and *Atg7*$^{F/F}$ VSMCs using the BCA method. Data were normalised to cell number (**, *P*<0.01; n=3 experiments in triplicate; Student t test). **(E)** Radioactive amino acid incorporation assay to assess protein synthesis in *Atg7*$^{+/+}$ and *Atg7*$^{F/F}$ VSMCs. Data are collected as counts per minute (CPMA), normalised to cell number and presented as a fold change. (***, P<0.001; n=3 experiments in tetraplicate; Student t test) **(F)** *Atg7*$^{+/+}$ and *Atg7*$^{F/F}$ VSMCs were treated with the ER-stressor thapsigargin (Tg) (20µmol/l) for 2h or left untreated (Ctrl). Activation of the UPR was evaluated by detection of mRNA of spliced (S) XBP1.

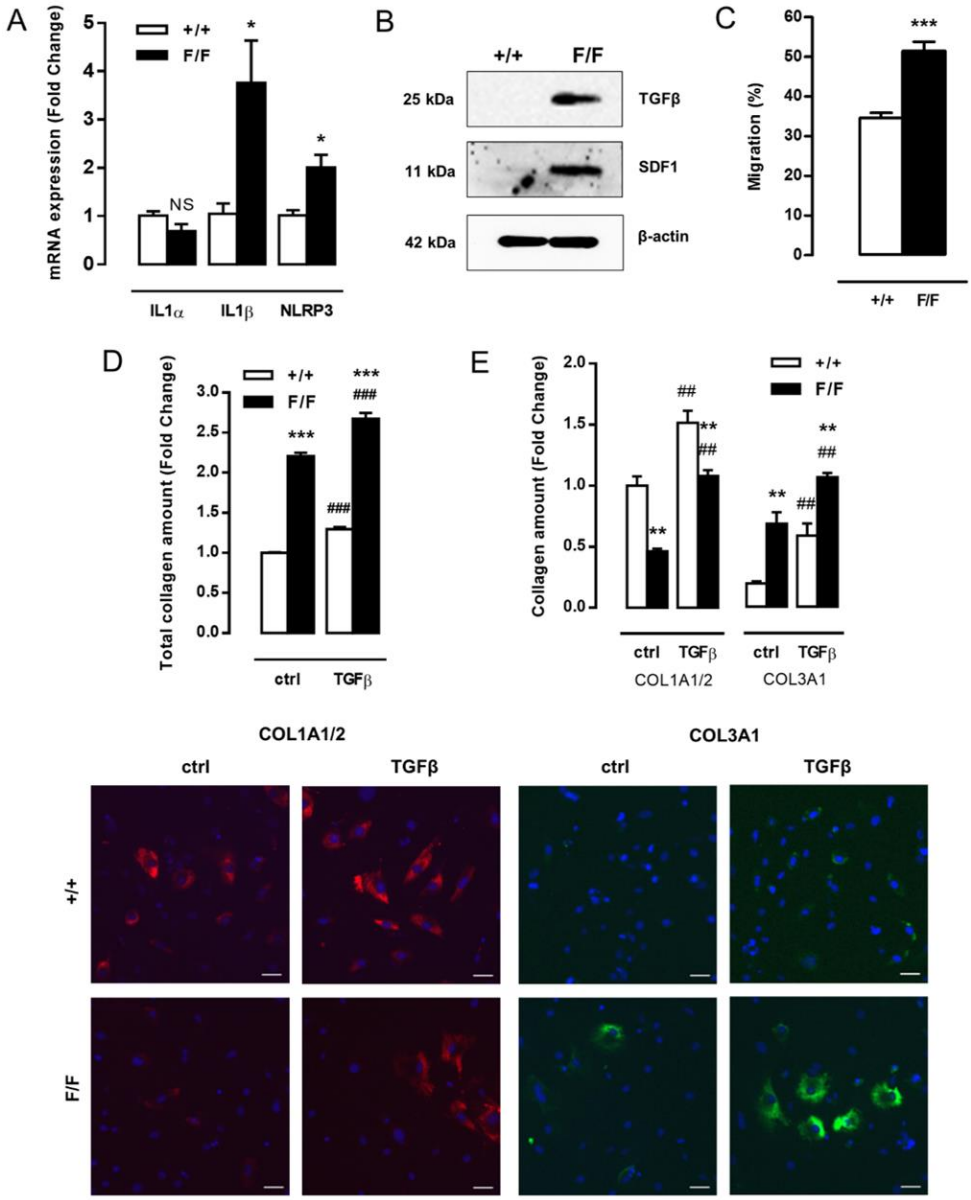

Figure 4.4: Defective autophagy in VSMCs increases migration capacity and synthesis of inflammasome components and collagen (A) Real time RT-PCR analysis of mRNA expression of IL1α, IL1β and NLRP3 in untreated *Atg7*$^{+/+}$ and *Atg7*$^{F/F}$ VSMCs. (n=4 independent experiments; NS, not significant, *, *P*<0.05 vs. *Atg7*$^{+/+}$) **(B)** Western blot analysis of TGFβ and SDF1 in *Atg7*$^{+/+}$ and *Atg7*$^{F/F}$ VSMCs. **(C)** Migratory capacity of *Atg7*$^{+/+}$ and *Atg7*$^{F/F}$ VSMCs was analysed using an Oris Migration Assay (***, *P*<0.001; n=2 experiments in triplicate; Student t test). **(D,E)** *Atg7*$^{+/+}$ and *Atg7*$^{F/F}$ VSMCs were left untreated or treated with 10ng/ml TGFβ for 48h and (D) stained with Sirius red to examine total collagen amount (***, *P*<0.001 vs. *Atg7*$^{+/+}$; ###, *P*<0.001 vs. ctrl; n=4 experiments in triplicate; Two-way ANOVA with genotype and treatment as category factors) or (E) analysed for COL1A1/2 (left panel, red) and COL3A1 (right panel, green) expression by immunofluorescence (**, *P*<0.01 vs. *Atg7*$^{+/+}$; ##, *P*<0.01 vs. ctrl; n=2 counting regions of 150 cells/region/condition; Two-way ANOVA with genotype and treatment as category factors). Scale bar: 25μm.

4.3.4 Defective autophagy in VSMCs accelerates senescence

A BrdU incorporation assay was performed to examine the proliferation capacity of *Atg7*$^{+/+}$ and *Atg7*$^{F/F}$ VSMCs. A nearly 2-fold reduction in proliferation of *Atg7*$^{F/F}$ VSMCs was observed as compared to *Atg7*$^{+/+}$ VSMCs **(Fig. 4.5A)**. Moreover, *Atg7*$^{F/F}$ VSMCs were characterised by a significant increase in nuclear size **(Fig. 4.5B)**. According to a cell cycle analysis, the percentage of *Atg7*$^{F/F}$ nuclei in G_1-phase was increased (36±5% vs. 55±1%) while the percentage of *Atg7*$^{F/F}$ nuclei in G_2/M-phase was strongly decreased (38±2% vs. 15±1%), suggestive of a G_1-cell cycle arrest and senescence **(Fig. 4.5C)**. Importantly, cell cycle analysis did not show signs of VSMC polyploidy in both cell types. Staining for senescence-associated (SA) β-galactosidase (β-gal) activity confirmed the presence of senescent cells in *Atg7*$^{F/F}$ VSMC cultures **(Fig. 4.5D)**. Because cellular senescence can be established by the activation of different tumour suppressor pathways including p16-RB (stress response) and p53-p21 (DNA damage response) pathways,[27, 28] these proteins were examined via western blotting. p16 was highly upregulated in *Atg7*$^{F/F}$ VSMCs and accompanied by hypophosphorylation and activation of RB while acetylated p53 and p21 levels remained unaltered **(Fig. 4.5E)**, indicating stress-induced premature senescence. Next, we performed a comet assay to determine possible DNA damage. Neither *Atg7*$^{+/+}$ nor *Atg7*$^{F/F}$ VSMCs showed comet tail formation. In contrast, *Atg7*$^{+/+}$ VSMCs treated with 0.5mmol/l H_2O_2 for 10min showed severe comet tail formation representing a large number of DNA strand breaks **(Fig. 4.5F)**. Given that the DNA damage response pathway was not activated and DNA strand breaks were absent, senescence in *Atg7*$^{F/F}$ VSMCs was not characterised by DNA damage.

Furthermore, we investigated a possible link between senescence and the Nrf2 pathway. Nrf2 silencing in *Atg7*$^{F/F}$ VSMCs did not affect p16 protein expression **(Fig. 4.6A)**. Overexpression of p16 in *Atg7*$^{+/+}$ VSMCs induced senescence (7±1% SA-β-gal vs. 27±1%, $P<0.001$) but altered neither NQO1 expression nor Nrf2 activation **(Fig. 4.6B)**. These experiments suggest that the senescence and Nrf2 pathway act independently in autophagy deficient VSMCs.

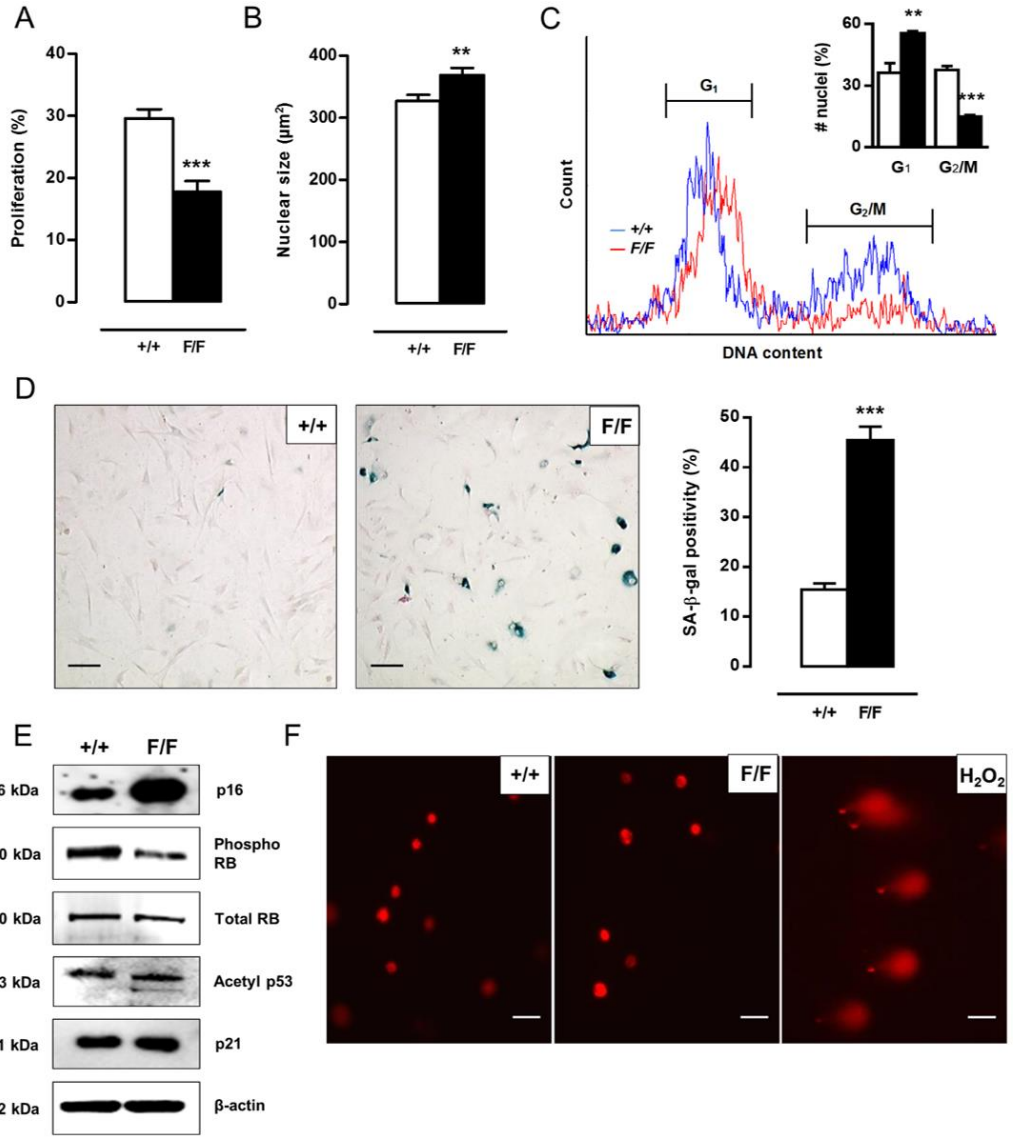

Figure 4.5 Defective autophagy in VSMCs accelerates senescence. (A) *Atg7*$^{+/+}$*SM22α-Cre*$^{+}$ (+/+) and *Atg7*$^{F/F}$*SM22α-Cre*$^{+}$ (F/F) VSMCs were treated with BrdU to examine proliferation (***, *P*<0.001; n=9 counting regions of 300 cells/region/condition; Student t test). **(B)** The size of *Atg7*$^{+/+}$ and *Atg7*$^{F/F}$ nuclei was measured to detect nuclear hypertrophy (**, *P*<0.01; n=50 nuclei; Student t test). **(C)** DNA cell cycle analysis of *Atg7*$^{+/+}$ (blue) and *Atg7*$^{F/F}$ (red) VSMCs. The bar graph shows the percentage of *Atg7*$^{+/+}$ and *Atg7*$^{F/F}$ nuclei in the G_1 and G_2/M phase of the cell cycle (**, *P*<0.01; ***, *P*<0.001; Student t test). **(D)** *Atg7*$^{+/+}$ and *Atg7*$^{F/F}$ VSMCs were stained with X-gal mixture for 24h, followed by Nuclear Fast Red staining. Scale bar: 125µm. The number of SA-β-gal-positive VSMCs was quantified. (***, *P*<0.001; n= 2 counting regions of 200 cells/region/condition; Student t test) **(E)** Western blot analysis of p16, phospho RB, total RB, acetylated p53 and p21 in *Atg7*$^{+/+}$ and *Atg7*$^{F/F}$ VSMCs. **(F)** Detection of DNA damage in *Atg7*$^{+/+}$ and *Atg7*$^{F/F}$ VSMCs by comet assay. *Atg7*$^{+/+}$ VSMCs treated with 0.5mM H_2O_2 for 10min were used as positive control. Scale bar: 25µm.

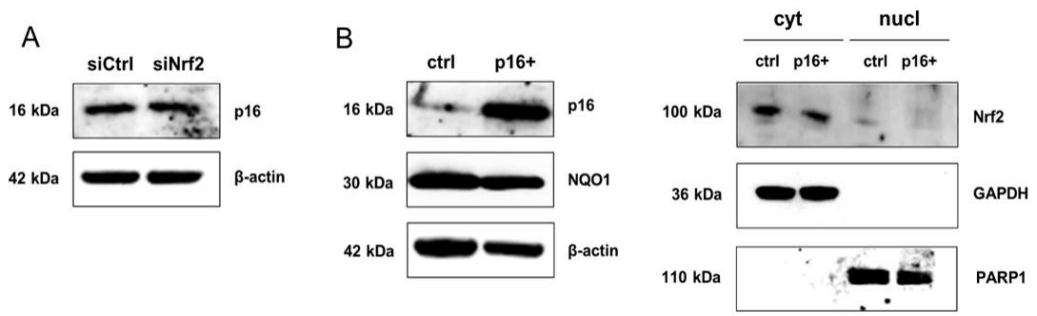

Figure 4.6 The senescence and Nrf2-ARE pathway act independently in autophagy deficient VSMCs. (A) *Atg7*$^{F/F}$ VSMCs were transfected with 100nmol/l siRNA against Nrf2 (siNrf2) or nontargeting siRNA (siCtrl). 72h after transfection, VSMCs were analysed for p16 expression by western blotting. **(B)** *Atg7*$^{+/+}$ VSMCs were transfected with 5µg plasmid DNA encoding p16 (p16+). 48h after transfection, VSMCs were analysed for p16, NQO1 and Nrf2 (in cytoplasmic and nuclear fractions) expression by western blotting**.**

To investigate the role of p62 accumulation (typical of defective autophagy, vide supra) in the induction of VSMC senescence, *Atg7*$^{+/+}$ VSMCs were transiently transfected with p62-encoding plasmid DNA. Overexpression of p62 in *Atg7*$^{+/+}$ VSMCs resulted in increased p16 expression and a slight decrease in RB phosphorylation **(Fig. 4.7A)**. Moreover, p62 overexpressing *Atg7*$^{+/+}$ VSMCs showed reduced proliferation **(Fig. 4.7B)** and increased SA-β-gal activity **(Fig. 4.7C)**. These experiments indicate that p62 mediates the induction of senescence in autophagy defective VSMCs.

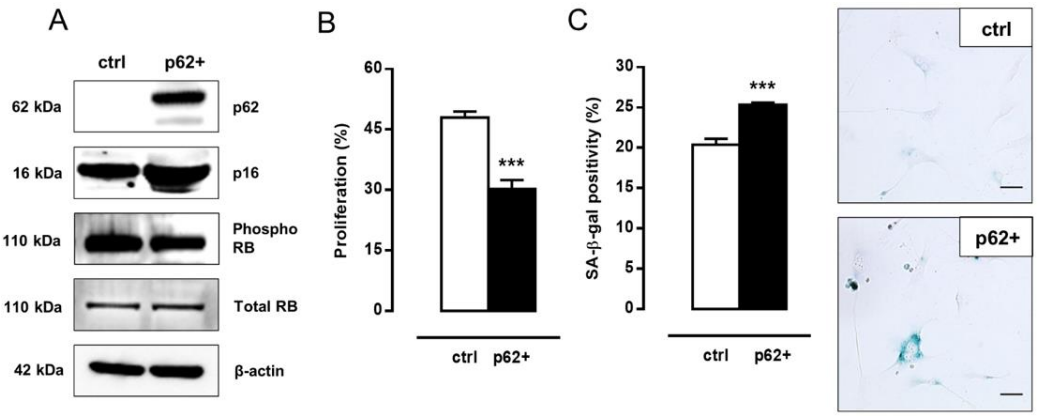

Figure 4.7 p62 accumulation links defective VSMC autophagy to senescence. (A) *Atg7*$^{+/+}$ VSMCs were transfected with 5µg plasmid DNA encoding p62 (p62+). 4 days after transfection, VSMCs were analysed for p62, p16, phospho RB and total RB expression by western blotting. **(B,C)** p62 overexpressing VSMCs were (B) incubated with BrdU to examine proliferation capacity (***, *P*<0.001; n=2 counting regions of 1000 cells/region/condition in duplicate; Student t test) or (C) stained with X-gal mixture for 24h to quantify the number of β-gal-positive VSMCs (***, *P*<0.001; n=3 counting regions of 150 cells/region/condition in duplicate; Student t test). Scale bar: 50µm**.**

4.3.5 Defective VSMC autophagy promotes neointima formation after ligation-induced injury

To evaluate the consequences of defective VSMC autophagy *in vivo*, neointimal lesion formation was induced by ligation of the left common carotid artery (LCCA) in *Atg7*$^{+/+}$*SM22α-Cre*$^{+}$ (*Atg7*$^{+/+}$) and *Atg7*$^{F/F}$*SM22α-Cre*$^{+}$ (*Atg7*$^{F/F}$) mice. Five days after ligation, the activity of the gelatinase MMP9 was already strongly elevated in *Atg7*$^{F/F}$ LCCA as shown by zymographic analysis **(Fig. 4.8A)**. Moreover, western blot analysis showed a significant increase in TGFβ and SDF1 expression in the LCCA of *Atg7*$^{F/F}$ mice **(Fig. 4.8B)**. To investigate the effect on neointimal thickening, LCCA of *Atg7*$^{+/+}$ and *Atg7*$^{F/F}$ mice were analysed 5 weeks after ligation. *Atg7*$^{F/F}$ mice showed a dramatic increase in stenosis (90±3%) as compared to *Atg7*$^{+/+}$ mice (54±6%) **(Fig. 4.9A)**. In addition, the total collagen content was significantly elevated in the neointima of *Atg7*$^{F/F}$ mice **(Fig. 4.9B)**. p62 staining confirmed the presence of autophagy deficient VSMCs in media and lesions of *Atg7*$^{F/F}$ mice **(Fig. 4.9C)**. Furthermore, neointimal *Atg7*$^{F/F}$ VSMCs were characterised by p16 upregulation **(Fig. 4.9D)**, SA-β-gal activity **(Fig. 4.9E)** and nuclear hypertrophy (28±1 vs. 23±1 μm^2), indicating that neointima formation in *Atg7*$^{F/F}$ mice was associated with VSMC senescence.

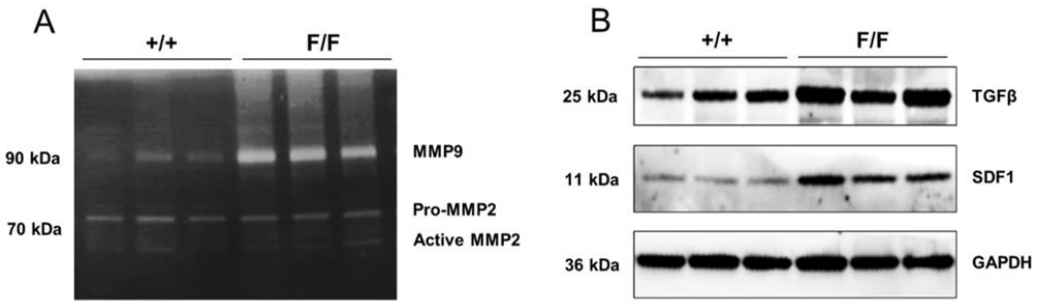

Figure 4.8: Defective VSMC autophagy promotes upregulation of MMP9, TGFβ and SDF1, 5 days after ligation-induced injury. (A) The left common carotid artery (LCCA) of *Atg7*$^{+/+}$*SM22α-Cre*$^{+}$ (+/+) and *Atg7*$^{F/F}$*SM22α-Cre*$^{+}$ (F/F) mice (n=3) was ligated for 5 days. Gelatin zymographic analysis of the LCCA to detect MMP9 and MMP2 activity. **(B)** Western blot analysis of the LCCA for TGFβ and SDF1. GAPDH was used as loading control.

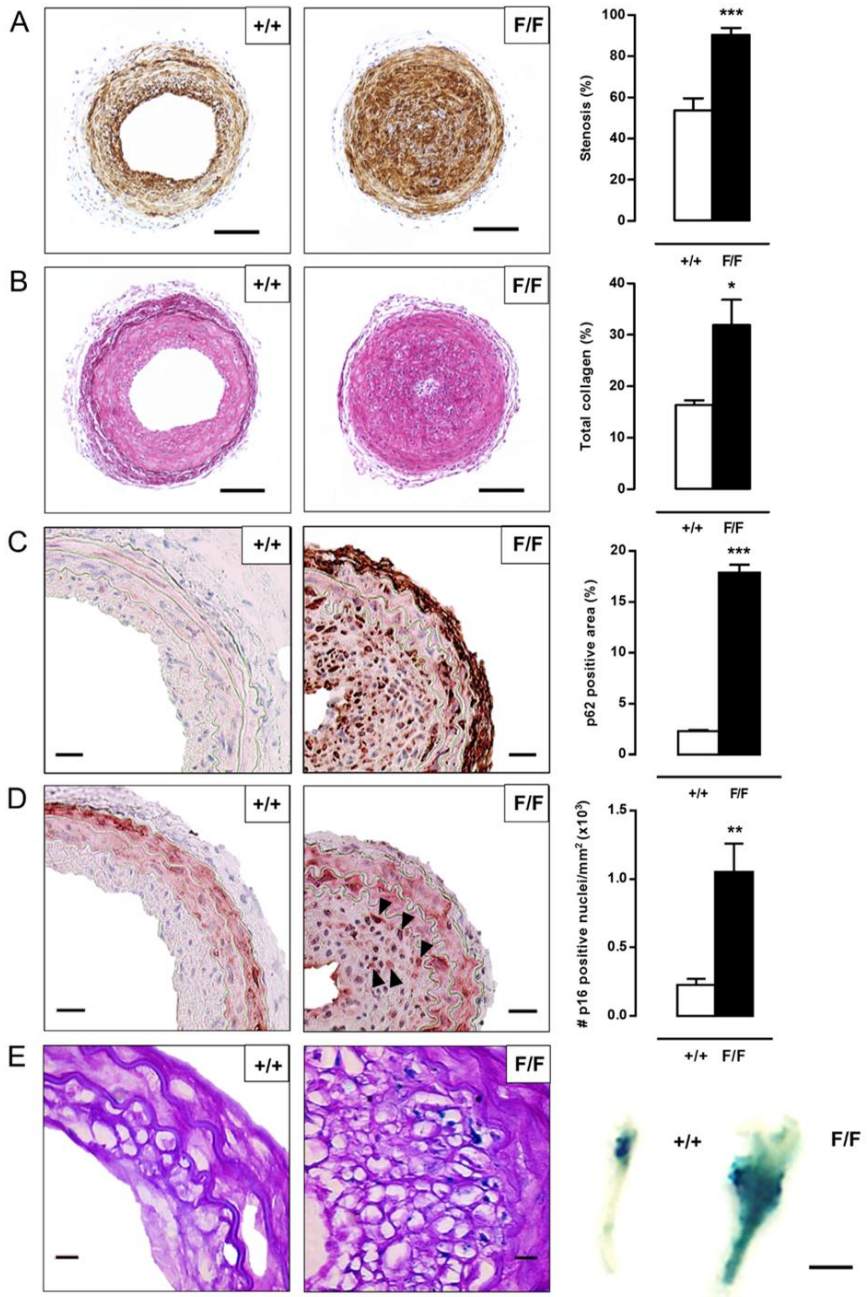

Figure 4.9 Defective VSMC autophagy promotes neointima formation 5 weeks after ligation-induced injury. (A,B) The left common carotid artery (LCCA) of *Atg7*$^{+/+}$*SM22α-Cre*$^{+}$ (+/+) (n=10) and *Atg7*$^{F/F}$*SM22α-Cre*$^{+}$ (F/F) (n=12) mice was ligated for 5 weeks. Sections of the LCCA were stained with anti-α-SMC-actin antibody (A) or Sirius red (B) to quantify the degree of stenosis and total collagen deposition, respectively. Scale bar: 100µm. **(C,D)** Sections of the LCCA were immunostained for p62 (C) or p16 (D) (black arrowheads). Scale bar: 25µm**. (E)** The LCCA was stained for SA-β-gal activity *ex vivo* (right panel). Scale bar: 250µm. Sections of the LCCA were then counterstained with periodic acid-Schiff (PAS) to identify senescent neointimal VSMCs (left panel). Note that the neointimal VSMCs are surrounded by a cage of PAS-positive basal lamina. Scale bar: 10µm. (***, *P*<0.001; **, *P*<0.01; *, *P*<0.05; Student t test).

4.3.6 Defective VSMC autophagy accelerates atherogenesis

To investigate the role of VSMC autophagy in atherosclerosis, *Atg7*$^{+/+}$*SM22α-Cre*$^{+}$ and *Atg7*$^{F/F}$*SM22α-Cre*$^{+}$ mice were crossbred with *ApoE*$^{-/-}$ mice and fed a western-type diet (WD) for 10 or 14 weeks. Body weight, total cholesterol and lipoproteins were not different between both groups after 10 and 14 weeks on WD **(Table 4.1 and Fig. 4.10)**, indicating that *Atg7* deletion in VSMCs does not influence normal growth and lipid metabolism.

Table 4.1. Characteristics of *Atg7*$^{+/+}$*SM22α-Cre*$^{+}$*ApoE*$^{-/-}$ (+/+) and *Atg7*$^{F/F}$*SM22α-Cre*$^{+}$*ApoE*$^{-/-}$ (F/F) mice after 10 and 14 weeks of western-type diet (WD).

	10 weeks WD		14 weeks WD	
	+/+	F/F	+/+	F/F
Body weight (g)	31±1	31±1	25±1	25±1
Total cholesterol (mg/dl)	825±58	1003±108	589±36	578±30

All data are represented as mean ± SEM; *P*>0.05; Student t test

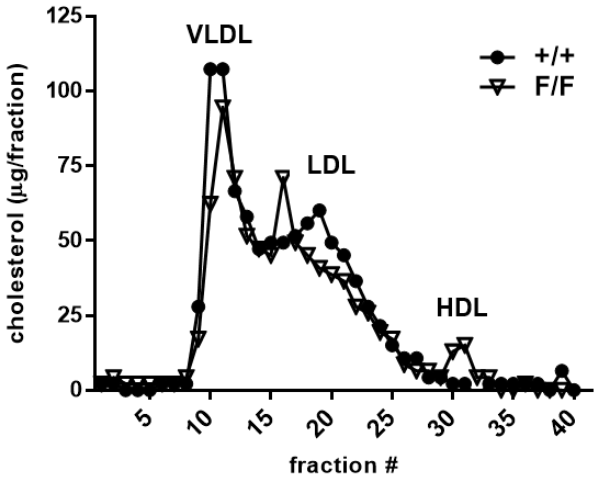

Figure 4.10 Defective VSMC autophagy accelerates atherogenesis without affecting lipid metabolism. Lipid profile of *Atg7*$^{+/+}$*SM22α-Cre*$^{+}$*ApoE*$^{-/-}$ (+/+) and *Atg7*$^{F/F}$*SM22α-Cre*$^{+}$*ApoE*$^{-/-}$ (F/F) mice fed a western-type diet for 10 and 14 weeks.

Analysis of plaques located in the brachiocephalic artery of *Atg7$^{F/F}$SM22α-Cre^{+}ApoE$^{-/-}$* (*Atg7$^{F/F}$ApoE$^{-/-}$*) revealed a 3-fold increase in size as compared to *Atg7$^{+/+}$SM22α-Cre^{+}ApoE$^{-/-}$* (*Atg7$^{+/+}$ApoE$^{-/-}$*) mice (156±19 vs. 58±9 x10^{3} µm^{2}; *P*<0.001) after 10 weeks of WD. Furthermore, plaques of *Atg7$^{F/F}$ApoE$^{-/-}$* mice were characterised by elevated plaque necrosis, plaque apoptosis, macrophage content, total collagen content and fibrous cap thickness **(Fig. 4.11A to 4.11E)**. Thus, *ApoE$^{-/-}$* mice with defective VSMC autophagy develop a more advanced and complex plaque phenotype.

After 14 weeks on WD, plaque size (171±11 µm^{2} vs. 166±9 x10^{3} µm^{2}; *P*>0.05), macrophage content as well as the degree of necrosis and apoptosis was similar in *Atg7$^{+/+}$ApoE$^{-/-}$* and *Atg7$^{F/F}$ApoE$^{-/-}$* mice **(Fig. 4.12A to 4.12C)**. However, total collagen content and fibrous cap thickness were still elevated in plaques of *Atg7$^{F/F}$ApoE$^{-/-}$* mice **(Fig. 4.12D and 4.12E)**. Interestingly, the amount of COL1A1/2 was significantly decreased in *Atg7$^{F/F}$ApoE$^{-/-}$* plaques while the amount of COL3A1 was increased **(Fig. 4.13A and 4.13B)**. Moreover, the deposition of cholesterol crystals, known to activate the NLRP3 inflammasome[29], was not different between plaques of *Atg7$^{+/+}$ApoE$^{-/-}$* mice and *Atg7$^{F/F}$ApoE$^{-/-}$* mice **(Fig. 4.13C)**. Finally, staining for p62 confirmed autophagy deficiency in VSMCs of the media and the plaque of *Atg7$^{F/F}$ApoE$^{-/-}$* mice **(Fig. 4.13D).**

Next, we investigated whether VSMCs in *Atg7$^{F/F}$ApoE$^{-/-}$* plaques revealed characteristics of senescence. VSMCs within the fibrous cap of *Atg7$^{F/F}$ApoE$^{-/-}$* plaques were characterised by enhanced SA-β-gal activity **(Fig. 4.14A)**, hypophosphorylation and activation of RB **(Fig. 4.14B)** and nuclear hypertrophy **(Fig. 4.14C)**, indicative of senescence. Importantly, plaque formation in *Atg7$^{F/F}$ApoE$^{-/-}$* mice was not attributed to increased proliferation of medial VSMCs as shown by severe hypophosphorylation of RB in the media **(Fig. 4.14D)**.

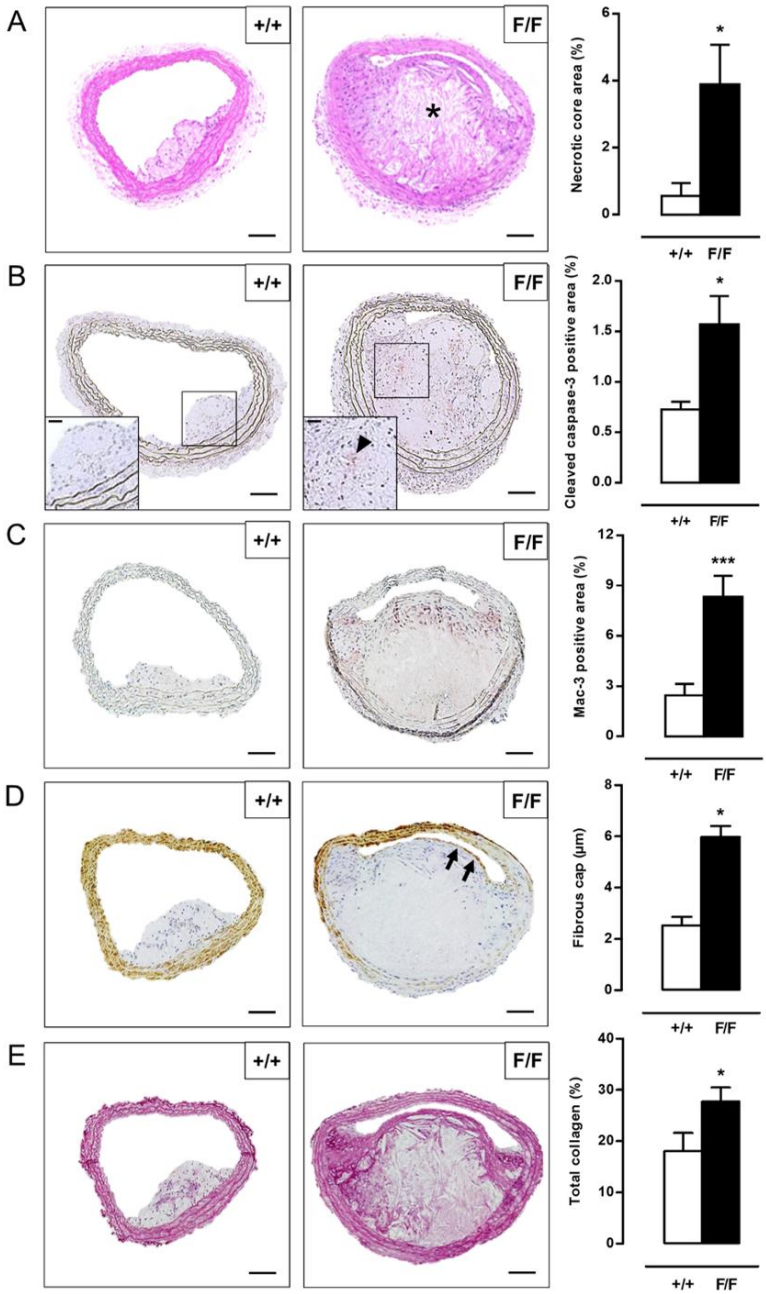

Figure 4.11 Defective VSMC autophagy accelerates atherogenesis after 10 weeks of western-type diet. (A) *Atg7*$^{+/+}$*SM22α-Cre*$^{+}$*ApoE*$^{-/-}$ (+/+) and *Atg7*$^{F/F}$*SM22α-Cre*$^{+}$*ApoE*$^{-/-}$ (F/F) mice (n=16) were fed a western-type diet for 10 weeks. Sections of the brachiocephalic artery were stained with H&E to quantify plaque size and percentage of necrosis. (*, *P*<0.05; Student t test). **(B to D)** Consecutive sections were immunostained for cleaved caspase-3 (B), Mac-3 (C) and α-SMC-actin (D) to measure the percentage of apoptosis (indicated by a black arrowhead in the high-power photograph of the boxed area in the left corner of each image), percentage of macrophages and fibrous cap thickness (indicated by black arrows), respectively (*, *P*<0.05; Student t test (B); ***, *P*<0.001; Student t test (C); *, *P*<0.05; n=10 measurements/mouse, Repeated Measure (D)). **(E)** Consecutive sections were stained with Sirius red to quantify total collagen. (*, *P*<0.05; Student t test). *, necrotic core. Scale bar: 100µm**.**

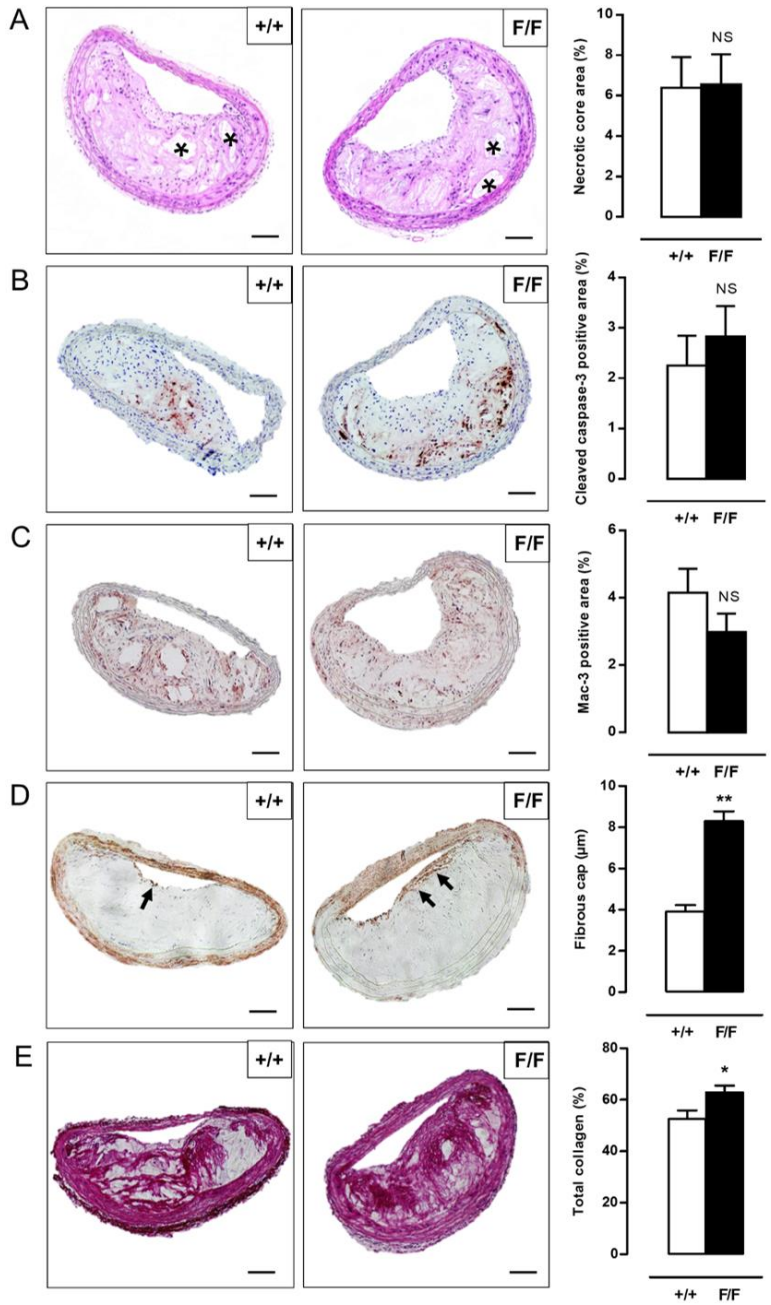

Figure 4.12 Defective VSMC autophagy promotes formation of a thick fibrous cap after 14 weeks of western-type diet. (A) *Atg7$^{+/+}$SM22α-Cre^{+}ApoE$^{-/-}$* (+/+) and *Atg7$^{F/F}$SM22α-Cre^{+}ApoE$^{-/-}$* (F/F) mice (n=16) were fed a western-type diet for 14 weeks. Sections of the brachiocephalic artery were stained with H&E to quantify plaque size and percentage of necrosis. (NS, not significant; Student t test). **(B to D)** Consecutive sections were immunostained for cleaved caspase-3 (B), Mac-3 (C) and α-SMC-actin (D) to measure the percentage of apoptosis, percentage of macrophages and fibrous cap thickness (indicated by black arrows), respectively. (NS, not significant; Student t test (B,C); **, *P*<0.01; n= 10 measurements/mouse, Repeated Measure (D)). (E) Consecutive sections were stained with Sirius red to quantify total collagen. (*, *P*<0.05; Student t test). *, necrotic core. Scale bar: 100µm**.**

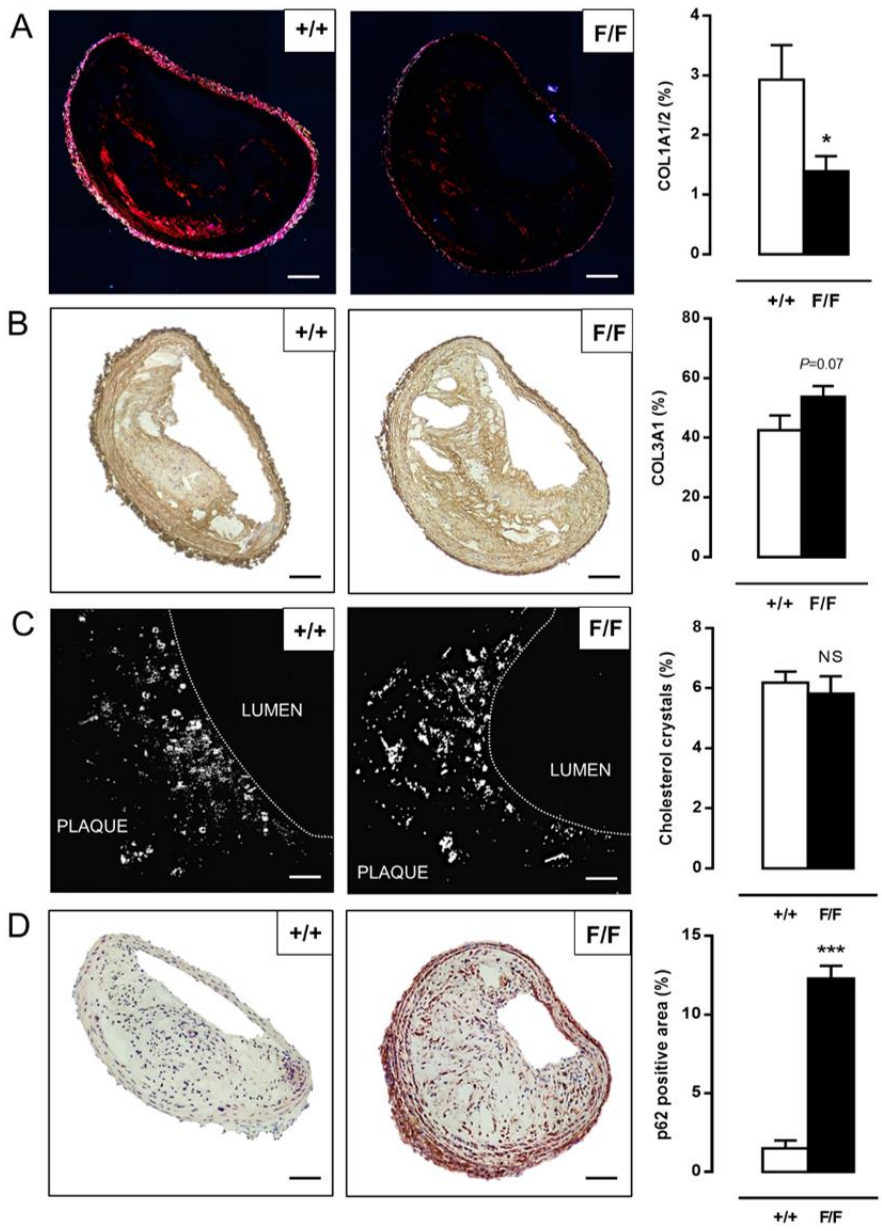

Figure 4.13 Defective VSMC autophagy is associated with p62 accumulation and alters collagen type I/III but not cholesterol crystal deposition after 14 weeks of western-type diet. *Atg7$^{+/+}$SM22α-Cre^{+}ApoE$^{-/-}$* (+/+) and *Atg7$^{F/F}$SM22α-Cre^{+}ApoE$^{-/-}$* (F/F) mice (n=16) were fed a western-type diet for 14 weeks. **(A,B)** Plaques of the brachiocephalic artery were stained with (A) Sirius red and visualised under polarised light to detect COL1A1/2 or (B) immunostained for COL3A1 (*, P<0.05; NS, not significant; Student t test). Scale bar: 100µm **(C)** Aortic root plaques were stained with Oil Red O and visualised under polarised light to detect cholesterol crystals. (NS, not significant; Univariate) Scale bar: 50µm. **(D)** Plaques of the brachiocephalic artery were immunostained for p62 as marker for defective autophagy. (***, P<0.001; Student t test). Scale bar: 100µm.

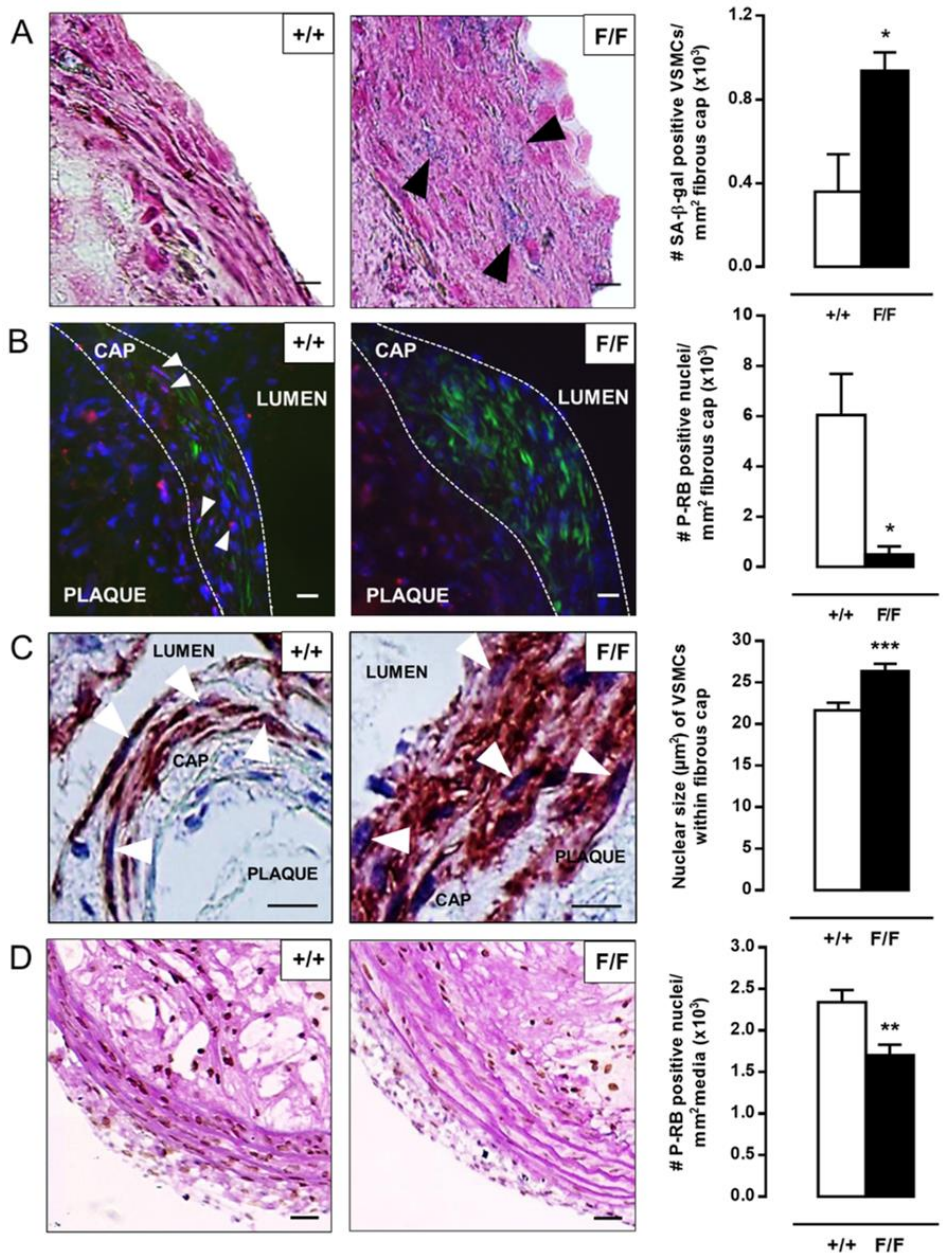

Figure 4.14 Atherosclerotic plaques of *Atg7$^{F/F}$SM22α-Cre^{+}ApoE$^{-/-}$* mice show several features of VSMC senescence. (A) Sections of the aortic root were stained for SA-β-gal activity (black arrowheads) and compared with serial SM22α staining (not shown) to locate the fibrous caps (*, *P*<0.05; n=5; Mann-Whitney U test). Scale bar: 10µm. **(B)** Consecutive sections of the aortic root were double stained for phospho-RB (red; white arrowheads) and α-SMC-actin (green) (*, *P*<0.05; n=5; Mann-Whitney U test). Scale bar: 25µm **(C)** Sections of the brachiocephalic artery were immunostained for α-SMC-actin to quantify the size of the nuclei (white arrowheads) of VSMCs within the fibrous cap. (***, *P*<0.001; n=10 nuclei/mouse; Univariate) Scale bar: 20µm. **(D)** Consecutive sections were stained for phospho-RB and periodic acid-Schiff to quantify P-RB-positive VSMC nuclei in the media. (**, *P*<0.01; n=10; Mann-Whitney U test). Scale bar: 50µm.

4.3.7 Activation of the Nrf2 and senescence pathway does not occur in autophagy defective macrophages

Because it was previously demonstrated that defective autophagy in macrophages led to increased apoptosis and plaque destabilisation,[30] we further explored the antioxidative mechanisms and cellular senescence in autophagy defective macrophages. Unlike *Atg7$^{F/F}$* VSMCs, *Atg7$^{F/F}$* macrophages did not overexpress GSTα and NQO1 **(Fig. 4.15A and 4.15B)** and were much more sensitive to tBHP-induced cell death as compared to controls **(Fig. 4.15C)**. This was attributed to the lack of Nrf2 activation in *Atg7$^{F/F}$* macrophages **(Fig. 4.15D)**.

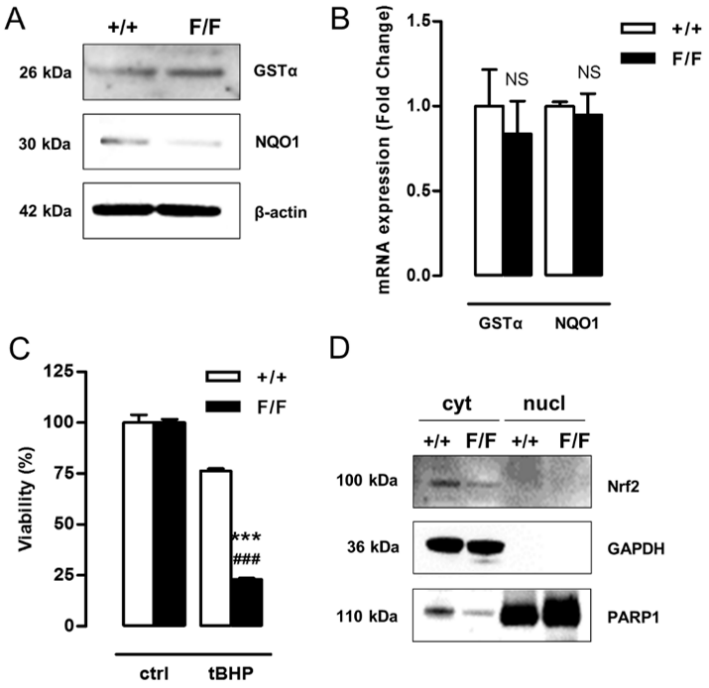

Figure 4.15 Defective autophagy in macrophages does not trigger an antioxidative backup mechanism. Bone marrow-derived macrophages were isolated from *Atg7$^{+/+}$LysM-Cre^{+}* (+/+) and *Atg7$^{F/F}$LysM-Cre^{+}* (F/F) mice **(A,B)** Western blot analysis (A) and real time RT-PCR (B) of GSTα and NQO1 in untreated *Atg7$^{+/+}$* and *Atg7$^{F/F}$* macrophages (NS, not significant; n=2 experiments in duplicate; Student t test). **(C)** *Atg7$^{+/+}$* and *Atg7$^{F/F}$* macrophages were treated with 50µmol/l tBHP for 24h (***, *P*<0.001 vs. Atg7$^{+/+}$; ###, *P*<0.001 vs. control; n=2 experiments in duplicate; Two-way ANOVA). **(D)** Western blot analysis of Nrf2 in cytoplasmic and nuclear fractions of *Atg7$^{+/+}$* and *Atg7$^{F/F}$* macrophages.

Furthermore, besides an unaltered proliferation **(Fig. 4.16A)**, *Atg7$^{F/F}$* macrophages showed neither cell cycle arrest nor upregulation of p16 **(Fig. 4.16B and 4.16C)**, indicating that defective autophagy in macrophages does not induce senescence.

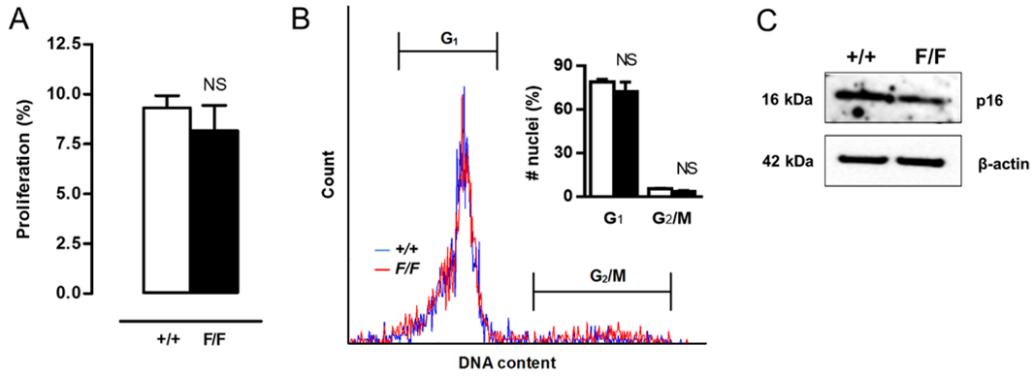

Figure 4.16 Defective autophagy in macrophages does not induce senescence. (A) Proliferation of *Atg7*$^{+/+}$ and *Atg7*$^{F/F}$ macrophages was examined by BrdU incorporation assay (NS, not significant; n=6 counting regions of 500 cells/region/condition; Student t test) **(B)** DNA cell cycle analysis of *Atg7*$^{+/+}$ (blue) and *Atg7*$^{F/F}$ (red) macrophages. The bar graph shows the percentage of *Atg7*$^{+/+}$ and *Atg7*$^{F/F}$ nuclei in G_1 and G_2/M phase of the cell cycle (NS, not significant; Student t test). **(C)** Western blot analysis of p16 in *Atg7*$^{+/+}$ and *Atg7*$^{F/F}$ macrophages.

To find a possible explanation for the discrepancy between autophagy defective VSMCs and macrophages, we examined the level of p62 expression in both cell types. According to western blot analysis, the p62 protein accumulation in *Atg7*$^{F/F}$ VSMCs was much more pronounced as compared to *Atg7*$^{F/F}$ macrophages **(Fig. 4.17A)**. Moreover, accumulation of p62 in *Atg7*$^{F/F}$ VSMCs is not only due to defective autophagy but also due to increased p62 mRNA expression **(Fig. 4.17B)**.

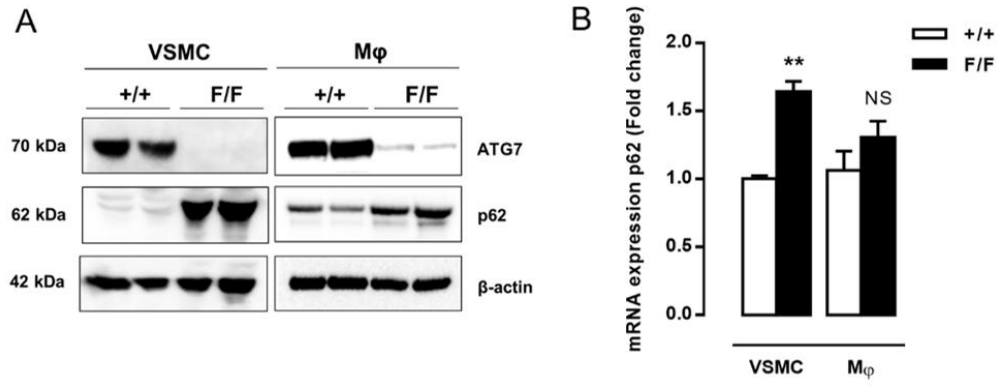

Figure 4.17 p62 expression level differs between autophagy deficient VSMCs and macrophages. (A) Western blot analysis of ATG7 and p62 in untreated *Atg7*$^{+/+}$ and *Atg7*$^{F/F}$ VSMCs (left) versus *Atg7*$^{+/+}$ and *Atg7*$^{F/F}$ macrophages (right). β-actin was used as loading control. **(B)** Real time RT-PCR of p62 in untreated *Atg7*$^{+/+}$ and *Atg7*$^{F/F}$ VSMCs versus macrophages (NS, not significant; **, P<0.01; n=4 experiments in duplicate; Student t test).

4.4 Discussion

In this study, we provide novel evidence for a prominent role of autophagy in the regulation of VSMC survival and phenotype. Defective autophagy has major effects on the mechanistic, functional and morphological properties of VSMCs, with significant implications for the development of cardiovascular diseases such as post-injury neointima formation and diet-induced atherosclerosis **(Fig. 4.18)**.

The relationship between autophagy and cell survival has been thoroughly investigated by several research groups. Because autophagy is considered as an important mechanism for the survival of VSMCs,[3, 4, 7] it is plausible to assume that defects in the autophagic machinery could aggravate VSMC death. Surprisingly, our data indicate that *Atg7*$^{F/F}$ VSMCs were highly resistant to oxidative stress as compared to *Atg7*$^{+/+}$ VSMCs. The protection against oxidative stress-mediated cell death was attributed to increased expression of different antioxidative enzymes such as GSTα and NQO1. These phase II enzymes serve as a detoxification mechanism to protect cells against electrophilic insults and oxidative stress. Accumulation of the protein p62, one of the hallmarks of defective autophagy,[31] plays a central role in the upregulation of these antioxidative enzymes. p62 accumulation triggers nuclear translocation of the transcription factor Nrf2,[26, 32] a well-known key regulator of the intracellular redox balance. Under basal conditions, Nrf2 is immobilised in the cytoplasm by binding to its inhibitor KEAP1 (kelch-like ECH-associated protein 1). However, when p62 accumulates, it will interfere with the Nrf2-KEAP1 binding complex by sequestrating KEAP1 into aggregates.[26, 32] As a result, Nrf2 is released from its inhibitor and translocated to the nucleus where it promotes transcription of multiple antioxidative genes by binding to the antioxidant response element (ARE) in their promoter region. Therefore, p62 is considered to be a crucial activator of Nrf2.[26] In the present study, *Atg7*$^{F/F}$ VSMCs showed increased nuclear translocation of Nrf2. Silencing of Nrf2 suppressed the expression of GSTα and NQO1 and abolished the protection of *Atg7*$^{F/F}$ VSMCs against oxidative stress. Importantly, *Atg7*$^{F/F}$ VSMCs did not reveal improved protection against ROS-independent apoptosis. Hence, *Atg7* deletion in VSMCs did not result in a general pro-survival status but only protected VSMCs against oxidative stress-mediated cell death. Interestingly, this antioxidative backup mechanism seems to be cell type specific. *Atg7*$^{F/F}$ macrophages revealed neither Nrf2 activation nor elevated phase II enzyme expression, which is in line with previous reports showing that various cell types including hepatic cells, neurons, pancreatic β cells and macrophages

are more susceptible to (oxidative stress-mediated) cell death under defective autophagy conditions.[13, 30, 33, 34]

Besides an improved antioxidant defence, *Atg7$^{F/F}$* VSMCs were characterised by cellular hypertrophy, nuclear hypertrophy, a decline in proliferative capacity due to a G_1-mediated cell cycle arrest and SA-β-gal activity, indicative of cellular senescence.[35] Moreover, *Atg7$^{F/F}$* VSMCs showed an increase in TGFβ and SDF1 expression, which is most likely related to the increase in migration potential and the development of a senescence-associated secretory phenotype.[36, 37] In addition, *Atg7$^{F/F}$* VSMCs showed a significant upregulation of IL1β and NLRP3, two key components of the inflammasome that have been recently described as additional characteristics of human senescent VSMCs.[38] Cellular senescence can be established by the activation of two different tumour suppressor pathways: p53-p21 and p16-RB.[27, 28] The p53 pathway is triggered by DNA damage and generally associated with p21 upregulation to initiate growth arrest. The p16-RB (retinoblastoma) pathway is engaged when cells are exposed to cellular stress, leading to the development of stress-induced premature senescence (SIPS).[39] During SIPS, the increased expression of p16 leads to hypophosphorylation and activation of RB, resulting in prevention of transcription of proliferation promoting genes.[27] In the present study, senescence in *Atg7$^{F/F}$* VSMCs was associated with the activation of the p16-RB pathway but not with DNA damage-mediated activation of the p53-p21 pathway. Importantly, the senescence pathway acts independently of the Nrf2-ARE pathway as shown by p16 overexpression and Nrf2 silencing experiments. Furthermore, analogous with the Nrf2 pathway, the induction of senescence seems cell-type dependent. In contrast to *Atg7$^{F/F}$* VSMCs, *Atg7$^{F/F}$* macrophages did not show any signs of cellular senescence. One possible reason for this discrepancy is that p62 plays a less central role in autophagy deficient macrophages. Indeed, *Atg7$^{F/F}$LysM-Cre^{+}* macrophages showed only a modest accumulation of p62 protein as result of defective autophagy whereas *Atg7$^{F/F}$SM22α-Cre^{+}* VSMCs show an increase in both p62 protein and mRNA expression.

Several research groups have shown that senescence contributes to the aging process and to the development of age-related pathologies.[36, 40] Given that p16 expression is elevated in aged VSMCs[41] and p16 is considered as a biomarker of aging,[36, 42] we define here a possible link between autophagy deficiency and VSMC aging. The relationship between autophagy and aging has been strongly investigated over the last 10 years.

Induction of autophagy by caloric restriction, spermidine, resveratrol or rapamycin extends life span in different organisms.[43] For example, the autophagy inducers rapamycin and resveratrol suppress cellular senescence,[44, 45] whereas inhibition of autophagy by knockdown of ATG7 or ATG12 induces premature senescence.[46] In the present study, we dissected out the molecular link between defective autophagy and VSMC senescence. Overexpression of p62 induced senescence in *Atg7*$^{+/+}$ VSMCs as shown by p16 accumulation, RB hypophosphorylation, reduced proliferation capacity and increased SA-β-gal activity. This experiment indicates that severe accumulation of p62, which occurs during defective VSMC autophagy, mediates the induction of senescence in VSMCs. Although some researchers have suggested that p62 could play a role in the induction of senescence in other pathologies,[47, 48] this is the first study that addresses p62 accumulation as the direct link between defective autophagy and VSMC senescence. The inverse relationship between autophagy and senescence seems logical if they are both considered as 2 cytoprotective pathways.[49] Indeed, autophagy is an important homeostatic regulator by eliminating damaged intracellular components and may play a critical role in the prevention of cellular senescence.[50] When autophagy is impaired, however, senescence can be engaged as a backup mechanism to protect the cell.[49]

Because changes in VSMC survival, phenotype, proliferation and migration are critical factors in the development of arterial vascular disease, we investigated their functional significance in 2 mouse models for post-injury neointima formation and atherosclerosis. Post-injury neointimal lesions are formed by the accumulation of VSMCs and extracellular matrix.[51] Five weeks after carotid ligation, *Atg7*$^{F/F}$ mice developed larger and more collagen-rich neointimal lesions as compared to *Atg7*$^{+/+}$ mice. The mechanism behind this excessive neointimal formation includes high MMP9 activity in the ligated LCCA of *Atg7*$^{F/F}$ mice already 5 days after ligation. Matrix metalloproteinases facilitate migration of VSMCs by remodelling the extracellular matrix.[52] In particular MMP9 and MMP2 are upregulated in response to vascular injury and to trigger intimal thickening.[53] Because MMP2 levels rise at a later time and remain lower than MMP9 levels,[54] we failed to detect MMP2 activity 5 days after ligation. Moreover, the expression of TGFβ and SDF1 was significantly increased in the LCCA of *Atg7*$^{F/F}$ mice. TGFβ plays a crucial role in intimal thickening and may stimulate MMP9 and MMP2 expression after arterial injury which in turn may augment the bioavailability of TGFβ, thereby creating a positive feedback loop promoting intimal thickening.[55] Given that TGFβ is also involved in

collagen synthesis, RB-dependent G_1-growth arrest and induction of several senescence markers (e.g. SA-β-gal activity),[56-58] this growth factor most likely plays a central role in both the development of senescence and the formation of post-injury neointima in *Atg7$^{F/F}$* mice. SDF1 is an important chemoattractant that is released by VSMCs after mechanical injury and triggers the recruitment of SMC progenitor cells to the lesion.[59, 60] All together, the excessive neointimal thickening in *Atg7$^{F/F}$* mice could be attributed to a combination of factors: cellular hypertrophy of neointimal VSMCs, increased deposition of collagen, improved VSMC migration and recruitment of smooth muscle progenitor cells due to increased MMP9 activity and elevated levels of TGFβ and SDF1. These findings support our *in vitro* data that autophagy defective VSMCs exhibit improved migration potential and develop a senescence-associated secretory phenotype which is characterised by the increased secretion of growth factors (TGFβ), cytokines (SDF1) and proteases (MMPs).[36, 37] Furthermore, neointimal *Atg7$^{F/F}$* VSMCs were characterised by p16 upregulation, SA-β-gal activity and nuclear hypertrophy, indicating that neointima formation in *Atg7$^{F/F}$* mice was associated with VSMC senescence.

Atherosclerotic lesions are characterised by the accumulation of VSMCs, immune cells, lipids and extracellular matrix within the arterial wall. Ten-week WD-fed *Atg7$^{F/F}$ApoE$^{-/-}$* mice developed larger and more advanced plaques as compared to *Atg7$^{+/+}$ApoE$^{-/-}$* mice, due to an increase in necrotic core size, fibrous cap thickness, macrophage and total collagen content. After 14 weeks on WD, the differences in plaque size, macrophage content, necrosis and apoptosis between both groups were no longer significant. Still, the fibrous cap thickness and total collagen content were significantly elevated in plaques of 14-week WD-fed *Atg7$^{F/F}$ApoE$^{-/-}$* mice. To assess the contribution of collagen to plaque stability, the amount of COL1A1/2 (more rigid) and COL3A1 (less rigid) was measured. In accordance with our *in vitro* findings, plaques of *Atg7$^{F/F}$ApoE$^{-/-}$* mice showed a significant decrease in COL1A1/2 while COL3A1 was increased. Taken together, we cannot define that plaque stability was improved in *Atg7$^{F/F}$ApoE$^{-/-}$* mice because several important criteria such as a sufficient decrease in plaque necrosis and plaque apoptosis and high amounts of COL1A1/2 were not evident. Moreover, VSMCs within the fibrous cap of atherosclerotic plaques of *Atg7$^{F/F}$ApoE$^{-/-}$* mice were characterised by several senescence markers including RB hypophosphorylation, SA-β-gal activity and nuclear hypertrophy. Different research groups have shown that VSMC senescence is present in atherosclerotic plaques and contributes to the pathogenesis of atherosclerosis.[28, 40, 61, 62] Our observations confirm once more the dual role of VSMCs in atherosclerosis. Although

VSMCs are considered beneficial in terms of plaque stability due to the formation of a thick fibrous cap that safeguards plaques from rupturing, VSMCs also play a fundamental role in promoting plaque development.[63]

It is important to note that longer *in vivo* studies were not feasible due to the development of heart failure in *Atg7$^{F/F}$ApoE$^{-/-}$* mice starting at the age of 20 weeks (unpublished data, Grootaert et al). The occurrence of heart failure in these mice most likely results from the short-term expression of *SM22α* in the primitive heart during embryonic development.[64] Cardiomyocytes isolated from *Atg7$^{F/F}$ApoE$^{-/-}$* mice showed decreased ATG7 mRNA expression and accumulation of p62 protein as compared to *Atg7$^{+/+}$ApoE$^{-/-}$* mice (unpublished data). These observations should be considered as an important limitation of the current study.

Because defective autophagy in VSMCs accelerates atherogenesis, we do not recommend inhibition of VSMC autophagy but rather suggest controlled stimulation of autophagy as a therapeutic strategy to treat atherosclerosis as recently suggested.[65-67] Caloric restriction for example, is a powerful tool to induce autophagy and has both life span-prolonging and anti-atherogenic properties in mice.[68] Also SIRT1 (sirtuin 1) deacetylase, an inducer of autophagy and a negative regulator of cellular aging, plays a protective role in atherosclerosis. VSMC-specific deletion of SIRT1 deacetylase in *ApoE$^{-/-}$* mice promotes atherosclerosis associated with increased DNA damage and senescence.[69] Finally, it is worthwhile to mention that mTOR-inhibitors such as rapamycin (or rapalogs) are able to stimulate autophagy and have significant promise to treat patients with unstable plaques, particularly in combination with statins or metformin.[70]

In conclusion, defective autophagy in VSMCs accelerates senescence and promotes ligation-induced neointima formation and diet-induced atherogenesis. Although neointimal and atherosclerotic lesions of VSMC-specific autophagy deficient mice show several features of senescence, we cannot exclude that other pathways, besides senescence, are engaged in response to defective VSMC autophagy and involved in the accelerated plaque formation. Overall, our study uncovers for the first time the role of VSMC autophagy in post-injury neointima formation and diet-induced atherosclerosis and reveals p62 as a key player in the induction of VSMC senescence, supporting the growing body of evidence that autophagic dysfunction plays a major role in cardiovascular disease.

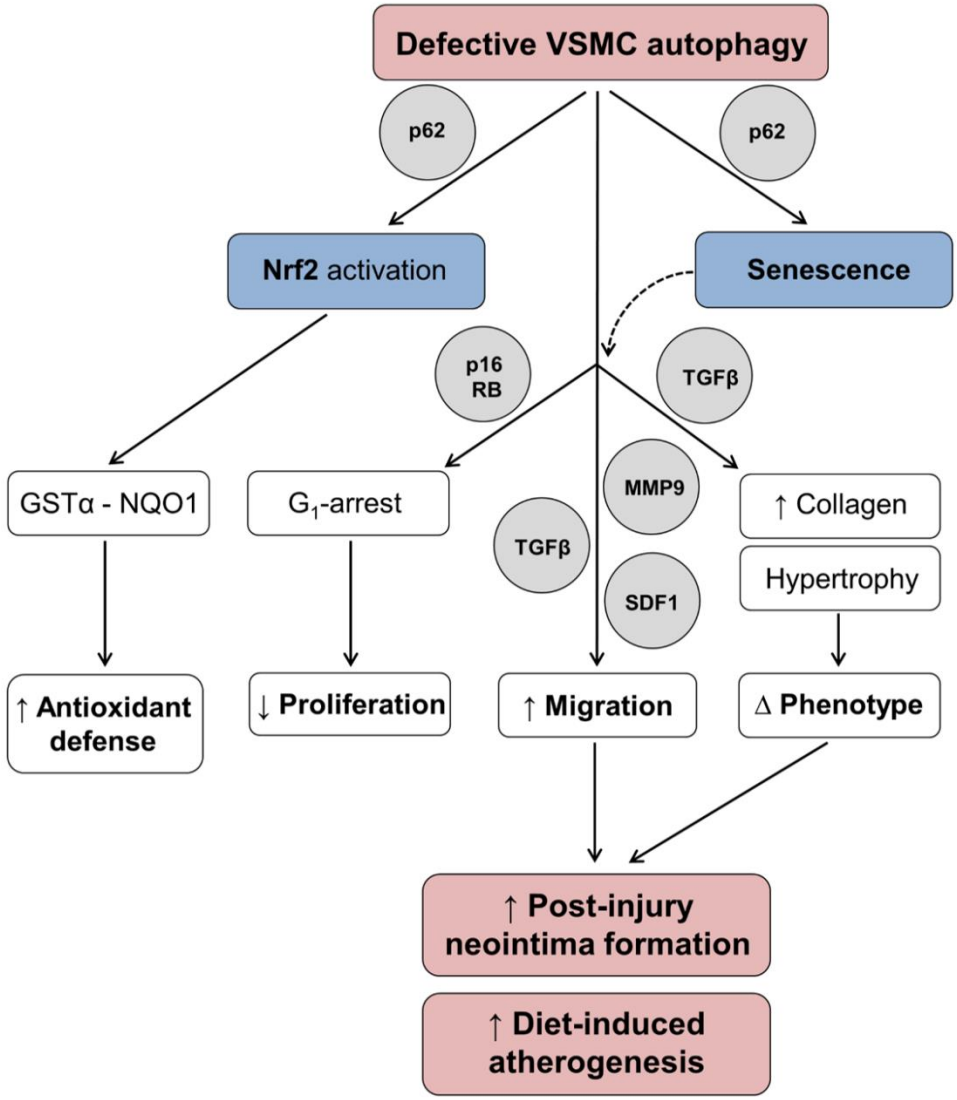

Figure 4.18 Overview of the mechanisms by which defective VSMC autophagy accelerates senescence and promotes post-injury neointima formation and diet-induced atherogenesis. p62 accumulation in autophagy defective VSMCs triggers Nrf2 activation and transcription of multiple antioxidative enzymes including GSTα and NQO1. Upregulation of GSTα and NQO1 promotes VSMC survival against oxidative stress under defective autophagy conditions. p62 accumulation in autophagy defective VSMCs triggers the development of stress-induced premature senescence. Autophagy defective VSMCs are characterised by p16-RB-mediated G_1 proliferation arrest, increased migration and changes in VSMC phenotype. Enhanced migration is associated with increased secretion of MMP9, TGFβ and SDF1. The phenotype of autophagy defective VSMCs is defined by nuclear and cellular hypertrophy, and by increased collagen content. Defective autophagy in VSMCs accelerates post-injury neointima formation and diet-induced atherogenesis.

4.5 References

(1) Martinet W, De Bie M, Schrijvers DM, De Meyer GRY, Herman AG, Kockx MM. 7-ketocholesterol induces protein ubiquitination, myelin figure formation, and light chain 3 processing in vascular smooth muscle cells. *Arterioscler Thromb Vasc Biol* 2004;24(12):2296-301.

(2) Jia G, Cheng G, Gangahar DM, Agrawal DK. Insulin-like growth factor-1 and TNF-alpha regulate autophagy through c-jun N-terminal kinase and Akt pathways in human atherosclerotic vascular smooth cells. *Immunol Cell Biol* 2006;84(5):448-54.

(3) Hill BG, Haberzettl P, Ahmed Y, Srivastava S, Bhatnagar A. Unsaturated lipid peroxidation-derived aldehydes activate autophagy in vascular smooth-muscle cells. *Biochem J* 2008;410(3):525-34.

(4) Xu K, Yang Y, Yan M, Zhan J, Fu X, Zheng X. Autophagy plays a protective role in free cholesterol overload-induced death of smooth muscle cells. *J Lipid Res* 2010;51(9):2581-90.

(5) Ding Z, Wang X, Schnackenberg L, Khaidakov M, Liu S, Singla S, Dai Y, Mehta JL. Regulation of autophagy and apoptosis in response to ox-LDL in vascular smooth muscle cells, and the modulatory effects of the microRNA hsa-let-7 g. *Int J Cardiol* 2013;168(2):1378-85.

(6) Salabei JK, Cummins TD, Singh M, Jones SP, Bhatnagar A, Hill BG. PDGF-mediated autophagy regulates vascular smooth muscle cell phenotype and resistance to oxidative stress. *Biochem J* 2013;451(3):375-88.

(7) He C, Zhu H, Zhang W, Okon I, Wang Q, Li H, Le YZ, Xie Z. 7-Ketocholesterol induces autophagy in vascular smooth muscle cells through Nox4 and Atg4B. *Am J Pathol* 2013;183(2):626-37.

(8) Salabei JK and Hill BG. Implications of autophagy for vascular smooth muscle cell function and plasticity. *Free Radic Biol Med* 2013;65:693-703.

(9) Grube E and Buellesfeld L. Everolimus for stent-based intracoronary applications. *Rev Cardiovasc Med* 2004;5 Suppl 2:S3-S8.

(10) Zhao HQ, Nikanorov A, Virmani R, Schwartz LB. Inhibition of experimental neointimal hyperplasia and neoatherosclerosis by local, stent-mediated delivery of everolimus. *J Vasc Surg* 2012;56(6):1680-8.

(11) Martinet W and De Meyer GRY. Autophagy in atherosclerosis: a cell survival and death phenomenon with therapeutic potential. *Circ Res* 2009;104(3):304-17.

(12) Perrotta I. The use of electron microscopy for the detection of autophagy in human atherosclerosis. *Micron* 2013;50:7-13.

(13) Komatsu M et al. Impairment of starvation-induced and constitutive autophagy in Atg7-deficient mice. *J Cell Biol* 2005;169(3):425-34.

(14) Owens GK, Loeb A, Gordon D, Thompson MM. Expression of smooth muscle-specific alpha-isoactin in cultured vascular smooth muscle cells: relationship between growth and cytodifferentiation. *J Cell Biol* 1986;102(2):343-52.

(15) Geisterfer AA, Peach MJ, Owens GK. Angiotensin II induces hypertrophy, not hyperplasia, of cultured rat aortic smooth muscle cells. *Circ Res* 1988;62(4):749-56.

(16) Lowik CW, Alblas MJ, van de Ruit M, Papapoulos SE, van der Pluijm G. Quantification of adherent and nonadherent cells cultured in 96-well plates using the supravital stain neutral red. *Anal Biochem* 1993;213(2):426-33.

(17) Martinet W, Timmermans JP, De Meyer GRY. Methods to assess autophagy in situ - Transmission electron microscopy versus immunohistochemistry. In: Galluzzi L, Kroemer G, eds. *Methods in Enzymology: cell-wide metabolic alterations associated with malignancy*.Waltham, Massachusetts: Academic Press; 2014. p. 89-114.

(18) Yu H, Stoneman V, Clarke M, Figg N, Xin HB, Kotlikoff M, Littlewood T, Bennett M. Bone marrow-derived smooth muscle-like cells are infrequent in advanced primary atherosclerotic plaques but promote atherosclerosis. *Arterioscler Thromb Vasc Biol* 2011;31(6):1291-9.

(19) Vindelov LL and Christensen IJ. Detergent and proteolytic enzyme-based techniques for nuclear isolation and DNA content analysis. *Methods Cell Biol* 1994;41:219-29.

(20) Martinet W, Knaapen MW, De Meyer GRY, Herman AG, Kockx MM. Oxidative DNA damage and repair in experimental atherosclerosis are reversed by dietary lipid lowering. *Circ Res* 2001;88(7):733-9.

(21) Seimon TA, Wang Y, Han S, Senokuchi T, Schrijvers DM, Kuriakose G, Tall AR, Tabas IA. Macrophage deficiency of p38alpha MAPK promotes apoptosis and plaque necrosis in advanced atherosclerotic lesions in mice. *J Clin Invest* 2009;119(4):886-98.

(22) Bennett MR. Reactive oxygen species and death: oxidative DNA damage in atherosclerosis. *Circ Res* 2001;88(7):648-50.

(23) Wang Y and Tabas I. Emerging roles of mitochondria ROS in atherosclerotic lesions: causation or association? *J Atheroscler Thromb* 2014;21(5):381-90.

(24) Filomeni G, De Zio D, Cecconi F. Oxidative stress and autophagy: the clash between damage and metabolic needs. *Cell Death Differ* 2015;22(3):377-88.

(25) Perrotta I and Aquila S. The role of oxidative stress and autophagy in atherosclerosis. *Oxid Med Cell Longev* 2015;2015:130315.
(26) Komatsu M et al. The selective autophagy substrate p62 activates the stress responsive transcription factor Nrf2 through inactivation of Keap1. *Nat Cell Biol* 2010;12(3):213-23.
(27) Campisi J and d'Adda di Fagagna F. Cellular senescence: when bad things happen to good cells. *Nat Rev Mol Cell Biol* 2007;8(9):729-40.
(28) Minamino T and Komuro I. Vascular cell senescence: contribution to atherosclerosis. *Circ Res* 2007;100(1):15-26.
(29) Duewell P et al. NLRP3 inflammasomes are required for atherogenesis and activated by cholesterol crystals. *Nature* 2010;464(7293):1357-61.
(30) Liao X, Sluimer JC, Wang Y, Subramanian M, Brown K, Pattison JS, Robbins J, Martinez J, Tabas I. Macrophage autophagy plays a protective role in advanced atherosclerosis. *Cell Metab* 2012;15(4):545-53.
(31) Komatsu M et al. Homeostatic levels of p62 control cytoplasmic inclusion body formation in autophagy-deficient mice. *Cell* 2007;131(6):1149-63.
(32) Lau A, Wang XJ, Zhao F, Villeneuve NF, Wu T, Jiang T, Sun Z, White E, Zhang DD. A noncanonical mechanism of Nrf2 activation by autophagy deficiency: direct interaction between Keap1 and p62. *Mol Cell Biol* 2010;30(13):3275-85.
(33) Komatsu M et al. Loss of autophagy in the central nervous system causes neurodegeneration in mice. *Nature* 2006;441(7095):880-4.
(34) Jung HS et al. Loss of autophagy diminishes pancreatic beta cell mass and function with resultant hyperglycemia. *Cell Metab* 2008;8(4):318-24.
(35) Blagosklonny MV. Cell senescence: hypertrophic arrest beyond the restriction point. *J Cell Physiol* 2006;209(3):592-7.
(36) Campisi J. Aging, cellular senescence, and cancer. *Annu Rev Physiol* 2013;75:685-705.
(37) Tchkonia T, Zhu Y, van Deursen J, Campisi J, Kirkland JL. Cellular senescence and the senescent secretory phenotype: therapeutic opportunities. *J Clin Invest* 2013;123(3):966-72.
(38) Gardner SE, Humphry M, Bennett MR, Clarke MC. Senescent Vascular Smooth Muscle Cells Drive Inflammation Through an Interleukin-1alpha-Dependent Senescence-Associated Secretory Phenotype. *Arterioscler Thromb Vasc Biol* 2015;35(9):1963-74.
(39) Wang JC and Bennett M. Aging and atherosclerosis: mechanisms, functional consequences, and potential therapeutics for cellular senescence. *Circ Res* 2012;111(2):245-59.
(40) Erusalimsky JD and Kurz DJ. Cellular senescence in vivo: its relevance in ageing and cardiovascular disease. *Exp Gerontol* 2005;40(8-9):634-42.
(41) Rodriguez-Menocal L, Pham SM, Mateu D, St-Pierre M, Wei Y, Pestana I, Aitouche A, Vazquez-Padron RI. Aging increases p16 INK4a expression in vascular smooth-muscle cells. *Biosci Rep* 2010;30(1):11-8.
(42) Krishnamurthy J, Torrice C, Ramsey MR, Kovalev GI, Al-Regaiey K, Su L, Sharpless NE. Ink4a/Arf expression is a biomarker of aging. *J Clin Invest* 2004;114(9):1299-307.
(43) Rubinsztein DC, Marino G, Kroemer G. Autophagy and aging. *Cell* 2011;146(5):682-95.
(44) Demidenko ZN, Zubova SG, Bukreeva EI, Pospelov VA, Pospelova TV, Blagosklonny MV. Rapamycin decelerates cellular senescence. *Cell Cycle* 2009;8(12):1888-95.
(45) Demidenko ZN and Blagosklonny MV. At concentrations that inhibit mTOR, resveratrol suppresses cellular senescence. *Cell Cycle* 2009;8(12):1901-4.
(46) Kang HT, Lee KB, Kim SY, Choi HR, Park SC. Autophagy impairment induces premature senescence in primary human fibroblasts. *PLoS One* 2011;6(8):e23367.
(47) Sasaki M, Miyakoshi M, Sato Y, Nakanuma Y. A possible involvement of p62/sequestosome-1 in the process of biliary epithelial autophagy and senescence in primary biliary cirrhosis. *Liver Int* 2012;32(3):487-99.
(48) Fujii S et al. Insufficient autophagy promotes bronchial epithelial cell senescence in chronic obstructive pulmonary disease. *Oncoimmunology* 2012;1(5):630-41.
(49) Gewirtz DA. Autophagy and senescence: a partnership in search of definition. *Autophagy* 2013;9(5):808-12.
(50) Takasaka N et al. Autophagy induction by SIRT6 through attenuation of insulin-like growth factor signaling is involved in the regulation of human bronchial epithelial cell senescence. *J Immunol* 2014;192(3):958-68.
(51) Carmeliet P, Moons L, Collen D. Mouse models of angiogenesis, arterial stenosis, atherosclerosis and hemostasis. *Cardiovasc Res* 1998;39(1):8-33.
(52) Newby AC. Matrix metalloproteinases regulate migration, proliferation, and death of vascular smooth muscle cells by degrading matrix and non-matrix substrates. *Cardiovasc Res* 2006;69(3):614-24.
(53) Louis SF and Zahradka P. Vascular smooth muscle cell motility: From migration to invasion. *Exp Clin Cardiol* 2010;15(4):e75-e85.

(54) Godin D, Ivan E, Johnson C, Magid R, Galis ZS. Remodeling of carotid artery is associated with increased expression of matrix metalloproteinases in mouse blood flow cessation model. *Circulation* 2000;102(23):2861-6.
(55) Khan R, Agrotis A, Bobik A. Understanding the role of transforming growth factor-beta1 in intimal thickening after vascular injury. *Cardiovasc Res* 2007;74(2):223-34.
(56) Rekhter MD. Collagen synthesis in atherosclerosis: too much and not enough. *Cardiovasc Res* 1999;41(2):376-84.
(57) Herrera RE, Makela TP, Weinberg RA. TGF beta-induced growth inhibition in primary fibroblasts requires the retinoblastoma protein. *Mol Biol Cell* 1996;7(9):1335-42.
(58) Debacq-Chainiaux F, Pascal T, Boilan E, Bastin C, Bauwens E, Toussaint O. Screening of senescence-associated genes with specific DNA array reveals the role of IGFBP-3 in premature senescence of human diploid fibroblasts. *Free Radic Biol Med* 2008;44(10):1817-32.
(59) Schober A, Knarren S, Lietz M, Lin EA, Weber C. Crucial role of stromal cell-derived factor-1alpha in neointima formation after vascular injury in apolipoprotein E-deficient mice. *Circulation* 2003;108(20):2491-7.
(60) Zernecke A et al. SDF-1alpha/CXCR4 axis is instrumental in neointimal hyperplasia and recruitment of smooth muscle progenitor cells. *Circ Res* 2005;96(7):784-91.
(61) Matthews C, Gorenne I, Scott S, Figg N, Kirkpatrick P, Ritchie A, Goddard M, Bennett M. Vascular smooth muscle cells undergo telomere-based senescence in human atherosclerosis: effects of telomerase and oxidative stress. *Circ Res* 2006;99(2):156-64.
(62) Gorenne I, Kavurma M, Scott S, Bennett M. Vascular smooth muscle cell senescence in atherosclerosis. *Cardiovasc Res* 2006;72(1):9-17.
(63) Johnson JL. Emerging regulators of vascular smooth muscle cell function in the development and progression of atherosclerosis. *Cardiovasc Res* 2014;103(4):452-60.
(64) Li L, Miano JM, Cserjesi P, Olsen EN. SM22 alpha, a marker of adult smooth muscle, is expressed in multiple myogenic lineages during embryogenesis. *Circ Res* 1996;78(2):188-95.
(65) Schrijvers DM, De Meyer GRY, Martinet W. Autophagy in atherosclerosis: a potential drug target for plaque stabilization. *Arterioscler Thromb Vasc Biol* 2011;31(12):2787-91.
(66) De Meyer GRY, Grootaert MOJ, Michiels CF, Kurdi A, Schrijvers DM, Martinet W. Autophagy in vascular disease. *Circ Res* 2015;116(3):468-79.
(67) Lavandero S, Chiong M, Rothermel BA, Hill JA. Autophagy in cardiovascular biology. *J Clin Invest* 2015;125(1):55-64.
(68) Guo Z, Mitchell-Raymundo F, Yang H, Ikeno Y, Nelson J, Diaz V, Richardson A, Reddick R. Dietary restriction reduces atherosclerosis and oxidative stress in the aorta of apolipoprotein E-deficient mice. *Mech Ageing Dev* 2002;123(8):1121-31.
(69) Gorenne I, Kumar S, Gray K, Figg N, Yu H, Mercer J, Bennett M. Vascular smooth muscle cell sirtuin 1 protects against DNA damage and inhibits atherosclerosis. *Circulation* 2013;127(3):386-96.
(70) Martinet W, De Loof H, De Meyer GRY. mTOR inhibition: a promising strategy for stabilization of atherosclerotic plaques. *Atherosclerosis* 2014;233(2):601-7.

CHAPTER 5

NecroX-7 reduces necrotic core formation in atherosclerotic plaques of ApoE knockout mice

Adapted from:
Grootaert MOJ, Schrijvers DM, Van Spaendonk H, Breynaert A, Hermans N, Van Hoof VO, Nozomi T, Vandenabeele P, Kim SH, De Meyer GRY, Martinet W. NecroX-7 reduces necrotic core formation in atherosclerotic plaques of *ApoE* knockout mice. *Atherosclerosis*, 2016, DOI: 10.1016/j.atherosclerosis. 2016.06.045

5.1 Introduction

Formation and enlargement of a necrotic core plays a key role in the pathology of unstable atherosclerotic plaques.[1, 2] The necrotic core is a major source of DAMPs, pro-inflammatory cytokines, proteases and pro-thrombotic factors[3] and thus can jeopardise plaque stability by promoting inflammation, plaque rupture (e.g. by thinning of the fibrous cap) and subsequent thrombosis.[1] Despite the importance and potential therapeutic relevance of necrosis in human atherosclerosis, plaque necrosis has not been a subject of interest for many years. Possible reasons are the lack of reliable markers to detect necrosis, the poor availability of therapeutic agents to specifically target necrosis and the incorrect view of necrosis as an accidental and uncontrolled form of cell death.

In this study, we aimed to inhibit necrosis formation in atherosclerotic plaques of WD-fed *ApoE*$^{-/-}$ mice to improve features of plaque stability using a novel small molecule necrosis inhibitor NecroX-7. NecroX compounds exhibit antioxidative properties through ROS and RNS scavenging,[4] NADPH oxidase inhibition[5] and inhibition of mitochondrial ROS generation.[6] Moreover, NecroX compounds have been shown to prevent oxidative stress-induced necrotic cell death,[4, 5] to inhibit HMGB1-mediated inflammatory responses[7] and to protect against myocardial necrosis after ischemia-reperfusion injury.[8] Furthermore, NecroX-7 is currently being tested in ST-segment elevated myocardial infarction (STEMI) patients undergoing percutaneous coronary intervention (https://clinicaltrials.gov, identifier NCT02070471).

5.2 Materials and Methods

5.2.1 Mice

Male *ApoE*$^{-/-}$ mice (C57BL/6, Jackson Laboratory, stock number 002052) were fed a western-type diet (4021.90, AB Diets) for 16 weeks. Simultaneously, mice were treated with NecroX-7 (LG Life Sciences, 30mg/kg body weight) (n=25) or vehicle (water for injection) (n=26) via intraperitoneal injections 3 times per week. At the end of the experiment, mice were fasted overnight and blood was collected by cardiac puncture. Total cholesterol, LDL cholesterol and triglyceride levels in plasma were measured on a Dimension Vista® System (Siemens Healthcare Diagnostics). Plasma levels of oxLDL

and malondialdehyde (MDA) were measured by an ELISA (USCNK, SEA527Mu) or HPLC-fluorescence detection method[9], respectively. Urinary excretion of 8-oxodG was determined with an ELISA kit (NWK-8OHDG01, Northwest Life Science Specialties) and normalised to creatinine levels (CR01, Oxford Biomedical Research). Tissues were imbedded in OCT or fixed in formalin 4% for 24h before paraffin imbedding. For *in vitro* experiments, wild-type mice (C57BL/6, stock number 000664) and *Ripk3*$^{-/-}$ mice[10] (gift from K. Newton and V. Dixit) were used. All experiments were approved by the Ethical Committee of the University of Antwerp.

5.2.2 Histological analysis

The thoracic aorta was stained *en face* with Oil Red O (ORO) to determine plaque burden. Atherosclerotic plaques located in the aortic root were analysed by immunohistochemistry at 3 different sections sliced at equally spaced intervals (every 50µm). The size of the necrotic core was determined by measuring the area of the necrotic core divided by the total plaque size on a haematoxylin-eosin (H&E) staining according to a standard method.[11] A 3000µm^2 minimum threshold was implemented in order to avoid counting of regions that likely do not represent necrotic core areas. A Sirius red staining was used for detection of total collagen. Collagen type I was detected on Sirius red-stained sections visualised under polarised light.[12] Apoptosis was determined by anti-cleaved caspase-3 (9661, Cell signaling Technology) and TUNEL (S7101, Millipore) staining. Plaques were further analysed by immunohistochemistry with the following primary antibodies: mouse anti-α-SMC-actin (A2547, Sigma-Aldrich) and rabbit anti-MMP13 (ab39012, Abcam). The minimal thickness of the fibrous cap within each plaque was determined on the α-SMC-actin staining. Frozen sections of the plaques were analysed with rabbit anti-Moma-2 (MCA519, Serotec), rabbit anti-8-oxodG (orb10011, Biorbyt) and rabbit anti-iNOS (BML-SA200, Enzo Life Sciences). Thereafter, tissue sections were incubated with species-appropriate HRP-conjugated secondary antibodies followed by 60min of reactive ABC. 3,3'-diaminobenzidine or 3-amino-9-ethyl-carbazole were used as a chromogen. All images were acquired with Universal Grab 6.1 software using an Olympus BX40 microscope and quantified with Image J software.

5.2.3 Cell culture

Bone marrow-derived macrophages (BMDM) were harvested by flushing bone marrow from the hind limbs of mice. Cells were cultured for 7 days in RPMI medium (Gibco Life

Technologies) supplemented with 15% L-cell conditioned medium (LCCM) containing monocyte colony stimulating factor (M-CSF). To polarise BMDM into M1 macrophages, cells were incubated for 24h with 100ng/ml LPS (Sigma-Aldrich). To induce oxidative stress-mediated necrosis, BMDM were treated with 0.5mmol/l and 1mmol/l *tert*-butyl hydroperoxide (tBHP, Sigma Aldrich) for 2h and 4h. Intracellular and mitochondrial ROS was measured using the fluorogenic marker 2',7'-dichlorofluorescin diacetate (DCFDA) and MitoSOX Red (Molecular Probes), respectively. After incubation with 25µmol/l carboxy-H_2DCFDA for 1h or 5µmol/l MitoSOX for 30min in HBSS (Gibco Life Technologies), cells were collected, resuspended in FACS-buffer (PBS with 0.1% BSA and 0.05% NaN_3) and analysed with BD Accuri flow cytometer. Necrosis was monitored by propidium iodide (PI) labelling. Briefly, cells were labelled with 1µg/ml PI (Molecular Probes) and 5µg/ml Hoechst (Life Technologies) and immediately visualised by fluorescence microscopy (EVOS FL Cell Imaging System). To induce apoptosis and necroptosis, BMDM were treated for 24h with 30µg/ml cycloheximide (Sigma-Aldrich) or 100ng/ml LPS and 20µmol/l zVAD-fmk (Enzo Life Sciences), respectively. Necrostatin-1 (Enzo Life Sciences) was used as RIPK1 inhibitor.

5.2.4 Western blotting

Cells were lysed in Laemmli sample buffer (Bio-rad) containing β-mercaptoethanol and boiled for 4min. Tissues samples were first homogenised in RIPA buffer and protein content was determined using BCA method before mixing with Laemmli sample buffer. Samples were loaded on Bolt 4-12% Bis-Tris gels (Life Technologies) and after electrophoresis transferred to Immobilon-P membranes (Millipore). Membranes were probed with rabbit anti-cleaved caspase-3 (9661, Cell signaling Technologies), rabbit anti-P-NF-κB (3031, Cell signaling Technologies), rabbit anti-total NF-κB (3034, Cell signaling Technologies), hamster anti-TNFα (1221-00, Genzyme) or mouse anti-β-actin (A5441, clone AC-15, Sigma-Aldrich) primary antibodies. Subsequently, membranes were incubated with HRP-conjugated secondary antibodies (Dako) to allow chemiluminescent detection. In some experiments, supernatant was collected and the extracellular proteins were precipitated with 10% trichloroacetic acid. After incubation on ice for 15min, supernatant was centrifuged for 10min at 2500g. The protein pellet was resuspended in Laemmli sample buffer containing β-mercaptoethanol. The release of HMGB1 in supernatant during necrosis was detected via western blotting using rabbit anti-HMGB1 (ab18256, Abcam) antibody.

5.2.5 Real time RT-PCR

Total RNA was prepared using the Nucleospin RNA Kit (Filter Service). Cell culture samples were analysed for iNOS using a TaqMan gene expression assay (Mm00440502_m1, Applied Biosystems). β-actin (Mm00607939_s1) was used as reference gene. Tissue samples were analysed using SYBR Green (GC Biotech) and gene-specific primers (Sigma-Aldrich) **(listed in Table 5.1)**. Real time RT-PCR was performed on a ABI Prism 7300 sequence detector system (Applied Biosystems). The parameters for PCR amplification were 95°C for 10min followed by 40 cycles of 95°C for 15sec and 60°C for 1min. In case of SYBR Green analysis, an additional step of 72°C for 30sec and a dissociation stage were added. Relative expression of mRNA was calculated using qBASE+ software (Biogazelle).[13]

Table 5.1 SYBR Green mouse primers

Gene	Forward primer (5'-3')	Reverse primer (5'-3')
TNFα	GGCAGGTCTACTTTGGAGTCATTG	ACATTCGAGGCTCCAGTGAATTCG
IL6	CTGGTGACAACCACGGCCTTCCCTA	ATGCTTAGGCATAACGCACTAGGTT
IL1α	AAGACAAGCCTGTGTTGCTGAAGG	TCCCAGAAGAAAATGAGGTCGGTC
IL1β	TGAAATGCCACCTTTTGACAG	CCACAGCCACAATGAGTGATAC
iNOS	CCCTTCCGAAGTTTCTGGCAGC	GGCTGTCAGAGCCTCGTGGCTTTGG
HMGB1	TGGCAAAGGCTGACAAGGCTC	GGATGCTCGCCTTTGATTTTGG
RAGE	CACTTGTGCTAAGCTGTAAGGG	CATCGACAATTCCAGTGGCTG
TLR4	GCCTTTCAGGGAATTAAGCTCC	GATCAACCGATGGACGTGTAAA
CPTa1	CAAAGATCAATCGGACCCTAGAC	CGCCACTCACGATGTTCTTC
ACOX1	GCCTGCTGTGTGGGTATGTCATT	GTCATGGGCGGGTGCAT
PNPLA2	CATGATGGTGCCCTATACTC	GTGAGAGGTTGTTTCGTACC
FASN	CTCCGTGGACCTTATCACTA	CTGGGAGAGGTTGTAGTCAG
DGAT1	GCTCTGGCATCATACTCCATC	CGGTAGGTCAGGTTGTCTGG
CD36	ATGGGCTGTGATCGGAACTG	GTCTTCCCAATAAGCATGTCTCC
GAPDH	CCAGTATGACTCCACTCACG	GACTCCACGACATACTCAGC
PPIA	GAAGCCATGGAGCGTTTTGG	CAGATGGGGTAGGGACGCTC
HPRT	TCAGTCAACGGGGGACATAAA	GGGGCTGTACTGCTTAACCAG

5.2.6 Statistical analysis

All data were analysed with SPSS 22.0 software (SPSS Inc.) and presented as mean ± SEM. Statistical tests are mentioned in the figure legends. Differences were considered significant at $P<0.05$.

5.3 Results

5.3.1 NecroX-7 reduces total aortic plaque burden in *ApoE*$^{-/-}$ mice without affecting total plasma cholesterol levels

ApoE$^{-/-}$ mice were treated with NecroX-7 (30mg/kg body weight) or vehicle 3 times per week and fed a western-type diet for 16 weeks to induce atherosclerotic plaque formation. Oil Red O staining of the thoracic aorta showed a significant decrease in atherosclerotic plaque formation, particularly in the aortic arch of NecroX-7-treated mice as compared to vehicle-treated control mice **(Fig. 5.1)**. Body weight, total cholesterol, LDL cholesterol and triglyceride plasma levels were not significantly altered in NecroX-7-treated mice as compared to controls **(Table 5.2)**. Moreover, NecroX-7 treatment did not affect [oxLDL]/[LDL] and malondialdehyde plasma levels **(Table 5.2)**, indicating that NecroX-7 does not inhibit oxidation of LDL and lipid peroxidation in WD-fed *ApoE*$^{-/-}$ mice. Also the urinary excretion of 8-oxodG, a well-known marker of oxidative stress-induced DNA damage, was not affected by NecroX-7 treatment **(Table 5.2)**.

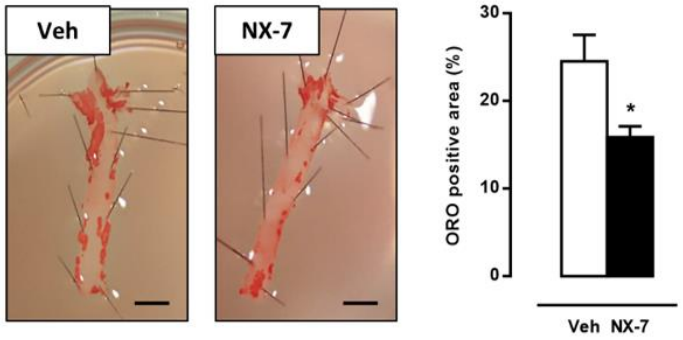

Figure 5.1: NecroX-7 reduces total aortic plaque burden in *ApoE*$^{-/-}$ mice. The thoracic aorta of vehicle-treated (Veh) and NecroX-7-treated (NX-7) *ApoE*$^{-/-}$ mice were stained *en face* with Oil Red O (ORO) to evaluate total aortic plaque burden (*P<0.05; n=5; Student t test). Scale bar: 2mm**.**

5.3.2 NecroX-7 increases features of atherosclerotic plaque stability in *ApoE*$^{-/-}$ mice

To evaluate the effect of NecroX-7 on plaque size and composition, atherosclerotic plaques located in the aortic root were analysed. NecroX-7 treatment significantly reduced the necrotic core area as illustrated by smaller and less abundant necrotic cores **(Fig. 5.2A)**, but did not affect plaque apoptosis **(Fig. 5.2B and Table 5.2)**. However, neither plaque size nor macrophage content were altered between both groups **(Table 5.2)**.

Table 5.2: Characteristics of vehicle-treated and NecroX-7-treated *ApoE*$^{-/-}$ mice after 16 weeks on western-type diet

	Vehicle	NecroX-7
General		
Body weight (g)[b]	34±1	33±1
Total cholesterol[a,b]	482±25	465±28
LDL cholesterol[a,b]	349±19	315±17
Triglycerides[a,b]	154±13	122±21
[oxLDL]/[LDL] [a,b]	0.12±0.01	0.11±0.01
Oxidative stress markers		
MDA (µmol/l) in plasma[b]	0.71±0.05	0.62±0.05
8-oxodG (ng/mg creatinine) in urine[b]	140±31	138±28
Aortic Root Plaque		
Plaque area (x10^{3}µm^2)[c]	176±6	168±5
# TUNEL positive cells/mm^2 plaque area[c]	46±10	52±7
Moma-2 positive area (%)[c]	1.2±0.1	1.4±0.1
α-SMC-actin positive area (%)[c]	2.5±0.2	3.2±0.2*

([a], mg/dl; [b], Student t test; [c], Repeated Measure;*P<0.05 vs. vehicle)

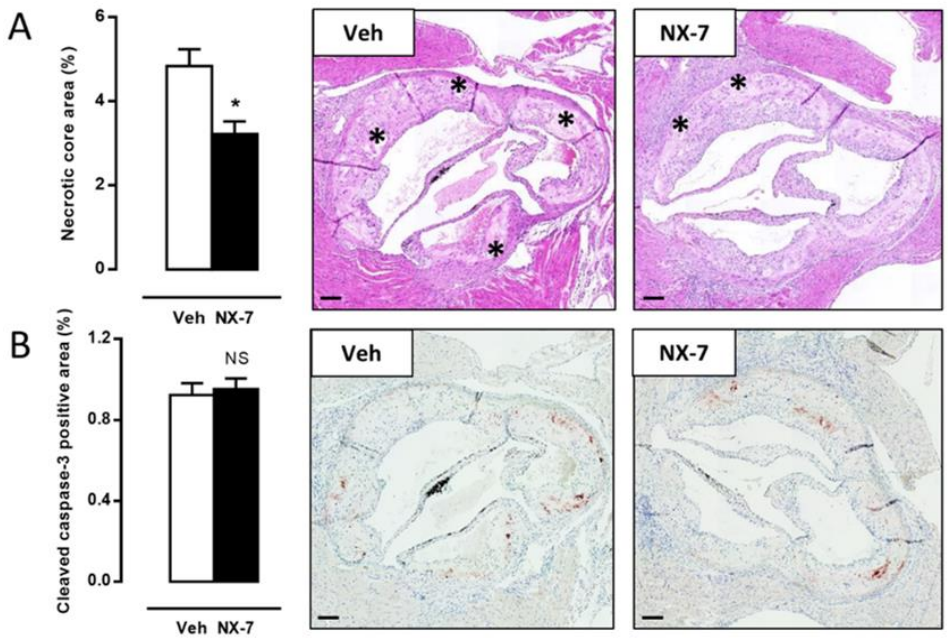

Figure 5.2: NecroX-7 reduces necrotic core formation in atherosclerotic plaques of *ApoE*$^{-/-}$ mice. **(A)** Sections of the aortic root of vehicle-treated (Veh) and NecroX-7-treated (NX-7) *ApoE*$^{-/-}$ mice were stained with H&E to quantify the necrotic core area (indicated by an asterisk) (*P<0.05 vs. vehicle; n=25; Repeated Measure). **(B)** Serial sections were immunostained for cleaved caspase-3 to measure the percentage of apoptosis (NS, not significant vs. vehicle; n=25; Repeated Measure). Scale bar: 100µm.

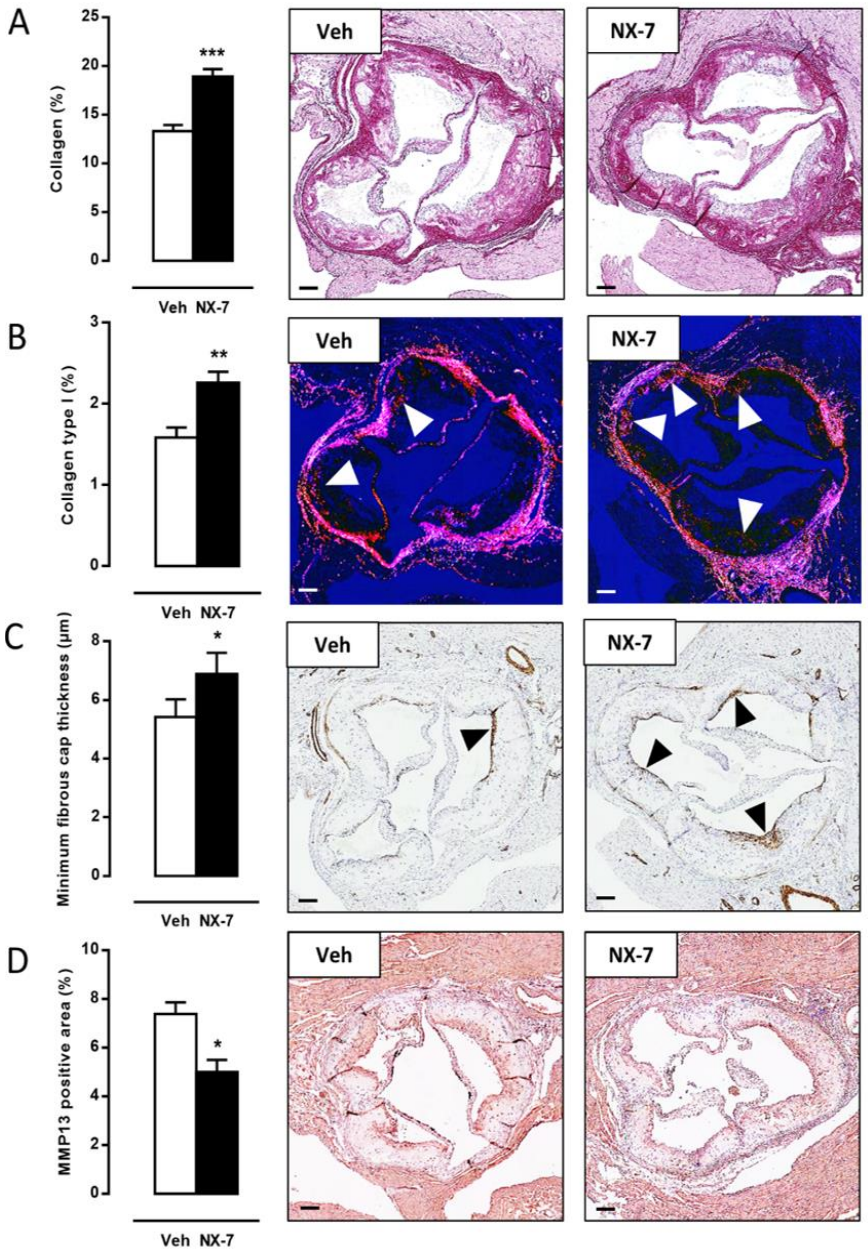

Figure 5.3 NecroX-7 increases collagen deposition and formation of a thick fibrous cap in atherosclerotic plaques of *ApoE*$^{-/-}$ mice. (A, B) Sections of the aortic root of vehicle-treated (Veh) and NecroX-7-treated (NX-7) *ApoE*$^{-/-}$ mice were stained with Sirius red to quantify total collagen (A) and collagen type I visualised under polarised light (B) (red, indicated by white arrowheads) (***P<0.001, **P<0.01, vs. vehicle; n=25; Repeated Measure). **(C)** Serial sections were immunostained for α-SMC-actin to measure the minimum fibrous cap thickness (indicated by black arrowheads). (*P<0.05 vs. vehicle;n=25; Repeated Measure). **(D)** Serial sections were immunostained for MMP13 (*P<0.05 vs. vehicle; n=10; Repeated Measure). Scale bar: 100µm.

Because a reduction in the necrotic core area is a key event in plaque stabilisation, other features of plaque stability were examined. Total collagen, in particular collagen type I, was significantly increased in plaques of NecroX-7-treated versus vehicle-treated mice **(Fig. 5.3A and 5.3B)**. Moreover, smooth muscle cell content and the minimal fibrous cap thickness were significantly elevated in plaques of NecroX-7-treated mice **(Table 5.2 and Fig. 5.3C)**. Interestingly, MMP13 expression, also known as collagenase 3, was significantly decreased in plaques of NecroX-7-treated mice **(Fig. 5.3D)**. Further analysis showed that there was a significant correlation between the amount of collagen and the number of smooth muscle cells (*P*=0.025) **(Fig. 5.4 left panel)** as well as an inverse association between collagen amount and MMP13 expression in the plaque (*P*=0.015) **(Fig. 5.4 right panel)**. These data suggest that the increase in collagen content in plaques of NecroX-7-treated *ApoE*$^{-/-}$ mice is likely due to a combination of increased smooth muscle cell content and decreased MMP13-mediated degradation.

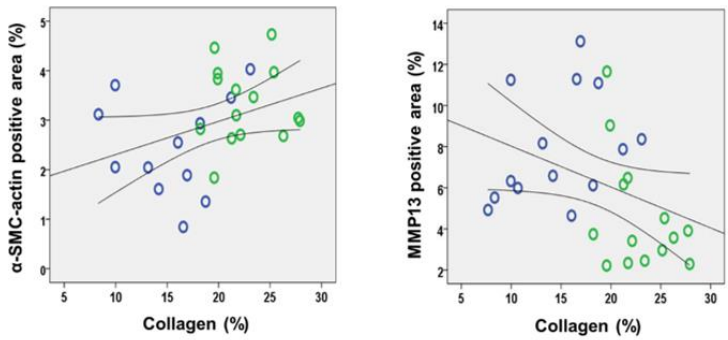

Figure 5.4 Correlation between the collagen deposition, smooth muscle cell content and MMP13 expression in atherosclerotic plaques of *ApoE*$^{-/-}$ mice. Sections of the aortic root of vehicle-treated (Veh) (blue dots) and NecroX-7-treated (NX-7) (green dots) *ApoE*$^{-/-}$ mice were stained with Sirius red, anti-α-SMC-actin antibody and anti-MMP13 antibody to quantify total collagen, smooth muscle cell content and MMP13 expression, respectively. A correlation analysis showed a positive relationship between total collagen content (%) and α-SMC-actin positive area (%) (Spearman's rho, *P*=0.025, left panel) whereas total collagen content (%) and MMP13 positive area (%) were negatively correlated (Spearman's rho, *P*=0.015, right panel).

5.3.3 NecroX-7 reduces atherosclerotic plaque oxidative stress and inflammation

According to an immunohistochemical staining of 8-oxodG, 4 out of 11 control plaques showed signs of oxidative stress while none of the plaques of NecroX-7-treated *ApoE*$^{-/-}$ mice stained positive for 8-oxodG **(Fig. 5.5A)**. In control mice, 8-oxodG-positivity was mostly observed in the proximity of the necrotic core and revealed both nuclear and non-nuclear oxidative DNA damage. Also iNOS expression was significantly decreased in plaques of NecroX-7-treated mice, suggestive of reduced oxidative stress and inflammation **(Fig. 5.5B)**. Real time RT-PCR analysis of whole plaque lysates of NecroX-7-treated mice revealed a significant decrease of multiple inflammation markers including TNFα, IL1β, iNOS, high mobility group box 1 (HMGB1) and receptor for advanced glycation end products (RAGE) as compared to vehicle-treated mice **(Fig. 5.5C)**. There was also a trend (*P*=0.06) for reduced IL6 mRNA expression in NecroX-7-treated plaques. The mRNA expression of IL1α and Toll-like receptor 4 (TLR4) in the atherosclerotic tissue were not altered by NecroX-7 treatment. Moreover, the reduced expression of inflammation markers in NecroX-7-treated plaques was associated with hypophosphorylation of NF-κB **(Fig. 5.5D)**.

5.3.4 NecroX-7 reduces hepatic steatosis in WD-fed *ApoE*$^{-/-}$ mice

Livers of *ApoE*$^{-/-}$ mice fed a western-type diet for 16 weeks displayed severe steatosis as shown by the macrovesicular steatosis pattern on a H&E staining and the large numbers of Oil Red O-positive lipid droplets **(Fig. 5.6A)**. Administration of NecroX-7 however, significantly reduced hepatic steatosis. To investigate this further, we performed real time RT-PCR analysis on the livers of NecroX-7 and vehicle-treated *ApoE*$^{-/-}$ mice for genes involved in lipid uptake (CD36), β-oxidation (CPTa1 and ACOX1), lipolysis (PNPLA2) and lipid synthesis (FASN and DGAT1). Only a significant decrease in FASN (fatty acid synthase) mRNA expression was observed in the livers of NecroX-7-treated *ApoE*$^{-/-}$ mice **(Fig. 5.6B)**, indicating a reduction in *de novo* fatty acid synthesis. We also observed a small trend for reduced CD36 mRNA expression in NecroX-7-treated livers. Moreover, the inflammation markers TNFα and IL1β were not significantly altered between both groups, suggesting that steatohepatitis was not (yet) established in WD-fed *ApoE*$^{-/-}$ mice.

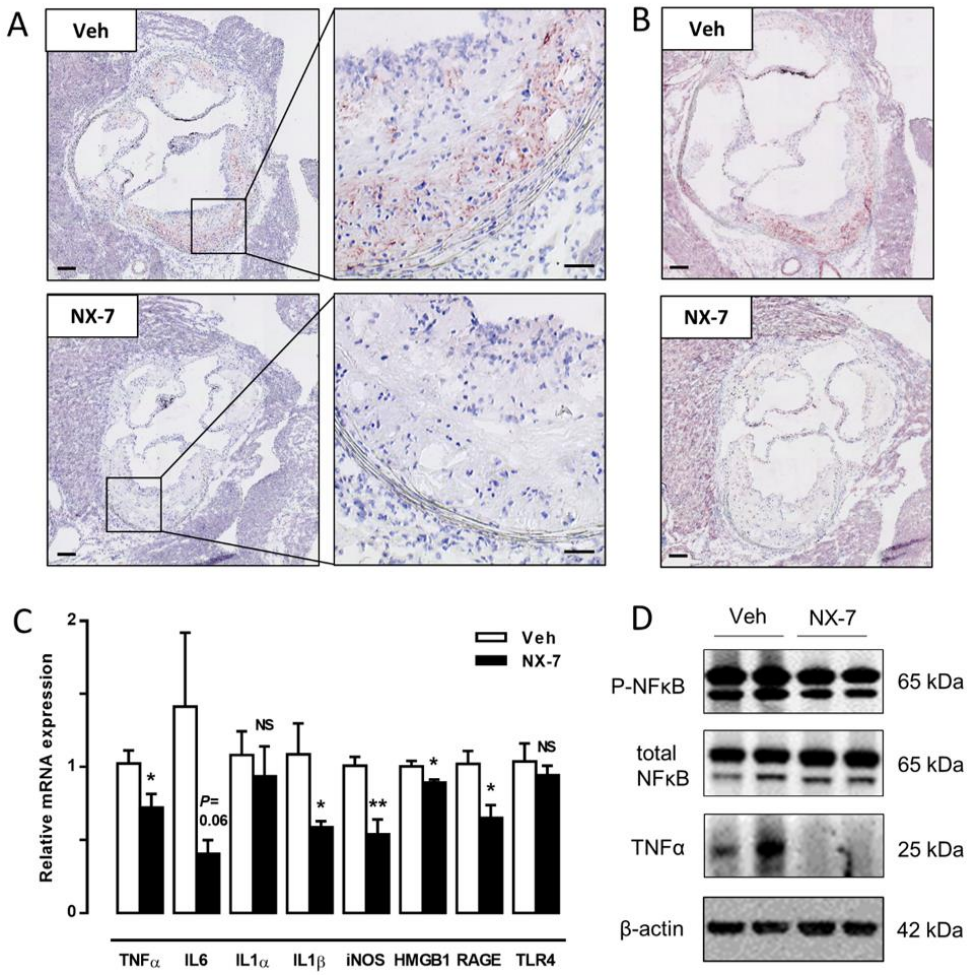

Figure 5.5 NecroX-7 reduces oxidative stress and inflammation in atherosclerotic plaques of *ApoE*$^{-/-}$ mice (A) Sections of the aortic root of vehicle-treated (Veh) and NecroX-7-treated (NX-7) *ApoE*$^{-/-}$ mice were immunostained for 8-oxodG to detect oxidative stress (P<0.05; Chi square, 4/11 (Veh) vs. 0/9 (NX-7)). Scale bars: 150µm and 25µm (detail). **(B)** Serial sections were immunostained for iNOS. Scale bar: 150µm. **(C)** Real time RT-PCR analysis on whole plaque lysates for TNFα, IL6, IL1α, IL1β, iNOS, HMGB1, RAGE and TLR4 mRNA expression. GAPDH and β-actin were used as housekeeping genes (*P<0.05, **P<0.01; NS, not significant vs. vehicle; n=6 aortas/group; Student t test). **(D)** Western blot analysis on plaque lysates for P-NF-κB, total NF-κB and TNFα. β-actin was used as loading control. n=2 pooled samples/group. Each pooled sample consists of atherosclerotic tissue from 3 different mice due to low protein amount.

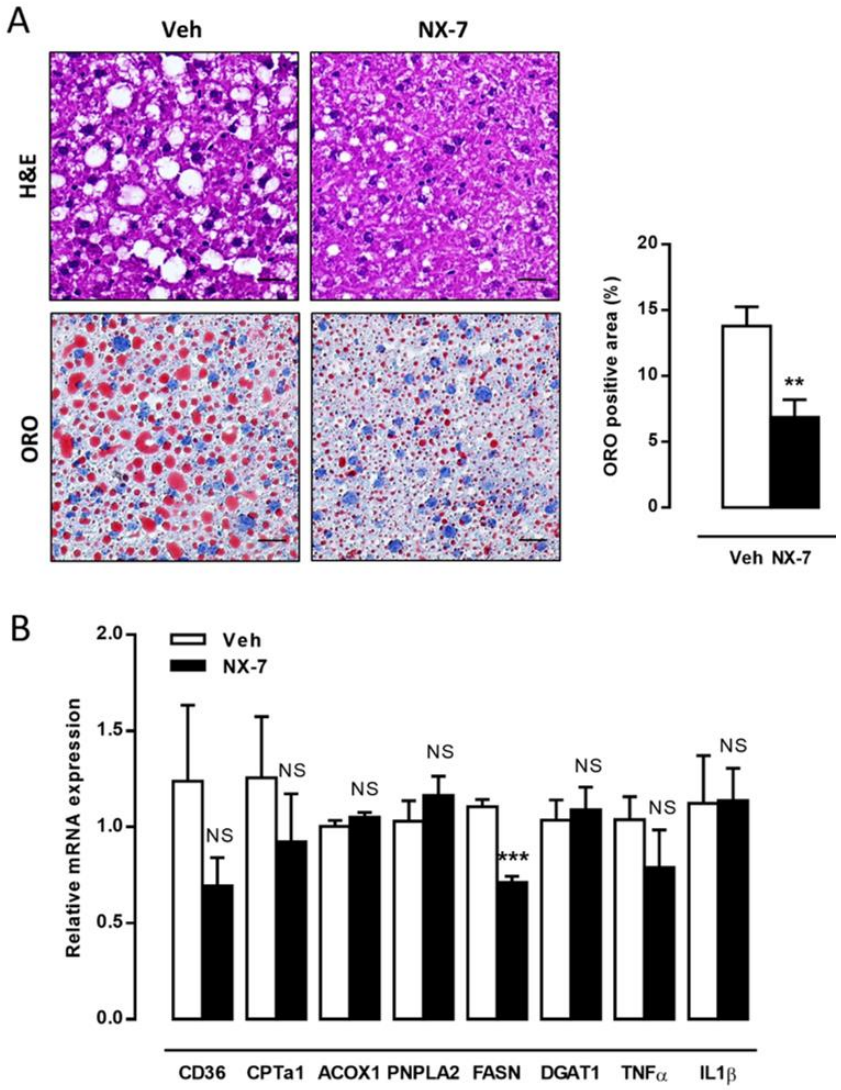

Figure 5.6: NecroX-7 reduces hepatic steatosis in WD-fed *ApoE*$^{-/-}$ mice. (A) Livers of WD-fed vehicle-treated (Veh) and NecroX-7-treated (NX-7) *ApoE*$^{-/-}$ mice were stained with H&E (upper panel) and Oil Red O (ORO) (lower panel; ***P*<0.01 vs. vehicle, Student t test) to determine the pattern of steatosis and the presence of lipid droplets, respectively. Scale bar: 25μm **(B)** Real time RT-PCR analysis of livers of WD-fed vehicle-treated (Veh) and NecroX-7-treated (NX-7) *ApoE*$^{-/-}$ mice for CD36, CPTa1, ACOX1, PNPLA2, FASN, DGAT1, TNFα, IL1β. GAPDH and HPRT were used as housekeeping genes (****P*<0.001; NS, not significant vs. vehicle; n=6/group; Student t test). CPTa1: carnitine palmitoyl transferase; ACOX1: acyl coA dehydrogenase; PNPLA2: patatin like phospholipase domain containing 2; FASN: fatty acid synthase; DGAT1: diacylglycerol O-acyltransferase.

5.3.5 NecroX-7 inhibits oxidative stress-induced necrosis in macrophages

Validation of tBHP as an inducer of oxidative stress-induced necrosis

To induce oxidative stress-induced necrosis in bone marrow-derived macrophages (BMDM), cells were treated with the free radical donor *tert*-butyl hydroperoxide (tBHP). High doses of tBHP (0.5 and 1mmol/l) and short incubation times (2h and 4h) were the most optimal conditions to induce oxidative stress-induced necrosis in macrophages. In these conditions, tBHP induced necrosis in a dose-dependent manner as determined by PI labelling **(Fig.5.7A white bars)** but did not stimulate RIPK1/RIPK3-dependent necroptosis **(Fig. 5.7A grey/black bars)**. Moreover, high doses of tBHP did not induce apoptosis as shown by the absence of cleaved caspase-3 expression on western blot **(Fig. 5.7B)**. These data were confirmed by a cleaved caspase-3 and TUNEL staining **(Fig. 5.7C)**.

Validation of NecroX-7 as an inhibitor of oxidative stress-induced necrosis

From 10µmol/l onwards NecroX-7 inhibited necrosis significantly as shown by decreased PI labelling **(Fig. 5.8A)**. Increasing the dosage up to 30µmol/l did not further improve its anti-necrotic effect. Henceforth, all experiments were performed with 10µmol/l NecroX-7. Importantly, NecroX-7 itself did not affect cell viability. Moreover, NecroX-7 diminished HMGB1 release in the supernatant of tBHP-treated BMDM **(Fig. 5.8B)**. Morphological analysis also revealed improved cell viability of tBHP-treated BMDM after NecroX-7 treatment **(Fig. 5.8C)**. In particular, the incidence of cell oncosis was decreased in NecroX-7-treated BMDM by about 90%. These data indicate that NecroX-7 inhibits necrosis in BMDM in the presence of a powerful oxidant.

Next, we investigated whether the anti-necrotic effects of NecroX-7 were associated with its antioxidative properties. High doses of tBHP generated high levels of intracellular and mitochondrial ROS after 2h and 4h treatment in a dose-dependent manner as shown by DCFDA and MitoSOX labelling, respectively **(Fig. 5.8D and 5.8E)**. NecroX-7 strongly decreased intracellular ROS as well as mitochondrial ROS levels in all conditions **(Fig. 5.8D and 5.8E)**. Moreover, NecroX-7 inhibited iNOS expression in M1-polarised BMDM exposed to tBHP **(Fig. 5.8F)**, an indirect measure for reduced oxidative stress.

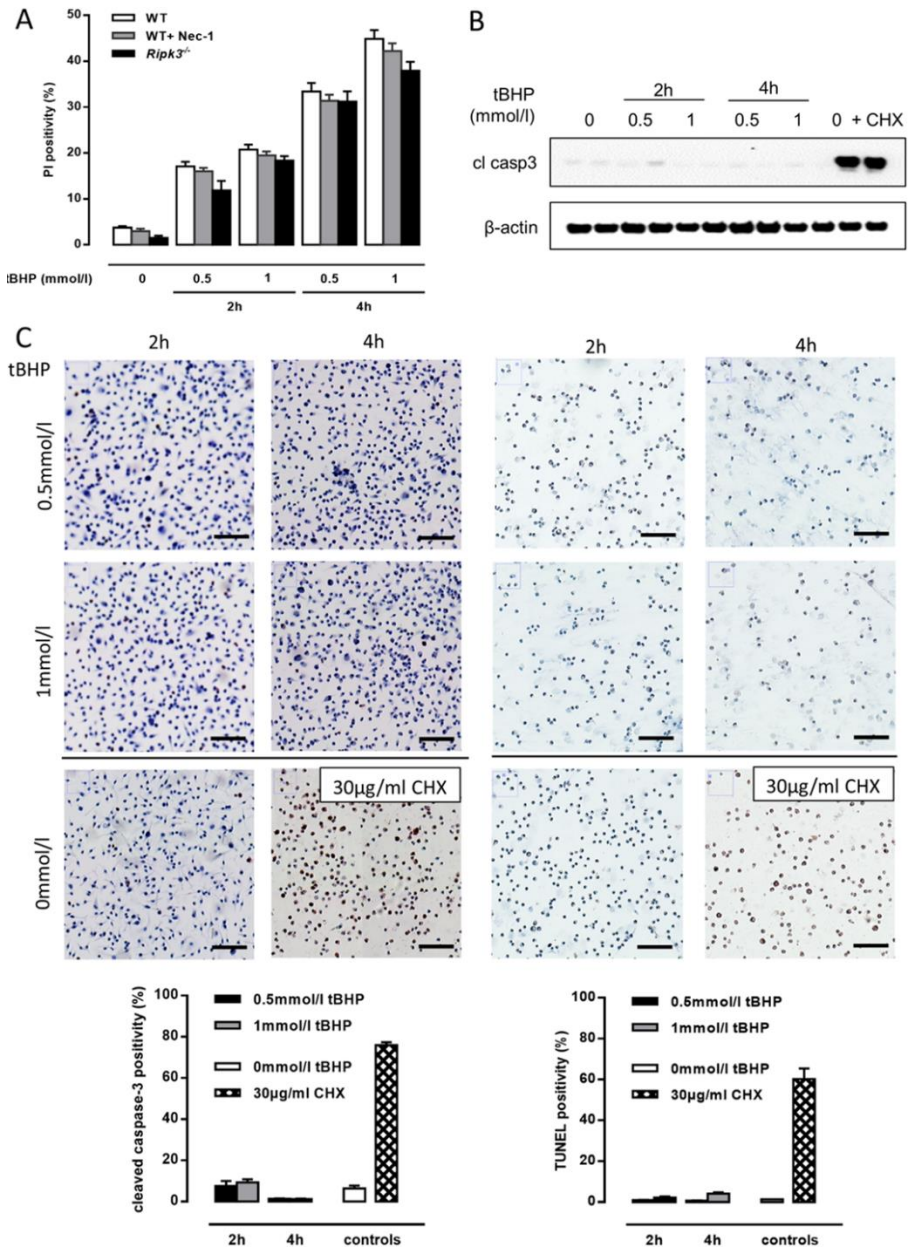

Figure 5.7 High doses of tBHP induce necrosis but not necroptosis and apoptosis. (A) Wild-type (WT) bone marrow-derived macrophages (BMDM) were exposed to 0, 0.5 or 1mmol/l tBHP for 2h or 4h. Necrosis was monitored by PI labelling. WT BMDM treated with 30µmol/l Necrostatin-1 (Nec-1) and *Ripk3*$^{-/-}$ BMDM were used as negative controls for necroptosis. (***P<0.001 vs. 0mmol/l; NS, not significant vs WT+Nec-1 and *Ripk3*$^{-/-}$; n=3 experiments with 3 counting regions of 200 cells/region in duplicate; Factorial ANOVA; Dunnett post hoc). **(B,C)** WT BMDM were exposed to 0.5 or 1mmol/l tBHP for 2h or 4h. Untreated (0mmol/l tBHP) or cycloheximide-treated BMDM (CHX, 30µg/ml for 24h) were used as negative and positive control, respectively. Apoptosis was monitored by (B) western blot analysis of cleaved caspase-3 and (C) immunohistochemical staining for cleaved caspase-3 and TUNEL. Scale bar: 75µm (NS, not significant vs. 0mmol/l; ***P<0.001 vs. CHX; n=2 counting regions of 500 cells/region in duplicate; Factorial ANOVA).

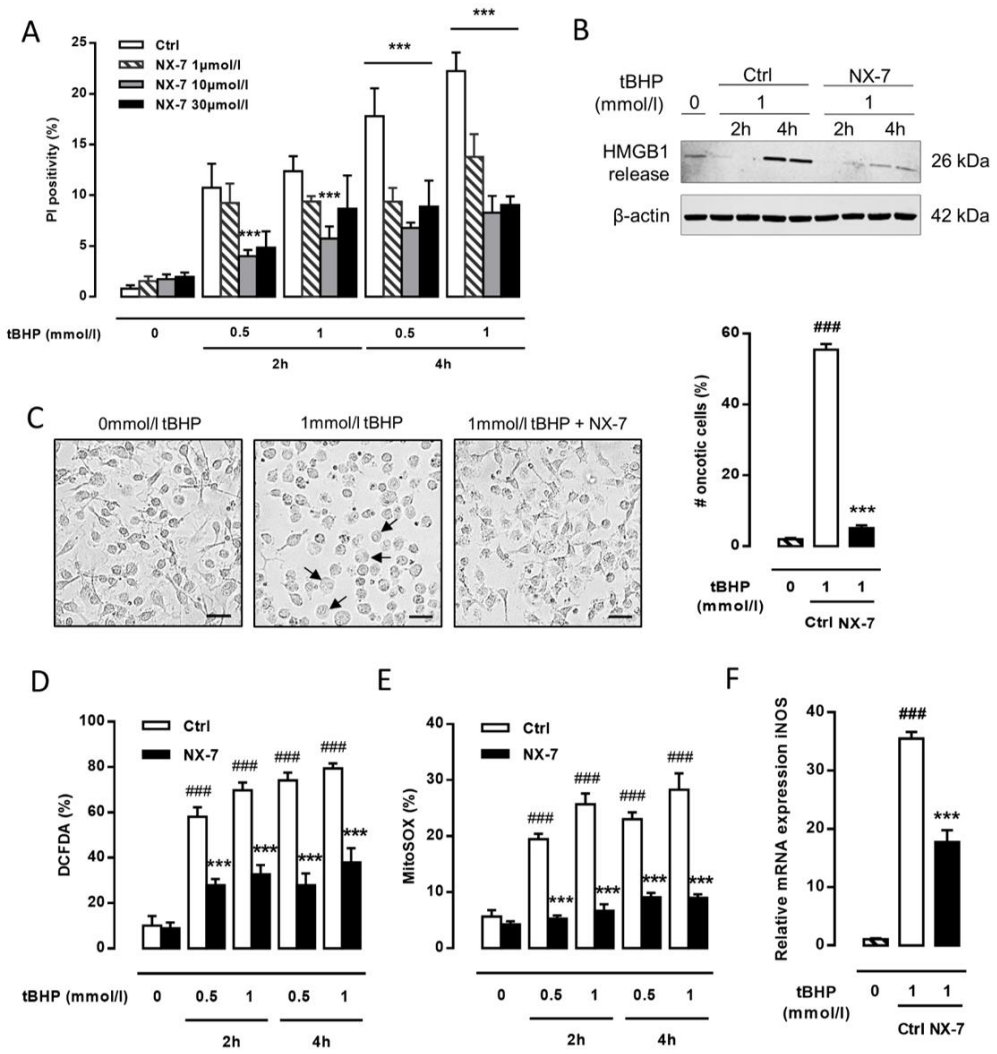

Figure 5.8 NecroX-7 inhibits oxidative stress-induced necrosis in macrophages. (A) Bone marrow-derived macrophages (BMDM) were exposed to 0, 0.5 or 1mmol/l tBHP for 2h or 4h and treated with 1,10 or 30µmol/l NecroX-7 (NX-7) or left untreated (Ctrl). Necrosis was monitored by PI labelling. (****P*<0.001 vs. Ctrl; n=3 experiments with 2 counting regions of 200 cells/region in duplicate; Factorial ANOVA, Bonferroni post hoc). **(B)** BMDM were exposed to 0 or 1mmol/l tBHP for 2h or 4h and treated with 10µmol/l NecroX-7 (NX-7) or left untreated (Ctrl). Necrosis was determined by western blot analysis of HMGB1 release in supernatant. Corresponding cell lysates were analysed for β-actin as internal control. **(C)** Representative images of BMDM exposed to 0mmol/l tBHP (left panel), 1mmol/l tBHP (middle panel), or 1mmol/l tBHP + 10µmol/l NecroX-7 (right panel) for 4h. Necrotic BMDM (indicated by black arrows) were characterised by an increase in cell volume (oncosis) (****P*<0.001 vs. Ctrl, n= 200 cells, One way ANOVA) and a translucent cytoplasm. Scale bar: 25µm. **(D,E)** BMDM were exposed to 0, 0.5 or 1mmol/l tBHP for 2h or 4h and treated with 10µmol/l NecroX-7 (NX-7) or left untreated (Ctrl). Intracellular and mitochondrial ROS generation was monitored by DCFDA (D) and MitoSOX (E) labelling, respectively. (****P*<0.001 vs. Ctrl; $^{\#\#\#}P$<0.001 vs. 0mmol/l; n=2 experiments in duplicate; Factorial ANOVA). **(F)** BMDM were polarised to M1 macrophages, exposed to 0 or 1mmol/l tBHP for 4h in the presence (NX-7) or absence (Ctrl) of 10µmol/l NecroX-7. iNOS expression was analysed by real time RT-PCR (****P*<0.001 vs. Ctrl; $^{\#\#\#}P$<0.001 vs. 0mmol/l; n=2 independent experiments in tetraplicate; One way ANOVA, Bonferroni post hoc test).

5.3.6 NecroX-7 inhibits neither LPS-induced necroptosis nor cycloheximide-induced apoptosis

To investigate whether NecroX-7 inhibits necroptosis, BMDM were treated with LPS (100ng/ml) and zVAD-fmk (20µmol/l) for 24h. Necroptosis was induced in wild-type BMDM but not in Necrostatin-1 (Nec-1, RIPK1 inhibitor) treated or *Ripk3*$^{-/-}$ BMDM **(Fig. 5.9A)**. However, NecroX-7 treatment did not affect LPS/zVAD-fmk-induced necroptosis.

To study whether NecroX-7 targets apoptosis, BMDM were treated with the protein synthesis inhibitor cycloheximide (30µg/ml) for 24h. According to western blot analysis and immunocytochemistry for cleaved caspase-3, NecroX-7 did not inhibit cycloheximide-induced macrophage apoptosis **(Fig.5.9B and 5.9C)**.

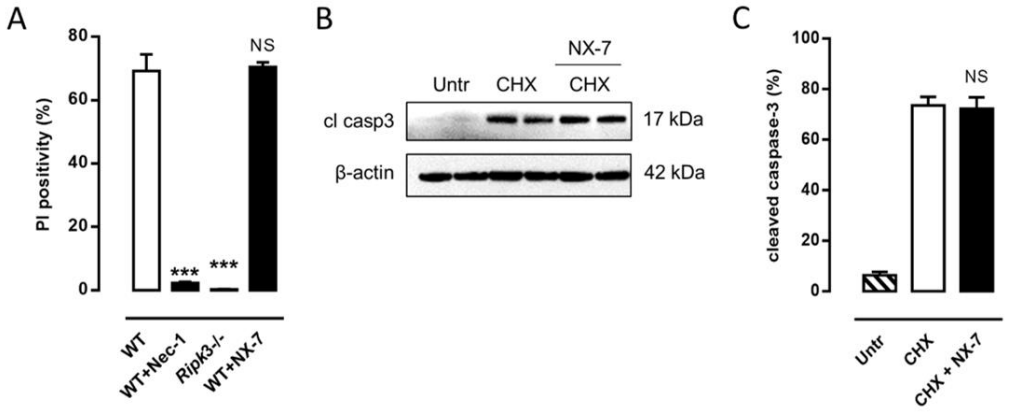

Figure 5.9 NecroX-7 inhibits neither LPS-induced necroptosis nor cycloheximide-induced apoptosis (A) Wild-type bone marrow-derived macrophages (BMDM) were exposed to 100ng/ml LPS + 20µmol/l zVAD-fmk in the presence or absence of NecroX-7 (10µmol/l). Necroptosis induction was evaluated via PI labelling. Necrostatin-1 (Nec-1, 30µmol/l) treated WT BMDM and *Ripk3*$^{-/-}$ BMDM were included as a negative control for necroptosis induction. (***P<0.001 vs. WT; NS, not significant vs. WT) (n=3 experiments with 2 counting regions of 300 cells/region in duplicate; One-way ANOVA with Dunnett post hoc). **(B,C)** Wild-type BMDM were treated with 30µg/ml cycloheximide (CHX) with or without NecroX-7 (10µmol/l). Apoptosis was assessed by detection of cleaved caspase-3 by western blotting (B) (bands are shown in duplicate; β-actin was used as loading control) or by immunocytochemistry (C) (NS, not significant vs. CHX; n=2 counting regions of 500 cells/region in duplicate, One-way ANOVA with Bonferroni post hoc) (scale bar: 75µm).

5.4 Discussion

Recently, NecroX compounds have been successfully tested in several pathologies including oxidative stress-induced cardiomyopathy, hepatic and renal ischemia-reperfusion injury, nonalcoholic steatohepatitis, allergic lung inflammation and acute graft-versus-host-disease.[5-7, 14-20] As a result, NecroX-7 is currently being tested in ST-segment elevated myocardial infarction (STEMI) patients before percutaneous coronary intervention to reduce myocardial infarct size (https://clinicaltrials.gov, identifier NCT02070471). In the present study, we tested the potential plaque stabilising effects of NecroX-7 in *ApoE*$^{-/-}$ mice, a model of atherosclerosis.

From a general point of view, unstable plaques are characterised by a high inflammatory cell content, a large necrotic core and a thin fibrous cap consisting of a low amount of smooth muscle cells and extracellular matrix (e.g. collagen).[21] NecroX-7 was able to improve plaque stability at different levels. Firstly, NecroX-7 reduced necrotic core area, albeit this effect did not result in smaller plaques. Secondly, we observed an increase in collagen content. A correlation analysis showed that the increase in total collagen content is most likely due to an increase in collagen deposition (owing to increased smooth muscle cell amount) and a decrease in MMP13-mediated collagen degradation. Though, to fully strengthen the latter view, measurement of MMP13 collagenolytic activity is required. Thirdly, even though the amount of macrophages was not different after NecroX-7 treatment, plaques developed a less inflammatory phenotype. Multiple inflammation markers such as TNFα, IL1β, iNOS, HMGB1 and RAGE were decreased in plaques of NecroX-7-treated *ApoE*$^{-/-}$ mice, which was associated with reduced NF-κB activation. There was also a trend (P=0.06) for reduced IL6 mRNA expression in NecroX-7-treated plaques whereas the expression of IL1α, typically released by necrotic VSMCs,[22] was not altered by NecroX-7 treatment. Of all pro-inflammatory mediators, HMGB1 is one of the most studied molecules associated with necrosis. HMGB1 is a nuclear protein that is passively released from necrotic or damaged cells, but not during apoptosis and secondary necrosis.[23] Once released, HMGB1 acts as a danger-associated molecular pattern (DAMP) signal and stimulates macrophages to produce pro-inflammatory cytokines such as TNFα, IL6 and IL1β via activation of NF-κB and MAPK signaling pathways upon binding with the receptor for advanced glycation end products (RAGE) or members of the toll-like receptor family (e.g. TLR4).[24-26] On the other hand, pro-inflammatory cytokines may stimulate HMGB1 mRNA expression in

macrophages and promote the release of HMGB1 in an active manner.[26, 27] Our data indicate that NecroX-7 downregulates the HMGB1/RAGE axis and attenuates inflammation in a NF-κB-dependent manner.

Our *in vitro* experiments demonstrated that NecroX-7 inhibited oxidative stress-induced necrosis in primary macrophages, but targeted neither LPS-induced necroptosis nor cycloheximide-induced apoptosis. NecroX-7 inhibited necrosis in tBHP-treated BMDM by preventing HMGB1 release and preserving cell membrane integrity as shown by reduced PI labelling. Moreover, NecroX-7 inhibited the generation of mitochondrial ROS (mtROS) in tBHP-treated BMDM. The antioxidative action of NecroX-7 may account, at least partially, for its anti-necrotic potential. Indeed, the imbalance between mtROS production and elimination may lead to excessive mtROS levels and subsequent cell death.[28] According to various reports, excessive mtROS promotes the progression of atherosclerosis in both patients and mouse models.[29-33] In the present study, NecroX-7 lowered oxidative stress in atherosclerotic plaques of *ApoE*$^{-/-}$ mice as detected by 8-oxodG. This structure is a typical oxidative modification of nuclear DNA and mtDNA,[34] and a recently accepted marker of mtROS in murine atherosclerotic lesions.[32]

Although the detrimental role of oxidative stress in atherosclerosis is broadly accepted, the results of clinical trials investigating antioxidative compounds (e.g. vitamin E) are rather disappointing (reviewed in [35,36]). Possibly, these compounds convert into pro-oxidants when scavenging ROS and/or impair mitochondrial function.[37] Moreover, these classical antioxidants are widely distributed throughout the body and block several oxidative reactions (e.g. propagation of lipid peroxidation) though they do not target mitochondrial oxidative damage directly.[38] Mitochondria-targeted antioxidants such as NecroX-7 are chemically designed in such a way that they selectively concentrate within the mitochondria in the tissue.[38] In this way, these antioxidants accumulate in high amounts at the site where most ROS are generated. The unique chemical moiety of 7-amino (indole) allows NecroX-7 to preferentially accumulate in the mitochondria and thus to inhibit the generation of mtROS, mitochondrial depolarisation, ATP depletion and subsequent necrosis **(Fig. 5.10)**. Additional evidence shows that NecroX-7 inhibits necrosis and preserves mitochondrial membrane potential much more effectively than the classical antioxidants, presumably by inhibition of the opening of the mitochondrial permeability transmission pore (mPTP).[8] Moreover, NecroX-7 significantly inhibits myocardial necrosis after ischemia-reperfusion injury in rats as compared to controls and

cyclosporine A, a well-known mPTP blocker.[8] To our knowledge, these anti-necrotic effects have not been described for other currently available antioxidative compounds in atherosclerosis studies. In addition, NecroX-7 was not able to lower oxLDL and malondialdehyde levels in plasma of WD-fed *ApoE*$^{-/-}$ mice, indicating that inhibition of lipid (per)oxidation reactions is not its main mode of action to reduce atherogenesis, in contrast to the classical antioxidants such as vitamin E.[39] Although we cannot exclude that the decrease in plaque inflammation in NecroX-7-treated mice is a result of reduced mtROS, above-mentioned data indicate that NecroX-7 exhibits discernible anti-necrotic effects which are likely accountable for the decreased inflammation. Furthermore, it is worthwhile to mention that comparable plaque stabilising effects were observed in *ApoE*$^{-/-}$ mice treated with MitoQ, one of the few antioxidants that selectively target the mitochondria. MitoQ does not affect total plaque size, smooth muscle content and apoptosis, but reduces the number of plaque macrophages.[40] Unfortunately, the effect of MitoQ on necrotic core formation was not examined.

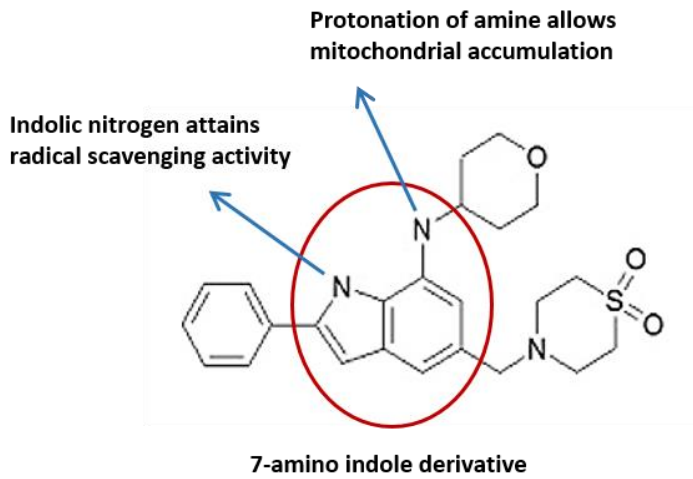

Figure 5.10 Chemical structure of NecroX-7. The chemical moiety of 7-amino indole allows NecroX-7 to preferentially accumulate in the mitochondria and to prevent mitochondrial oxidative damage and mtROS-induced necrosis.

Furthermore, we examined the livers of vehicle and NecroX-7-treated mice, which are, besides the vasculature, heavily subjected to a western life style. NecroX-7 treatment reduced hepatic steatosis significantly in WD-fed *ApoE*$^{-/-}$ mice. Similar results were recently described in a NASH (non-alcoholic steatohepatitis) ob/ob mouse model. In this study, the reduced hepatic steatosis upon NecroX-7 treatment was associated with increased β-oxidation.[6] In the present study, we did not observe a significant upregulation of β-oxidation-related genes in the livers of NecroX-7-treated *ApoE*$^{-/-}$ mice, though FASN (fatty acid synthase) mRNA expression was significantly decreased. These data indicate that the reduction in hepatic steatosis in NecroX-7-treated *ApoE*$^{-/-}$ mice was not attributed to increased lipid degradation (via β-oxidation or PNPLA2-regulated lipolysis) but was associated with decreased *de novo* lipogenesis. Because the livers of *ApoE*$^{-/-}$ mice did not show signs of inflammation after 16 weeks on WD, the effect of NecroX-7 on NASH could not be examined. Nevertheless, these findings underscore the potential of NecroX-7 in the treatment of atherosclerosis, not only by exerting a direct effect on plaque stability, but possibly also by affecting whole body lipid metabolism. Further and probably longer studies are required to establish an effect on the circulating lipids.

Taken together, our study demonstrates that inhibition of important triggers of necrosis such as mitochondrial oxidative stress during atherogenesis attenuates the severity of the disease. However, from a translational point of view, more experiments evaluating the effect of NecroX-7 on established plaques would be extremely valuable. With regard to its suitability in humans, NecroX-7 is now being tested in phase II clinical trials to evaluate its efficacy, safety and pharmacokinetic properties (https://clinicaltrials.gov, identifier NCT02070471). Moreover, analysis of the cytokine profiles of healthy subjects showed that NecroX-7 does not induce a pathological inflammatory response, at least not after one single injection.[18] Because the treatment of atherosclerosis requires a chronic approach, the evaluation of the safety of NecroX-7 during chronic administration should be included in future trials.

In conclusion, NecroX-7 improves features of atherosclerotic plaque stability in 16 week western-type diet-fed *ApoE*$^{-/-}$ mice by reducing necrotic core formation, oxidative stress and inflammation, and by increasing collagen deposition and fibrous cap thickness **(Fig. 5.11)**. Given the multifaceted pathophysiology of atherosclerosis and the pleiotropic efficacy of NecroX-7, this compound could be a new attractive therapeutic drug in the treatment of atherosclerosis.

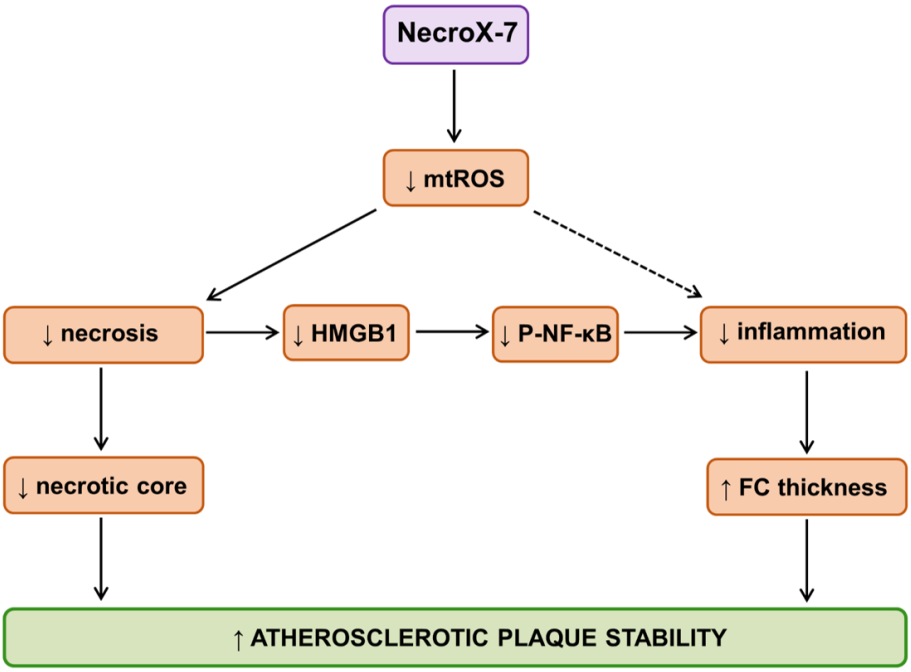

Figure 5.11 Schematic overview of the mechanism by which NecroX-7 improves features of atherosclerotic plaque stability in *ApoE*$^{-/-}$ mice. NecroX-7 inhibits oxidative stress-induced necrosis by targeting mtROS. Inhibition of necrosis attenuates HMGB1 release and subsequent activation of the NF-κB pathway, resulting in reduced inflammation. NecroX-7 improves plaque stability by reducing necrotic core formation and exerting anti-inflammatory effects, resulting in a thicker fibrous cap (FC).

5.5 References

(1) Virmani R, Burke AP, Willerson J, Farb A, Narula J, Kolodgie FD. The pathology of vulnerable plaque. In: Virmani R, Narula J, Leon M, Willerson J, eds. *The vulnerable atherosclerotic plaque: strategies for diagnosis and management*. Malden: Blackwell Futura; 2007. p. 21-36.

(2) Fok PW. Growth of necrotic cores in atherosclerotic plaque. *Math Med Biol* 2012;29(4):301-27.

(3) Seimon T and Tabas I. Mechanisms and consequences of macrophage apoptosis in atherosclerosis. *J Lipid Res* 2009;50 Suppl:S382-S387.

(4) Kim HJ et al. NecroX as a novel class of mitochondrial reactive oxygen species and ONOO scavenger. *Arch Pharm Res* 2010;33(11):1813-23.

(5) Park J et al. NecroX-7 prevents oxidative stress-induced cardiomyopathy by inhibition of NADPH oxidase activity in rats. *Toxicol Appl Pharmacol* 2012;263(1):1-6.

(6) Chung HK et al. The indole derivative NecroX-7 improves nonalcoholic steatohepatitis in ob/ob mice through suppression of mitochondrial ROS/RNS and inflammation. *Liver Int* 2015;35(4):1341-53.

(7) Im KI, Kim N, Lim JY, Nam YS, Lee ES, Kim EJ, Kim HJ, Kim SH, Cho SG. The Free Radical Scavenger NecroX-7 Attenuates Acute Graft-versus-Host Disease via Reciprocal Regulation of Th1/Regulatory T Cells and Inhibition of HMGB1 Release. *J Immunol* 2015;194(11):5223-32.

(8) Cho HJ, Hwang IC, Kim JY, Lee HS, Lee J, Park J, Yang HM, Kwon YW, Kim SH, Kim HS. Therapeutic Potential of a Novel Necrosis Inhibitor in Myocardial Ischemia-reperfusion Injury. Circ.Res. 117:A263. 2015.

(9) Hermans N, Cos P, Berghe DV, Vlietinck AJ, de BT. Method development and validation for monitoring in vivo oxidative stress: evaluation of lipid peroxidation and fat-soluble vitamin status by HPLC in rat plasma. *J Chromatogr B Analyt Technol Biomed Life Sci* 2005;822(1-2):33-9.

(10) Newton K, Sun X, Dixit VM. Kinase RIP3 is dispensable for normal NF-kappa Bs, signaling by the B-cell and T-cell receptors, tumor necrosis factor receptor 1, and Toll-like receptors 2 and 4. *Mol Cell Biol* 2004;24(4):1464-9.

(11) Seimon TA, Wang Y, Han S, Senokuchi T, Schrijvers DM, Kuriakose G, Tall AR, Tabas IA. Macrophage deficiency of p38alpha MAPK promotes apoptosis and plaque necrosis in advanced atherosclerotic lesions in mice. *J Clin Invest* 2009;119(4):886-98.

(12) Whittaker P, Kloner RA, Boughner DR, Pickering JG. Quantitative assessment of myocardial collagen with picrosirius red staining and circularly polarized light. *Basic Res Cardiol* 1994;89(5):397-410.

(13) Hellemans J, Mortier G, De PA, Speleman F, Vandesompele J. qBase relative quantification framework and software for management and automated analysis of real-time quantitative PCR data. *Genome Biol* 2007;8(2):R19.

(14) Thu VT et al. NecroX-5 prevents hypoxia/reoxygenation injury by inhibiting the mitochondrial calcium uniporter. *Cardiovasc Res* 2012;94(2):342-50.

(15) Choi JM, Park KM, Kim SH, Hwang DW, Chon SH, Lee JH, Lee SY, Lee YJ. Effect of necrosis modulator necrox-7 on hepatic ischemia-reperfusion injury in beagle dogs. *Transplant Proc* 2010;42(9):3414-21.

(16) Park JH et al. An indole derivative protects against acetaminophen-induced liver injury by directly binding to N-acetyl-p-benzoquinone imine in mice. *Antioxid Redox Signal* 2013;18(14):1713-22.

(17) Kim SR, Kim DI, Kim SH, Lee H, Lee KS, Cho SH, Lee YC. NLRP3 inflammasome activation by mitochondrial ROS in bronchial epithelial cells is required for allergic inflammation. *Cell Death Dis* 2014;5:e1498.

(18) Shin E, Lee YC, Kim SR, Kim SH, Park J. Drug Signature-based Finding of Additional Clinical Use of LC28-0126 for Neutrophilic Bronchial Asthma. *Sci Rep* 2015;5:17784.

(19) Li X, Kwon O, Kim DY, Taketomi Y, Murakami M, Chang HW. NecroX-5 suppresses IgE/Ag-stimulated anaphylaxis and mast cell activation by regulating the SHP-1-Syk signaling module. *Allergy* 2015.

(20) Jin SA et al. Beneficial Effects of Necrosis Modulator, Indole Derivative NecroX-7, on Renal Ischemia-Reperfusion Injury in Rats. *Transplant Proc* 2016;48(1):199-204.

(21) Falk E, Nakano M, Bentzon JF, Finn AV, Virmani R. Update on acute coronary syndromes: the pathologists' view. *Eur Heart J* 2013;34(10):719-28.

(22) Clarke MC, Talib S, Figg NL, Bennett MR. Vascular smooth muscle cell apoptosis induces interleukin-1-directed inflammation: effects of hyperlipidemia-mediated inhibition of phagocytosis. *Circ Res* 2010;106(2):363-72.

(23) Scaffidi P, Misteli T, Bianchi ME. Release of chromatin protein HMGB1 by necrotic cells triggers inflammation. *Nature* 2002;418(6894):191-5.

(24) Andersson U et al. High mobility group 1 protein (HMG-1) stimulates proinflammatory cytokine synthesis in human monocytes. *J Exp Med* 2000;192(4):565-70.

(25) Erlandsson HH and Andersson U. Mini-review: The nuclear protein HMGB1 as a proinflammatory mediator. *Eur J Immunol* 2004;34(6):1503-12.

(26) Kalinina N, Agrotis A, Antropova Y, DiVitto G, Kanellakis P, Kostolias G, Ilyinskaya O, Tararak E, Bobik A. Increased expression of the DNA-binding cytokine HMGB1 in human atherosclerotic lesions: role of activated macrophages and cytokines. *Arterioscler Thromb Vasc Biol* 2004;24(12):2320-5.
(27) Gardella S, Andrei C, Ferrera D, Lotti LV, Torrisi MR, Bianchi ME, Rubartelli A. The nuclear protein HMGB1 is secreted by monocytes via a non-classical, vesicle-mediated secretory pathway. *EMBO Rep* 2002;3(10):995-1001.
(28) Li X, Fang P, Mai J, Choi ET, Wang H, Yang XF. Targeting mitochondrial reactive oxygen species as novel therapy for inflammatory diseases and cancers. *J Hematol Oncol* 2013;6:19.
(29) Ballinger SW et al. Mitochondrial integrity and function in atherogenesis. *Circulation* 2002;106(5):544-9.
(30) Harrison CM, Pompilius M, Pinkerton KE, Ballinger SW. Mitochondrial oxidative stress significantly influences atherogenic risk and cytokine-induced oxidant production. *Environ Health Perspect* 2011;119(5):676-81.
(31) Ari E, Kaya Y, Demir H, Cebi A, Alp HH, Bakan E, Odabasi D, Keskin S. Oxidative DNA damage correlates with carotid artery atherosclerosis in hemodialysis patients. *Hemodial Int* 2011;15(4):453-9.
(32) Wang Y, Wang GZ, Rabinovitch PS, Tabas I. Macrophage mitochondrial oxidative stress promotes atherosclerosis and nuclear factor-kappaB-mediated inflammation in macrophages. *Circ Res* 2014;114(3):421-33.
(33) Tabas I and Wang Y. Emerging Roles of Mitochondria ROS in Atherosclerotic Lesions: Causation or Association? *J Atheroscler Thromb* 2014.
(34) de Souza-Pinto NC, Eide L, Hogue BA, Thybo T, Stevnsner T, Seeberg E, Klungland A, Bohr VA. Repair of 8-oxodeoxyguanosine lesions in mitochondrial dna depends on the oxoguanine dna glycosylase (OGG1) gene and 8-oxoguanine accumulates in the mitochondrial dna of OGG1-defective mice. *Cancer Res* 2001;61(14):5378-81.
(35) Madamanchi NR, Vendrov A, Runge MS. Oxidative stress and vascular disease. *Arterioscler Thromb Vasc Biol* 2005;25(1):29-38.
(36) Cherubini A, Vigna GB, Zuliani G, Ruggiero C, Senin U, Fellin R. Role of antioxidants in atherosclerosis: epidemiological and clinical update. *Curr Pharm Des* 2005;11(16):2017-32.
(37) Otani H. Site-specific antioxidative therapy for prevention of atherosclerosis and cardiovascular disease. *Oxid Med Cell Longev* 2013;2013:796891.
(38) Smith RA and Murphy MP. Mitochondria-targeted antioxidants as therapies. *Discov Med* 2011;11(57):106-14.
(39) Upston JM, Kritharides L, Stocker R. The role of vitamin E in atherosclerosis. *Prog Lipid Res* 2003;42(5):405-22.
(40) Mercer JR et al. The mitochondria-targeted antioxidant MitoQ decreases features of the metabolic syndrome in ATM+/-/ApoE-/- mice. *Free Radic Biol Med* 2012;52(5):841-9.

CHAPTER 6

Discussion and Conclusion

6.1 Discussion

Cell death plays a central role in the pathophysiology of atherosclerotic plaque destabilisation. Unstable, rupture-prone plaques are characterised by a thin fibrous cap, a high inflammatory cell content and a large necrotic core.[1] Death of vascular smooth muscle cells (VSMCs) and macrophages in atherosclerotic plaques does not only increase plaque vulnerability, but also promotes plaque inflammation and thrombosis.

The goal of this thesis was to investigate whether inhibition of cell death, in particular of apoptosis, autophagy, or necrosis, could be a beneficial strategy to improve atherosclerotic plaque stability. In this thesis, we kind of travel through time as the three main chapters reflect the historical changes in cell death research in atherosclerosis **(Fig. 6.1)**. During this time travelling, we started-off with a mouse model for apoptosis deficiency to investigate its impact on plaque development and stability (chapter 3). Because cell death research gradually switched from apoptosis to autophagy about 10 years ago, we were encouraged to investigate the role of VSMC autophagy in post-injury neointima formation and atherosclerosis in a second study (chapter 4). In the third study, we tested the plaque stabilising potential of NecroX-7, a newly developed necrosis inhibitor (chapter 5). Only since the last few years, necrosis has been considered as a highly regulated form of cell death, and therefore, the development of new inhibitors and their applications in atherosclerosis is expected to rise in the upcoming years.

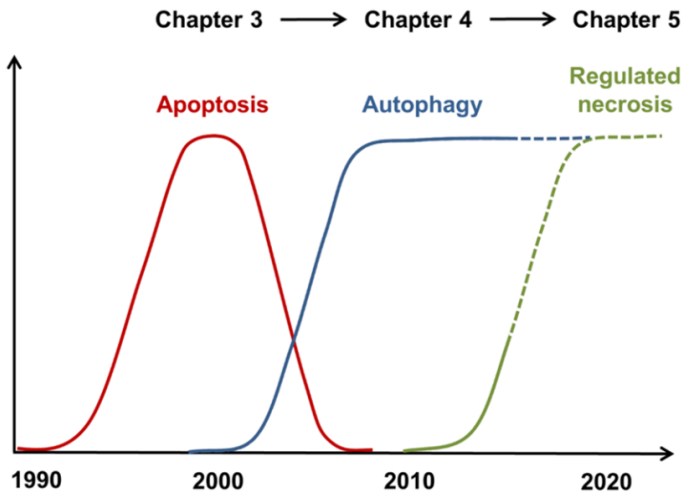

Figure 6.1 Historical overview of cell death research in atherosclerosis

In this discussion, we will review the different approaches implemented in this thesis to inhibit cell death in atherosclerosis and provide an answer to the three main research questions before formulating a general conclusion.

6.1.1 Does apoptosis impairment improve plaque stability?

In the first study of this thesis (chapter 3), we used caspase-3 deficient mice as a model for apoptosis deficiency to investigate its impact on plaque development and stability. Many other mouse models (listed in Table 1.2) have previously been generated to impair apoptosis, though these models target only one route of apoptosis. Deletion of caspase-3 enables us to block the execution of both the extrinsic and intrinsic apoptotic pathway. Moreover, by targeting apoptosis, we aimed to prevent secondary necrosis and concomitant enlargement of the necrotic core.

We could demonstrate that caspase-3 deficient macrophages and VSMCs were resistant to apoptosis and did not activate the analogous compensatory executioner caspase-7. However, caspase-3 deficient macrophages and VSMCs showed increased susceptibility to necrosis when exposed to apoptotic stimuli. Thus inactivation of caspase-3 inhibits apoptosis but does not prevent cell death. The switch to necrotic cell death did not involve induction of necroptosis, but is possibly attributed to the downstream activity of caspase-3 in the apoptotic pathway.[2] Caspase-3 inactivation prevents the final execution of apoptosis by inhibiting all the morphological changes associated with apoptosis but does not affect the biochemical events that occur upstream in the pathway. For example, different cell death stimuli can still reach the mitochondria and cause mitochondrial membrane permeabilisation. When mitochondrial ROS levels increase and ATP levels drop, a point-of-no-return is trespassed and the cell is forced to die by necrosis.[3]

In vivo, caspase-3 deficiency reduced plaque apoptosis but promoted necrosis in atherosclerotic plaques in WD-fed *ApoE*$^{-/-}$ mice resulting in increased plaque size. Although plaques of *Casp3*$^{-/-}$*ApoE*$^{-/-}$ mice showed a decrease in macrophage content, this should not be considered as a feature of increased plaque stability since it likely reflects an increase in macrophage necrosis. Thus instead of preventing secondary necrosis by inhibiting apoptosis, caspase-3 deletion promotes necrotic core enlargement by increasing primary necrosis. Hence, caspase-3 deficiency promotes plaque growth and plaque instability, indicating that inhibition of apoptosis is not a favourable strategy

to improve plaque stability. These findings are in line with previous observations in mice lacking the pro-apoptotic protein p53.[4-6]

Our study has a number of limitations. Firstly, we used full-knockout mice in which caspase-3 is deleted in every cell type. VSMC-specific or macrophage-specific caspase-3 knockout mice could have been extremely valuable to investigate the contribution of each cell type to necrotic core formation. Secondly, given that macrophage apoptosis is considered beneficial in early but not in advanced lesions, macrophage-specific deletion of caspase-3, using mice that contain an inducible *Cre* recombinase, could have made it possible to inhibit macrophage apoptosis only in advanced plaques.

Taken together, repression of apoptosis promotes atherosclerosis and plaque necrosis and may not be of therapeutic benefit in atherosclerosis considering the pro-inflammatory and pro-thrombotic properties of necrosis.

6.1.2 What are the consequences of defective autophagy in VSMCs in atherosclerosis?

Next, we investigated the impact of defective VSMC autophagy on post-injury neointima formation and atherosclerosis. This study differs from the other two studies in this thesis (related to apoptosis [chapter 4] and necrosis [chapter 5]) as the role of VSMC autophagy in atherosclerotic plaque stabilisation was completely unknown. Because autophagy has both pro-survival and cell death potential, the outcome of this experiment was impossible to predict, though very intriguing to uncover.

We demonstrated that defective autophagy in VSMCs accelerated the development of stress-induced premature senescence (SIPS) as shown by cellular and nuclear hypertrophy, a decline in proliferative capacity due to a p16/RB-mediated G_1 cell cycle arrest and SA-β-galactosidase activity. Moreover, autophagy defective VSMCs were characterised by an augmented migration potential, elevated expression of TGFβ and SDF1, and upregulation of the inflammasome components IL1β and NLRP3. These findings are in line with the characteristics of senescent human VSMCs as recently described by Gardner et al.[7] However, the senescence-associated secretory phenotype in human VSMCs is IL1α-dependent while *Atg7$^{F/F}$SM22α-Cre^{+}* VSMCs did not show upregulation of IL1α. Moreover, *Atg7$^{F/F}$SM22α-Cre^{+}* VSMCs were characterised by increased collagen synthesis, which is not consistent with the observations in the senescent human VSMCs. The discrepancies between both studies can be explained by

multiple factors. First of all, we are comparing two different species. Numerous studies have shown that senescence in mice can be regulated differently as compared to senescence in humans.[8, 9] Secondly, human VSMCs investigated in the study of Gardner et al., develop senescence by repetitive replication and have a competent autophagic machinery while *Atg7$^{F/F}$SM22α-Cre^{+}* VSMCs developed senescence as result of defective autophagy. Nevertheless, we have gathered sufficient evidence to state that autophagy defective VSMCs develop a senescent phenotype. However, we must be aware that some characteristics of *Atg7$^{F/F}$SM22α-Cre^{+}* VSMCs could be related to the activation of other cellular pathways - which we did not investigate - rather than being part of the senescent phenotype.

Furthermore, we revealed that the induction of senescence in *Atg7$^{F/F}$SM22α-Cre^{+}* VSMCs was mediated by severe accumulation of p62, which typically occurs during defective autophagy. This is the first study that addresses p62 accumulation as a direct link between defective autophagy and senescence in VSMCs. The inverse relationship between autophagy and senescence has previously been described by others[10-12] and seems highly conceivable when they are considered as two cytoprotective pathways. When autophagy is impaired, senescence can be engaged as a backup mechanism to protect the cell[13] while, vice versa, autophagy may prevent cellular senescence by facilitating the removal of damaged organelles and promoting self-renewal.[14] Nonetheless, other studies favour a direct relationship between autophagy and senescence.[15-17] Besides the fact that this theory, so far, only accounts for oncogene-induced or DNA damage-induced senescence, and not SIPS, a direct relationship between autophagy and senescence seems intuitively less logical. Why would autophagy, a process known for its life-expanding and anti-aging properties, take place in senescent cells?

Besides the development of senescence, *Atg7$^{F/F}$SM22α-Cre^{+}* VSMCs were highly resistant to oxidative stress-mediated cell death as compared to *Atg7$^{+/+}$SM22α-Cre^{+}* VSMCs. This phenomenon is attributed to activation of the transcription factor Nrf2 resulting in upregulation of several anti-oxidative enzymes such as GSTα and NQO1. According to literature, accumulation of p62 triggers nuclear translocation and activation of Nrf2.[18] Thus, the Nrf2 pathway is activated in autophagy defective VSMCs as a protective backup mechanism to maintain cell survival against oxidative insults. Although senescent cells may show apoptotic resistance (e.g. senescent fibroblasts),[19, 20] our

experiments revealed that the senescence and the Nrf2/ARE pathway acted independently in *Atg7$^{F/F}$SM22α-Cre^{+}* VSMCs.

Because changes in VSMC survival, phenotype, proliferation and migration are critical factors in the development of arterial vascular disease, we investigated their functional significance in two mouse models for post-injury neointima formation and diet-induced atherosclerosis. Defective VSMC autophagy accelerated neointima formation 5 weeks after ligation of the left common carotid artery. The mechanism behind neointima formation included high MMP9 activity and increased expression of TGFβ and SDF1 in the ligated vessel of *Atg7$^{F/F}$SM22α-Cre^{+}* mice. Moreover, neointimal *Atg7$^{F/F}$SM22α-Cre^{+}* VSMCs showed typical markers of VSMC senescence. Along these lines, *ApoE$^{-/-}$* mice with defective VSMC autophagy developed larger and more complex atherosclerotic plaques after 10 weeks of western-type diet as compared to *Atg7$^{+/+}$SM22α-Cre^{+}ApoE$^{-/-}$* mice. Differences in plaque size were no longer evident after 14 weeks of WD, though the fibrous cap thickness and total collagen content remained significantly elevated in plaques of *Atg7$^{F/F}$SM22α-Cre^{+}ApoE$^{-/-}$* mice. Moreover, VSMCs within the fibrous cap of *Atg7$^{F/F}$SM22α-Cre^{+}ApoE$^{-/-}$* mice were characterised by several senescence markers. Both experiments show that defective VSMC autophagy is closely associated with VSMC senescence and exerts pro-atherogenic effects by promoting the migration of monocytes and/or smooth muscle cell progenitor cells and by remodelling the extracellular matrix. Although VSMC senescence is known to contribute to the pathogenesis of atherosclerosis,[21-24] we cannot state that VSMC senescence is exclusively involved in the accelerated plaque formation in *Atg7$^{F/F}$SM22α-Cre^{+}ApoE$^{-/-}$* mice.

During the completion of this study, Liao et al. published that defective autophagy in macrophages increases plaque instability after 12 and 16 weeks of WD.[25] Moreover, autophagy deficient macrophages showed increased susceptibility to apoptotic cell death. These observations encouraged us to further explore the antioxidative mechanisms and cellular senescence in autophagy deficient macrophages. *Atg7$^{F/F}$LysM-Cre^{+}* macrophages did not overexpress GSTα and NQO1 due to the lack of Nrf2 activation. Moreover, *Atg7$^{F/F}$LysM-Cre^{+}* macrophages did not show any signs of cellular senescence. The opposite response of VSMCs and macrophages to defective autophagy, is most intriguing. One possible reason is that p62 plays a less central role in autophagy deficient macrophages. Indeed, *Atg7$^{F/F}$LysM-Cre^{+}* macrophages show only a modest accumulation of p62 protein as result of defective autophagy whereas

Atg7$^{F/F}$SM22α-Cre^{+} VSMCs show an increase in both p62 protein and mRNA expression. It is tempting to speculate that p62 should exceed a certain threshold before it is able to induce senescence and to activate Nrf2. In addition, the dissimilarity between VSMCs and macrophages in response to defective autophagy may simply be predetermined by the cell's origin. Hematopoietic cells preferentially respond to stress by inducing apoptosis rather than undergoing senescence whereas mesenchymal cells (.e.g. fibroblast-like cells) respond in the opposite direction.[26]

Taken together, targeting autophagy has oppossite effects in VSMCs versus macrophages and implies that autophagy may have a distinct role in both cell types. The induction of senescence in autophagy defective VSMCs favors a pro-survival role for autophagy and opens the current debate on whether or not autophagy should be classified as a typical cell death pathway.

6.1.3 Is inhibition of necrosis a good strategy for plaque stabilisation?

In the last part of this thesis, we evaluated the plaque stabilising potential of the necrosis inhibitor NecroX-7. *In vitro* validation of this compound revealed that NecroX-7 inhibits oxidative stress-induced necrosis in primary macrophages. NecroX-7 inhibited the generation of mtROS and reduced necrosis both at the morphological and biochemical level: NecroX-7 prevented cell oncosis, preserved membrane integrity and inhibited the release of HMGB1 in tBHP-exposed macrophages. Neither LPS-induced necroptosis nor cycloheximide-induced apoptosis was inhibited by NecroX-7.

Examination of atherosclerotic plaques in WD-fed *ApoE$^{-/-}$* mice revealed no difference in the level of apoptosis between the NecroX-7-treated group and controls. When we evaluated necrosis into more detail, we observed that NecroX-7 reduced necrotic core size by about 38%. Although the necrotic core also consists of cholesterol deposits and thus does not represent 100% necrosis, these data still imply that NecroX-7 only targeted approximately one third of all plaque necrosis. The other two third possibly reflects RIPK3-dependent necroptosis and/or secondary necrosis. Similarly, in *Ripk3$^{-/-}$ApoE$^{-/-}$* mice, necrotic core size was reduced by 50%,[27] indicating that the other 50% likely reflects RIPK3-independent primary necrosis and/or secondary necrosis. Different lessons can be drawn from these studies. First of all, secondary necrosis is a major contributor to necrotic core formation and should be considered as an important target for future research. Although prevention of secondary necrosis by inhibition of apoptosis

was ineffective in reducing plaque necrosis (vide supra), improving efferocytosis might be an alternative approach. Secondly, given that necrosis can be regulated by diverse mechanisms may challenge the approach of targeting plaque necrosis as a whole.

Nevertheless, besides reducing necrosis, NecroX-7 improved plaque stability at different levels. NecroX-7 lowered plaque inflammation and oxidative stress, and increased collagen deposition and fibrous cap thickness in WD-fed *ApoE*$^{-/-}$ mice. It is likely that the anti-inflammatory effects of NecroX-7 are a secondary event and thus occur downstream of necrosis inhibition. Specifically, inhibition of necrosis attenuates HMGB1 release and the subsequent binding to the RAGE receptor on adjacent cells. Consequently, the NF-κB pathway is hypo-activated and the production of pro-inflammatory cytokines is hindered. In turn, adjacent cells are less stimulated to synthesise HMGB1, creating a viscous circle. This theory is based on the observed downregulation of the HMGB1/RAGE axis and the decreased expression of NF-κB-dependent pro-inflammatory cytokines in plaques of NecroX-7-treated *ApoE*$^{-/-}$ mice, combined with the recently published paper of Im et al. In this paper, the authors state that NecroX-7 inhibits HMGB1-induced release of TNFα and IL6 in a model for graft-versus-host-disease.[28] Although our data point towards a central role for HMGB1 between necrosis and inflammation, we should not exclude that other pathways, including the decrease in mtROS, may be involved in the reduced inflammation in NecroX-7-treated plaques.

Overall, NecroX-7 improves plaque stability in WD-fed *ApoE*$^{-/-}$ mice by interfering with key atherosclerotic processes including oxidative stress, necrosis and inflammation, and could therefore be an attractive anti-atherosclerotic drug. It would be interesting to study the effect of NecroX-7 also on established plaques since patients often present themselves to the hospital with advanced lesions characterised by a large necrotic core. However, we must take into account that NecroX-7 cannot eliminate necrosis that is already present in the plaque. It may only inhibit further enlargement of the necrotic core. Nevertheless, we presume that NecroX-7 would still exerts its anti-inflammatory and plaque stabilising effects on advanced lesions.

6.2 Conclusion

From the three different cell death inhibiting strategies tested in this thesis, only one was effective in improving plaque stability **(Fig. 6.2)**. The necrosis inhibitor NecroX-7 improved features of plaque stability by reducing necrotic core formation, increasing fibrous cap thickness and lowering plaque inflammation and oxidative stress in WD-fed *ApoE*$^{-/-}$ mice. These pleiotropic effects delineate NecroX-7 as a promising compound to treat a multifaceted pathology such as atherosclerosis. However, from a translational point of view, future experiments are required to evaluate its efficacy as a curative therapy in advanced atherosclerotic plaques. Also the safety of NecroX-7 during chronic administration should be assessed in future trials.

The other two approaches exerted detrimental effects on atherosclerosis in WD-fed *ApoE*$^{-/-}$ mice. Repression of apoptosis through caspase-3 deletion aggravated plaque stability by increasing primary necrosis. Impairment of autophagy in VSMCs did not dramatically affect plaque stability but greatly accelerated atherogenesis and induced VSMC senescence, indicating that inhibition of VSMC autophagy is not a favourable strategy to treat atherosclerosis. Instead, we rather recommend controlled stimulation of autophagy as an anti-atherosclerotic strategy as recently suggested[29, 30].

Moreover, this thesis supports the general concept that inhibition of one cell death pathway often results in the compensatory activation of other cellular (death) routes. Of course, these compensatory reactions challenge the therapeutic application of cell death inhibitors in general. To date, necrosis is the only cell death pathway that can be inhibited (by NecroX-7 or *Ripk3* knockout[27, 31]) without evoking a compensatory switch to other cell death pathways and that confers true cytoprotection.

Finally, we report the very first study wherein necrosis is specifically targeted in atherosclerosis using a pharmacological compound. Giving the detrimental role of necrosis in atherosclerotic plaque destabilisation, the new concept of necrosis as a highly regulated form of cell death, and the upcoming development of new necrosis inhibitors, we may stand at the beginning of a new era in (atherosclerosis) cell death research.

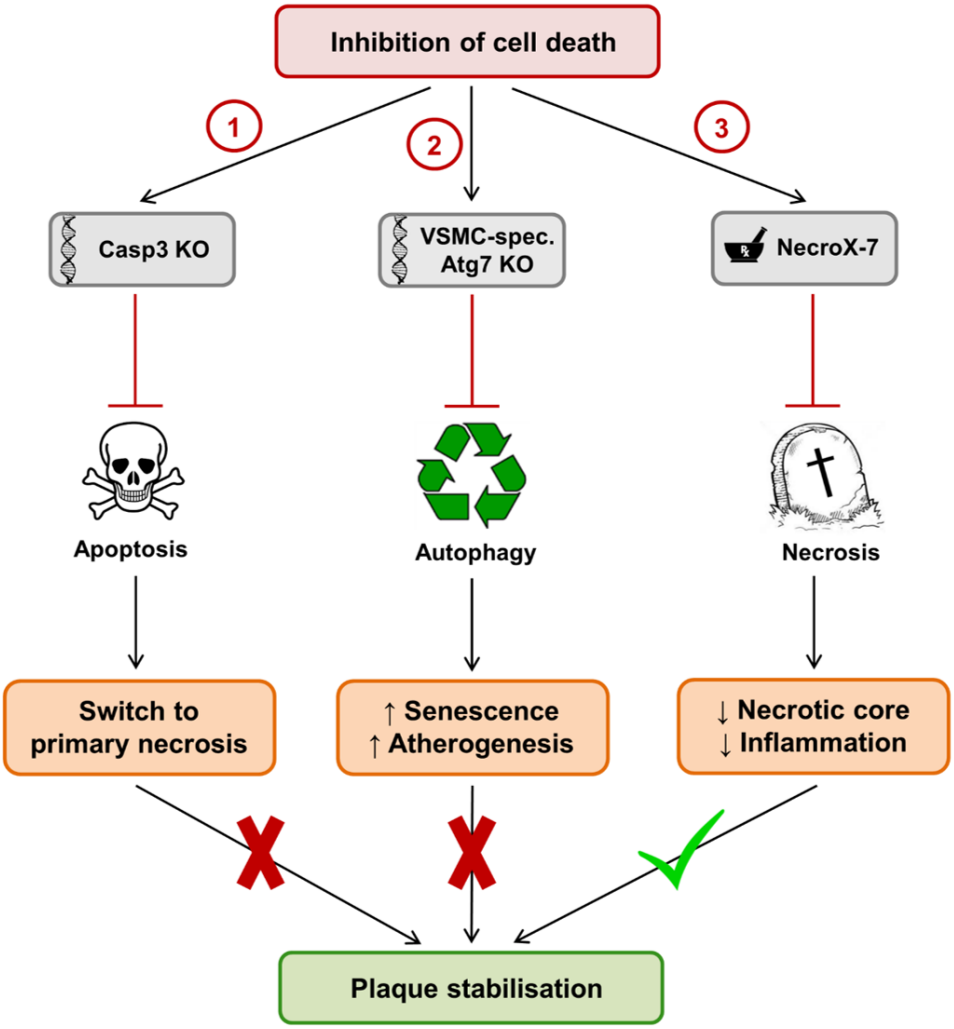

Figure 6.2 Evaluation of the three different approaches to inhibit cell death in atherosclerosis as potential plaque stabilising strategies. (1) Genetic disruption of the effector caspase-3 in *ApoE*$^{-/-}$ mice reduced plaque apoptosis but induced a switch to primary necrosis, leading to increased plaque instability**. (2)** VSMC-specific deletion of *Atg7* accelerated senescence and promoted atherogenesis in *ApoE*$^{-/-}$ mice and is therefore unsuitable as an anti-atherosclerotic therapy. **(3)** The necrosis inhibitor NecroX-7 reduced necrotic core formation and lowered inflammation, indicating that pharmacological inhibition of necrosis by NecroX-7 is the only suitable strategy, tested in this thesis, for plaque stabilisation.

6.3 References

(1) Falk E, Nakano M, Bentzon JF, Finn AV, Virmani R. Update on acute coronary syndromes: the pathologists' view. *Eur Heart J* 2013;34(10):719-28.
(2) Hirsch T, Marchetti P, Susin SA, Dallaporta B, Zamzami N, Marzo I, Geuskens M, Kroemer G. The apoptosis-necrosis paradox. Apoptogenic proteases activated after mitochondrial permeability transition determine the mode of cell death. *Oncogene* 1997;15(13):1573-81.
(3) Kroemer G and Reed JC. Mitochondrial control of cell death. *Nat Med* 2000;6(5):513-9.
(4) van Vlijmen BJ et al. Macrophage p53 deficiency leads to enhanced atherosclerosis in APOE*3-Leiden transgenic mice. *Circ Res* 2001;88(8):780-6.
(5) Merched AJ, Williams E, Chan L. Macrophage-specific p53 expression plays a crucial role in atherosclerosis development and plaque remodeling. *Arterioscler Thromb Vasc Biol* 2003;23(9):1608-14.
(6) Boesten LS et al. Macrophage p53 controls macrophage death in atherosclerotic lesions of apolipoprotein E deficient mice. *Atherosclerosis* 2009;207(2):399-404.
(7) Gardner SE, Humphry M, Bennett MR, Clarke MC. Senescent Vascular Smooth Muscle Cells Drive Inflammation Through an Interleukin-1alpha-Dependent Senescence-Associated Secretory Phenotype. *Arterioscler Thromb Vasc Biol* 2015;35(9):1963-74.
(8) Wright WE and Shay JW. Telomere dynamics in cancer progression and prevention: fundamental differences in human and mouse telomere biology. *Nat Med* 2000;6(8):849-51.
(9) Itahana K, Campisi J, Dimri GP. Mechanisms of cellular senescence in human and mouse cells. *Biogerontology* 2004;5(1):1-10.
(10) Kang HT, Lee KB, Kim SY, Choi HR, Park SC. Autophagy impairment induces premature senescence in primary human fibroblasts. *PLoS One* 2011;6(8):e23367.
(11) Wang Y et al. Autophagic activity dictates the cellular response to oncogenic RAS. *Proc Natl Acad Sci U S A* 2012;109(33):13325-30.
(12) Zhang CF et al. Suppression of autophagy dysregulates the antioxidant response and causes premature senescence of melanocytes. *J Invest Dermatol* 2015;135(5):1348-57.
(13) Gewirtz DA. Autophagy and senescence: a partnership in search of definition. *Autophagy* 2013;9(5):808-12.
(14) Takasaka N et al. Autophagy induction by SIRT6 through attenuation of insulin-like growth factor signaling is involved in the regulation of human bronchial epithelial cell senescence. *J Immunol* 2014;192(3):958-68.
(15) Young AR et al. Autophagy mediates the mitotic senescence transition. *Genes Dev* 2009;23(7):798-803.
(16) White E and Lowe SW. Eating to exit: autophagy-enabled senescence revealed. *Genes Dev* 2009;23(7):784-7.
(17) Goehe RW, Di X, Sharma K, Bristol ML, Henderson SC, Valerie K, Rodier F, Davalos AR, Gewirtz DA. The autophagy-senescence connection in chemotherapy: must tumor cells (self) eat before they sleep? *J Pharmacol Exp Ther* 2012;343(3):763-78.
(18) Komatsu M et al. The selective autophagy substrate p62 activates the stress responsive transcription factor Nrf2 through inactivation of Keap1. *Nat Cell Biol* 2010;12(3):213-23.
(19) Wang E. Senescent human fibroblasts resist programmed cell death, and failure to suppress bcl2 is involved. *Cancer Res* 1995;55(11):2284-92.
(20) Sanders YY, Liu H, Zhang X, Hecker L, Bernard K, Desai L, Liu G, Thannickal VJ. Histone modifications in senescence-associated resistance to apoptosis by oxidative stress. *Redox Biol* 2013;1:8-16.
(21) Erusalimsky JD and Kurz DJ. Cellular senescence in vivo: its relevance in ageing and cardiovascular disease. *Exp Gerontol* 2005;40(8-9):634-42.
(22) Matthews C, Gorenne I, Scott S, Figg N, Kirkpatrick P, Ritchie A, Goddard M, Bennett M. Vascular smooth muscle cells undergo telomere-based senescence in human atherosclerosis: effects of telomerase and oxidative stress. *Circ Res* 2006;99(2):156-64.
(23) Gorenne I, Kavurma M, Scott S, Bennett M. Vascular smooth muscle cell senescence in atherosclerosis. *Cardiovasc Res* 2006;72(1):9-17.
(24) Minamino T and Komuro I. Vascular cell senescence: contribution to atherosclerosis. *Circ Res* 2007;100(1):15-26.
(25) Liao X, Sluimer JC, Wang Y, Subramanian M, Brown K, Pattison JS, Robbins J, Martinez J, Tabas I. Macrophage autophagy plays a protective role in advanced atherosclerosis. *Cell Metab* 2012;15(4):545-53.
(26) Fridlyanskaya I, Alekseenko L, Nikolsky N. Senescence as a general cellular response to stress: A mini-review. *Exp Gerontol* 2015;72:124-8.

(27) Lin J et al. A role of RIP3-mediated macrophage necrosis in atherosclerosis development. *Cell Rep* 2013;3(1):200-10.
(28) Im KI, Kim N, Lim JY, Nam YS, Lee ES, Kim EJ, Kim HJ, Kim SH, Cho SG. The Free Radical Scavenger NecroX-7 Attenuates Acute Graft-versus-Host Disease via Reciprocal Regulation of Th1/Regulatory T Cells and Inhibition of HMGB1 Release. *J Immunol* 2015;194(11):5223-32.
(29) De Meyer GRY, Grootaert MOJ, Michiels CF, Kurdi A, Schrijvers DM, Martinet W. Autophagy in vascular disease. *Circ Res* 2015;116(3):468-79.
(30) Lavandero S, Chiong M, Rothermel BA, Hill JA. Autophagy in cardiovascular biology. *J Clin Invest* 2015;125(1):55-64.
(31) Vanlangenakker N, Bertrand MJ, Bogaert P, Vandenabeele P, Vanden Berghe T. TNF-induced necroptosis in L929 cells is tightly regulated by multiple TNFR1 complex I and II members. *Cell Death Dis* 2011;2:e230.

CHAPTER 7

Summary

Atherosclerosis is a chronic, inflammatory disease characterised by the formation of atherosclerotic plaques in the arterial blood vessel wall. These atherosclerotic plaques may narrow the lumen of the artery (i.e. stenosis) or completely occlude the vessel by the formation of thrombi following plaque rupture, resulting in clinical manifestations such as myocardial infarction or stroke. Despite remarkable advances in cardiovascular research, atherosclerosis remains a leading cause of death and morbidity in the western world (± 370 000 deaths/year in the USA). Therefore, we are searching for new strategies that prevent plaque rupture and can augment the current anti-atherosclerotic therapies. Atherosclerotic plaque rupture is facilitated by the conversion of a stable lesion into a vulnerable, unstable plaque. An atherosclerotic plaque is defined unstable when it consists of a high inflammatory cell content, a large necrotic core and a thin fibrous cap. One of the main mechanisms leading to plaque destabilisation is cell death of lesional macrophages and vascular smooth muscle cells (VSMCs).

There are 3 main cell death pathways: apoptosis, autophagy and necrosis. Apoptotic cell death is characterised by several morphological changes such as cellular shrinkage, membrane blebbing and DNA fragmentation, and is regulated by so-called caspases, whereas necrotic cells oppositely undergo cell swelling followed by cell lysis. Autophagy is characterised by the formation of double-membraned vacuoles, under control of ATG proteins, wherein damaged proteins and/or cell organelles are degraded. The catabolic function of autophagy may promote cell survival by generating nutrients and energy but may also induce cell death by degrading vital cell organelles. Apoptotic and necrotic cell death of macrophages and VSMCs promotes plaque destabilisation by causing thinning of the protective fibrous cap, enlargement of the necrotic core and induction of inflammatory responses. Defective autophagy in macrophages aggravates plaque stability whereas the role of autophagy in VSMCs in atherosclerosis requires further elucidation.

Based on the current knowledge, we decided to investigate whether inhibition of apoptosis, VSMC autophagy, or necrosis, could have beneficial effects on the stability of atherosclerotic plaques in Apolipoprotein E deficient (*ApoE*$^{-/-}$) mice. To accelerate plaque development, mice were fed a western-type diet (WD). First, we used caspase-3 deficient (*Casp3*$^{-/-}$) mice crossbred with *ApoE*$^{-/-}$ mice as a model for apoptosis deficiency in atherosclerosis. *In vitro*, caspase-3 deficient macrophages and VSMCs were resistant to apoptosis, but showed increased susceptibility to necrosis. However, caspase-3

deficiency did not induce a switch to RIPK1-dependent necroptosis. Thus, defective apoptosis, through caspase-3 deletion, does not prevent cell death but triggers a switch to primary necrosis. *In vivo*, caspase-3 deficiency reduced plaque apoptosis but promoted necrotic core formation in atherosclerotic plaques of *ApoE*$^{-/-}$ mice. Moreover, *Casp3*$^{-/-}$*ApoE*$^{-/-}$ mice were characterised by increased plaque size and reduced macrophage content, both presumably due to an increase in necrosis. VSMC and collagen content were not different between both groups. Hence, apoptosis deficiency, via deletion of caspase-3, aggravates plaque stability in WD-fed *ApoE*$^{-/-}$ mice by promoting plaque growth and plaque necrosis.

To investigate the role of VSMC autophagy in arterial disease, a mouse model was constructed in which the essential autophagy gene *Atg7* was specifically deleted in VSMCs. Loss of *Atg7* in murine VSMCs (*Atg7*$^{F/F}$ VSMCs) caused accumulation of the ubiquitin-binding scaffold protein p62 and accelerated the development of stress-induced premature senescence as shown by cellular and nuclear hypertrophy, p16-RB-mediated G_1 proliferative arrest and senescence-associated β-Gal activity. Transfection of p62-encoding plasmid DNA in *Atg7*$^{+/+}$ VSMCs induced similar features, suggesting that accumulation of p62 promotes VSMC senescence. Interestingly, *Atg7*$^{F/F}$ VSMCs were resistant to oxidative stress-induced cell death as compared to controls. This effect was attributed to nuclear translocation of the transcription factor Nrf2 resulting in upregulation of several antioxidative enzymes. *In vivo*, defective VSMC autophagy led to upregulation of MMP9, TGFβ and SDF1 and promoted post-injury neointima formation and diet-induced atherogenesis. Lesions of VSMC-specific *Atg7* knockout mice were characterised by increased total collagen deposition, nuclear hypertrophy, p16 upregulation, RB hypophosphorylation and SA-β-Gal activity, features typical of cellular senescence. We can conclude that defective autophagy in VSMCs accelerates senescence and promotes ligation-induced neointima formation and diet-induced atherogenesis.

To test the plaque stabilising potential of the necrosis inhibitor NecroX-7, WD-fed *ApoE*$^{-/-}$ mice were treated with the compound (30mg/kg, i.p.) three times per week for 16 weeks. NecroX-7 reduced total plaque burden in the thoracic aorta as compared to controls without affecting total plasma cholesterol. Plaques of NecroX-7-treated mice showed a significant decrease in necrotic core area, 8-oxodG, iNOS and MMP13 expression while collagen content and minimum fibrous cap thickness were increased. Moreover, NecroX-

7 treatment reduced the expression of multiple inflammation markers such as TNFα, IL1β, iNOS, HMGB1 and RAGE in a NF-κB-dependent manner. *In vitro*, NecroX-7 prevented *tert*-butyl hydroperoxide (tBHP)-induced mitochondrial ROS formation, necrosis, iNOS expression and HMGB1 release in primary macrophages. Taken together, NecroX-7 improves features of plaque stability in *ApoE*$^{-/-}$ mice by reducing necrotic core formation, oxidative stress and inflammation, and by increasing collagen deposition and fibrous cap thickness.

We can conclude that inhibition of apoptosis and VSMC autophagy are unfavourable strategies to improve atherosclerotic plaque stability. In contrast, inhibition of necrosis proved to be effective as a plaque stabilising strategy. The necrosis inhibitor NecroX-7 reduced plaque necrosis without the compensatory activation of an alternative cell death pathway. Moreover, NecroX-7 improved several features of plaque stability in WD-fed *ApoE*$^{-/-}$ mice including fibrous cap thickening and reduced inflammation, and could therefore be a potential pleiotropic drug for the treatment of atherosclerosis.

CHAPTER 8

Samenvatting

Atherosclerose is een chronische, inflammatoire aandoening gekarakteriseerd door de vorming van atherosclerotische plaques in de arteriële bloedvatwand. Deze atherosclerotische plaques kunnen het lumen van de arterie vernauwen (i.e. stenose) of het bloedvat volledig afsluiten door de vorming van bloedklonters als gevolg van plaqueruptuur, resulterend in klinische verschijnselen zoals een hartinfarct of een beroerte. Ondanks de opmerkelijke voortuitgang in het cardiovasculair onderzoek, blijft atherosclerose één van de grootste doodsoorzaken in de westerse wereld (± 370 000 doden/jaar in de VS). Daarom blijven we onderzoek doen naar nieuwe strategieën die plaqueruptuur kunnen voorkomen en de huidige anti-atherosclerotische therapieën kunnen verbeteren of aanvullen. Plaqueruptuur wordt bewerkstelligd wanneer een stabiele plaque evolueert naar een kwetsbare, onstabiele plaque. Een plaque wordt gedefinieerd als zijnde onstabiel als die bestaat uit een groot aantal inflammatoire cellen, een grote necrotische kern en een dunne fibreuze kap. Een van de belangrijkste mechanismen die aanleiding geven tot plaque destabilisatie is het optreden van celdood van macrofagen en gladde spiercellen (GSC) in de plaque.

De drie belangrijkste vormen van celdood zijn apoptose, autofagie en necrose. Apoptose wordt gekarakteriseerd door verschillende morfologische veranderingen zoals cel inkrimping, membraan blebbing en DNA fragmentatie, en wordt gereguleerd door zogenaamde caspasen, terwijl necrotische cellen juist cel zwelling ondergaan en vervolgens lyseren. Autofagie wordt gekarakteriseerd door de vorming van dubbelmembraan vacuolen, onder de controle van ATG eiwitten, waarin beschadigde eiwitten en/of celorganellen worden afgebroken. De katabole functie van autofagie kan bijdragen tot cel overleving door de vrijstelling van nutriënten en energie maar kan ook celdood induceren door de afbraak van levensnoodzakelijke celorganellen. Apoptose en necrose van macrofagen en GSC bevordert plaque destabilisatie door de fibreuze kap te verzwakken, de necrotische kern te vergroten en inflammatoire reacties uit te lokken. Autofagie deficiëntie in macrofagen leidt tot plaque destabilisatie terwijl de rol van autofagie in GSC in atherosclerose nog ongekend is.

Gebaseerd op de huidige kennis, besloten we te onderzoeken of inhibitie van apoptose, GSC autofagie of necrose, een positieve invloed zou kunnen hebben op de stabiliteit van atherosclerotische plaques in Apolipoprotein E deficiënte (*ApoE*$^{-/-}$) muizen. De ontwikkeling van de plaques werd versneld door de muizen te voeden met een cholesterolrijk dieet. Ten eerste werden caspase-3 deficiënte (*Casp3*$^{-/-}$) muizen gekruist

met *ApoE*$^{-/-}$ muizen als model voor apoptose deficiëntie in atherosclerose. *In vitro* waren caspase-3 deficiënte macrofagen en GSC resistent voor apoptose maar vertoonden ze een verhoogde gevoeligheid voor necrose. Nochtans lokte de caspase-3 deficiëntie geen switch uit naar RIPK1-afhankelijke necroptose. Apoptose deficiëntie via deletie van caspase-3 beschermt dus niet tegen celdood maar veroorzaakt een switch naar primaire necrose. *In vivo* leidde caspase-3 deficiëntie tot een vermindering in plaque apoptose maar ook tot een vergroting van de necrotische kern in plaques van *ApoE*$^{-/-}$ muizen. Bovendien vertoonden *Casp3*$^{-/-}$*ApoE*$^{-/-}$ muizen een toename in plaquegrootte en een afname in het aantal macrofagen, hoogstwaarschijnlijk te wijten aan een toename in necrose. Het aantal GSC en de hoeveelheid collageen in de plaques waren niet verschillend tussen beide groepen. Hieruit kunnen we besluiten dat apoptose deficiëntie via deletie van caspase-3 de plaque stabiliteit in *ApoE*$^{-/-}$ muizen verslechtert door het bevorderen van plaque groei en necrose.

Om de rol van autofagie in GSC in arteriële aandoeningen te onderzoeken, werd een muismodel ontwikkeld waarin het essentiële autofagie gen *Atg7* specifiek in de GSC werd uitgeschakeld. Deletie van *Atg7* in muis GSC (*Atg7*$^{F/F}$ GSC) leidde tot de accumulatie van het ubiquitine-bindende eiwit p62 en versnelde de ontwikkeling van stress-geïnduceerde premature senescentie aangetoond door het optreden van cellulaire en nucleaire hypertrofie, een p16-RB-gemedieerde G_1 groeistop en senescentie-geassocieerde β-Gal activiteit. Transfectie van een p62-coderend plasmide DNA in *Atg7*$^{+/+}$ GSC veroorzaakte gelijkaardige verschijnselen en toont dus aan dat accumulatie van p62 senescentie in GSC kan bevorderen. Daarenboven vertoonden *Atg7*$^{F/F}$ GSC een verhoogde resistentie tegen oxidatieve stress-geïnduceerde celdood in vergelijking met controles. Dit effect was te wijten aan de nucleaire translocatie van de transcriptiefactor Nrf2 wat resulteert in de opregulatie van verscheidene anti-oxidatieve enzymen. *In vivo* leidde defecte GSC autofagie tot de opregulatie van MMP9, TGFβ en SDF1 en bevorderde de ontwikkeling van neointima vorming (post-ligatie) en dieet-geïnduceerde atherogenese. Plaques van GSC-specifieke *Atg7* knockout muizen werden gekarakteriseerd door een toename in collageen, nucleaire hypertrofie, p16 opregulatie, RB hypofosforylatie en SA-β-Gal activiteit, typische kenmerken van cellulaire senescentie. We kunnen concluderen dat autofagie deficiëntie in GSC het optreden van senescentie doet versnellen en de ontwikkeling van neointima vorming (post-ligatie) en dieet- geïnduceerde atherogenese bevordert.

Om het potentiële plaquestabiliserende effect van de necrose inhibitor NecroX-7 te onderzoeken, werden *ApoE*$^{-/-}$ muizen 3 keer per week gedurende 16 weken met deze remmer (30mg/kg, i.p.) behandeld. Behandeling met NecroX-7 verminderde de totale plaque vorming in de thoracale aorta in vergelijking met controles zonder invloed op de totale cholesterol. Plaques van NecroX-7 behandelde muizen vertoonden een significante daling in de grootte van de necrotische kern, 8-oxodG, iNOS en MMP13 expressie terwijl de hoeveelheid collageen en de dikte van de fibreuze kap waren toegenomen. Bovendien verlaagde NecroX-7 de expressie van verschillende inflammatoire merkers zoals TNFα, IL1β, iNOS, HMGB1 en RAGE via een NF-κB-afhankelijke wijze. *In vitro* beschermde NecroX-7 primaire macrofagen tegen *tert*-butyl hydroperoxide (tBHP)-geïnduceerde mitochondriale oxidatieve stress, necrose, iNOS expressie en vrijstelling van HMGB1. We kunnen concluderen dat NecroX-7 verschillende aspecten van plaquestabiliteit bevordert in *ApoE*$^{-/-}$ muizen door de vorming van de necrotische kern, oxidatieve stress en inflammatie te verminderen en door de hoeveelheid collageen en de dikte van de fibreuze kap te verhogen.

We kunnen besluiten dat inhibitie van apoptose en GSC autofagie geen wenselijke strategieën zijn om de stabiliteit van atherosclerotische plaques te bevorderen. Uitsluitend inhibitie van necrose was effectief als plaquestabiliserende strategie. De necrose inhibitor NecroX-7 leidde tot een vermindering in plaque necrose zonder een compensatoire activatie van een alternatieve celdoodroute uit te lokken. Bovendien verbeterde NecroX-7 verschillende kenmerken van plaquestabiliteit waaronder een verdikking van de fibreuze kap en een vermindering in inflammatie, en zou dus een mogelijk pleiotroop geneesmiddel kunnen zijn voor de behandeling van atherosclerose.